



Faculteit Farmaceutische, Biomedische en Diergeneeskundige Wetenschappen
Departement Farmaceutische Wetenschappen
Medicinale Chemie

Implementation of Carboxylate Isosteres to Improve Inflammatory Caspase Inhibitors

Implementatie van Carboxylaatisosteren met als doel
Remmers van Inflammatoire Caspasen te Optimaliseren

Proefschrift voorgelegd tot het behalen van de graad
van doctor in de farmaceutische wetenschappen
aan de Universiteit Antwerpen te verdedigen door

Yves Adriaenssens

**Promotoren: Prof. dr. Pieter Van Der Veken
Prof. dr. Koen Augustyns**

Antwerpen, 2017

Table of contents

| | |
|--|-----------|
| List of abbreviations..... | IX |
| Preface..... | XI |
| 1 The therapeutic relevance of caspases..... | 3 |
| 1.1 Caspases in the cysteine protease family | 3 |
| 1.2 C14A subfamily | 3 |
| 1.3 Heterotetrameric structure of caspases | 4 |
| 1.4 Biological functions of caspases | 5 |
| 1.4.1 Caspases in apoptosis | 5 |
| 1.4.2 Caspases in inflammation | 6 |
| 1.4.2.1 Caspase-1..... | 6 |
| 1.4.2.2 Caspase-4, -5 and -11 | 8 |
| 1.4.2.3 Caspase-12..... | 9 |
| 1.4.2.4 Caspase-14..... | 9 |
| 1.4.3 Other roles of caspases | 9 |
| 1.5 Caspases in diseases | 10 |
| 1.6 Catalytic mechanism of caspases | 11 |
| 1.7 Overlapping substrate specificity..... | 12 |
| 1.8 Caspase inhibitors..... | 15 |
| 1.8.1 Warhead functionality and prime side alterations | 15 |
| 1.8.2 Carboxylate isosteres..... | 17 |
| 1.8.3 Peptidomimetic inhibitors | 19 |
| 1.8.4 Hybrid inhibitors | 19 |
| 1.8.5 Nonpeptidic inhibitors..... | 21 |
| 1.8.6 Allosteric inhibitors | 21 |
| 1.9 Caspase inhibitors in the clinic | 22 |
| 1.9.1 Pralnacasan (VX-740)..... | 22 |
| 1.9.2 Belnacasan (VX-765)..... | 24 |
| 1.9.3 Emricasan (IDN-6556) | 25 |

| | | |
|----------|--|-----------|
| 1.9.4 | Nivocasan (GS-9450)..... | 26 |
| 1.9.5 | NCX-1000..... | 26 |
| | References..... | 27 |
| 2 | Objectives of this thesis | 41 |
| 2.1 | Objective 1: Identification and implementation of carboxylate isosteres in caspase inhibitors..... | 41 |
| 2.2 | Objective 2: Convenient library synthesis and on-target experiments..... | 43 |
| 2.3 | Objective 3: Approach to induce caspase-1 degradation via thalidomide conjugates 44 | |
| | References..... | 45 |
| 3 | Carboxylate isosteres for caspase inhibitors: the acylsulfonamide case revisited 49 | |
| 3.1 | Abstract..... | 49 |
| 3.2 | Introduction..... | 49 |
| 3.2.1 | Caspase inhibition..... | 49 |
| 3.2.2 | Caspase selectivity issues..... | 50 |
| 3.3 | Objectives of this chapter..... | 51 |
| 3.4 | Results and discussion..... | 52 |
| 3.4.1 | Design and synthesis..... | 52 |
| 3.4.2 | Inhibitory potency..... | 54 |
| 3.4.2.1 | Human caspase panel..... | 54 |
| 3.4.2.2 | Murine caspase panel..... | 56 |
| 3.4.3 | Structural elaboration of the P1-moiety..... | 57 |
| 3.4.4 | Stability measurements..... | 61 |
| 3.4.5 | Biological assays..... | 63 |
| 3.5 | Conclusions..... | 65 |
| 3.6 | Experimental..... | 65 |
| 3.6.1 | Chemistry..... | 65 |
| 3.6.2 | Phenylhydrazine kinetic study..... | 74 |
| 3.6.3 | Biochemical evaluation: IC ₅₀ determination..... | 75 |

| | | |
|----------|---|-----------|
| 3.6.4 | Chemical stability protocol | 75 |
| 3.6.5 | Metabolic stability protocol | 76 |
| 3.6.6 | Macrophage differentiation, stimulation and evaluation | 76 |
| | References..... | 77 |
| | Supporting information | 80 |
| 4 | The identification of isosteric replacements for carboxylic acids in caspase inhibitors, determined by the Modified Substrate Activity Screening (MSAS)..... | 95 |
| 4.1 | Introduction..... | 95 |
| 4.1.1 | Caspases | 95 |
| 4.1.2 | Overcoming selectivity problems with respect to caspase inhibitors | 95 |
| 4.1.3 | Methodology: the Modified Substrate Activity Screening (MSAS) | 96 |
| 4.2 | Objectives of this chapter | 97 |
| 4.3 | Results and discussion..... | 97 |
| 4.3.1 | Library synthesis | 97 |
| 4.3.2 | Inhibitor screening (step 1)..... | 100 |
| 4.3.2.1 | N-Acyl aminomethylcoumarins | 100 |
| 4.3.2.2 | Acetic acid isosteres | 105 |
| 4.3.3 | Substrate screening (step 2)..... | 107 |
| 4.3.4 | Validation through emerging with warhead (step 3)..... | 108 |
| 4.3.4.1 | Replacement of the amide bond by a warhead | 108 |
| 4.3.4.2 | Incorporation of identified isosteres in existing caspase inhibitors | 110 |
| 4.3.4.3 | Physicochemical profile | 113 |
| 4.4 | Conclusions..... | 114 |
| 4.5 | Outlook..... | 115 |
| 4.6 | Experimental section..... | 116 |
| 4.6.1 | Chemistry | 116 |
| 4.6.2 | Biochemical assays..... | 141 |
| 4.6.3 | Physicochemical profile..... | 143 |
| | References..... | 144 |

| | |
|---|------------|
| 5 Oxadiazolones: a challenge to implement | 149 |
| 5.1 Introduction..... | 149 |
| 5.1.1 General synthesis of oxadiazolones..... | 149 |
| 5.2 Objectives..... | 150 |
| 5.3 Results and discussion..... | 150 |
| 5.3.1 Protecting groups | 150 |
| 5.3.2 Via the acyliminium-Strecker reaction | 151 |
| 5.3.3 Via Schiff base formation | 153 |
| 5.3.3.1 Synthesis of the oxadiazolone building block: attempt 1..... | 153 |
| 5.3.3.2 Synthesis of the oxadiazolone building block: attempt 2..... | 154 |
| 5.3.3.3 Synthesis of the oxadiazolone building block: attempt 3..... | 154 |
| 5.3.4 Transformation of aminonitriles into amino aldehydes | 155 |
| 5.4 Conclusions | 155 |
| 5.5 Experimental section | 155 |
| 5.5.1 Chemistry | 155 |
| References..... | 161 |
| 6 Optimization of the acyliminium-Strecker reaction for convenient library synthesis and on-target experiments | 165 |
| 6.1 Introduction..... | 165 |
| 6.1.1 Target-assisted drug discovery | 165 |
| 6.1.2 The Strecker and “acyliminium-Strecker” reaction | 168 |
| 6.2 Study design..... | 170 |
| 6.3 Results and discussion..... | 172 |
| 6.3.1 Experiments involving isolation of acylaminoalkylsulfone intermediates..... | 172 |
| 6.3.1.1 Synthesis of acylaminoalkylsulfones..... | 172 |
| 6.3.1.2 Transformation of acylaminoalkylsulfones in the corresponding carbonitriles | 173 |
| 6.3.1.3 One-pot protocols for the acyliminium-Strecker reaction | 175 |
| 6.3.2 Preliminary experiments to produce a one-pot protocol without phenylsulfonic acid catalysis | 177 |

| | | |
|-----------|--|------------|
| 6.4 | Future perspectives..... | 177 |
| 6.5 | Conclusion..... | 179 |
| 6.6 | Experimental section..... | 179 |
| 6.6.1 | Chemistry..... | 179 |
| | References..... | 185 |
| 7 | Approach to induce caspase-1 degradation via thalidomide conjugates..... | 191 |
| 8 | Conclusions and Outlook..... | 195 |
| 8.1 | Conclusions..... | 195 |
| 8.2 | Outlook..... | 196 |
| 8.2.1 | Further investigation of acylsulfonamide prodrugs..... | 196 |
| 8.2.2 | Screening of the fragment library against other enzymatic targets..... | 196 |
| 8.2.3 | Taking oxadiazolones to the next level with respect to caspase inhibitor discovery | 196 |
| 8.2.3.1 | Modifications to the warhead..... | 196 |
| 8.2.3.2 | Scaffold-based inhibitors..... | 197 |
| 8.2.3.3 | Modifications to the oxadiazolone heterocycle..... | 197 |
| 8.2.4 | Further optimization of the acyliminium-Strecker synthesis..... | 198 |
| | References..... | 199 |
| 9 | Summary..... | 203 |
| 9.1 | The therapeutic relevance of caspases..... | 203 |
| 9.2 | Carboxylate isosteres for caspase inhibitors: the acylsulfonamide case revisited | 203 |
| 9.3 | The identification of isosteric replacements for carboxylic acids in (inflammatory) caspase inhibitors, determined by the Modified Substrate Activity Screening (MSAS) ... | 204 |
| 9.4 | Optimization of the acyliminium-Strecker synthesis..... | 206 |
| | References..... | 208 |
| 10 | Samenvatting..... | 213 |
| 10.1 | Therapeutisch belang van caspasen..... | 213 |
| 10.2 | Carbonzuurisosteren voor remmers van caspasen: acylsulfonamides herbekeken | 213 |

| | | |
|-----------|--|------------|
| 10.3 | Identificatie van carbonzuurisosteren voor remmers van inflammatoire caspases, bepaald door de Gemodificeerde Substraat Activiteit Screening (MSAS)..... | 215 |
| 10.4 | Optimalisatie van de acyliminium-Streckersynthese | 217 |
| | Referenties | 218 |
| 11 | Curriculum Vitae | 223 |
| 12 | Dankwoord | 229 |

List of abbreviations

| | |
|---------|---|
| Å | Ångström |
| ACN | Acetonitrile |
| ADME | Absorption-Distribution-Metabolism-Excretion |
| AFC | 7-Amino-4-trifluoromethylcoumarin |
| AMC | 7-Amino-4-methylcoumarin |
| Aq | Aqueous |
| Boc | <i>tert</i> -Butoxycarbonyl |
| CARD | Caspase Recruitment Domain |
| CDI | 1,1'-Carbonyldiimidazole |
| CHAPS | 3-[(3-Cholamidopropyl)dimethylammonio]-1-propanesulfonate |
| DBU | 1,8-Diazabicyclo[5.4.0]undec-7-ene |
| DCM | Dichloromethane |
| DCC | Dynamic Combinatorial Chemistry |
| DED | Death Effector Domain |
| DIPEA | <i>N,N</i> -Diisopropylethylamine |
| DMAP | 4-Dimethylaminopyridine |
| DMBA | 1,3-Dimethylbarbituric acid |
| DME | Dimethoxyethane |
| DMF | <i>N,N</i> -Dimethylformamide |
| DMSO | Dimethylsulfoxide |
| EDC·HCl | <i>N</i> -(3-Dimethylaminopropyl)- <i>N'</i> -ethylcarbodiimide hydrochloride |
| EDTA | Ethylenediaminetetraacetic acid |
| ESI | Electrospray ionization |
| EtOAc | Ethyl acetate |
| Eq | Equivalent |
| FA | Formic acid |
| HATU | 1-[Bis(dimethylamino)methylene]-1H-1,2,3-triazolo[4,5-b]pyridinium 3-oxide hexafluorophosphate |
| HEPES | 2-[4-(2-Hydroxyethyl)piperazin-1-yl]ethanesulfonic acid |
| Hept | <i>n</i> -Heptane |
| Hex | Hexanes |
| HPLC | High Performance Liquid Chromatography |
| HOBt | 1-Hydroxybenzotriazole |

| | |
|------------------|---|
| (HR)MS | (High Resolution) Mass Spectrometry |
| IC ₅₀ | Half maximal inhibitory concentration |
| IL | Interleukin |
| KTGS | Kinetic target-guided synthesis |
| LC | Liquid Chromatography |
| LDH | Lactate dehydrogenase |
| LPS | Lipopolysaccharide |
| MRM | Multiple Reaction Monitoring |
| MSAS | Modified Substrate Activity Screening |
| NMR | Nuclear Magnetic Resonance |
| PIPES | Piperazine- <i>N,N'</i> -bis(2-ethanesulfonic acid) |
| PMA | Phosphomolybdic Acid |
| <i>p</i> TsOH | <i>para</i> -toluenesulfonic acid |
| Ref | Reference |
| RT | Room temperature |
| SAS | Substrate Activity Screening |
| TBAF | tetra- <i>n</i> -butylammonium fluoride |
| TEA | Triethylamine |
| TFA | Trifluoroacetic acid |
| TFAA | Trifluoroacetic anhydride |
| THF | Tetrahydrofuran |
| UPLC | Ultra Performance Liquid Chromatography |
| Z | Carboxybenzyl |

Preface

As part of the ongoing interest of our research group in inhibitor-mediated blocking of protease activity, this project focused on caspases as promising targets. In **Chapter 1**, the different members of the caspase family will be discussed, as well as their therapeutic relevance as consequence of their important roles in several diseases. The second part of this chapter will cover the structural aspects belonging to caspase inhibitor design, while setting the emphasis on inhibitors that have entered clinical trials. The different objectives that were set at the beginning and updated throughout this PhD, are described in **Chapter 2**.

In order to structurally differ from existing caspase inhibitors, part of this work aimed at implementing carboxylic acid isosteres. Based on previous reports, **Chapter 3** continues the investigation of the incorporation of acylsulfonamides as worthy carboxylate replacements in existing caspase inhibitors. Further identification of other promising isosteres was achieved in **Chapter 4**, where the focus is set on MSAS, a methodology that has been recently devised and validated by our group. Specifically, oxadiazolone heterocycles were found to be favorable in terms of affinity and selectivity towards caspase-1 and -4. Similar to the previous chapter, this chapter also covers the implementation of this isostere in existing caspase inhibitors. However, since the synthesis of these molecules appeared to be a real challenge, **Chapter 5** is devoted to the different approaches that have been attempted but appeared unsuccessful.

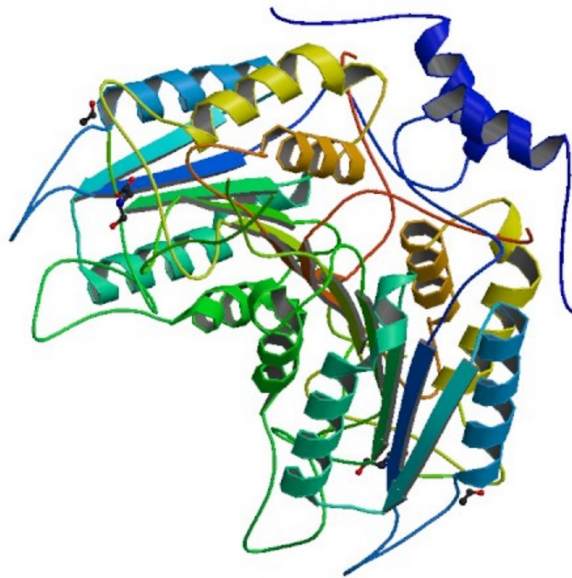
Due to our interest in designing protease inhibitors, we explored an easy and efficient way to create large library sets of aminonitriles that are believed to have the potential of blocking specific proteases. **Chapter 6** has therefore been devoted to an exploratory study of this methodology, which is mainly based on the acyliminium-Strecker reaction.

While the rest of this thesis is focusing on caspase inhibition, **Chapter 7** aims for caspase degradation. However, due to limited intellectual property rights, this chapter has been removed from this thesis.

The concluding remarks, as well as some future perspectives in order to complete this work, have been described in **Chapter 8**. In the end, a complete summary of this work has been added; **Chapter 9** covers the English version while **Chapter 10** the Dutch version.

Chapter 1

The therapeutic relevance of caspases



1 The therapeutic relevance of caspases

1.1 Caspases in the cysteine protease family

Proteases, enzymes that catalyze the hydrolysis of peptide bonds in proteins, are generally classified into seven categories depending on the nature of their catalytic residues and their mechanism of action (**Figure 1.1**).¹ Cysteine proteases share a common mechanism that involves a nucleophilic attack of the cysteine thiol present in its active center. This class of enzymes counts 14 superfamilies, from which clan CD is the second biggest one. Clan CD was proposed in 1994, after the determination of the 3D crystal structure of human interleukin-1 β -converting enzyme (ICE), later renamed as caspase-1.²⁻³ Family C14, often referred to as the caspase family, is one of the seven peptidase families that are members of clan CD. In turn, family C14 is divided into subfamilies C14A (caspases) and C14B (metacaspases and paracaspases).⁴

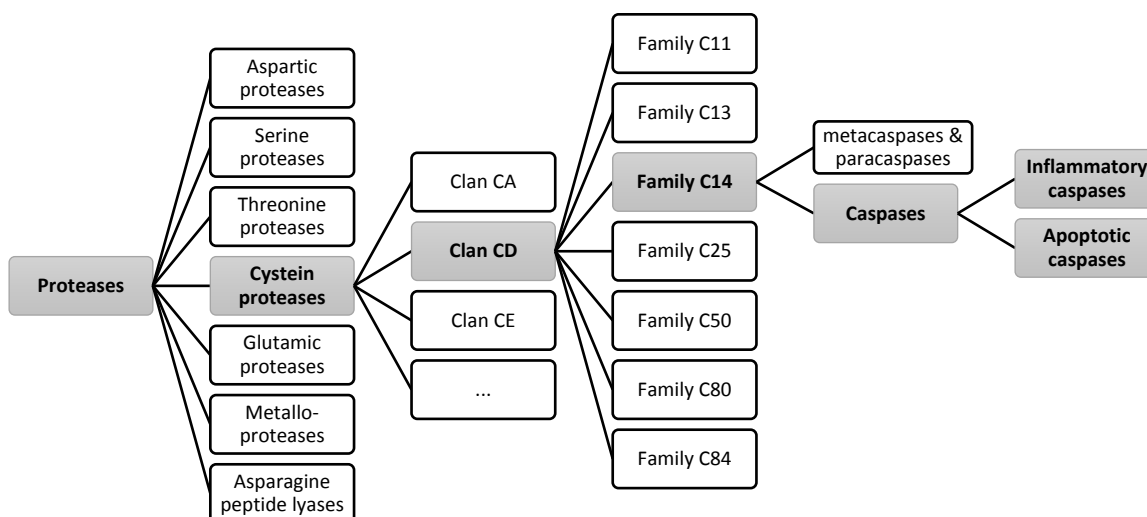


Figure 1.1. Hierarchical representation of the caspases.

1.2 C14A subfamily

In humans, the C14A subfamily consists of 12 caspases which can be allocated to two main groups, depending on their structural similarities, which are generally associated with their cellular functions. The first group includes caspase-1, -4, -5 and -12, and is called the inflammatory caspases. Except for caspase-12, all inflammatory caspases participate in the activation of inflammasomes to initiate inflammation and pyroptosis, an inflammatory and lytic form of programmed cell death.⁵ The second group, the apoptotic caspases, are typically subdivided into initiators (caspase-2, -8, -9 and -10) and executioners (caspase-3, -6 and -7) of an immunologically silent form of programmed cell death known as apoptosis.⁶⁻⁷ These caspases are supplemented with a functional outlier, caspase-14, which has a primary role in cornification and protection of underlying layers of skin.⁸ In spite of being a structurally

highly conserved group of enzymes, functional differentiation within the family seems not fully identical between species. For example, mice lack caspase-4 and -5 but possess an alternative caspase, namely caspase-11.⁹ A summary of all human and murine caspases is presented in **Figure 1.2**.

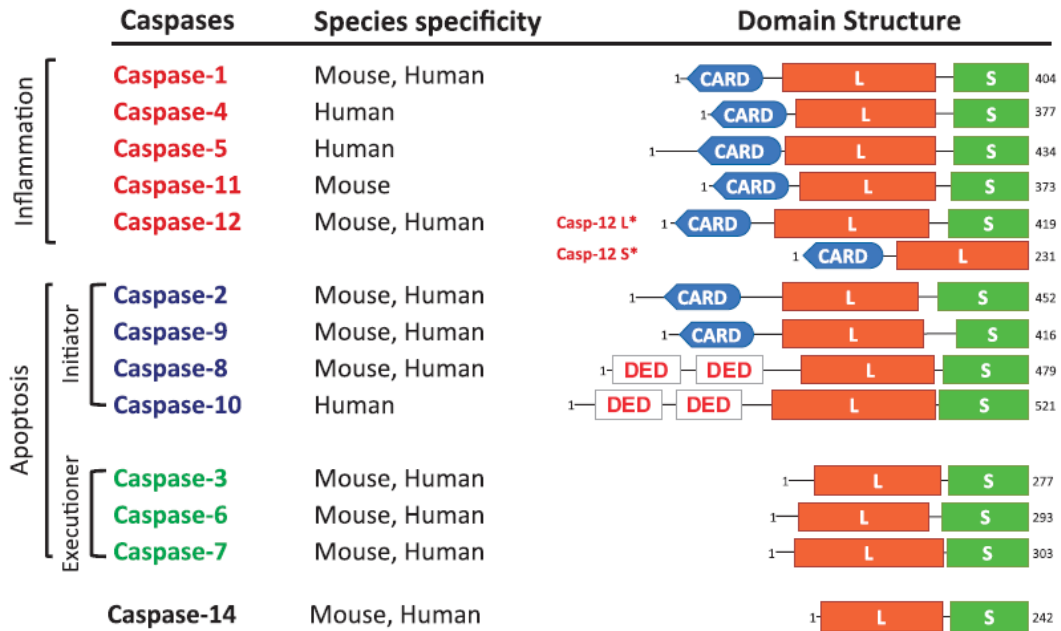


Figure 1.2. Domain structure and functional classification of human and murine caspases. CARD, caspase recruitment domain; DED, death effector domain; L, large subunit; S, small subunit; S*, short form; L*, long form. Figure was taken from ref [10].

1.3 Heterotetrameric structure of caspases

In general, caspases are found in the cytoplasm of cells as inactive monomeric zymogens, which consist of a carboxy-terminal protease effector domain comprised of a large subunit and a small subunit (**Figure 1.2**). The initiator and inflammatory caspases structurally differ from the executioners by the presence of specific protein interaction domains toward the *N*-terminus, namely death effector domains (DED) or caspase-recruitment domains (CARD). These additional domains mediate dimerization and/or recruitment into larger complexes to facilitate caspase activation.¹⁰⁻¹¹ Executioner caspases on the other hand, have a short prodomain and exist as inactive homodimers until they are cleaved and activated by initiator caspases. In general, after the autocatalytic cleavage at the intersubunit linkers, caspases become mature, proteolytically active heterotetramers (**Figure 1.3**), containing two small (p10) and two large subdomains (p20).¹² The two heterodimers align in a head-to-tail configuration. Correspondingly, two active sites are positioned at opposite ends of the molecule.¹³

Caspase-12 is the only member that can be expressed in different variants due to mutations in the human caspase-12 gene. Most individuals express the truncated form of caspase-12 (casp-12-S) that

has only a CARD domain and large subunit, therefore lacking the possibility to generate a catalytic active heterotetramer. Only in about 20 % of individuals of African descent the full length variant of caspase-12 (casp-12-L) is expressed because of a single nucleotide polymorphism.¹⁴

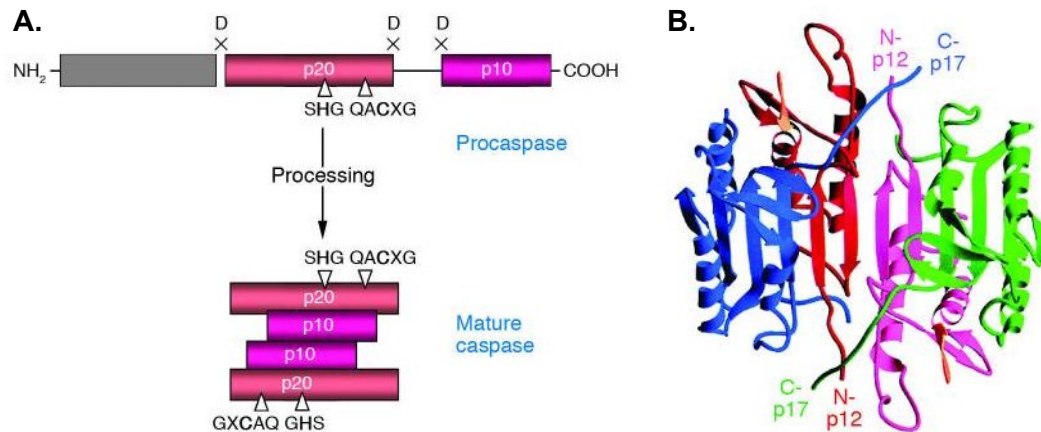


Figure 1.3. (A) Scheme of procaspase activation. Cleavage of the procaspase at the specific Asp-X bonds leads to the formation of the mature caspase, which comprises the heterotetramer and the release of the prodomain. The residues involved in the formation of the active center are shown. (B) The 3D structure of caspase-3 heterotetramer. Figure was taken from ref [13].

1.4 Biological functions of caspases

As previously mentioned, caspases possess essential roles in pyroptosis and apoptosis. Though many mechanistic pathways have been described, the domain of caspase biology is still fraught with numerous unanswered questions. The discovery of yet unknown functional mechanisms for each caspase is ongoing, especially in respect to biological functions besides the two central roles. In this part, all caspases are described with their most important functions in human cells.

1.4.1 Caspases in apoptosis

In multicellular organisms, homeostasis is maintained through a balance between cell proliferation and cell death. Because of the role of apoptosis in the elimination of damaged cells, it serves as a protagonist in the prevention of disease. Apoptosis is a regulated process that leads to dismantling of intracellular components without causing inflammation or damage to surrounding cells. Activated initiator caspases trigger executioner caspases to cleave key structural proteins that will lead to DNA fragmentation, membrane blebbing and eventually cell death.

Apoptotic caspase activation pathways can be divided into an extrinsic and intrinsic category (**Figure 1.4**). Caspase-8 plays a key role in the extrinsic pathway of apoptosis, that is believed to be activated by ligand binding to death receptors. These ligands include tumor necrosis factor alpha (TNF- α), Fas ligand (FasL), TNF-related apoptosis-inducing ligand (TRAIL), and many others. Caspase-10, showing high similarity with caspase-8, is also an apoptotic initiator in the extrinsic pathway. However, due to

the fact that this caspase is not encoded in rodent genomes, much less functional studies have been performed on caspase-10.¹⁵ Furthermore, both enzymes have shown to possess additional functions besides the apoptotic pathway. Caspase-10, for example, was found to maintain a balanced level of autophagy, therefore suggesting a significant role in the regulation of acute myeloid leukemia cell death.¹⁶⁻¹⁷ Intrinsic apoptosis, also known as mitochondrial apoptosis, relies on the activation of caspase-9 through a various number of cellular stresses, such as growth factor deprivation, cytoskeletal disruption, oxidative stress, DNA damage and accumulation of unfolded proteins.¹⁸⁻¹⁹ Caspase-8, -9 and -10, regardless of which pathway, will in their turn activate the executioner caspases-3, -6 and -7, leading to apoptosis. Apoptotic cells attract macrophages to find and phagocytose them without mounting an inflammatory response.²⁰

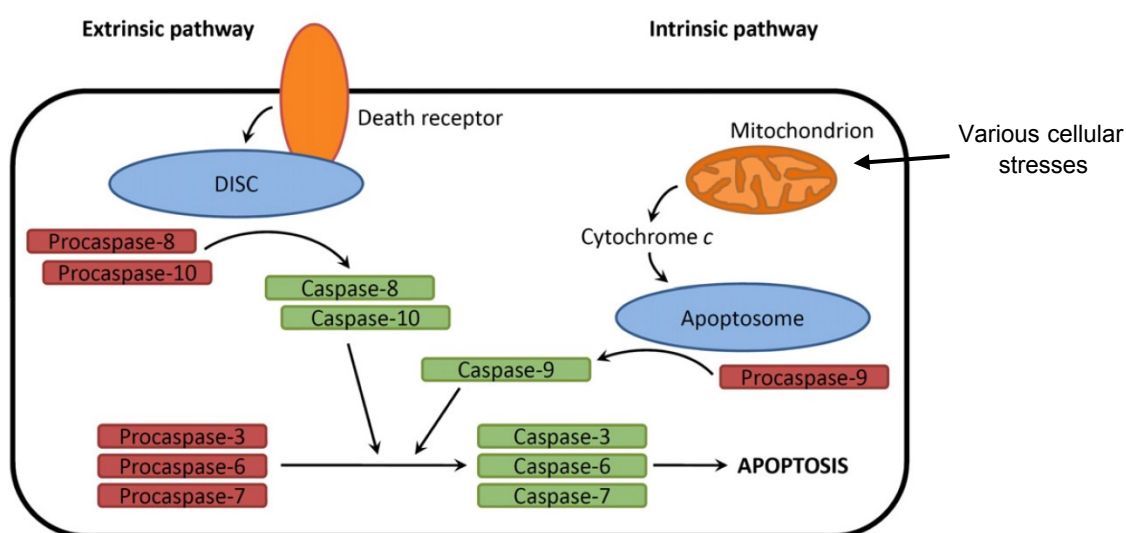


Figure 1.4. Major apoptotic pathways of caspase activation. Figure was adjusted from ref [125].

The last member of the apoptotic category is caspase-2. Though this enzyme is classified as a long prodomain initiator caspase, it is also considered to share executioner features.²¹ This unique member is the only caspase that is localized in both cytoplasm and nucleus. Diverse research groups have demonstrated important roles for caspase-2 in apparently diverse functions, such as tumor suppression, regulation of oxidative stress response pathways and aging. Nevertheless, the precise role of caspase-2 in physiology and disease is still poorly understood and controversial.²²⁻²⁴

1.4.2 Caspases in inflammation

1.4.2.1 Caspase-1

Of the inflammatory caspases, caspase-1 has thus far been the most studied. In response to bacterial and viral infections or when subjected to bacterial toxins, specific pathogen- or danger-related molecular patterns cause the formation of different inflammasome complexes (**Figure 1.5**).²⁵ Such a protein complex, the so-called canonical inflammasome, initiates caspase-1, that is known to be

responsible for processing of pro-interleukins-1 β and -18 into its mature biologically active form. The release of these mature interleukins (ILs) is an important factor in innate immunity and host resistance to pathogens as it induces inflammation. Consequently, it exerts various effects on different tissues, resulting, for example, in the induction of anorexia, fatigue, fat catabolism, fever, as well as the secretion of acute phase proteins and activation of immune cells leading to the release of other cytokines and chemokines. Furthermore, parallel to the processing of IL-1 family cytokines, caspase-1 executes an inflammatory form of programmed cell death, distinct from the immunologically silent apoptosis, termed pyroptosis.²⁶ This involves an osmotic water flow into the cell after the formation of membrane pores. As a result, the cell swells and lysis occurs.²⁷ This leads to the release of pro-inflammatory molecules, such as ATP, or proteins, such as proIL-1 α and HMGB1, which are able to recruit neutrophils and induce inflammation.²⁰ Remarkably, mitochondrial membranes remain intact.

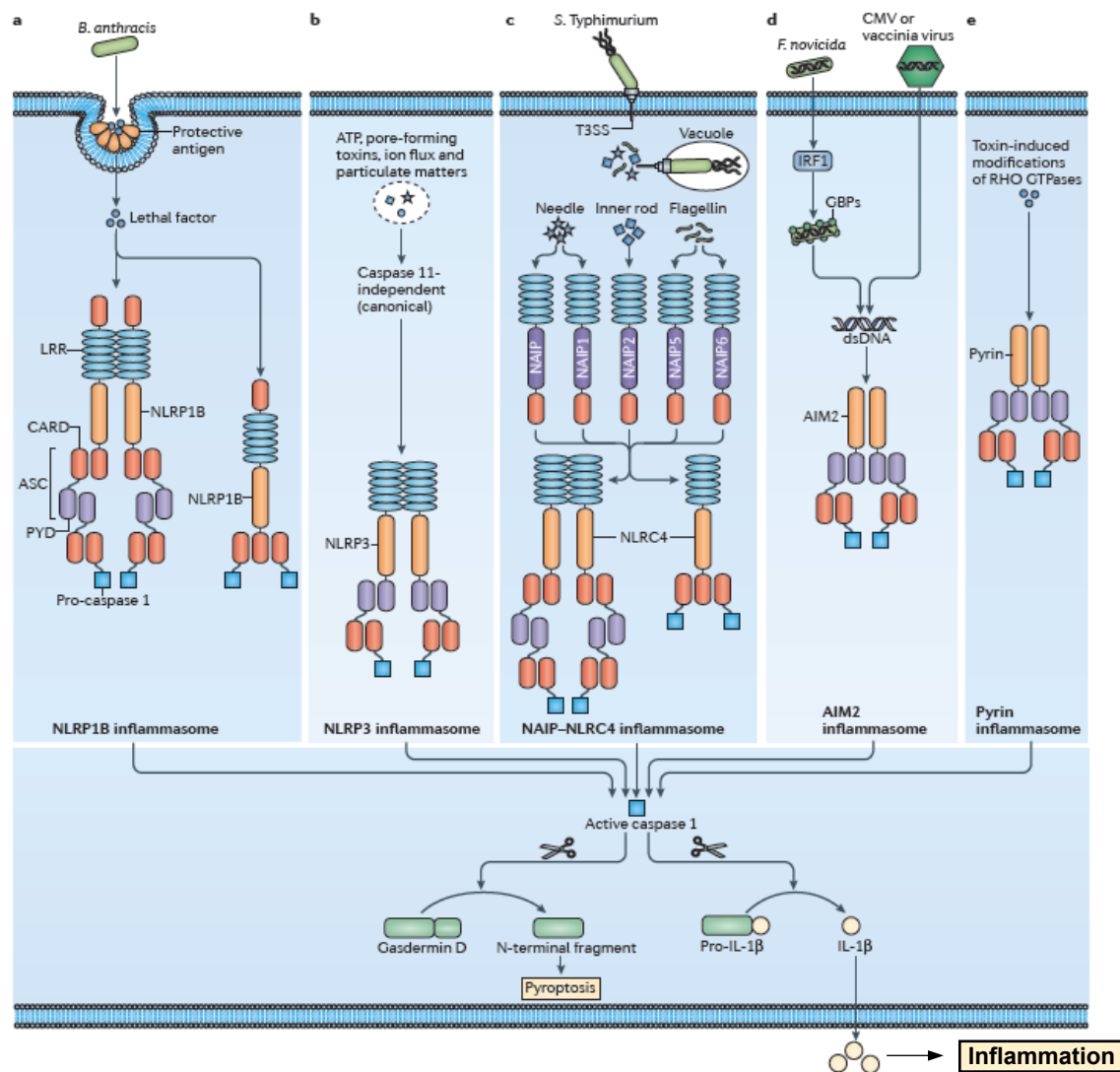


Figure 1.5. Caspase-1 and the canonical inflammasome. Figure adjusted from ref [6].

1.4.2.2 Caspase-4, -5 and -11

While humans possess caspases-4 and -5, mice only express caspase-11. Even though these three members of the caspase family are considered the most homologous, it remains unclear whether human caspase-4 and/or -5 represent functional orthologs of murine caspase-11. Some apparent differences between these enzymes can be considered. For example, the amino acid identity between caspase-11 and caspase-4 or -5 has been determined to be less than 60%, insinuating that these enzymes may carry out distinct functions.²⁸ Furthermore, caspase-11 and -5 are characterized by relatively low expression levels, while caspase-4 expression is substantially bigger.

Throughout the years, a lot of effort has been done to generate a better insight into the structural and functional parameters of the comparison between these three caspases.^{9, 29-32} For example, recent studies in mice have demonstrated that caspase-11 has the ability to, independently of caspase-1, induce pyroptosis and IL-1 α in response to infections by Gram-negative bacteria, such as *E. coli* or *Vibrio cholerae* (**Figure 1.6**).³³ Furthermore, an immune response is initiated through the activation of the caspase-11-dependent inflammasomes, also referred to as the non-canonical inflammasomes.³⁴ Next, caspase-1 gets activated, causing cytokine maturation and consecutive inflammation.

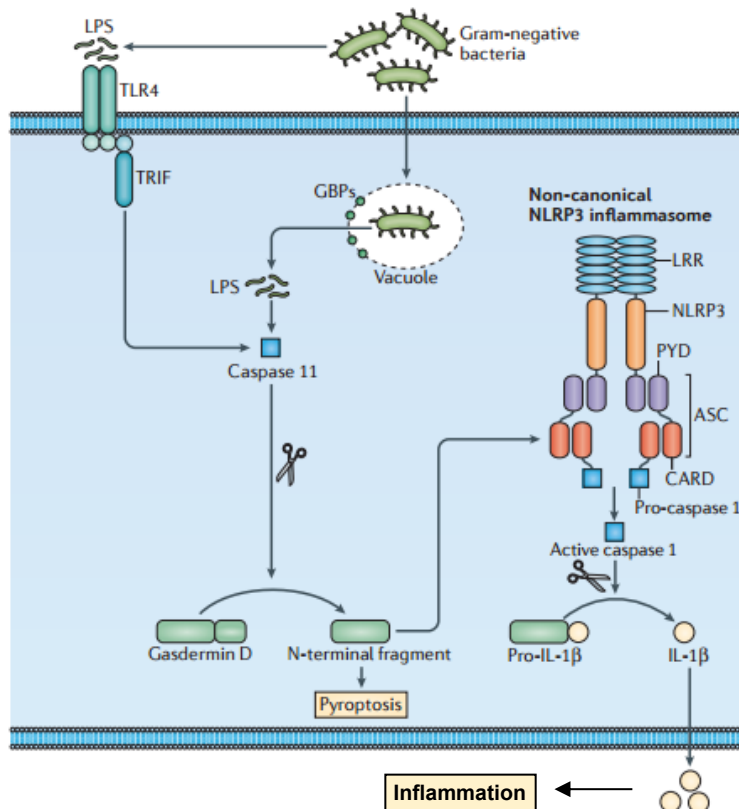


Figure 1.6. Caspase-11 and the non-canonical inflammasome. Figure adjusted from ref [6].

To compare with human caspases, investigations have indicated that both caspase-4 and caspase-5 detect cytoplasmic lipopolysaccharides (LPS), components of the outer membrane of Gram-negative

bacteria. As a result, both enzymes mediate IL-1 α and IL-1 β release, but only caspase-4 has been identified in a human monocytic cell line to mediate intracellular LPS responses leading to cell death.³⁵⁻³⁶ However, the mechanism underlying this process has not yet been confirmed.³⁷ Moreover, caspase-4 remains uncleaved, while caspase-5 undergoes rapid processing upon LPS treatment. Another research group observed that caspase-4 indeed contributes to IL-1 β release in response to cytosolic LPS but does not play a major role in controlling IL-1 β release from human macrophages during bacterial infection.³⁸

The described differences in the regulation of non-canonical inflammasome pathways in murine and human cells calls for further extensive research in this field. Obviously, further insight is required into the many mechanisms that underlay the processes where these caspases are participated in.

1.4.2.3 Caspase-12

Caspase-12 in its active heterotetrameric conformation was first reported as a dominant-negative regulator of caspase-1 activation.³⁹⁻⁴⁰ However, Lamkanfi and co-workers questioned these findings in a later study.⁴¹ Moreover, they reported that caspase-12-deficient mice also lack caspase-11 expression, thus preventing only non-canonical caspase-1 activation. Next, caspase-12 was found to lead to the downregulation of antimicrobial responses.⁴² Humans expressing this full-length caspase-12 protein show reduced inflammatory and innate responses to endotoxins and thus an increased risk of developing severe sepsis.⁴³

1.4.2.4 Caspase-14

Caspase-14 is a unique caspase. First, unlike apoptotic caspases, expression of caspase-14 is restricted to stratified epithelia, such as the skin. Next, it has a distinguished function; it is responsible for proteolytic processing and degradation of profilaggrin to yield filaggrin monomers, a structural protein that binds to keratin fibers in epithelial cells, thereby protecting the cells of the skin from UVB irradiation and water loss.^{20,44}

1.4.3 Other roles of caspases

Besides their prominent role in cell death and inflammation, increasing evidence suggests that caspases are involved in regulating multiple cellular processes that do not lead to cell death. For example, it is found that various caspases play significant roles in cell proliferation⁴⁵⁻⁴⁶, migration⁴⁷⁻⁴⁸ and differentiation⁴⁸⁻⁴⁹, but also in neural development, scar remediation, synaptic plasticity, stem cells and self-renewal, DNA damage and aging in many biological events associated with restoring and regeneration.^{10, 50-51} The molecular mechanisms behind these biological processes still remain incomplete and are therefore subject of many ongoing investigations.

1.5 Caspases in diseases

Caspases have key functions in fundamental processes like pro-inflammatory cytokine maturation and cellular apoptosis. Upon dysregulation of caspases, these processes become impaired and consequently play central roles in many common medical conditions.

Cytokines are at the core of a wide variety of inflammatory and autoimmune diseases. Specifically, gout⁵², type 2 diabetes⁵³, familial Mediterranean fever⁵⁴ and systemic-onset juvenile idiopathic arthritis⁵⁵ are examples of disorders that have been linked with elevated IL-1 β levels. A direct link between these increased levels and inflammatory caspases has been established during several recent developments.¹⁹ Moreover, human trials with existing caspase-1 inhibitors have proven their role in rheumatoid arthritis, SLE, psoriatic arthritis and osteoarthritis.⁵⁶⁻⁵⁷

On the other hand, dysregulated apoptotic caspases could initiate disorders by two ways: upon excessive/inappropriate activation and upon deficient activity. In the first case, cells would prematurely undergo cell death, potentially leading to neurodegenerative diseases, hematologic diseases and tissue damage. More specifically, activated caspase-8 has been identified in degenerating neurons from Huntington's disease patients.⁵⁸⁻⁵⁹ Furthermore, caspase-3 expression is up-regulated in apoptotic hippocampal neurons in Alzheimer's disease.⁶⁰⁻⁶¹ In the heart, caspases are also activated in a variety of human cardiomyopathies that lead to progressive loss of cardiac myocytes and congestive heart failure.⁶²

In case the dysregulation of apoptotic caspases consists of deficient caspase activity, cell death levels are lower than normal. Activators of caspases could in that perspective be the elemental therapeutic solution. Such activators will not be discussed in detail. Nevertheless, it is important to understand that excessive inhibition of cell death could at last, in theory, lead to tumor developing pathologies. A thorough investigation should be performed when using caspase inhibitors as therapeutic drugs.

It is obvious that caspases are important mediators of diverse diseases. For that reason they have emerged as extremely valuable therapeutic targets. Unfortunately, available drug therapies are still remarkably poor in this field. This has encouraged a great deal of effort to find potent and selective inhibitors with pharmaceutically acceptable properties. In the next section of this chapter, a thorough analysis will be described of the structural mechanism of caspases, along with the many obstacles that researchers are facing in respect to the discovery of selective caspase inhibitors with acceptable biopharmaceutical properties.

1.6 Catalytic mechanism of caspases

As the name implies, caspases are **cysteine-dependent aspartate-specific peptidases**. These enzymes catalytically hydrolyze amide bonds, specifically at the carboxyl side of an aspartate amino acid of a peptide (**Figure 1.7**).

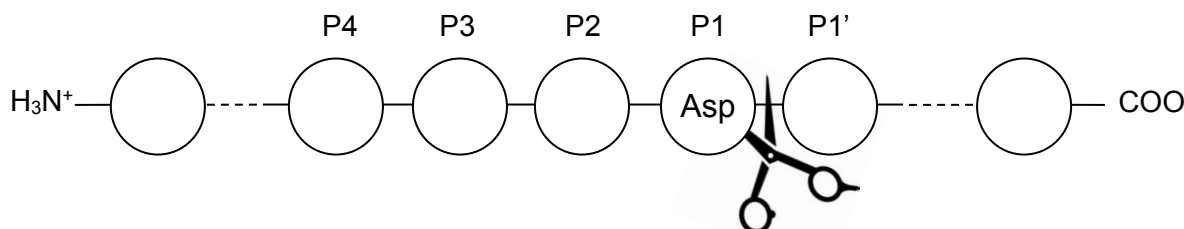


Figure 1.7. Representation of substrate cleavage by caspases. Caspases have a strict preference for aspartic acid in the P1 substrate position.

The preference for an aspartate moiety in the P1 position of the peptide substrates of caspases is due to direct charge-charge interactions with side chains of Arg179 and Arg341 amino acid and hydrogen bonds with the side chain NH of Gln283, illustrated for the caspase-1 active-site pocket in **Figure 1.8**. The interactions with Arg179 are considered the most important, taking into account hydrogen bond distances and geometry. With exception of the amino acid numbering, the interactions are identical for each member of the caspase family. The amide hydrolysis is achieved by a nucleophilic attack of the caspase cysteine. Cysteine's relatively high pK_a (8.00) is compensated by the presence of a conserved histidine residue near the active site. This so-called catalytic dyad increases the nucleophilicity of cysteine. Histidine not only acts as a general base, but also activates a water molecule to complete the release of a hydrolyzed product.^{3, 63-64}

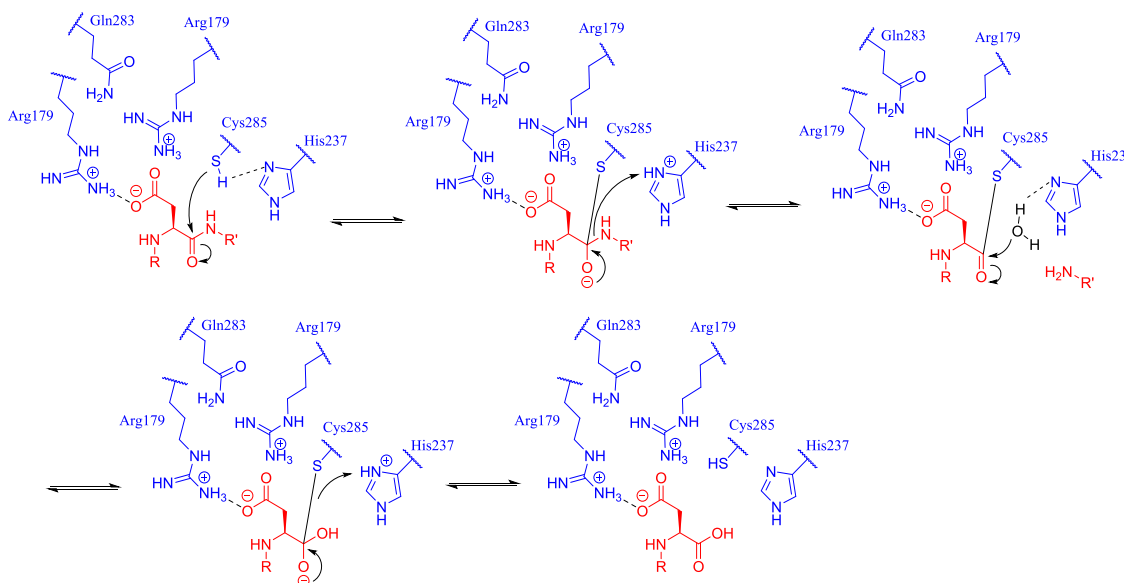


Figure 1.8. Mechanism for substrate cleavage by caspases. The amino acid numbering is illustrated for caspase-1. The enzyme and substrate are highlighted in blue and red, respectively. Electrostatic and hydrogen bond interactions are indicated by dashed lines. Figure was derived from ref [65].⁶⁵

1.7 Overlapping substrate specificity

Many studies have been performed in the search for specific synthetic substrates for each caspase in order to elucidate caspase-mediated mechanisms in various cellular processes. Nevertheless, the design of selective substrates appears to be a huge obstacle. The inevitable similarity of all caspases causes a problem of cross-reactivity. It is therefore important to realize that the majority of the substrates are useful for studies on individual purified caspases but are less effective for research on complex biological samples.⁶⁶

The substrate preference for caspases is generally characterized by a tetrapeptide moiety, fitting the S1-S4 caspase subsites. Only caspase-2 appears to favor a pentapeptide to obtain efficient cleavage.⁶⁷ Several strategies have been developed to identify subsite preferences for caspases, generally based on attaching a reporter group to the peptide sequences. Caspase cleavage of the P1 adjacent scissile bond will release the reporter group, which can be quantified by fluorescence, light absorption or other detection modes. Several examples of various reporters are presented in **Figure 1.9**. Reporter groups, such as chromophore *para*-nitroaniline (*p*NA) and fluorophores 7-amino-4-methylcoumarin (AMC) and 7-amino-4-(trifluoromethyl)coumarin (AFC) are not only suitable for rapid and reliable determination of substrate specificity, but such measurements also provide data on reaction kinetics.⁶⁸⁻⁶⁹ Use of the bifunctional 7-amino-4-carbamoylmethylcoumarin (ACC), allowed solid-phase synthesis, providing a less time-consuming way for library synthesis.⁷⁰ While the previous methods are based on measurements with increasing fluorescence after caspase cleavage, 2-aminoacridone (AMAC) has been used as a reporting group with decrease of fluorescence upon cleavage.⁷¹ This strategy has the advantage that background correction is avoided. Furthermore, incorporation of luminophore aminoluciferin is suitable for the examination of *in vitro* and *in vivo* assays. Upon release of this reporter group it gets oxidized by luciferase resulting in the emission of light.⁷²⁻⁷³

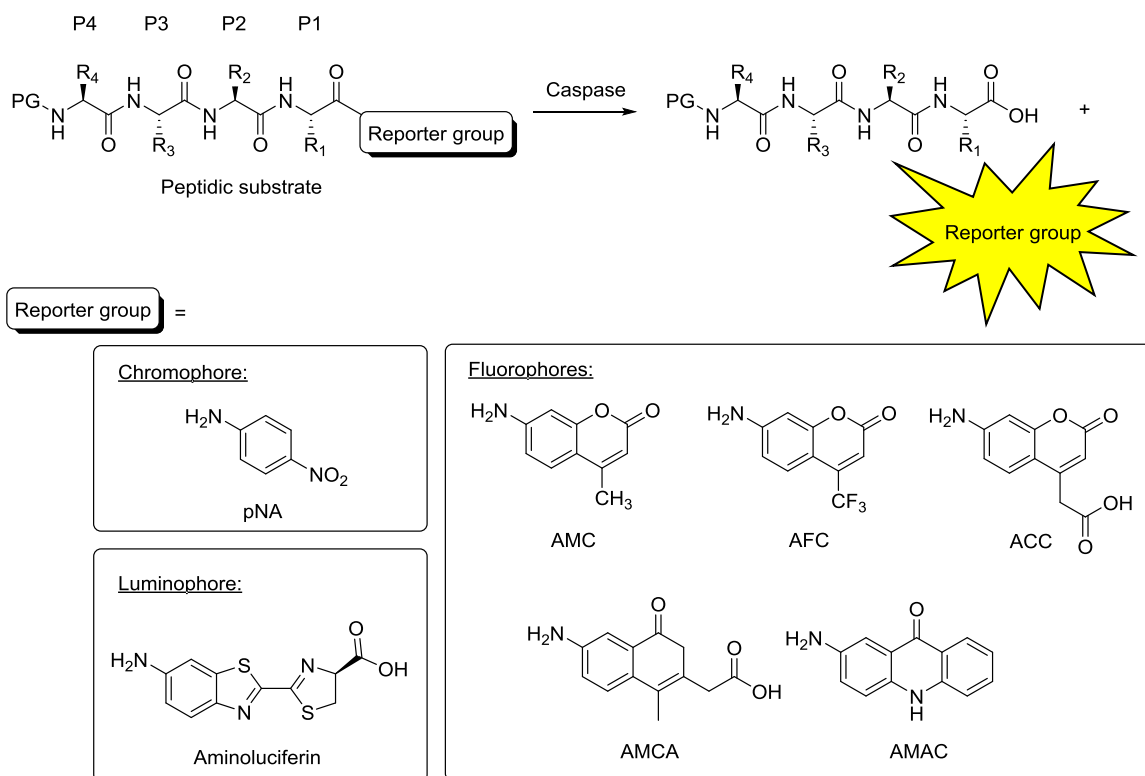


Figure 1.9. Caspase cleavage of tetrapeptidic substrates carrying a reporter group and some examples of reporter groups, categorized in three groups depending on their required detection mode.

Benkova and co-workers created an alternative experimental set-up using HPLC measurements to quantify caspase activity for specific peptide substrates.⁷⁴ Each caspase was added to a mixture of competitive AMAC-based substrates. The analysis of fluorescence over time made it possible to calculate the relative enzyme specificities (k_{cat}/K_m) for each substrate with a given caspase. The entire experimental outcome was reanalyzed and summarized in **Table 1.1**. The results clearly indicate that all caspases exhibit activity toward more than one substrate, except for caspase-2. Also, none of the used peptide sequences was found to be highly selective for a defined caspase. Nevertheless, a clearly expressed group specificity exists among the caspases. Sequence YVAD, a selective substrate for caspase-1 and -4, was also tested during this experiment but appeared to be unaffected by all enzymes because of its poor kinetic constants (data not shown).⁶⁷

Table 1.1: Representation of the specificity of each caspase toward competitive substrates ^{[a][b]}

| Caspase | | Substrate | | | | | | | |
|--------------|-----|---------------|--------------|--------------|--------------|--------------|--------------|--------------|--------------|
| | | Ac-YDAVD-AMAC | Ac-DEVD-AMAC | Ac-LEVD-AMAC | Ac-WEHD-AMAC | Ac-VEID-AMAC | Ac-IETD-AMAC | Ac-LEHD-AMAC | Ac-AEVD-AMAC |
| Inflammatory | -1 | | | | | | | | |
| | -4 | | | | | | | | |
| | -5 | | | | | | | | |
| Executioner | -3 | | | | | | | | |
| | -6 | | | | | | | | |
| | -7 | | | | | | | | |
| Initiator | -2 | | | | | | | | |
| | -8 | | | | | | | | |
| | -9 | | | | | | | | |
| | -10 | | | | | | | | |

[a] Relative enzyme specificities for the substrates are quantified as the intensity of the red color. The highest “specific constant” (k_{cat}/K_m) is given the most intense color. Substrates are 2-aminoacridone (AMAC) derivatives. [b] Data was reanalyzed from ref [74].

Not unexpectedly, all caspase substrates have an aspartate amino acid in common at the P1 position. The deep, highly basic pocket of a caspase is optimally shaped to accommodate the aspartate side chain. It appears that upon alteration of this amino acid into a glutamate, a notable decrease in catalytic efficiency up to four orders of magnitude was observed.⁷⁵ Moreover, after replacement by any other amino acid, no hydrolysis was detected at all, making the preference for aspartic acid in P1 extremely strict. Also, *N*-methylation of the P1 amide caused a negative effect. This proved that the hydrogen bond interactions of this NH are crucial to maintain inhibitor-enzyme binding potency.⁷⁶

It is important to notice that the described methods only identify nonprime substrate specificity. To achieve substrate specificity on the other side of scissile bond, other approaches have been developed. One method comprises design of peptidic substrates with a donor (fluorogenic group) at one side, and an acceptor (quenching group) on the other side (**Figure 1.10**). The intact molecules do not show any fluorescent signal. Upon caspase cleavage of the substrate, the fluorophore gets separated from the quenching group and increased fluorescence emission can be observed.^{75, 77}

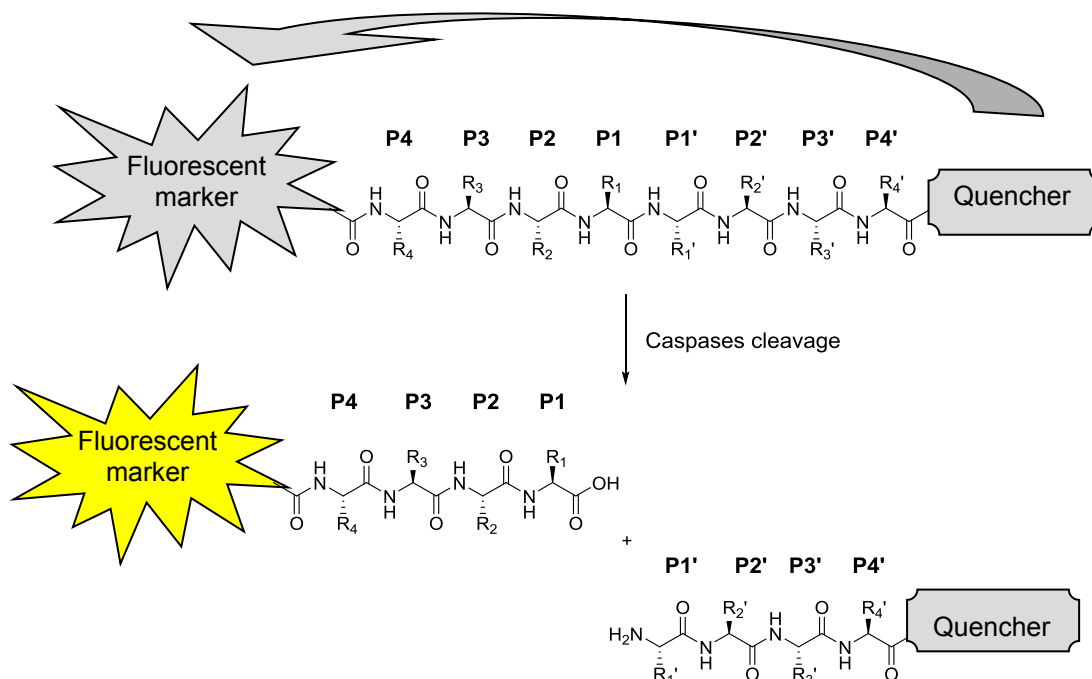


Figure 1.10. Schematic representation of fluorescence-quenched substrates.

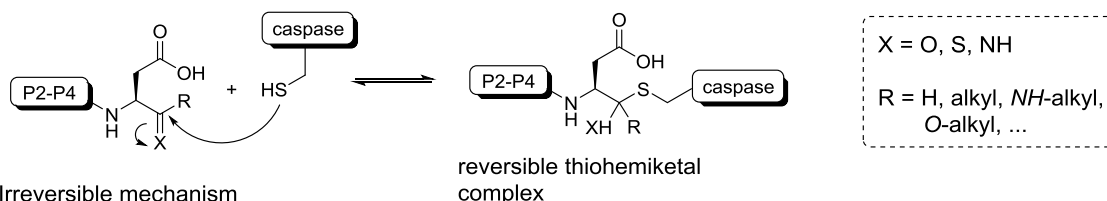
1.8 Caspase inhibitors

In comparison with the struggle of creating caspase substrates, even bigger effort has been put in designing caspase inhibitors that are characterized by high selectivity for one member of the caspase family, high potency, high bioavailability and high pharmacological activity *in vivo*. However, to date, no caspase inhibitors have been approved by FDA or EMA. The main reason is most likely related to the selectivity issue. The overlapping substrate specificity has already pointed out that caspases have a similar preference in their catalytic pocket, making it extremely difficult to find inhibitors that are accommodated in the active site of only one specific caspase. In that perspective, several attempts will be pointed out that have been described to overcome the lack of selectivity for orthosteric inhibitors. Also, the influence of allosteric inhibitors will be discussed. At the end of this section, focus is set on designed inhibitors that entered clinical trials.

1.8.1 Warhead functionality and prime side alterations

A warhead is an electrophilic moiety that covalently binds to the active site cysteine of caspases, thus forming the basis of the enzyme inactivation. The mechanism of the inactivation can either be reversible, through formation of a reversible thiohemiketal, or irreversible, when the enzyme is permanently inactivated by formation of a thioether adduct after an S_N2 mechanism (Figure 1.11).⁷⁸ In addition, bimodal patterns of inhibition have also been described, when a thiohemiketal is slowly transformed into a thioether adduct.⁷⁹

A. Reversible mechanism



B. Irreversible mechanism

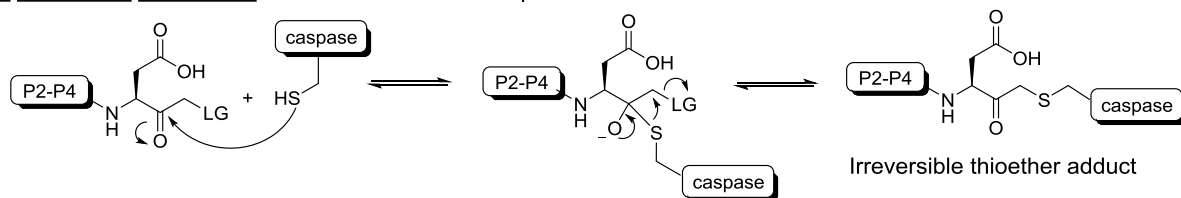
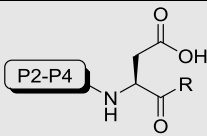


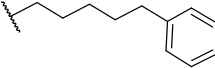
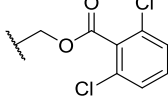
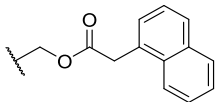
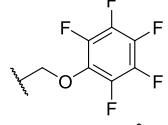
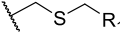
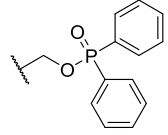
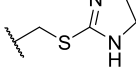
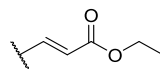
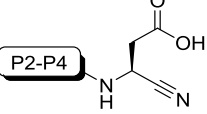
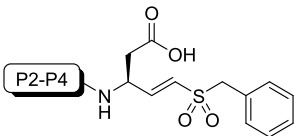
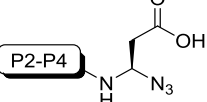


Figure 1.11. Mechanisms for reversible (A) and irreversible (B) binding and inhibition. LG stands for leaving group. Mechanisms are based on ref [65].

Warhead functionalities seem essential for the discovery of orthosteric drugs targeting caspases. Proof was given by replacement of an aldehyde warhead moiety by a hydrogen atom in an existing inhibitor, which resulted in a 280 000-fold decrease of potency.⁷⁹ Besides aldehydes, many other different warheads have been developed throughout the years. A list of some examples is presented in **Table 1.2**.

Table 1.2. Examples of warhead functionalities for caspase inhibitor design

|  | | | |
|---|-----|--|-----|
| Reversible R = | Ref | Irreversible R = | Ref |
|  | 80 |  | 81 |
|  | 82 |  | 83 |
|  | 84 |  | 85 |
|  | 86 |  | 87 |
|  | 88 |  | 90 |
|  | 89 |  | 92 |
|  | 91 | | |

In line with improving selectivity toward single caspases, Ganesan *et al.* explored inhibitor interactions with the S1' subsite of the enzyme by employing epoxide warhead-based inhibitors (**Figure 1.12**).⁹³ To increase the electrophilicity of the epoxide, they positioned two carbonyl functional groups adjacent of the epoxide. Also, analysis of the crystal structures revealed that epoxide protonation occurred with the help of the catalytic histidine, resulting in irreversible thioether formation at the C3 carbon of the epoxide ring. To improve selectivity at the prime side, different substituents can be positioned on the C2 carbon of the ring, as well as on the second carbonyl group (R). It is also worth stressing that this group employs aza-aspartate in the P1 position, resulting in a configuration change from L to intermediate planar D/L geometry. Whereas caspases recognize compounds with this geometry as normal peptidic substrates with similar efficiency, no other proteases appear to show affinity for such inhibitors.

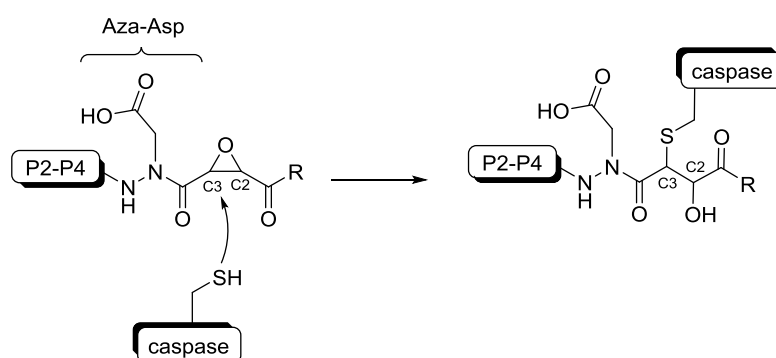


Figure 1.12. Nucleophilic attack of caspase cysteinyl active site on aza-peptide epoxide inhibitors

Similarly, acyloxymethyl ketones, vinyl sulfones and other Michael acceptor scaffolds are examples of warheads that can positively contribute to the selectivity by additional interactions at the prime side of the scissile bond.

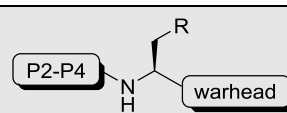
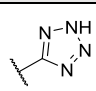
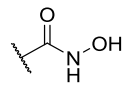
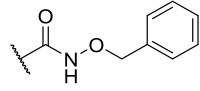
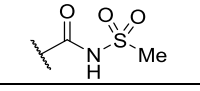
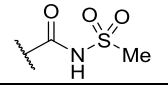
1.8.2 Carboxylate isosteres

Since all caspases use a P1 aspartate residue as a main recognition point in their substrates, most reported caspase inhibitors incorporate a carboxylate that mimics the aspartate residue and acts as an affinity-enhancing structural element. Another potential, hitherto underexplored approach to gain selectivity could consist of isosterically modifying the carboxylate function. Replacement of this carboxylate by another acidic group with distinctive size or electronic properties, can reasonably be expected to have differing impacts on the process of substrate/inhibitor recognition by individual members of the caspase family. This in turn would translate into a more pronounced differentiation by individual caspases between inhibitors or substrates possessing such a modification. Additionally, isosteric replacement could provide biopharmaceutical advantages for caspase-targeting compounds: the carboxylate's "hard" ionic character at physiological pH and its potential for toxic metabolite

formation have convincingly been demonstrated to often critically discount on the cellular permeability and ADME-Tox properties of caspase inhibitors.⁹⁴⁻⁹⁵

So far, the number of reports on isosteric carboxylate replacement in caspase-targeting compounds has been limited, and existing publications have mainly focused on improvement of physicochemical and/or biopharmaceutical properties of inhibitors (**Table 1.3**). Prasad *et al.* replaced the carboxylate function in Z-protected, aspartate-derived α -(arylacyl)oxymethyl ketones with a tetrazole moiety. The resulting enzyme affinity undershot the detection limit.⁷⁶ Similarly, Boxer *et al.* investigated a tetrazole analogue of caspase-1 inhibitor VRT-043198. Despite improved resistance to degradation, its potency for all caspases dropped at least 50-fold compared to the carboxylic analogue.⁸⁹ In a third case, Okamoto *et al.* found that the use of benzyloxyaminocarbonyl and hydroxyaminocarbonyl groups also resulted in a dramatic decrease of caspase-1 inhibitory potency. An *N*-acylsulfonamide, on the other hand, resulted in similar potency as its carboxylic acid analogue. Moreover, they reported a fourfold increase of inhibitory activity in cellular assays and a drastically improved cell permeability.⁹⁶ Notwithstanding these promising results and the number of successful applications of acylsulfonamide isosteres in other domains⁹⁷⁻¹⁰⁰, the full potential of this functional group for caspase research was never investigated in further detail. Likewise, no data on caspase selectivity, physicochemical properties and *in vitro* pharmacokinetic profile of such compounds are available.

Table 1.3. All isosteric replacements in caspase inhibitors, described in literature.

|  | | |
|---|---------------------------------|-----|
| Isostere R = | Relative potency ^[a] | Ref |
|  | n.d. ^[b] | 76 |
|  | 0.9% | 89 |
|  | 1% | 96 |
|  | 2% | 96 |
|  | 34% | 96 |

[a] in comparison with the carboxylic acid analogue;

[b] Not determined because signal of isostere was under the detection limit.

1.8.3 Peptidomimetic inhibitors

The easiest way to create inhibitors is by incorporation of an electrophilic warhead functionality at the position of the scissile bond in identified peptidic substrates. However, as mentioned before, peptidic substrates are rather specific for caspase groups than for sole caspases. Moreover, rapid proteolytic metabolism and low cell permeability are major drawbacks that limit their use in drug discovery. With respect to this matter, Vickers and co-workers investigated the optimization of peptide-based caspase inhibitors through implementation of unnatural amino acids and hydrophobic natural residues in order to diversify beyond the standard amino acid chemistry. The increased structural diversity introduced an optimized fit in the target active subsite, leading to enhanced selective affinity toward single caspases.¹⁰¹⁻¹⁰³ In one particular case they reported an inhibitor that selectively recognized caspase-3 over caspase-7 (**Figure 1.13**). This inhibitor consisted of unnatural amino acids homoleucine (P2), β -homoleucine (P3) and 3-pyridylalanine (P5).

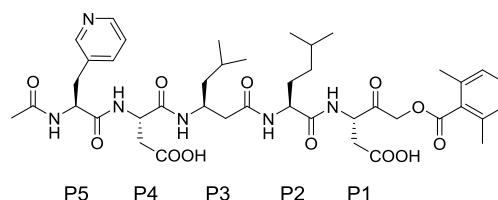


Figure 1.13. Selective inhibitor for caspase-3 by implementation of unnatural amino acids.¹⁰²

Besides improving selectivity, peptidomimetics offer several other advantages, such as improved *in vivo* stability, better oral absorption and improved tissue distribution.¹⁰⁴

1.8.4 Hybrid inhibitors

Analogous to the peptidomimetic inhibitors, this group also consists of aspartic acid derivatives. However, instead of a peptidomimetic chain, hybrid inhibitors comprise nonpeptidic tails. By including aromatic cycles to this kind of inhibitors, easy derivation can be achieved. For example, Shahripour *et al.* used the X-ray crystallographic analysis of a YVAD-based inhibitor with caspase-1 as a basis for the incorporation of a nonpeptidic structure next to the aspartic acid moiety.¹⁰⁵ Following, the reported hit in **Figure 1.14** was further optimized in another structure-based study published by the same research group.¹⁰⁶

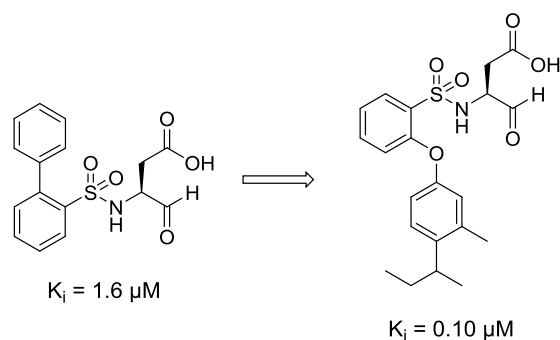


Figure 1.14. Structure-based drug design of caspase-1 hybrid inhibitors, reported by Shahripour *et al.*¹⁰⁵⁻¹⁰⁶

These results show that sufficiently effective interaction of small-molecule inhibitors with caspases is possible, even in the absence of peptidic elements in the inhibitor structure. Consequently, other attempts to design caspase inhibitors with nonpeptidic moieties have been published. Some examples are presented in **Table 1.4**, pointing out that reducing the peptidyl nature of inhibitors is considered a good strategy for the discovery of potent and more druglike inhibitors of caspases.¹⁰⁷ Though this field is rather unexplored, hybrid inhibitors serve as an evolving class of molecules with promising potential for drug development.

Table 1.4. Examples of hybrid inhibitors of caspases.

| Structure | Target caspase | Inhibitory potency | Ref |
|-----------|----------------|-----------------------------|---------|
| | -3 | $K_i = 0.05 \mu\text{M}$ | 108-109 |
| | -3 | $K_i = 0.02 \mu\text{M}$ | 108-109 |
| | -3 | $IC_{50} = 3.6 \mu\text{M}$ | 110 |
| | -3 | $IC_{50} = 6.1 \mu\text{M}$ | 111-112 |
| | -3 | $IC_{50} = 1.7 \mu\text{M}$ | 111-112 |

1.8.5 Nonpeptidic inhibitors

While peptidomimetic and hybrid caspase inhibitors consist of an aspartic acid residue, heterocyclic scaffold-based inhibitors have been developed that lack this structural moiety. It is believed that the nonpeptidic character of these molecules could provide better biopharmaceutical properties. The most promising inhibitors of this kind contain an isatin core. Isatin sulfonamides have been subject of many SAR developments, resulting in the discovery of potent and selective caspase-3 and -7 inhibitors (**Figure 1.15**).¹¹³⁻¹¹⁷ The convenient chemical modification at different anchor points of the heterocyclic core led to an improved metabolic profile and biodistribution, without altering the high affinity. An interesting feature of these heterocyclic compounds is that none of these inhibitors possesses an acidic functionality, to interact via salt-bridging within the S1 pocket. Nevertheless, they are very potent caspase-3 and -7 inhibitors. A significant part of their inhibitory potency is derived from reversible covalent bonding of the catalytic cysteine to the isatin's ketone function.¹¹³

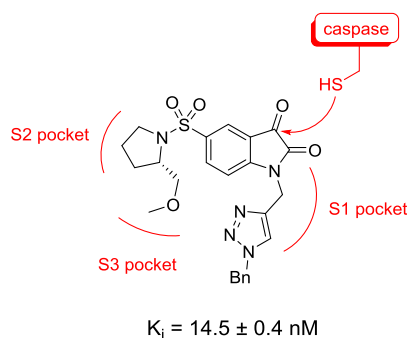


Figure 1.15. Example of an isatin sulfonamide inhibitor of caspase-3.¹¹³ The enzyme binding pockets and active site are highlighted in red.

The family of nonpeptidic caspase inhibitors also contain several other scaffolds in their structure, such as isoquinoline-1,3,4-triones¹¹⁸, quinazolines¹¹⁹, quinones¹²⁰ and more.

1.8.6 Allosteric inhibitors

One of the most promising strategies in terms of design and optimization of selective inhibitors is through allosteric binding sites. This approach is still in its infancy but the few identified allosteric inhibitors prospect good caspase selectivity.⁶⁶

While orthosteric inhibitors are known to bind in the caspase active site, identifying allosteric binding sites and targeting them is much more challenging. In general, an allosteric area comprises a site on the enzyme that is topographically distinct from the active site, that by small molecule binding can lead to enzyme regulation via opening/closing or changes to conformation/electrostatic properties of the active site.¹²¹ In case of caspases, inhibitors that prevent the dimerization of the enzyme (essential for its activation), are also considered allosteric inhibitors.¹²² For example, two allosteric inhibitors of

caspase-3 (**Figure 1.16**) have been identified that bind to the dimerization interface of the enzyme. As a result, they trap the caspase in an inactive, zymogen-like conformation. Interestingly, the mercaptoethyl chain of these inhibitors was found to be crucial for inhibition, as it selectively forms of a disulfide bond with one out of six cysteines (Cys264) that are exposed at the protein surface. This distinct cysteine residue was found to be located in a cleft at the dimerization interface in a distance of 15 Å from the active site.¹²³

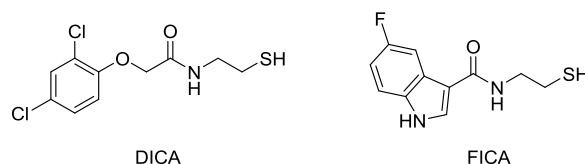


Figure 1.16. Two examples of allosteric inhibitors of caspase-3.

Currently, further investigations are ongoing in order to transform these inhibitor into drugs with good biopharmaceutical properties. In addition, similar research focuses on providing reliable techniques that identify other allosteric sites and inhibitors that bind to these sites in a caspase selective way.¹²⁴⁻

125

1.9 Caspase inhibitors in the clinic

Though many caspase substrates have been identified and easy conversion into inhibitors is possible, such compounds have little therapeutic utility based on poor potency, solubility, stability and selectivity. From the many peptidomimetic, hybrid and nonpeptidic inhibitors that have been developed only a limited number of inhibitors have entered clinical trials. Moreover, none of these drugs have been approved by FDA of EMA.

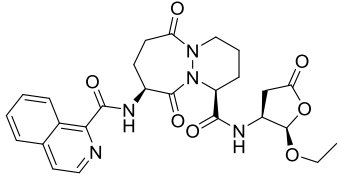
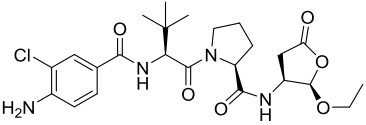
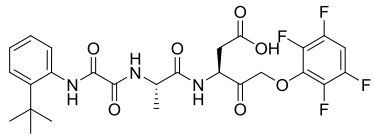
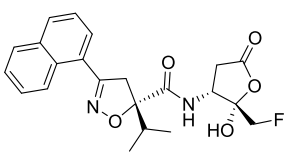
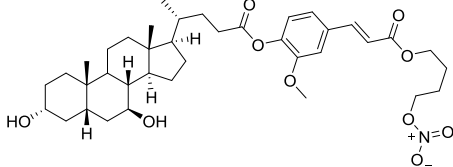
So far, five inhibitors have been clinically tested and are presented in **Table 1.5**. The focus in the following discussion is set on the development of their chemical structure and the different treatments they were tested for in patients. Though these inhibitors were subject of extensive research in rat and mouse models with several other types of diseases, no details concerning this matter will be covered.

1.9.1 Pralnacasan (VX-740)

Pralnacasan, or VX-740, a drug developed by Vertex Pharmaceuticals Inc., was the first caspase inhibitor to enter clinical trials. The design of this heterocyclic caspase-1 inhibitor was based on tetrapeptide sequence YVAD, one of the preferred recognition sequences of caspase-1. The hydrophobic preference in the P4 position was preserved by changing the tryptophane amino acid by an isoquinoline substituent. Because Dolle and co-workers proved that replacing the P2 Ala residue by

other amino acids including secondary piperidine or proline moieties does not affect inhibitory potency of caspase-1, a pyridazinodiazepine group was

Table 1.5. Summary of clinically tested caspase inhibitors.

| Name | Structure | Target caspase | (human) Disease | Clinical trials | Ref |
|----------|---|-----------------------|--|--|---------------------------|
| VX-740 |  | casp-1 | Rheumatoid arthritis Osteoarthritis | Terminated in phase IIb in RA due to liver toxicity in animals | 128-129 |
| VX-765 |  | casp-1 | Psoriasis Epilepsy | No results published Terminated in phase IIb due to lack of efficacy | 130 |
| IDN-6556 |  | pan-caspase inhibitor | Hepatitis C Liver transplantation Other chronic liver diseases | Completed phase II Completed phase II Ongoing clinical trials (phase II) | 131-133 134 135-137 |
| GS-9450 |  | casp-1, -8, -9 | NASH Chronic HCV | Completed phase II Terminated in phase IIb due to abnormalities | 138 139 |
| NCX-1000 |  | casp-3, -8, -9 | Chronic liver disease (cirrhosis, portal hypertension) | Discontinued after phase II due to lack of efficacy | 140 |

implemented to mimick valine and alanine in the P3-P2 positions.¹²⁶ With respect to the P1 position, a masked aspartic aldehyde was implemented, resulting in a drastic increase of cell permeability. This lactone prodrug comprises an ethyl hemiacetal that requires activation through plasma and liver esterases (**Figure 1.17**).¹²⁷ Upon activation, an equilibrium arises between the (cyclic) hemiacetal and the aldehyde. The latter is the formation responsible for caspase inhibition.

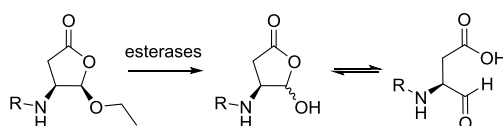


Figure 1.17. Activation of an ethyl hemiacetal prodrug and the equilibrium formed.

The active form of pralnacasan (VRT-18858) selectively inhibits caspase-1 with an IC_{50} of 1.3 nM, compared to 2.3 μ M for caspase-3 and 0.12 μ M for caspase-8.¹⁴¹ Furthermore, pralnacasan inhibits LPS-induced IL-1 β release with an IC_{50} value of 850 nM from human peripheral blood mononuclear cells (PBMCs) *in vitro*.¹⁴² Upon oral administration *in vivo*, pralnacasan has shown to decrease IL-1 β levels up to 80 % after LPS inducement.¹⁴¹ Further preclinical studies proved that pralnacasan had anti-inflammatory activity in several mice models focusing on collagen-induced arthritis and osteoarthritis.¹⁴³ Because of its efficacious effect, the inhibitor was transferred to clinical trials. In clinical phase I studies, pralnacasan displayed good oral bioavailability (50%) and was well tolerated in healthy, rheumatoid arthritis and osteoarthritis patients.¹²⁸ Though phase II trials were initiated, Vertex Pharmaceuticals Inc. announced a discontinuation due to liver abnormalities detected in animal toxicology studies when administered for prolonged periods (9 months) in high doses.¹²⁹

1.9.2 Belnacasan (VX-765)

Belnacasan, also an orally absorbed prodrug developed by Vertex Pharmaceuticals Inc., is a rare example of a peptidomimetic caspase inhibitor, possessing a good pharmacokinetic profile. Analogous to the previously described drug, its structure is derived from the YVAD tetrapeptide. P4 also consists of a hydrophobic moiety, specifically an aniline derivative, and an identical lactone has been placed in the P1 position of belnacasan. Instead of valine in P3, the unnatural amino acid *tert*-leucine was implemented and alanine in P2 was replaced by a proline. The afforded compound, VX-765, is converted into its active form, VRT-043198, in a similar way as pralnacasan.

VRT-043198 has a K_i of 0.8 nM for caspase-1, compared to 21.5 μ M for caspase-3 and 0.1 μ M for caspase-8.¹²⁷ Next, the prodrug form has shown to inhibit IL-1 β release with an IC_{50} value of 470 nM upon LPS treatment in PBMCs.¹⁴² These numbers suggest that belnacasan has a higher inhibitory potency and caspase selectivity than pralnacasan. Belnacasan has reached clinical trials for the treatment of epilepsy and psoriasis. Phase I clinical trials demonstrated a dose-dependent reduction of cytokine levels in plasma and a phase II trial proved safety, tolerability and clinical activity. A phase IIb study to evaluate the efficacy and safety of belnacasan was started in subjects with treatment-resistant partial epilepsy. The drug appeared safe but not sufficiently effective for treatment of epilepsy. Regarding patients with psoriasis, the drug progressed into phase IIa clinical trials. However, the efficacy in the treatment for psoriasis is still to be reported.¹⁴⁴

Although also other diseases are currently investigated using belnacasan, it is worth mentioning that experiments are ongoing with this drug in the treatment of HIV-1 infection. Specifically, belnacasan has been shown to inhibit CD4 T-cell death (and the corresponding pyroptosis) in HIV-infected hosts

and thus raising the possibility of developing a new class of anti-AIDS therapeutics targeting the host rather than the virus.¹⁴⁵⁻¹⁴⁶

In 2007 belnacasan was considered the most promising caspase-1 inhibitor. Nonetheless, it is important to acknowledge that the selectivity for that specific caspase was still rather low. Wannamaker and Boxer have separately published that VRT-043198 had considerable inhibitory potency towards caspase-4. Moreover, Boxer *et al.* reported high potencies for caspase-5, -8 and -9 as well.^{89, 127} In response to this selectivity problem, Boxer and co-workers altered the aldehyde warhead in belnacasan by a carbonitrile, resulting in compound NCGC-00183434 (a.k.a. ML-132 or CID-4462093). They reported enhanced selectivity for this inhibitor towards caspase-1 by at least ten times. Specifically in the inflammatory subset, the IC₅₀ values of caspases-1, -4, and -5 were respectively quantified as 0.023 nM, 13.8 nM and 3.60 nM. Since its publication, this carbonitrile-containing inhibitor has been recognized as the most selective and potent inhibitor of caspase-1.

1.9.3 Emricasan (IDN-6556)

Emricasan, or IDN-6556, is an irreversible *pan*-caspase inhibitor, designed by Conatus Pharmaceuticals Inc. The irreversible character of this inhibitor is derived from a 2,3,5,6-tetrafluorophenoxymethyl ketone warhead. Furthermore, it contains the dipeptide Asp-Ala to fill the S1-S2 caspase subsites. The two other positions (P3-P4) contain an adjacent diamide moiety and a terminal *tert*-butyl substituted phenyl residue.

This broad spectrum inactivator is characterized by IC₅₀ values in the low to subnanomolar range against caspases-1, -3, -6, -7, -8, and -9 as well as submicromolar efficacy in a variety of cellular assays.¹⁴⁷ Investigations of oral administration indicated rapid absorption and uptake by the liver. Besides the advantageous lower systemic exposure, this drug is therefore considered an excellent candidate for treating several liver diseases because these are characterized by high amounts of apoptosis.¹⁴⁷ Conatus Pharmaceuticals Inc. reports that, to date, emricasan has been studied in over 650 subjects in a total of eight phase I and eight phase II clinical trials. This includes healthy volunteers, subjects with elevated liver biomarker levels, liver cirrhosis, hepatitis C and liver transplant subjects. While emricasan has been generally well-tolerated in completed clinical trials, this drug is currently still subject of several clinical trials.¹³¹⁻¹³³

Regarding the inactivation of a broad spectrum of caspases, it is important to acknowledge that the use of an apoptosis inhibitor has the theoretical potential of disrupting the normal homeostatic cell death mechanism. A possible consequence could be the promotion of tumor formation. However, Spada *et al.* have shown that emricasan does not affect caspase activity and apoptosis in healthy subjects and that it is unlikely to affect normal homeostatic processes that may be modulated by

caspase enzymes. Additionally, emricasan was found to have no tumorigenic potential in a recently reported carcinogenicity study.¹⁴⁸⁻¹⁴⁹ Other research groups have described the shift towards other pathways that effect programmed cell death and repair to compensate for apoptosis inhibition.¹⁵⁰

1.9.4 Nivocasan (GS-9450)

Nivocasan, or GS-9450, is an orally active irreversible peptidomimetic inhibitor developed by Gilead Sciences, with selective activity against caspase-1, -8, -9. Its P1 position consists of an aspartic acid residue with a fluoromethylketone warhead. The rest of the molecule consists of a naphthyl group that is connected to the *N*-terminus of the aspartic acid moiety via an *iso*-propyl substituted oxazole ring structure.

Nivocasan showed potential in treating apoptosis-mediated liver injury.¹⁵¹ This drug has also been tested in patients with chronic hepatitis C virus infection, but these clinical trials were terminated due to abnormalities and adverse events in a number of clinical study participants.¹³⁹ Furthermore, nivocasan has been administered in subjects with nonalcoholic steatohepatitis (NASH). Although the results were promising, inhibitors with higher selectivity profiles would be more suitable.¹³⁸

1.9.5 NCX-1000

NCX-1000 is a small-molecule caspase inhibitor that differs from the other inhibitors with respect to its structure. It contains a steroid-based moiety, connected to a nitrate ester warhead via a caffeic acid-derived linker. It covalently binds to the catalytic cysteine of caspases, presumably via *S*-nitrosylation, thereby causing enzyme inhibition.¹⁵² This drug is considered a selective inhibitor of caspase-3, -8 and -9 with IC₅₀ values in the micromolar range.¹⁵³ NCX-1000 entered phase II clinical trials for the treatment of chronic liver disease. Furthermore, the results of a phase II trial for treatment of patients with cirrhosis and portal hypertension revealed that NCX-1000 administration was safe, but did not reduce portal pressure. Presumably because of a lack of selective release of NO in the intrahepatic circulation.¹⁴⁰ The development of this compound has since been discontinued.

References

1. Oda, K., New families of carboxyl peptidases: serine-carboxyl peptidases and glutamic peptidases. *J. Biochem.* **2012**, *151* (1), 13-25.
2. Walker, N. P. C.; Talanian, R. V.; Brady, K. D.; Dang, L. C.; Bump, N. J.; Ferez, C. R.; Franklin, S.; Ghayur, T.; Hackett, M. C.; Hammill, L. D.; Herzog, L.; Hugunin, M.; Houy, W.; Mankovich, J. A.; McGuiness, L.; Orlewicz, E.; Paskind, M.; Pratt, C. A.; Reis, P.; Summani, A.; Terranova, M.; Welch, J. P.; Xiong, L.; Moller, A.; Tracey, D. E.; Kamen, R.; Wong, W. W., Crystal-Structure of the Cysteine Protease Interleukin-1-Beta-Converting Enzyme - a (P20/P10)(2) Homodimer. *Cell* **1994**, *78* (2), 343-352.
3. Wilson, K. P.; Black, J. A. F.; Thomson, J. A.; Kim, E. E.; Griffith, J. P.; Navia, M. A.; Murcko, M. A.; Chambers, S. P.; Aldape, R. A.; Raybuck, S. A.; Livingston, D. J., Structure and Mechanism of Interleukin-1-Beta Converting-Enzyme. *Nature* **1994**, *370* (6487), 270-275.
4. McLuskey, K.; Mottram, J. C., Comparative structural analysis of the caspase family with other clan CD cysteine peptidases. *Biochem. J.* **2015**, *466*, 219-232.
5. Lamkanfi, M.; Dixit, V. M., Mechanisms and Functions of Inflammasomes. *Cell* **2014**, *157* (5), 1013-1022.
6. Man, S. M.; Kanneganti, T. D., Converging roles of caspases in inflammasome activation, cell death and innate immunity. *Nat. Rev. Immunol.* **2016**, *16* (1), 7-21.
7. Fuchs, Y.; Steller, H., Live to die another way: modes of programmed cell death and the signals emanating from dying cells. *Nat. Rev. Mol. Cell Biol.* **2015**, *16* (6), 329-344.
8. Hoste, E.; Kemperman, P.; Devos, M.; Denecker, G.; Kezic, S.; Yau, N.; Gilbert, B.; Lippens, S.; De Groote, P.; Roelandt, R.; Van Damme, P.; Gevaert, K.; Presland, R. B.; Takahara, H.; Puppels, G.; Caspers, P.; Vandenabeele, P.; Declercq, W., Caspase-14 Is Required for Filaggrin Degradation to Natural Moisturizing Factors in the Skin. *J. Invest. Dermatol.* **2011**, *131* (11), 2233-2241.
9. Stowe, I.; Lee, B.; Kayagaki, N., Caspase-11: arming the guards against bacterial infection. *Immunol. Rev.* **2015**, *265* (1), 75-84.
10. Shalini, S.; Dorstyn, L.; Dawar, S.; Kumar, S., Old, new and emerging functions of caspases. *Cell Death Differ.* **2015**, *22* (4), 526-539.
11. Boatright, K. M.; Renatus, M.; Scott, F. L.; Sperandio, S.; Shin, H.; Pedersen, I. M.; Ricci, J. E.; Edris, W. A.; Sutherlin, D. P.; Green, D. R.; Salvesen, G. S., A unified model for apical caspase activation. *Mol. Cell* **2003**, *11* (2), 529-541.
12. Creagh, E. M., Caspase crosstalk: integration of apoptotic and innate immune signalling pathways. *Trends Immunol.* **2014**, *35* (12), 631-640.
13. Lavrik, I. N.; Golks, A.; Krammer, P. H., Caspases: pharmacological manipulation of cell death. *J. Clin. Invest.* **2005**, *115* (10), 2665-2672.
14. de la Cadena, S. G.; Massieu, L., Caspases and their role in inflammation and ischemic neuronal death. Focus on caspase-12. *Apoptosis* **2016**, *21* (7), 763-777.
15. Wachmann, K.; Pop, C.; van Raam, B. J.; Drag, M.; Mace, P. D.; Snipas, S. J.; Zmasek, C.; Schwarzenbacher, R.; Salvesen, G. S.; Riedl, S. J., Activation and Specificity of Human Caspase-10. *Biochemistry* **2010**, *49* (38), 8307-8315.
16. Guo, W. J.; Dong, A. S.; Pan, X. H.; Lin, X. J.; Lin, Y.; He, M. Q.; Zhu, B. L.; Jin, L. M.; Yao, R. X., Role of caspase-10 in the death of acute leukemia cells. *Oncol. Lett.* **2016**, *12* (2), 1623-1629.

17. Lamy, L.; Ngo, V. N.; Emre, N. C. T.; Shaffer, A. L.; Yang, Y. D.; Tian, E. M.; Nair, V.; Kruhlak, M. J.; Zingone, A.; Landgren, O.; Staudt, L. M., Control of Autophagic Cell Death by Caspase-10 in Multiple Myeloma. *Cancer Cell* **2013**, *23* (4), 435-449.
18. Brenner, D.; Mak, T. W., Mitochondrial cell death effectors. *Curr. Opin. Cell Biol.* **2009**, *21* (6), 871-877.
19. McIlwain, D. R.; Berger, T.; Mak, T. W., Caspase Functions in Cell Death and Disease. *Cold Spring Harbor Perspect. Biol.* **2013**, *5* (4).
20. Sollberger, G.; Strittmatter, G. E.; Garstkiewicz, M.; Sand, J.; Beer, H. D., Caspase-1: The inflammasome and beyond. *Innate Immun.* **2014**, *20* (2), 115-125.
21. Aksenova, V. I.; Kopeina, G. S.; Zamaraev, A. V.; Zhivotovsky, B. D.; Lavrik, I. N., Mechanism of caspase-2 activation upon DNA damage. *Dokl. Biochem. Biophys.* **2016**, *467* (1), 132-135.
22. Shalini, S.; Dorstyn, L.; Wilson, C.; Puccini, J.; Ho, L.; Kumar, S., Impaired antioxidant defence and accumulation of oxidative stress in caspase-2-deficient mice. *Cell Death Differ.* **2012**, *19* (8), 1370-1380.
23. Li, J.; Yuan, J., Caspases in apoptosis and beyond. *Oncogene* **2008**, *27* (48), 6194-6206.
24. Wilson, C. H.; Dorstyn, L.; Kumar, S., Fat, sex and caspase-2. *Cell Death Dis.* **2016**, *7*.
25. Bergsbaken, T.; Fink, S. L.; Cookson, B. T., Pyroptosis: host cell death and inflammation. *Nat. Rev. Microbiol.* **2009**, *7* (2), 99-109.
26. LeBlanc, P. M.; Saleh, M., Caspases in Inflammation and Immunity. In *Encyclopedia of Life Sciences*, 2009.
27. Aachoui, Y.; Sagulenko, V.; Miao, E. A.; Stacey, K. J., Inflammasome-mediated pyroptotic and apoptotic cell death, and defense against infection. *Curr. Opin. Microbiol.* **2013**, *16* (3), 319-326.
28. Wang, S. Y.; Miura, M.; Jung, Y. K.; Zhu, H.; Gagliardini, V.; Shi, L. F.; Greenberg, A. H.; Yuan, J. Y., Identification and characterization of Ich-3, a member of the interleukin-1 beta converting enzyme (ICE)/Ced-3 family and an upstream regulator of ICE. *J. Biol. Chem.* **1996**, *271* (34), 20580-20587.
29. Shi, J. J.; Zhao, Y.; Wang, Y. P.; Gao, W. Q.; Ding, J. J.; Li, P.; Hu, L. Y.; Shao, F., Inflammatory caspases are innate immune receptors for intracellular LPS. *Nature* **2014**, *514* (7521), 187-+.
30. Kajiwara, Y.; Schiff, T.; Voloudakis, G.; Sosa, M. A. G.; Elder, G.; Bozdagi, O.; Buxbaum, J. D., A Critical Role for Human Caspase-4 in Endotoxin Sensitivity. *J. Immunol.* **2014**, *193* (1), 335-343.
31. Knodler, L. A.; Crowley, S. M.; Sham, H. P.; Yang, H. J.; Wrande, M.; Ma, C. X.; Ernst, R. K.; Steele-Mortimer, O.; Celli, J.; Vallance, B. A., Noncanonical Inflammasome Activation of Caspase-4/Caspase-11 Mediates Epithelial Defenses against Enteric Bacterial Pathogens. *Cell Host Microbe* **2014**, *16* (2), 249-256.
32. Sollberger, G.; Strittmatter, G. E.; Kistowska, M.; French, L. E.; Beer, H. D., Caspase-4 is required for activation of inflammasomes. *J. Immunol.* **2012**, *188* (4), 1992-2000.
33. Kayagaki, N.; Wong, M. T.; Stowe, I. B.; Ramani, S. R.; Gonzalez, L. C.; Akashi-Takamura, S.; Miyake, K.; Zhang, J.; Lee, W. P.; Muszynski, A.; Forsberg, L. S.; Carlson, R. W.; Dixit, V. M., Noncanonical Inflammasome Activation by Intracellular LPS Independent of TLR4. *Science* **2013**, *341* (6151), 1246-1249.
34. Uchiyama, R.; Tsutsui, H., Caspases as the Key Effectors of Inflammatory Responses Against Bacterial Infection. *Arch. Immunol. Ther. Exp.* **2015**, *63* (1), 1-13.

35. Vigano, E.; Diamond, C. E.; Spreafico, R.; Balachander, A.; Sobota, R. M.; Mortellaro, A., Human caspase-4 and caspase-5 regulate the one-step non-canonical inflammasome activation in monocytes. *Nat. Commun.* **2015**, *6*.
36. Schmid-Burgk, J. L.; Gaidt, M. M.; Schmidt, T.; Ebert, T. S.; Bartok, E.; Hornung, V., Caspase-4 mediates non-canonical activation of the NLRP3 inflammasome in human myeloid cells. *Eur. J. Immunol.* **2015**, *45* (10), 2911-2917.
37. Baker, P. J.; Boucher, D.; Bierschenk, D.; Tebartz, C.; Whitney, P. G.; D'Silva, D. B.; Tanzer, M. C.; Monteleone, M.; Robertson, A. A. B.; Cooper, M. A.; Alvarez-Diaz, S.; Herold, M. J.; Bedoui, S.; Schroder, K.; Masters, S. L., NLRP3 inflammasome activation downstream of cytoplasmic LPS recognition by both caspase-4 and caspase-5. *Eur. J. Immunol.* **2015**, *45* (10), 2918-2926.
38. Casson, C. N.; Yu, J.; Reyes, V. M.; Taschuk, F. O.; Yadav, A.; Copenhaver, A. M.; Nguyen, H. T.; Collman, R. G.; Shin, S., Human caspase-4 mediates noncanonical inflammasome activation against gram-negative bacterial pathogens. *Proc. Natl. Acad. Sci. U. S. A.* **2015**, *112* (21), 6688-6693.
39. Saleh, M.; Mathison, J. C.; Wolinski, M. K.; Bensinger, S. J.; Fitzgerald, P.; Droin, N.; Ulevitch, R. J.; Green, D. R.; Nicholson, D. W., Corrigendum: Enhanced bacterial clearance and sepsis resistance in caspase-12-deficient mice *Nature* **2014**, *508* (7495), 274-274.
40. Saleh, M.; Mathison, J. C.; Wolinski, M. K.; Bensinger, S. J.; Fitzgerald, P.; Droin, N.; Ulevitch, R. J.; Green, D. R.; Nicholson, D. W., Enhanced bacterial clearance and sepsis resistance in caspase-12-deficient mice. *Nature* **2006**, *440* (7087), 1064-1068.
41. Walle, L. V.; Fernandez, D. J.; Demon, D.; Van Laethem, N.; Van Hauwermeiren, F.; Van Gorp, H.; Van Opdenbosch, N.; Kayagaki, N.; Lamkanfi, M., Does caspase-12 suppress inflammasome activation? *Nature* **2016**, *534* (7605), E1-+.
42. LeBlanc, P. M.; Yeretssian, G.; Rutherford, N.; Doiron, K.; Nadiri, A.; Zhu, L.; Green, D. R.; Gruenheid, S.; Saleh, M., Caspase-12 modulates NOD signaling and regulates antimicrobial peptide production and mucosal immunity. *Cell Host Microbe* **2008**, *3* (3), 146-157.
43. Saleh, M.; Vaillancourt, J. P.; Graham, R. K.; Huyck, M.; Srinivasula, S. M.; Alnemri, E. S.; Steinberg, M. H.; Nolan, V.; Baldwin, C. T.; Hotchkiss, R. S.; Buchman, T. G.; Zehnauer, B. A.; Hayden, M. R.; Farrer, L. A.; Roy, S.; Nicholson, D. W., Differential modulation of endotoxin responsiveness by human caspase-12 polymorphisms. *Nature* **2004**, *429* (6987), 75-79.
44. Joehlin-Price, A. S.; Elkins, C. T.; Stephens, J. A.; Cohn, D. E.; Knobloch, T. J.; Weghorst, C. M.; Suarez, A. A., Comprehensive evaluation of caspase-14 in vulvar neoplasia: An opportunity for treatment with black raspberry extract. *Gynecol. Oncol.* **2014**, *135* (3), 503-509.
45. Su, H.; Bidere, N.; Zheng, L. X.; Cubre, A.; Sakai, K.; Dale, J.; Salmena, L.; Hakem, R.; Straus, S.; Lenardo, M., Requirement for caspase-8 in NF-kappa B activation by antigen receptor. *Science* **2005**, *307* (5714), 1465-1468.
46. Beisner, D. R.; Ch'en, I. L.; Kolla, R. V.; Hoffmann, A.; Hedrick, S. M., Cutting edge: Innate Immunity conferred by B cells is regulated by caspase-8. *J. Immunol.* **2005**, *175* (6), 3469-3473.
47. Li, J. Y.; Briehner, W. M.; Scimone, M. L.; Kang, S. J.; Zhu, H.; Yin, H.; von Andrian, U. H.; Mitchison, T.; Yuan, J. Y., Caspase-11 regulates cell migration by promoting Aip1-Cofilin-mediated actin depolymerization. *Nat. Cell Biol.* **2007**, *9* (3), 276-+.
48. Helfer, B.; Boswell, B. C.; Finlay, D.; Cipres, A.; Vuori, K.; Kang, T. B.; Wallach, D.; Dorfleutner, A.; Lahti, J. M.; Flynn, D. C.; Frisch, S. M., Caspase-8 promotes cell motility and calpain activity under nonapoptotic conditions. *Cancer Res.* **2006**, *66* (8), 4273-4278.

49. Fernando, P.; Megeney, L. A., Is caspase-dependent apoptosis only cell differentiation taken to the extreme? *FASEB J.* **2007**, *21* (1), 8-17.
50. Bolkent, S.; Oztay, F.; Gezginci Oktayoglu, S.; Sancar Bas, S.; Karatug, A., A matter of regeneration and repair: caspases as the key molecules. *Turk. J. Biol.* **2016**, *40* (2), 333-352.
51. Miura, M., Apoptotic and Nonapoptotic Caspase Functions in Animal Development. *Cold Spring Harbor Perspect. Biol.* **2012**, *4* (10).
52. Hornung, V.; Bauernfeind, F.; Halle, A.; Samstad, E. O.; Kono, H.; Rock, K. L.; Fitzgerald, K. A.; Latz, E., Silica crystals and aluminum salts activate the NALP3 inflammasome through phagosomal destabilization. *Nat. Immunol.* **2008**, *9* (8), 847-856.
53. Maedler, K.; Dharmadhikari, G.; Schumann, D. M.; Storling, J., Interleukin-1 beta targeted therapy for type 2 diabetes. *Expert Opin. Biol. Ther.* **2009**, *9* (9), 1177-1188.
54. Roldan, R.; Ruiz, A. A.; Miranda, M. D.; Collantes, E., Anakinra: New therapeutic approach in children with Familial Mediterranean Fever resistant to colchicine. *Joint Bone Spine* **2008**, *75* (4), 504-505.
55. Pascual, V.; Allantaz, F.; Arce, E.; Punaro, M.; Banchereau, J., Role of interleukin-1 (IL-1) in the pathogenesis of systemic onset juvenile idiopathic arthritis and clinical response to IL-1 blockade. *J. Exp. Med.* **2005**, *201* (9), 1479-1486.
56. Alten, R.; Gram, H.; Joosten, L. A.; van den Berg, W. B.; Sieper, J.; Wassenberg, S.; Burmester, G.; van Riel, P.; Diaz-Lorente, M.; Bruin, G. J. M.; Woodworth, T. G.; Rordorf, C.; Batard, Y.; Wright, A. M.; Jung, T., The human anti-IL-1 beta monoclonal antibody ACZ885 is effective in joint inflammation models in mice and in a proof-of-concept study in patients with rheumatoid arthritis. *Arthritis Res. Ther.* **2008**, *10* (3).
57. Finckh, A.; Gabay, C., At the horizon of innovative therapy in rheumatology: new biologic agents. *Curr. Opin. Rheumatol.* **2008**, *20* (3), 269-275.
58. Sanchez, I.; Xu, C. J.; Juo, P.; Kakizaka, A.; Blenis, J.; Yuan, J. Y., Caspase-8 is required for cell death induced by expanded polyglutamine repeats. *Neuron* **1999**, *22* (3), 623-633.
59. Squitieri, F.; Maglione, V.; Orobello, S.; Fornai, F., Genotype-, aging-dependent abnormal caspase activity in Huntington disease blood cells. *J. Neural Transm.* **2011**, *118* (11), 1599-1607.
60. Gervais, F. G.; Xu, D. G.; Robertson, G. S.; Vaillancourt, J. P.; Zhu, Y. X.; Huang, J. Q.; LeBlanc, A.; Smith, D.; Rigby, M.; Shearman, M. S.; Clarke, F. E.; Zheng, H.; Van Der Ploeg, L. H. T.; Ruffolo, S. C.; Thornberry, N. A.; Xanthoudakis, S.; Zamboni, R. J.; Roy, S.; Nicholson, D. W., Involvement of caspases in proteolytic cleavage of Alzheimer's amyloid-beta precursor protein and amyloidogenic A beta peptide formation. *Cell* **1999**, *97* (3), 395-406.
61. Rohn, T. T.; Head, E., Caspases as Therapeutic Targets in Alzheimer's Disease: Is It Time to "Cut" to the Chase? *Int. J. Clin. Exp. Pathol.* **2009**, *2* (2), 108-118.
62. Narula, J.; Pandey, P.; Arbustini, E.; Haider, N.; Narula, N.; Kolodgie, F. D.; Dal Bello, B.; Semigran, M. J.; Bielsa-Masdeu, A.; Dec, G. W.; Israels, S.; Ballester, M.; Virmani, R.; Saxena, S.; Kharbanda, S., Apoptosis in heart failure: Release of cytochrome c from mitochondria and activation of caspase-3 in human cardiomyopathy. *Proc. Natl. Acad. Sci. U. S. A.* **1999**, *96* (14), 8144-8149.
63. Rotonda, J.; Nicholson, D. W.; Fazil, K. M.; Gallant, M.; Gareau, Y.; Labelle, M.; Peterson, E. P.; Rasper, D. M.; Ruel, R.; Vaillancourt, J. P.; Thornberry, N. A.; Becker, J. W., The three-dimensional structure of apopain/CPP32, a key mediator of apoptosis. *Nat. Struct. Biol.* **1996**, *3* (7), 619-625.

64. Watt, W.; Koeplinger, K. A.; Mildner, A. M.; Heinrikson, R. L.; Tomasselli, A. G.; Watenpaugh, K. D., The atomic-resolution structure of human caspase-8, a key activator of apoptosis. *Struct. Fold. Des.* **1999**, *7* (9), 1135-1143.
65. O'Brien, T.; Linton, S. D., *Design of Caspase Inhibitors as Potential Clinical Agents*. CRC Press: Cardiff, UK, 2009.
66. Poreba, M.; Strozyk, A.; Salvesen, G. S.; Drag, M., Caspase Substrates and Inhibitors. *Cold Spring Harbor Perspect. Biol.* **2013**, *5* (8), a008680.
67. Talanian, R. V.; Quinlan, C.; Trautz, S.; Hackett, M. C.; Mankovich, J. A.; Banach, D.; Ghayur, T.; Brady, K. D.; Wong, W. W., Substrate specificities of caspase family proteases. *J. Biol. Chem.* **1997**, *272* (15), 9677-9682.
68. Rano, T. A.; Timkey, T.; Peterson, E. P.; Rotonda, J.; Nicholson, D. W.; Becker, J. W.; Chapman, K. T.; Thornberry, N. A., A combinatorial approach for determining protease specificities: Application to interleukin-1 beta converting enzyme (ICE). *Chem. Biol.* **1997**, *4* (2), 149-155.
69. Thornberry, N. A.; Rano, T. A.; Peterson, E. P.; Rasper, D. M.; Timkey, T.; Garcia-Calvo, M.; Houtzager, V. M.; Nordstrom, P. A.; Roy, S.; Vaillancourt, J. P.; Chapman, K. T.; Nicholson, D. W., A Combinatorial Approach Defines Specificities of Members of the Caspase Family and Granzyme B: FUNCTIONAL RELATIONSHIPS ESTABLISHED FOR KEY MEDIATORS OF APOPTOSIS. *J. Biol. Chem.* **1997**, *272* (29), 17907-17911.
70. Maly, D. J.; Leonetti, F.; Backes, B. J.; Dauber, D. S.; Harris, J. L.; Craik, C. S.; Ellman, J. A., Expedient solid-phase synthesis of fluorogenic protease substrates using the 7-amino-4-carbamoylmethylcoumarin (ACC) fluorophore. *J. Org. Chem.* **2002**, *67* (3), 910-915.
71. Lozanov, V.; Ivanov, I. P.; Benkova, B.; Mitev, V., Peptide substrate for caspase-3 with 2-aminoacridone as reporting group. *Amino Acids* **2009**, *36* (3), 581-586.
72. Hickson, J.; Ackler, S.; Klaubert, D.; Bouska, J.; Ellis, P.; Foster, K.; Oleksijew, A.; Rodriguez, L.; Schlessinger, S.; Wang, B.; Frost, D., Noninvasive molecular imaging of apoptosis in vivo using a modified firefly luciferase substrate, Z-DEVD-aminoluciferin. *Cell Death Diff.* **2010**, *17* (6), 1003-1010.
73. O'Brien, M. A.; Daily, W. J.; Hesselberth, P. E.; Moravec, R. A.; Scurria, M. A.; Klaubert, D. H.; Bulleit, R. F.; Wood, K. V., Homogeneous, bioluminescent protease assays: Caspase-3 as a model. *J. Biomol. Screening* **2005**, *10* (2), 137-148.
74. Benkova, B.; Lozanov, V.; Ivanov, I. P.; Mitev, V., Evaluation of recombinant caspase specificity by competitive substrates. *Anal. Biochem.* **2009**, *394* (1), 68-74.
75. Stennicke, H. R.; Renatus, M.; Meldal, M.; Salvesen, G. S., Internally quenched fluorescent peptide substrates disclose the subsite preferences of human caspases 1, 3, 6, 7 and 8. *Biochem. J.* **2000**, *350*, 563-568.
76. Prasad, C. V. C.; Prouty, C. P.; Hoyer, D.; Ross, T. M.; Salvino, J. M.; Awad, M.; Graybill, T. L.; Schmidt, S. J.; Kelly Osifo, I.; Dolle, R. E.; Helaszek, C. T.; Miller, R. E.; Ator, M. A., Structural and stereochemical requirements of time-dependent inactivators of the interleukin-1 β converting enzyme. *Bioorg. Med. Chem. Lett.* **1995**, *5* (4), 315-318.
77. Petrassi, H. M.; Williams, J. A.; Li, J.; Tumanut, C.; Ek, J.; Nakai, T.; Masick, B.; Backes, B. J.; Harris, J. L., A strategy to profile prime and non-prime proteolytic substrate specificity. *Bioorg. Med. Chem. Lett.* **2005**, *15* (12), 3162-6.
78. Powers, J. C.; Asgian, J. L.; Ekici, O. D.; James, K. E., Irreversible inhibitors of serine, cysteine, and threonine proteases. *Chem. Rev.* **2002**, *102* (12), 4639-4750.

79. Brady, K. D., Bimodal inhibition of caspase-1 by aryloxymethyl and acyloxymethyl ketones. *Biochemistry* **1998**, 37 (23), 8508-8515.
80. Graybill, T. L.; Dolle, R. E.; Helaszek, C. T.; Miller, R. E.; Ator, M. A., Preparation and Evaluation of Peptidic Aspartyl Hemiacetals as Reversible Inhibitors of Interleukin-1-Beta Converting-Enzyme (Ice). *Int. J. Pept. Protein Res.* **1994**, 44 (2), 173-182.
81. Revesz, L.; Briswalter, C.; Heng, R.; Leutwiler, A.; Mueller, R.; Wuethrich, H. J., Synthesis of P1 Aspartate-Based Peptide Acyloxymethyl and Fluoromethyl Ketones as Inhibitors of Interleukin-1-Beta-Converting Enzyme. *Tetrahedron Lett.* **1994**, 35 (52), 9693-9696.
82. Harter, W. G.; Albrect, H.; Brady, K.; Caprathe, B.; Dunbar, J.; Gilmore, J.; Hays, S.; Kostlan, C. R.; Lunney, B.; Walker, N., The design and synthesis of sulfonamides as caspase-1 inhibitors. *Bioorg. Med. Chem. Lett.* **2004**, 14 (3), 809-812.
83. Dolle, R. E.; Hoyer, D.; Prasad, C. V. C.; Schmidt, S. J.; Helaszek, C. T.; Miller, R. E.; Ator, M. A., P-1 Aspartate-Based Peptide Alpha-((2,6-Dichlorobenzoyl)Oxy)Methyl Ketones as Potent Time-Dependent Inhibitors of Interleukin-1-Beta-Converting Enzyme. *J. Med. Chem.* **1994**, 37 (5), 563-564.
84. Galatsis, P.; Caprathe, B.; Downing, D.; Gilmore, J.; Harter, W.; Hays, S.; Kostlan, C.; Linn, K.; Lunney, E.; Para, K.; Thomas, A.; Warmus, J.; Allen, H.; Brady, K.; Talanian, R.; Walker, N., Inhibition of interleukin-1 beta converting enzyme (ICE or caspase 1) by aspartyl acyloxyalkyl ketones and aspartyl amidooxyalkyl ketones. *Bioorg. Med. Chem. Lett.* **2010**, 20 (17), 5089-5094.
85. Thornberry, N. A.; Peterson, E. P.; Zhao, J. J.; Howard, A. D.; Griffin, P. R.; Chapman, K. T., Inactivation of Interleukin-1-Beta Converting-Enzyme by Peptide (Acyloxy)Methyl Ketones. *Biochemistry* **1994**, 33 (13), 3934-3940.
86. Mjalli, A. M. M.; Chapman, K. T.; Maccoss, M.; Thornberry, N. A.; Peterson, E. P., Activated Ketones as Potent Reversible Inhibitors of Interleukin-1-Beta Converting-Enzyme. *Bioorg. Med. Chem. Lett.* **1994**, 4 (16), 1965-1968.
87. Dolle, R. E.; Singh, J.; Whipple, D.; Osifo, I. K.; Speier, G.; Graybill, T. L.; Gregory, J. S.; Harris, A. L.; Helaszek, C. T.; Miller, R. E.; Ator, M. A., Aspartyl Alpha-((Diphenylphosphinyl)Oxy)Methyl Ketones as Novel Inhibitors of Interleukin-1-Beta Converting-Enzyme - Utility of the Diphenylphosphinic Acid Leaving Group for the Inhibition of Cysteine Proteases. *J. Med. Chem.* **1995**, 38 (2), 220-222.
88. Ullman, B. R.; Aja, T.; Chen, N.; Diaz, J. L.; Gu, X.; Herrmann, J.; Kalish, V. J.; Karanewsky, D. S.; Kodandapani, L.; Krebs, J. J.; Linton, S. D.; Meduna, S. P.; Nalley, K.; Robinson, E. D.; Roggo, S. P.; Sayers, R. O.; Schmitz, A.; Ternansky, R. J.; Tomaselli, K. J.; Wu, J. C., Structure-activity relationships within a series of caspase inhibitors. Part 2: Heterocyclic warheads. *Bioorg. Med. Chem. Lett.* **2005**, 15 (15), 3632-3636.
89. Boxer, M. B.; Quinn, A. M.; Shen, M.; Jadhav, A.; Leister, W.; Simeonov, A.; Auld, D. S.; Thomas, C. J., A highly potent and selective caspase 1 inhibitor that utilizes a key 3-cyanopropanoic acid moiety. *ChemMedChem* **2010**, 5 (5), 730-8.
90. Sexton, K. B.; Kato, D.; Berger, A. B.; Fonovic, M.; Verhelst, S. H. L.; Bogyo, M., Specificity of aza-peptide electrophile activity-based probes of caspases. *Cell Death Diff.* **2007**, 14 (4), 727-732.
91. Le, G. T.; Abbenante, G.; Madala, P. K.; Hoang, H. N.; Fairlie, D. P., Organic azide inhibitors of cysteine proteases. *J. Am. Chem. Soc.* **2006**, 128 (38), 12396-12397.

92. Newton, A. S.; Gloria, P. M.; Goncalves, L. M.; dos Santos, D. J.; Moreira, R.; Guedes, R. C.; Santos, M. M., Synthesis and evaluation of vinyl sulfones as caspase-3 inhibitors. A structure-activity study. *Eur. J. Med. Chem.* **2010**, *45* (9), 3858-63.
93. Ganesan, R.; Jelakovic, S.; Campbell, A. J.; Li, Z. Z.; Asgian, J. L.; Powers, J. C.; Grutter, M. G., Exploring the S4 and S1 prime subsite specificities in caspase-3 with aza-peptide epoxide inhibitors. *Biochemistry* **2006**, *45* (30), 9059-9067.
94. Meanwell, N. A., Synopsis of some recent tactical application of bioisosteres in drug design. *J. Med. Chem.* **2011**, *54* (8), 2529-91.
95. Ballatore, C.; Hury, D. M.; Smith, A. B., Carboxylic Acid (Bio)Isosteres in Drug Design. *ChemMedChem* **2013**, *8* (3), 385-395.
96. Okamoto, Y.; Anan, H.; Nakai, E.; Morihira, K.; Yonetoku, Y.; Kurihara, H.; Sakashita, H.; Terai, Y.; Takeuchi, M.; Shibamura, T.; Isomura, Y., Peptide based interleukin-1 beta converting enzyme (ICE) inhibitors: Synthesis, structure activity relationships and crystallographic study of the ICE-inhibitor complex. *Chem. Pharm. Bull.* **1999**, *47* (1), 11-21.
97. Yee, Y. K.; Bernstein, P. R.; Adams, E. J.; Brown, F. J.; Cronk, L. A.; Hebbel, K. C.; Vacek, E. P.; Krell, R. D.; Snyder, D. W., A Novel Series of Selective Leukotriene Antagonists - Exploration and Optimization of the Acidic Region in 1,6-Disubstituted Indoles and Indazoles. *J. Med. Chem.* **1990**, *33* (9), 2437-2451.
98. Uehling, D. E.; Donaldson, K. H.; Deaton, D. N.; Hyman, C. E.; Sugg, E. E.; Barrett, D. G.; Hughes, R. G.; Reitter, B.; Adkison, K. K.; Lancaster, M. E.; Lee, F.; Hart, R.; Paulik, M. A.; Sherman, B. W.; True, T.; Cowan, C., Synthesis and evaluation of potent and selective beta(3) adrenergic receptor agonists containing acylsulfonamide, sulfonylsulfonamide, and sulfonylurea carboxylic acid isosteres. *J. Med. Chem.* **2002**, *45* (3), 567-583.
99. Glunz, P. W.; Zhang, X. J.; Zou, Y.; Delucca, I.; Nirschl, A. H.; Cheng, X. H.; Weigelt, C. A.; Cheney, D. L.; Wei, A. Z.; Anumula, R.; Luetttgen, J. M.; Rendina, A. R.; Harpel, M.; Luo, G.; Knabb, R.; Wong, P. C.; Wexler, R. R.; Priestley, E. S., Nonbenzamidine acylsulfonamide tissue factor-factor VIIa inhibitors. *Bioorg. Med. Chem. Lett.* **2013**, *23* (18), 5244-5248.
100. Pelz, N. F.; Bian, Z. G.; Zhao, B.; Shaw, S.; Tarr, J. C.; Belmar, J.; Gregg, C.; Camper, D. V.; Goodwin, C. M.; Arnold, A. L.; Sensintaffar, J. L.; Friberg, A.; Rossanese, O. W.; Lee, T.; Olejniczak, E. T.; Fesik, S. W., Discovery of 2-Indole-acylsulfonamide Myeloid Cell Leukemia 1 (Mcl-1) Inhibitors Using Fragment-Based Methods. *J. Med. Chem.* **2016**, *59* (5), 2054-2066.
101. Vickers, C. J.; Gonzalez-Paez, G. E.; Litwin, K. M.; Umotoy, J. C.; Coutasias, E. A.; Wolan, D. W., Selective Inhibition of Initiator versus Executioner Caspases Using Small Peptides Containing Unnatural Amino Acids. *ACS Chem. Biol.* **2014**, *9* (10), 2194-2198.
102. Vickers, C. J.; Gonzalez-Paez, G. E.; Wolan, D. W., Selective Detection of Caspase-3 versus Caspase-7 Using Activity-Based Probes with Key Unnatural Amino Acids. *ACS Chem. Biol.* **2013**, *8* (7), 1558-1566.
103. Vickers, C. J.; Gonzalez-Paez, G. E.; Wolan, D. W., Selective Detection and Inhibition of Active Caspase-3 in Cells with Optimized Peptides. *J. Am. Chem. Soc.* **2013**, *135* (34), 12869-12876.
104. Stevenazzi, A.; Marchini, M.; Sandrone, G.; Vergani, B.; Lattanzio, M., Amino acidic scaffolds bearing unnatural side chains: An old idea generates new and versatile tools for the life sciences. *Bioorg. Med. Chem. Lett.* **2014**, *24* (23), 5349-5356.
105. Shahripour, A. B.; Plummer, M. S.; Lunney, E. A.; Albrecht, H. P.; Hays, S. J.; Kostlan, C. R.; Sawyer, T. K.; Walker, N. P. C.; Brady, K. D.; Allen, H. J.; Talanian, R. V.; Wong, W. W.; Humblet, C., Structure-Based design of nonpeptide inhibitors of interleukin-1 β converting enzyme (ICE, Caspase-1). *Bioorg. Med. Chem.* **2002**, *10* (1), 31-40.

106. Shahripour, A. B.; Plummer, M. S.; Lunney, E. A.; Sawyer, T. K.; Stankovic, C. J.; Connolly, M. K.; Rubin, J. R.; Walker, N. P. C.; Brady, K. D.; Allen, H. J.; Talanian, R. V.; Wong, W. W.; Humblet, C., Structure-based design of caspase-1 inhibitor containing a diphenyl ether sulfonamide. *Bioorg. Med. Chem. Lett.* **2001**, *11* (20), 2779-2782.
107. Zhenodarova, S. M., Small-molecule caspase inhibitors. *Russ. Chem. Rev.* **2010**, *79* (2), 119-143.
108. Erlanson, D. A.; Lam, J. W.; Wiesmann, C.; Luong, T. N.; Simmons, R. L.; DeLano, W. L.; Choong, I. C.; Burdett, M. T.; Flanagan, W. M.; Lee, D.; Gordon, E. M.; O'Brien, T., In situ assembly of enzyme inhibitors using extended tethering. *Nat. Biotechnol.* **2003**, *21* (3), 308-14.
109. Choong, I. C.; Lew, W.; Lee, D.; Pham, P.; Burdett, M. T.; Lam, J. W.; Wiesmann, C.; Luong, T. N.; Fahr, B.; DeLano, W. L.; McDowell, R. S.; Allen, D. A.; Erlanson, D. A.; Gordon, E. M.; O'Brien, T., Identification of Potent and Selective Small-Molecule Inhibitors of Caspase-3 through the Use of Extended Tethering and Structure-Based Drug Design. *J. Med. Chem.* **2002**, *45* (23), 5005-5022.
110. Vazquez, J.; Garcia-Jareno, A.; Mondragon, L.; Rubio-Martinez, J.; Perez-Paya, E.; Albericio, F., Conformationally restricted hydantoin-based peptidomimetics as inhibitors of caspase-3 with basic groups allowed at the S3 enzyme subsite. *ChemMedChem* **2008**, *3* (6), 979-85.
111. Isabel, E.; Black, W. C.; Bayly, C. I.; Grimm, E. L.; Janes, M. K.; McKay, D. J.; Nicholson, D. W.; Rasper, D. M.; Renaud, J.; Roy, S.; Tam, J.; Thornberry, N. A.; Vaillancourt, J. P.; Xanthoudakis, S.; Zamboni, R., Nicotinyl aspartyl ketones as inhibitors of caspase-3. *J. Med. Chem. Lett.* **2003**, *13* (13), 2137-2140.
112. Becker, J. W.; Rotonda, J.; Soisson, S. M.; Aspiotis, R.; Bayly, C.; Francoeur, S.; Gallant, M.; Garcia-Calvo, M.; Giroux, A.; Grimm, E.; Han, Y.; McKay, D.; Nicholson, D. W.; Peterson, E.; Renaud, J.; Roy, S.; Thornberry, N.; Zamboni, R., Reducing the Peptidyl Features of Caspase-3 Inhibitors: A Structural Analysis. *J. Med. Chem.* **2004**, *47* (10), 2466-2474.
113. Jiang, Y.; Hansen, T. V., Isatin 1,2,3-triazoles as potent inhibitors against caspase-3. *Bioorg. Med. Chem. Lett.* **2011**, *21* (6), 1626-9.
114. Chu, W. H.; Rothfuss, J.; Chu, Y. X.; Zhou, D.; Mach, R. H., Synthesis and in Vitro Evaluation of Sulfonamide Isatin Michael Acceptors as Small Molecule Inhibitors of Caspase-6. *J. Med. Chem.* **2009**, *52* (8), 2188-2191.
115. Chu, W. H.; Rothfuss, J.; d'Avignon, A.; Zeng, C. B.; Zhou, D.; Hotchkiss, R. S.; Mach, R. H., Isatin sulfonamide analogs containing a michael addition acceptor: A new class of caspase 3/7 inhibitors. *J. Med. Chem.* **2007**, *50* (15), 3751-3755.
116. Chu, W. H.; Zhang, J.; Zeng, C. B.; Rothfuss, J.; Tu, Z. D.; Chu, Y. X.; Reichert, D. E.; Welch, M. J.; Mach, R. H., N-benzylisatin sulfonamide analogues as potent caspase-3 inhibitors: Synthesis, in vitro activity, and molecular modeling studies. *J. Med. Chem.* **2005**, *48* (24), 7637-7647.
117. Wang, Q.; Mach, R. H.; Reichert, D. E., Docking and 3D-QSAR Studies on Isatin Sulfonamide Analogues as Caspase-3 Inhibitors. *J. Chem. Inf. Model.* **2009**, *49* (8), 1963-1973.
118. Chen, Y. H.; Zhang, Y. H.; Zhang, H. J.; Liu, D. Z.; Gu, M.; Li, J. Y.; Wu, F.; Zhu, X. Z.; Li, J.; Nan, F., Design, synthesis, and biological evaluation of isoquinoline-1,3,4-trione derivatives as potent caspase-3 inhibitors. *J. Med. Chem.* **2006**, *49* (5), 1613-1623.
119. Scott, C. W.; Sobotka-Briner, C.; Wilkins, D. E.; Jacobs, R. T.; Folmer, J. J.; Frazee, W. J.; Bhat, R. V.; Ghanekar, S. V.; Aharony, D., Novel small molecule inhibitors of caspase-3 block cellular and biochemical features of apoptosis. *J. Pharmacol. Exp. Ther.* **2003**, *304* (1), 433-440.
120. Hazel, B. A.; Baum, C.; Kalf, G. F., Hydroquinone, a bioreactive metabolite of benzene, inhibits apoptosis in myeloblasts. *Stem Cells* **1996**, *14* (6), 730-742.

121. Laskowski, R. A.; Gerick, F.; Thornton, J. M., The structural basis of allosteric regulation in proteins. *Febs Lett.* **2009**, *583* (11), 1692-1698.
122. Huber, K. L.; Ghosh, S.; Hardy, J. A., Inhibition of caspase-9 by stabilized peptides targeting the dimerization interface. *Biopolymers* **2012**, *98* (5), 451-465.
123. Hardy, J. A.; Lam, J.; Nguyen, J. T.; O'Brien, T.; Wells, J. A., Discovery of an allosteric site in the caspases. *Proc. Natl. Acad. Sci. U. S. A.* **2004**, *101* (34), 12461-12466.
124. Feldman, T.; Kabaleeswaran, V.; Jang, S. B.; Antczak, C.; Djaballah, H.; Wu, H.; Jiang, X., A class of allosteric caspase inhibitors identified by high-throughput screening. *Mol. Cell* **2012**, *47* (4), 585-95.
125. Hacker, H. G.; Sisay, M. T.; Gutschow, M., Allosteric modulation of caspases. *Pharmacol. Ther.* **2011**, *132* (2), 180-195.
126. Dolle, R. E.; Prasad, C. V. C.; Prouty, C. P.; Salvino, J. M.; Awad, M. M. A.; Schmidt, S. J.; Hoyer, D.; Ross, T. M.; Graybill, T. L.; Speier, G. J.; Uhl, J.; Miller, B. E.; Helaszek, C. T.; Ator, M. A., Pyridazinodiazepines as a high-affinity, P-2-P-3 peptidomimetic class of interleukin-1 beta-converting enzyme inhibitor. *J. Med. Chem.* **1997**, *40* (13), 1941-1946.
127. Wannamaker, W.; Davies, R.; Namchuk, M.; Pollard, J.; Ford, P.; Ku, G.; Decker, C.; Charifson, P.; Weber, P.; Germann, U. A.; Kuida, K.; Randle, J. C., (S)-1-((S)-2-([1-(4-amino-3-chlorophenyl)-methanoyl]-amino)-3,3-dimethyl-butanoyl)-pyrrolidine-2-carboxylic acid ((2R,3S)-2-ethoxy-5-oxo-tetrahydro-furan-3-yl)-amide (VX-765), an orally available selective interleukin (IL)-converting enzyme/caspase-1 inhibitor, exhibits potent anti-inflammatory activities by inhibiting the release of IL-1beta and IL-18. *J. Pharmacol. Exp. Ther.* **2007**, *321* (2), 509-16.
128. Siegmund, B.; Zeitz, M., Pralnacasan Vertex Pharmaceuticals. *Drugs* **2003**, *6* (2), 154-158.
129. Linton, S. D., Caspase inhibitors: A pharmaceutical industry perspective. *Curr. Top. Med. Chem.* **2005**, *5* (16), 1697-1716.
130. Chen, Y. X.; Huang, J. Y.; Paskavitz, J.; Hooek, T.; Wright, C., Evaluation of Drug-Drug Interactions between VX-765 and Common Anti-Epileptic Medications in Subjects with Treatment-Resistant Partial-Onset Epilepsy. *Neurology* **2013**, *80*.
131. Spada, A. P.; Contreras, P.; Burgess, G. C., Inhibition of caspase activity with emricasan in HCV patients: potential implications for chronic dosing and long term safety. *Hepatology* **2012**, *56*, 1123a-1123a.
132. Pockros, P. J.; Schiff, E. R.; Shiffman, M. L.; McHutchison, J. G.; Gish, R. G.; Afdhal, N. H.; Makhviladze, M.; Huyghe, M.; Hecht, D.; Oltersdorf, T.; Shapiro, D. A., Oral IDN-6556, an antiapoptotic caspase inhibitor, may lower aminotransferase activity in patients with chronic hepatitis C. *Hepatology* **2007**, *46* (2), 324-329.
133. Shiffman, M. L.; Pockros, P.; McHutchison, J. G.; Schiff, E. R.; Morris, M.; Burgess, G., Clinical trial: the efficacy and safety of oral PF-03491390, a pancaspase inhibitor - a randomized placebo-controlled study in patients with chronic hepatitis C. *Aliment. Pharmacol. Ther.* **2010**, *31* (9), 969-978.
134. Spada, A. P.; Contreras, P. C.; Huyghe, M. C.; Morris, M.; Burgess, G. C., Rapid and statistically significant reduction of markers of apoptosis and cell death in subjects with mild, moderate and severe hepatic impairment treated with a single dose of the pan caspase inhibitor, emricasan. *Hepatology* **2014**, *60* (6), 1277a-1277a.
135. Garcia-Tsao, G.; Fuchs, M.; Shiffman, M. L.; Chan, J. L.; Morris, M.; Yamashita, M.; Spada, A. P.; Hagerty, D.; Bosch, J., Emricasan (IDN-6556) administered orally for 28 days lowers portal

- pressure in patients with compensated cirrhosis and severe portal hypertension. *Hepatology* **2015**, *62* (6), 1382a-1383a.
136. Jalan, R.; Wright, G.; McPherson, S.; Frenette, C.; Cave, M.; Morris, M.; Huyghe, M.; Burgess, G., A Placebo-Controlled, Multicenter, Double-Blind, Randomised, Pharmacokinetic and Pharmacodynamic Trial of Emricasan (Idn-6556) in Subjects with Acute-on Chronic Liver Failure (Aclf). *J. Hepatol.* **2015**, *62*, S281-S281.
137. Shiffman, M.; Freilich, B.; Vuppalanchi, R.; Watt, K.; Burgess, G.; Morris, M.; Sheedy, B.; Schiff, E., A Placebo-Controlled, Multicenter, Double-Blind, Randomised Trial of Emricasan in Subjects with Non-Alcoholic Fatty Liver Disease (Nafld) and Raised Transaminases. *J. Hepatol.* **2015**, *62*, S282-S282.
138. Ratziu, V.; Sheikh, M. Y.; Sanyal, A. J.; Lim, J. K.; Conjeevaram, H.; Chalasani, N.; Abdelmalek, M.; Bakken, A.; Renou, C.; Palmer, M.; Levine, R. A.; Bhandari, B. R.; Cornpropst, M.; Liang, W.; King, B.; Mondou, E.; Rousseau, F. S.; McHutchison, J.; Chojkier, M., A phase 2, randomized, double-blind, placebo-controlled study of GS-9450 in subjects with nonalcoholic steatohepatitis. *Hepatology* **2012**, *55* (2), 419-428.
139. Manns, M.; Palmer, M.; Flisiak, R.; DeJesus, E.; Hazan, L.; Liang, W.; Oldach, D.; McHutchison, J.; Hirsch, K., A Phase-2b Trial to Evaluate the Safety, Tolerability and Efficacy of a Caspase Inhibitor, Gs-9450, in Adults Failing Peg/Rbv Therapy for Chronic Hcv Infection. *J. Hepatol.* **2011**, *54*, S55-S56.
140. Berzigotti, A.; Bellot, P.; De Gottardi, A.; Garcia-Pagan, J. C.; Gagnon, C.; Spenard, J.; Bosch, J., NCX-1000, a Nitric Oxide-Releasing Derivative of UDCA, Does Not Decrease Portal Pressure in Patients With Cirrhosis: Results of a Randomized, Double-Blind, Dose-Escalating Study. *Am. J. Gastroenterol.* **2010**, *105* (5), 1094-1101.
141. Ku, G.; Ford, P.; Raybuck, S. A.; Harding, M. W.; Randle, J. C. R., Selective interleukin-1 beta converting enzyme (ICE/caspase-1) inhibition with pralnacasan (HMR 3480/VX.(-)40) reduces inflammation and joint destruction in murine type II collagen-induced arthritis (CIA). *Arthritis Rheum.* **2001**, *44* (9), S241-S241.
142. Braddock, M.; Quinn, A., Targeting IL-1 in inflammatory disease: New opportunities for therapeutic intervention. *Nat. Rev. Drug Discovery* **2004**, *3* (4), 1-10.
143. Rudolphi, K.; Gerwin, N.; Verzijl, N.; van der Kraan, P.; van den Berg, W., Pralnacasan, an inhibitor of interleukin-1 beta converting enzyme, reduces joint damage in two murine models of osteoarthritis. *Osteoarthr. Cartil.* **2003**, *11* (10), 738-746.
144. Kudelova, J.; Fleischmannova, J.; Adamova, E.; Matalova, E., Pharmacological Caspase Inhibitors: Research Towards Therapeutic Perspectives. *J. Physiol. Pharmacol.* **2015**, *66* (4), 473-482.
145. Doitsh, G.; Galloway, N. L. K.; Geng, X.; Yang, Z. Y.; Monroe, K. M.; Zepeda, O.; Hunt, P. W.; Hatano, H.; Sowinski, S.; Munoz-Arias, I.; Greene, W. C., Cell death by pyroptosis drives CD4 T-cell depletion in HIV-1 infection. *Nature* **2014**, *505* (7484), 509-+.
146. Galloway, N. L. K.; Doitsh, G.; Monroe, K. M.; Yang, Z. Y.; Munoz-Arias, I.; Levy, D. N.; Greene, W. C., Cell-to-Cell Transmission of HIV-1 Is Required to Trigger Pyroptotic Death of Lymphoid-Tissue-Derived CD4 T Cells. *Cell Rep.* **2015**, *12* (10), 1555-1563.
147. Hoglen, N. C.; Chen, L. S.; Fisher, C. D.; Hirakawa, B. P.; Groessl, T.; Contreras, P. C., Characterization of IDN-6556(3-{2-(2-tert-butylphenylaminoxy)amino}-propionylamino}-4-oxo-5-(2,3,5,6-tetrafluoro-phenoxy)-pentanoic Acid): a liver-targeted caspase inhibitor. *J. Pharmacol. Exp. Ther.* **2004**, *309* (2), 634-640.

148. Spada, A. P.; Contreras, P. C.; Huyghe, M. C.; Morris, M.; Burgess, G. C., Emricasan, a Potent Pan Caspase Inhibitor, Rapidly Reduces Caspase Activity and Biomarkers of Apoptosis in Patients with Hepatic Impairment but Not in Healthy Volunteers: Implications for Safety, Selectivity and Mechanism of Action. *J. Hepatol.* **2015**, *62*, S462-S462.
149. Elbekai, R. H.; Paranjpe, M. G.; Contreras, P. C.; Spada, A., Carcinogenicity assessment of the pan-caspase inhibitor, emricasan, in Tg.rasH2 mice. *Regul. Toxicol. Pharmacol.* **2015**, *72* (2), 169-178.
150. Marino, G.; Niso-Santano, M.; Baehrecke, E. H.; Kroemer, G., Self-consumption: the interplay of autophagy and apoptosis. *Nat. Rev. Mol. Cell Biol.* **2014**, *15* (2), 81-94.
151. Hoppener, F. J. P.; Ebes, F.; Kim, J. A.; Park, M. J.; Choi, H. J., Caspase inhibition a promising new treatment for various liver diseases, report of two phase I studies with gs-9450. *Br. J. Clin. Pharmacol.* **2010**, *69* (6), 709-709.
152. Fiorucci, S.; Antonelli, E.; Tocchetti, P.; Morelli, A., Treatment of portal hypertension with NCX-1000, a liver-specific NO donor. A review of its current status. *Cardiovasc. Drug Rev.* **2004**, *22* (2), 135-146.
153. MacKenzie, S. H.; Schipper, J. L.; Clark, A. C., The potential for caspases in drug discovery. *Curr. Opin. Drug Discovery Dev.* **2010**, *13* (5), 568-576.

Chapter 2

Objectives of this thesis

2 Objectives of this thesis

Though the primary objective of this thesis is the production of new and improved inflammatory caspase inhibitors by implementing carboxylate isosteres, two other objectives have emerged through this study; optimization of the acyliminium-Strecker reaction for convenient library synthesis and the development of an approach to induce caspase-1 degradation.

2.1 Objective 1: Identification and implementation of carboxylate isosteres in caspase inhibitors

As mentioned in the introduction, all caspases use a P1-aspartate residue as a main recognition point in their substrates. For this reason, most reported caspase inhibitors also incorporate a carboxylate that mimics the aspartate residue and acts as an affinity-enhancing structural element.¹ The close phylogenetical relationship between the caspases however, makes specific caspase targeting a huge obstacle in drug discovery and biological research.² This study therefore focuses on exploring the incorporation of carboxylate isosteres for target recognition in order to overcome this lack of selectivity, hitherto an underexplored approach in terms of caspase inhibitor design. Replacement of this carboxylate by other acidic groups with distinctive size or electronic properties, can reasonably be expected to have differing impacts on the process of substrate/inhibitor recognition by individual members of the caspase family. This in turn would translate into a more pronounced differentiation by individual caspases between inhibitors or substrates possessing such a modification. So far, the number of reports on isosteric carboxylate replacement in caspase-targeting compounds has been limited, and existing publications have mainly focused on improvement of physicochemical and/or biopharmaceutical properties of inhibitors rather than increasing caspase selectivity. In one case, Okamoto *et al.* found that the use of *N*-acylsulfonamides resulted in similar potencies as its carboxylate analogues. Moreover, they reported a fourfold increase of inhibitory activity in cellular assays and a drastically improved cell permeability.³ Notwithstanding these promising results and the number of successful applications of acylsulfonamide isosteres in other domains⁴⁻⁷, the full potential of this functional group for caspase research was never investigated in further detail. As part of our ongoing effort to discover inhibitors of caspase-1 with an optimized selectivity and biopharmaceutical profile, we decided to investigate acylsulfonamide-containing analogues of VRT-043198 (**2.1, Figure 2.1**). Considering the spatial confinement of the caspase P1-pocket, only analogues with a small (methyl, ethyl) sulfonyl substituent were selected (**2.2-2.3**). To optimally probe the acylsulfonamide's potential as a tool to increase selectivity for individual caspase family members, we also opted to incorporate it into analogues of the well-known *pan*-caspase targeting inhibitor Z-VAD-CHO (**2.4-2.5**).⁸ In part of the designed molecules, the aldehyde warhead of the parent compounds was conserved. Taking into account the relatively high reactivity of aldehydes and the resulting likelihood for erratic behavior in *in*

vivo conditions, we also decided to synthesize analogues with a carbonitrile warhead, based on the existing inhibitor NCGC-00183434 (**2.6-2.7**).⁹ The milder electrophilicity of the latter could lead to a significant improvement of selectivity and biopharmaceutical compound quality.¹⁰⁻¹¹ Besides the inhibitory potency and caspase selectivity, a thorough structural elaboration of these compounds should point out the full potential of this isostere. The development of acylsulfonamide-containing caspase inhibitors will be the subject of **Chapter 3** of this PhD thesis.

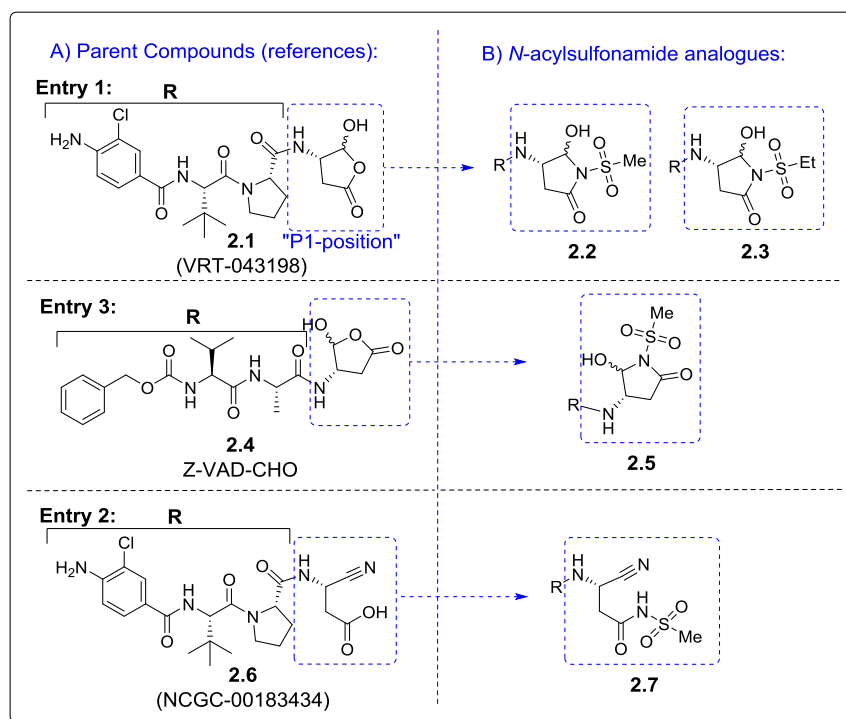


Figure 2.1. Incorporation of acylsulfonamide isosteres in existing caspase inhibitors.

Besides acylsulfonamides, we are also aiming at discovering other isosteric replacements for carboxylic acids that generate a good fit in the S1 pocket/region of inflammatory caspases. To achieve this goal, a systematic approach will be applied that has recently been developed in our lab: the Modified Substrate Activity Screening (**Figure 2.2**).¹²⁻¹³ This fragment-based methodology comprises the production of a library of *N*-acyl 7-amino-4-methylcoumarins containing a number of acidic residues (carboxylates, sulfonates, phosphonates or bioisosteres thereof). An easy biochemical 2-step protocol (inhibitor - and substrate screening) will then allow the identification of the most promising isosteres for caspase drug discovery. Emerging these fragments with warhead functionalities should finally lead to new inhibitors with improved characteristics in terms of caspase blocking. The application of the MSAS methodology on caspase-1 and -4 will be the subject of **Chapters 4 and 5** of this PhD thesis.

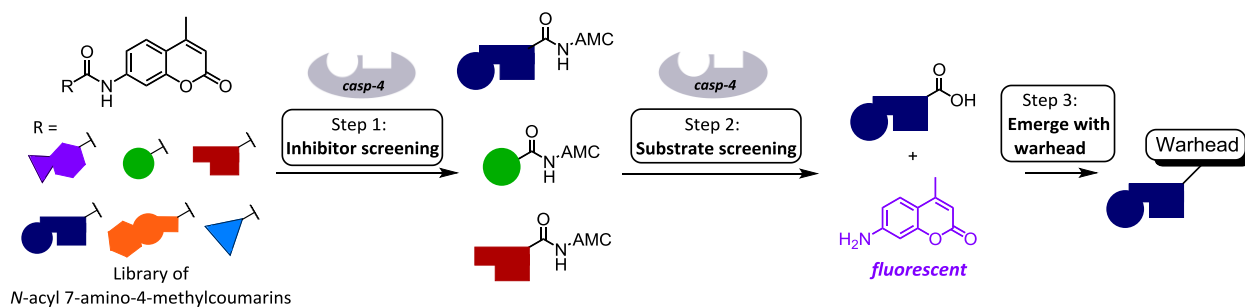


Figure 2.2. Outline of the MSAS approach. Figure was taken from ref. [13]

2.2 Objective 2: Convenient library synthesis and on-target experiments

The second objective of this PhD project consists of investigating and implementing target-assisted synthetic approaches for the assembly of inhibitor building blocks, as an efficient means to produce high-affinity caspase inhibitors. Developing target-assisted versions of multicomponent reactions that can be used in diversity-oriented drug discovery seems highly attractive for this project, given the possibility to simultaneously assemble multiple building blocks (including carboxylate isosteres) and deliver complex, functionalized molecular structures in a single, target-catalyzed step. Due to its proven potential in caspase inhibition, 1-aminoalkylcarbonitriles seem highly attractive in the context of this project.¹⁴ Such molecules are typically generated by the Strecker reaction. Moreover, besides on-target experiments, this multicomponent reaction could also provide an easy and efficient way to create large inhibitor libraries. Importantly however, the basic properties of the amine function present in products of the classical Strecker protocol seemed undesirable, taking into account the strict endopeptidase properties of caspases. We therefore decided to focus on a variant of the Strecker reaction that has the potential to produce compounds with an acylated amine function, starting from the corresponding amide or carbamate building blocks (**Figure 2.3**). This reaction will be named the “acyliminium-Strecker”.

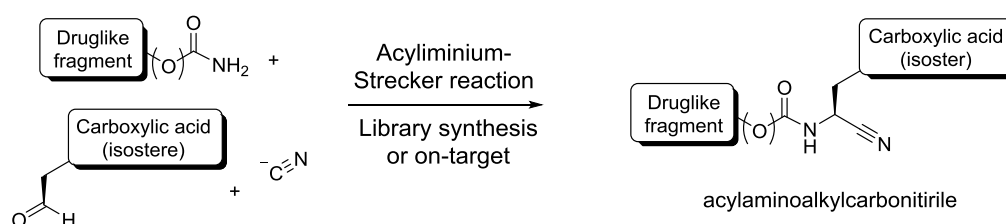


Figure 2.3. Library synthesis and target-assisted drug discovery based on the acyliminium-Strecker reaction to obtain acylaminoalkylcarbonitriles that could serve as caspase inhibitors.

A prospective synthetic study will be performed in this part of the PhD, aiming at providing a clearer view on the different parameters that determine the kinetics, outcome and scope of the acyliminium-Strecker reaction. We hope to create two reliable and cross-optimized protocols for this reaction: 1) an “aqueous” protocol that can be used in target-guided synthesis; 2) a traditional protocol that would

allow efficient and versatile library synthesis of protease inhibitors with an acylaminoalkylcarbonitrile core. Application of both protocols would involve a diversified library of druglike amides and/or carbamates, an optimal cyanide source, and either 3-oxopropanoic acid (or a protected derivative thereof) or a suitable bioisostere of the carboxylate group equipped with an aldehyde function (**Figure 2.3**). The exploratory study towards an optimized acyliminium-Strecker protocol will be the focus in **Chapter 6** of this PhD thesis.

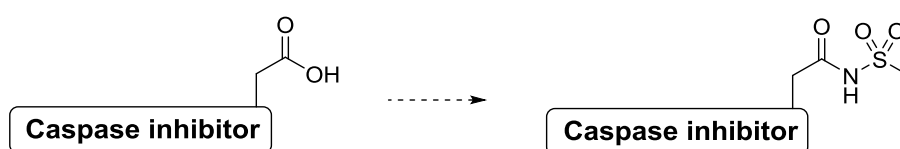
2.3 Objective 3: Approach to induce caspase-1 degradation via thalidomide conjugates

This part of the objectives has been removed from this thesis due to limited Intellectual Property rights.

References

1. Poreba, M.; Strozyk, A.; Salvesen, G. S.; Drag, M., Caspase substrates and inhibitors. *Cold Spring Harbor Perspect. Biol.* **2013**, *5* (8), a008680.
2. Poreba, M.; Szalek, A.; Kasperkiewicz, P.; Rut, W.; Salvesen, G. S.; Drag, M., Small Molecule Active Site Directed Tools for Studying Human Caspases. *Chem. Rev.* **2015**, *115* (22), 12546-12629.
3. Okamoto, Y.; Anan, H.; Nakai, E.; Morihira, K.; Yonetoku, Y.; Kurihara, H.; Sakashita, H.; Terai, Y.; Takeuchi, M.; Shibamura, T.; Isomura, Y., Peptide based interleukin-1 beta converting enzyme (ICE) inhibitors: Synthesis, structure activity relationships and crystallographic study of the ICE-inhibitor complex. *Chem. Pharm. Bull.* **1999**, *47* (1), 11-21.
4. Yee, Y. K.; Bernstein, P. R.; Adams, E. J.; Brown, F. J.; Cronk, L. A.; Hebbel, K. C.; Vacek, E. P.; Krell, R. D.; Snyder, D. W., A Novel Series of Selective Leukotriene Antagonists - Exploration and Optimization of the Acidic Region in 1,6-Disubstituted Indoles and Indazoles. *J. Med. Chem.* **1990**, *33* (9), 2437-2451.
5. Uehling, D. E.; Donaldson, K. H.; Deaton, D. N.; Hyman, C. E.; Sugg, E. E.; Barrett, D. G.; Hughes, R. G.; Reitter, B.; Adkison, K. K.; Lancaster, M. E.; Lee, F.; Hart, R.; Paulik, M. A.; Sherman, B. W.; True, T.; Cowan, C., Synthesis and evaluation of potent and selective beta(3) adrenergic receptor agonists containing acylsulfonamide, sulfonylsulfonamide, and sulfonylurea carboxylic acid isosteres. *J. Med. Chem.* **2002**, *45* (3), 567-583.
6. Glunz, P. W.; Zhang, X. J.; Zou, Y.; Delucca, I.; Nirschl, A. H.; Cheng, X. H.; Weigelt, C. A.; Cheney, D. L.; Wei, A. Z.; Anumula, R.; Luetgen, J. M.; Rendina, A. R.; Harpel, M.; Luo, G.; Knabb, R.; Wong, P. C.; Wexler, R. R.; Priestley, E. S., Nonbenzamidine acylsulfonamide tissue factor-factor VIIa inhibitors. *Bioorg. Med. Chem. Lett.* **2013**, *23* (18), 5244-5248.
7. Pelz, N. F.; Bian, Z. G.; Zhao, B.; Shaw, S.; Tarr, J. C.; Belmar, J.; Gregg, C.; Camper, D. V.; Goodwin, C. M.; Arnold, A. L.; Sensintaffar, J. L.; Friberg, A.; Rossanese, O. W.; Lee, T.; Olejniczak, E. T.; Fesik, S. W., Discovery of 2-Indole-acylsulfonamide Myeloid Cell Leukemia 1 (Mcl-1) Inhibitors Using Fragment-Based Methods. *J. Med. Chem.* **2016**, *59* (5), 2054-2066.
8. Fahr, B. T.; O'Brien, T.; Pham, P.; Waal, N. D.; Baskaran, S.; Raimundo, B. C.; Lam, J. W.; Sopko, M. M.; Purkey, H. E.; Romanowski, M. J., Tethering identifies fragment that yields potent inhibitors of human caspase-1. *Bioorg. Med. Chem. Lett.* **2006**, *16* (3), 559-562.
9. Boxer, M. B.; Quinn, A. M.; Shen, M.; Jadhav, A.; Leister, W.; Simeonov, A.; Auld, D. S.; Thomas, C. J., A highly potent and selective caspase 1 inhibitor that utilizes a key 3-cyanopropanoic acid moiety. *ChemMedChem* **2010**, *5* (5), 730-8.
10. MacKenzie, S. H.; Schipper, J. L.; Clark, A. C., The potential for caspases in drug discovery. *Curr. Opin. Drug Discovery Dev.* **2010**, *13* (5), 568-576.
11. Zhenodarova, S. M., Small-molecule caspase inhibitors. *Russ. Chem. Rev.* **2010**, *79* (2), 119-143.
12. Cleenewerck, M.; Grootaert, M. O. J.; Gladysz, R.; Adriaenssens, Y.; Roelandt, R.; Joossens, J.; Lambeir, A.-M.; De Meyer, G. R. Y.; Declercq, W.; Augustyns, K.; Martinet, W.; Van der Veken, P., Inhibitor screening and enzymatic activity determination for autophagy target Atg4B using a gel electrophoresis-based assay. *Eur. J. Med. Chem.* **2016**, *123*, 631-638.
13. Gladysz, R.; Cleenewerck, M.; Joossens, J.; Lambeir, A. M.; Augustyns, K.; Van der Veken, P., Repositioning the Substrate Activity Screening (SAS) Approach as a Fragment-Based Method for Identification of Weak Binders. *ChemBioChem* **2014**, *15* (15), 2238-47.
14. Merino, P.; Marqués-López, E.; Tejero, T.; Herrera, R. P., Organocatalyzed Strecker reactions. *Tetrahedron* **2009**, *65* (7), 1219-1234.

Carboxylate Isosteres for Caspase Inhibitors: the Acylsulfonamide Case Revisited



The content of this chapter is based on:

Adriaenssens, Y.; Fernández, D. J.; Vande Walle, L.; Elvas, F.; Joossens, J.; Lambeir, A. M.; Augustyns, K.; Lamkanfi, M.; Van der Veken, P.; Carboxylate Isosteres for Caspase Inhibitors: the Acylsulfonamide Case Revisited; *Submitted to Organic and Biomolecular Chemistry*.

3 Carboxylate isosteres for caspase inhibitors: the acylsulfonamide case revisited

3.1 Abstract

As part of an ongoing effort to discover inhibitors of caspase-1 with an optimized selectivity and biopharmaceutical profile, acylsulfonamides were explored as carboxylate isosteres in caspase inhibitors. Acylsulfonamide analogues of the clinically investigated caspase-1 inhibitor VRT-043198 and of the *pan*-caspase inhibitor Z-VAD-CHO were synthesized. The isostere-containing analogues with an aldehyde warhead had inhibitory potencies comparable to the carboxylate references. In addition, the conformational and tautomeric characteristics of these molecules were determined using ^1H - and ^{13}C -based NMR. The propensity of acylsulfonamides with an aldehyde warhead to occur in a ring-closed conformation at physiological pH, significantly increases sensitivity to hydrolysis of the acylsulfonamide moiety, yielding the parent carboxylate containing inhibitors. These results indicate that the acylsulfonamide analogues of the aldehyde-based inhibitor VRT-043198 might have potential as a novel prodrug type for the latter. Finally, inhibition of caspase-1 and -11 mediated inflammation in mouse macrophages were found to correlate with the compounds' potencies in the enzymatic assays.

3.2 Introduction

3.2.1 Caspase inhibition

The caspases are a family of aspartate selective cysteine proteases, of which orthologues occur in a wide range of species. Human caspases are typically classified into two subfamilies on the basis of their sequence homologies and biological functions.^{1, 2} Members of the first subfamily ("death caspases") have key roles in the initiation (caspase-8, -9, -10) and execution (caspase-3, -6, -7) of apoptosis (programmed cell death). The second subfamily consists of the inflammatory caspases. This subfamily controls inflammatory and host defense responses during infection and in the context of autoimmune and -inflammatory diseases by a threefold mode of action; 1) by modulating the maturation and secretion of inflammatory cytokines interleukin (IL)-1 β and IL-18, 2) by inducing a lytic cell death mode termed pyroptosis and 3) by releasing additional alarmin molecules that contribute to pathogen eradication.^{3, 4} Caspase-1 (interleukin-1 β -converting enzyme, ICE) is by far the best studied member, while the other human inflammatory caspases (caspase-4 and -5) have so far received less attention. Dysregulated caspase-1 is involved in the pathogenesis of many inflammatory diseases such as atherosclerosis, Alzheimer's disease, type-2 diabetes, gout and rare auto-inflammatory disorders.⁵ Caspase-1 is therefore considered as a target for influencing these pathological processes through inhibitor-mediated blocking of protease activity. So far, no caspase inhibitors have been approved as drugs by FDA or EMA. Only two inhibitors of caspase-1 have found their way into clinical trials; VX-765

(**3.1**, belnacasan) and VX-740 (prlnacasan). The latter however was withdrawn from clinical trials due to liver toxicity in long-term animal studies.⁶ VX-765 is an orally absorbed ethyl hemiacetal prodrug that is rapidly converted into VRT-043198 (**3.2**) under the action of plasma and liver esterases (**Figure 3.1**). VRT-043198, like other aspartylaldehyde-based caspase inhibitors, is known to occur mainly as an acyl hemiacetal and, to a lesser extent, in a hydrated form in aqueous solution.⁷ All these forms equilibrate with the ring-opened, aldehyde-containing carboxylate form that binds to caspase-1. This drug has been tested for the treatment of chronic epilepsy and psoriasis,⁸⁻¹⁰ and more recently in HIV-1 infected individuals and in patients with rheumatoid arthritis.¹¹⁻¹³

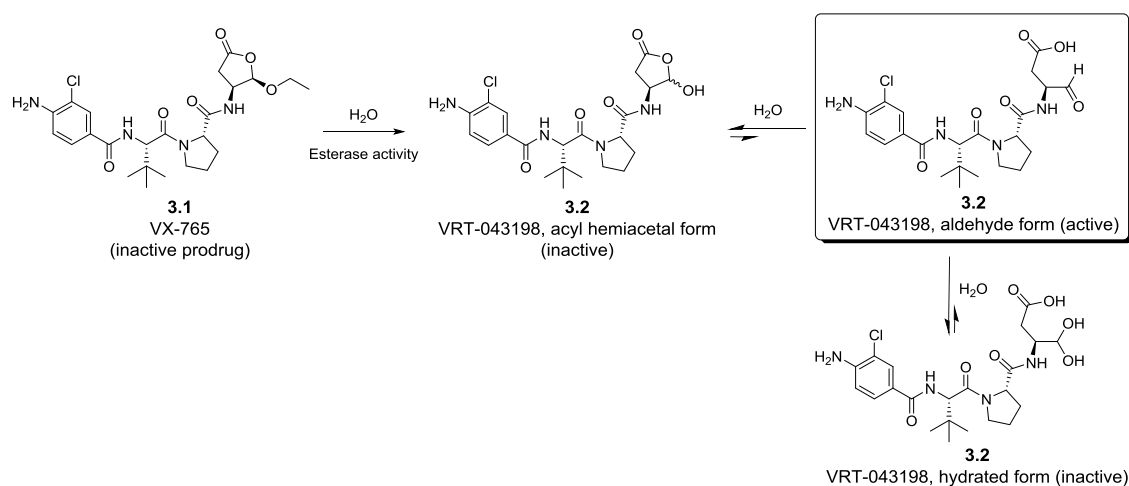


Figure 3.1. Structures of prodrug VX-765 and its active metabolite VRT-043198.

3.2.2 Caspase selectivity issues

All caspases use the P1-aspartate residue in their physiological peptide substrates as a main molecular recognition feature. Consequently, most reported caspase inhibitors also incorporate a carboxylate function as an affinity-enhancing structural element. The close phylogenetic relationship between caspases makes selective caspase targeting a huge obstacle in drug discovery and biological research.¹⁴ In the past, several strategies have been explored to overcome this lack of selectivity. Vickers *et al.* have demonstrated that significant selectivity can be obtained via the incorporation of unnatural amino acids in peptide substrates and inhibitors.¹⁵⁻¹⁷ In the same way, Ganesan *et al.* achieved reasonable selectivity towards caspase-3, using aza-peptide epoxide inhibitors that interact with the S1' subsite of the enzyme.¹⁸ Another potential approach to gain selectivity could consist of isosterically modifying the carboxylate function that caspases use for substrate and inhibitor recognition. Replacement of this carboxylate by another acidic group with distinctive size or electronic properties could reasonably be expected to have differing impacts on the recognition process by individual members of the caspase family. Isosteric replacement could also provide biopharmaceutical advantages for caspase-targeting compounds: the carboxylate's "hard" ionic character at physiological pH and its potential for toxic metabolite formation have convincingly been demonstrated to critically

discount on cellular permeability and ADME-Tox properties of compounds.^{19, 20} Illustrative thereof, most caspase inhibitors are used as ester-type prodrugs in preclinical and clinical settings. So far, the number of reports on isosteric carboxylate replacement in caspase-targeting compounds has been limited, and existing reports have mainly focused on improvement of physicochemical and/or biopharmaceutical properties of inhibitors. Prasad *et al.* replaced the carboxylate function in aspartate-derived α -(arylacyl)oxymethyl ketones with a tetrazole moiety. These analogues however lacked notable target affinity.²¹ Similarly, Boxer *et al.* investigated a tetrazole analogue of VRT-043198. In spite of improved resistance to degradation, its potency for all caspases dropped at least 50-fold compared to the carboxylate analogue.²² In a third case, Okamoto *et al.* found that the use of an *N*-acyl hydroxamate isostere resulted in a dramatic decrease of caspase-1 inhibitory potency. An *N*-acylsulfonamide evaluated by the same authors, resulted in similar potency as the carboxylate-containing compound. Moreover, a fourfold increase of inhibitory activity was reported in cellular assays and a drastically improved cell permeability compared to the parent molecule.²³ Notwithstanding these promising results and the number of successful applications of acylsulfonamide isosteres in other domains of drug discovery, the full potential of this functional group for caspase research has not been further investigated.²⁴⁻²⁷ Likewise, no data on caspase selectivity, physicochemical properties and *in vitro* pharmacokinetic profile are available for this compound type.

3.3 Objectives of this chapter

Part of our ongoing effort to discover inhibitors of caspase-1 with an optimized selectivity and biopharmaceutical profile, we decided to investigate acylsulfonamide-containing analogues of **3.2** (VRT-043198) (**Figure 3.2, entry 1**). Taking into account the spatial confinement of the caspase P1-pocket, only analogues **3.3** and **3.4** with a small (methyl, ethyl) sulfonyl substituent were planned. In addition, **3.2**'s carbonitrile analogue (**3.5**, NCGC-00183434) and the acylsulfonamide derivative thereof (**3.6**) were synthesized (**Figure 3.2, entry 2**).²² Compared to the aldehyde warhead, the milder electrophilicity of the carbonitrile function could in itself contribute to a potentially improved selectivity and biopharmaceutical profile for **3.5** and **3.6**.^{6, 28} As an illustration, several compounds with a carbonitrile warhead, including the cysteine protease inhibitor odanacatib, have been successfully approved as drugs by the FDA during recent years.²⁹⁻³¹ Third, we also opted to include *pan*-caspase inhibitor **3.7** (Z-VAD-CHO) and its acylsulfonamide analogue **3.8** in the study. (**Figure 3.2, entry 3**) The lack of selectivity of parent molecule **3.7** seemed interesting as an additional reference point to benchmark the acylsulfonamide's potential to increase selectivity for individual caspase family members.³²

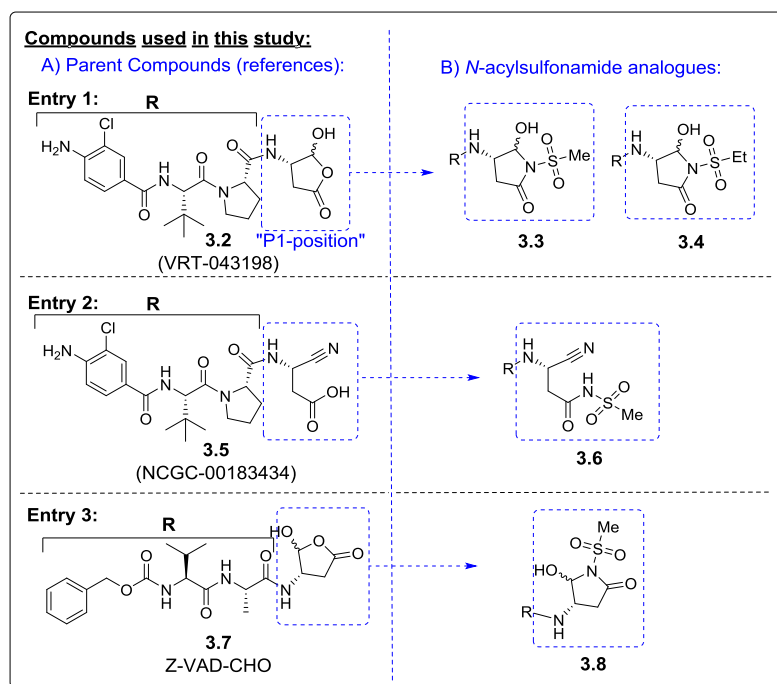
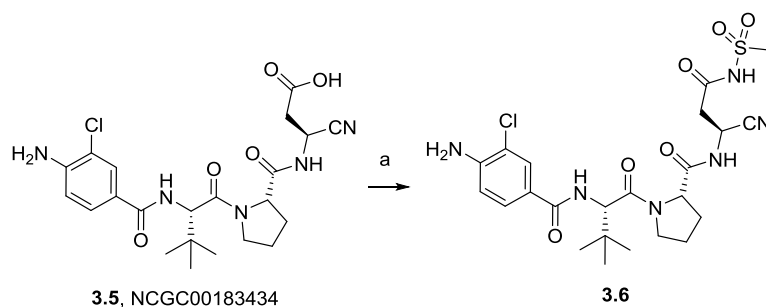


Figure 3.2. Overview of compounds used in this study. Aldehyde-containing inhibitors (**3.2-3.4** and **3.7-3.8**) are represented as the corresponding acyl hemiacetal or acyl hemiaminal tautomers (*vide infra*).

3.4 Results and discussion

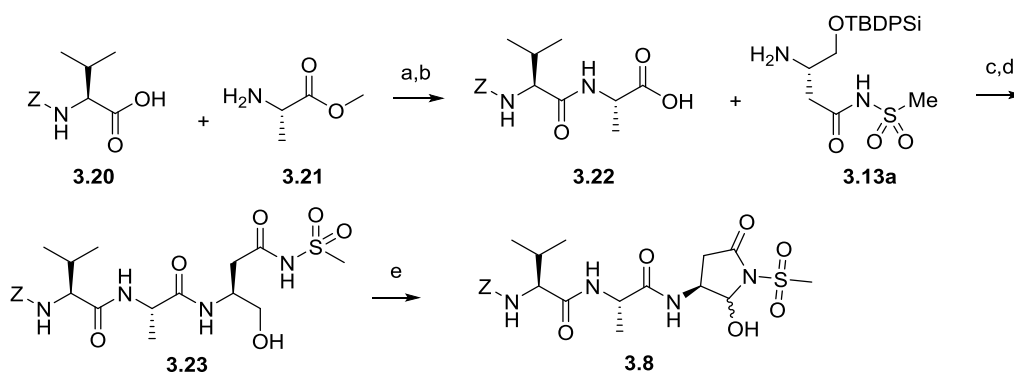
3.4.1 Design and synthesis

The synthetic strategy for aldehyde-based acylsulfonamide analogues of VRT-043198 (**3.3** and **3.4**) consisted of separately synthesizing advanced precursors of the required P1-building blocks (**Scheme 3.1**), after which coupling to the acylated peptide tail of VRT-043198 and oxidative installation of the aldehyde group, was expected to deliver the final products (**Scheme 3.2**). First, side-chain protected Z-Asp(OtBu)-OH was activated with isobutyl chloroformate and the adduct was cleanly reduced with NaBH₄ to yield **3.10**. The resulting primary alcohol was protected with a *tert*-butyldiphenylsilyl protecting group (TBDPS), which proved to be stable under the conditions of the subsequent acidolytic deprotection of the side-chain carboxylate, affording intermediate **3.11**. In the latter, an isosteric acylsulfonamide group was installed through coupling of the free carboxylate with either methane- or ethanesulfonamide using carbonyl diimidazole (CDI) as the coupling reagent to produce **3.12a** and its homologue **3.12b**, respectively.³³ Hydrogenolytic removal of the Z-protecting group, delivered the advanced P1-building block precursors. Standard peptide synthesis procedures were then used for the preparation of dipeptide **3.16**. *N*-acylation of the latter with *N*-Boc-4-amino-3-chlorobenzoic acid (**3.11**) provided the protected peptide tail **3.18**. Protection of the aminobenzoate building block was considered advisory due to concerns of potential aniline incompatibility with the oxidizing agent used in the penultimate step (*vide infra*). Next, P1-building blocks **3.13a** and **3.13b** were coupled with the protected peptide tail and the TBDPS function in intermediates **3.19a** and **3.19b** was cleaved off with



Scheme 3.3. Reagents and conditions: a) $\text{CH}_3\text{SO}_2\text{NH}_2$, EDC.HCl, DMAP, DCM, RT, overnight, 81 %.

To obtain acylsulfonamide analogue **3.8** of Z-VAD-CHO (**Scheme 3.4**), the dipeptide precursor Z-VA-OH (**3.22**) was synthesized from Z-protected valine (**3.20**) and alanine methyl ester (**3.21**), followed by deprotection in basic aqueous media. Next, **3.22** was coupled to P1-building block **3.13a** and transformed into final compound **3.8** after TBDPS-deprotection and oxidation to produce the aldehyde warhead.



Scheme 3.4. Reagents and conditions: a) EDC.HCl, HOBT, DIPEA, DCM, RT, overnight, 52 %; b) LiOH, H_2O , MeOH, RT, 2 h, 54 %; c) isobutyl chloroformate, 4-methylmorpholine, THF, $-20\text{ }^\circ\text{C}$, 3 h; d) TBAF, THF, RT, overnight, 83 % over 2 steps; e) Dess-Martin, DCM, RT, 2 h, 39 %.

3.4.2 Inhibitory potency

3.4.2.1 Human caspase panel

The prepared set of compounds was first evaluated for their inhibitory potency against a panel of human caspases using published protocols.³⁵ The panel was composed of all inflammatory caspases, supplemented with the most relevant representatives of the initiator and executioner subgroups. Reference inhibitors VRT-043198 (**3.2**) and Z-VAD-CHO (**3.7**) displayed IC_{50} values that were in good agreement with data published by other groups (**Tables 3.1 and 3.2**).^{22, 36, 37} Reference **3.5** (NCGC00183434) however, showed slight differences in comparison with published results (*vide infra*).

In the aldehyde series, potencies of the acylsulfonamide-containing inhibitors (**3.3-3.4, 3.8**) were generally similar to those of VRT-043198 and Z-VAD-CHO. These data indeed indicate that the acylsulfonamide group is a promising carboxylate surrogate for caspase ligands. Noteworthy however, this type of isosteric replacement did not turn out to be a proficient instrument to increase selectivity

for a specific caspase. This is directly illustrated by comparison of the caspase-1 selectivity indices (SIs) for VRT-043198 and its analogues, which are roughly comparable for each enzyme. A very limited but consistent increase in caspase-8 and caspase-9 affinity of the isostere-containing analogues **3.3** and **3.4** seems nonetheless present. However, this effect is absent for acylsulfonamide analogue **3.8** of Z-VAD-CHO. It therefore remains to be demonstrated that introduction of an acylsulfonamide isostere in reported caspase-8 or caspase-9 inhibitors would be a good strategy to obtain more selective compounds. Finally, it deserves mentioning that no significant differences were detected between the methyl- and ethyl acylsulfonamide analogues.

Looking at the evaluation data for carbonitriles **3.5** and **3.6**, three observations can be made. First, the presence of a carbonitrile warhead leads to a pronounced decrease in caspase potency, potentially directly related to the lower electrophilicity of this warhead type. As an exception to that trend, the affinity for human caspase-1 of reference **3.5** remains grossly conserved, making this one of the most selective caspase-1 inhibitors known to date. Second, as mentioned above, a noticeable difference is observed with the experiments from Boxer *et al.*²² This group reported a ninefold improvement in potency for human caspase-1 upon changing the warhead from an aldehyde to a carbonitrile group. Moreover, their selectivity indices appear to be generally lower than ours. A potential cause is most likely the use of different substrates in the potency assays. While our potency assays were run with five optimized substrates for the enzymes in the panel, Boxer *et al.* used two general caspase substrates in their experiments.^{38, 39} Furthermore, the acylsulfonamide-containing carbonitrile **3.6** displayed a further decrease in caspase potency. Although we have no definitive rationalization for this finding, it is not inconceivable that introduction of the isosteric replacement significantly impacts on the parts of conformational space that are accessible to the inhibitor. This could preclude optimal positioning of the warhead to efficiently engage in covalent bond formation with the caspases' catalytic cysteine residue.

Table 3.1. IC₅₀ values (in nM) and selectivity indices with respect to h casp-1 for inhibitors **3.2-3.8** in a human caspase panel^a

| Human caspases ^(a) | | | | | | | | | | | | | |
|-------------------------------|-------------|--------------------------|--------------------------|-------------------|--------------------------|--------|--------------------------|--------------------|--------------------------|--------|--------------------------|--------|--|
| Cmp | War-head | Inflammatory caspases | | | | | | Apoptotic caspases | | | | | |
| | | casp-1 | | casp-4 | | casp-5 | | casp-3 | | casp-8 | | casp-9 | |
| | | IC ₅₀ (nM) | IC ₅₀ (nM) | SI ^(b) | IC ₅₀ (nM) | SI | IC ₅₀ (nM) | SI | IC ₅₀ (nM) | SI | IC ₅₀ (nM) | SI | |
| 3.2 | -CHO | 10.5 ± 0.41 | 62.1 ± 4.1 | 5.9 | 190 ± 60 | 18.1 | 10 910 ± 1 151 | 1039 | 59.6 ± 4.2 | 5.7 | 110 ± 29 | 10.4 | |
| 3.3 | -CHO | 20.6 ± 1.8 | 123 ± 48 | 5.9 | 289 ± 118 | 14 | >25 000 | >1214 | 38.9 ± 4.6 | 1.9 | 80 ± 14 | 3.9 | |
| 3.4 | -CHO | 22.1 ± 1.2 | 101 ± 15 | 4.6 | 214 ± 59 | 9.7 | >25 000 | >1132 | 51.9 ± 3.4 | 2.3 | 113 ± 15 | 5.1 | |
| 3.5 | -CN | 34.9 ± 7.4 | 1 272 ± 253 | 36.4 | 850 ± 91 | 24.3 | >100 000 | >2865 | 4 184 ± 853 | 118.9 | 2 846 ± 225 | 81.5 | |
| 3.6 | -CN | 5 264 ± 866 | >100 000 | >19 | >50 000 | >9.5 | >100 000 | >19 | >100 000 | >19 | >25 000 | >4.7 | |
| 3.7 | -CHO | 685 ± 70 | >50 000 | >73 | 2 813 ± 180 | 4.1 | >100 000 | >146 | 6 309 ± 1 297 | 9.2 | 405 ± 35 | 0.6 | |
| 3.8 | -CHO | 1 966 ± 382 | >50 000 | 25.4 | 7 840 ± 2 038 | 4 | >100 000 | >51 | 13 464 ± 2 928 | 6.85 | >25 000 | >12.7 | |

^(a)Substrates tested were Ac-WEHD-AMC for casp-1,-4,-5; Ac-DEVD-AMC for casp-3; Ac-IETD-AMC for casp-8 and Ac-LEHD-AMC for casp-9. ^(b)Selectivity Indices (SIs) were calculated as (IC₅₀(caspase-x)/IC₅₀(caspase-1))

3.4.2.2 Murine caspase panel

Since caspase-1 inhibitors **3.2-3.6** were evaluated in a mouse-derived model of cellular inflammation (*vide infra*), these compounds were also evaluated against a panel of murine inflammatory caspases (**Table 3.2**). Similar to the human caspase panel, acylsulfonamides **3.3** and **3.4** show comparable potencies as for the reference inhibitor (**3.2**). However, in contrast to the human inflammatory panel, the selectivity has been largely favored for murine caspase-1, which is surprising since caspase-11 is considered the murine homolog of human caspase-4 and -5. While carbonitrile-containing reference inhibitor **3.5** shows a moderate potency decrease, its selectivity towards murine caspase-1 is even more distinct. Similar to the human caspase panel, the acylsulfonamide analogue **3.6** does not present promising inhibitory potencies.

Table 3.2. IC₅₀ values (in nM) and selectivity indices with respect to m casp-1 for inhibitors **3.2-3.6** in a murine caspase panel^a

| Murine inflammatory caspases ^(a) | | | | | | | |
|---|-------------|--------------------------|-------------------|--------------------------|-------------------|--------------------------|---------|
| Cmp | Warhead | casp-1 | | casp-11 | | casp-12 | |
| | | IC ₅₀ (nM) | SI ^(b) | IC ₅₀ (nM) | SI ^(b) | IC ₅₀ (nM) | SI |
| 3.2 | -CHO | 5.47 ± 0.28 | | 5 604 ± 767 | 1024 | >100 000 | >18 281 |
| 3.3 | -CHO | 15.5 ± 1.8 | | 11 409 ± 4 598 | 736 | >100 000 | >6 451 |
| 3.4 | -CHO | 7.0 ± 1.2 | | 7 991 ± 1 312 | 1142 | >100 000 | >14 285 |
| 3.5 | -CN | 145 ± 20 | | >100 000 | >689.7 | >100 000 | >689.7 |
| 3.6 | -CN | 6 503 ± 623 | | >100 000 | >15.4 | >100 000 | >15.4 |

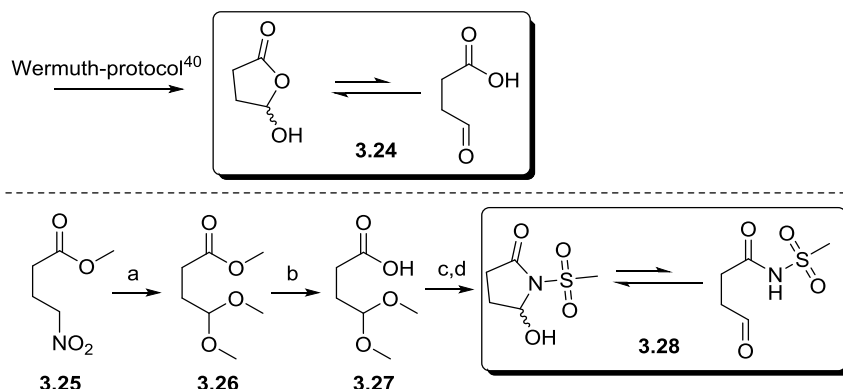
^(a)Substrates tested were Ac-WEHD-AMC for m casp-1 and -11 and Ac-ATAD-AFC for m casp-12. ^(b)Selectivity indices were calculated as (IC₅₀(caspase-x)/IC₅₀(caspase-1))

3.4.3 Structural elaboration of the P1-moiety

The IC₅₀-values in **Tables 3.1** and **3.2** clearly indicate that the acylsulfonamide function could serve as a carboxylate surrogate in caspase drug discovery. Nonetheless, gaining insight in the inhibitors' conformational behavior seemed essential for further understanding of the potency data. Analogous to the well-known intramolecular acyl hemiacetal formation in **3.2** and **3.7**, acylsulfonamides could theoretically engage in intramolecular cyclization by addition of the acylsulfonamide onto the warhead function. Furthermore, this reaction could be reversible or (practically) irreversible under ambient conditions. Since cyclic products would lack both the acidity required for caspase recognition and the electrophilic warhead function, ring-closed products can reasonably be expected to lack enzyme affinity, similar to the situation with carboxylate-based compounds. The following factors were therefore important to address for the acylsulfonamides: 1) their tendency to form cyclic tautomers, and, if so, 2) the relative stabilities of the open and ring-closed forms. 3) Finally, to assess whether equilibration between both forms is possible under ambient conditions, the reversibility and activation energy of the tautomerization process would be interesting to probe. No literature data were present that address these issues.

A first hint at the tautomeric behavior of the acylsulfonamides was obtained from the NMR-spectra of the molecules. In the ¹³C spectra of **3.3**, **3.4** and **3.8** (that combine an acylsulfonamide and aldehyde function) in MeOD-*d*₄ or DMSO-*d*₆, no aldehyde carbons were detected. Instead, in each case one specific signal around 87 ppm was present that could not be assigned to a carbon of the corresponding peptidomimetic/peptidic tail, therefore suggesting that these acylsulfonamide-containing inhibitors adapt other tautomeric forms. A similar pattern was observed in the corresponding carboxylate-based reference compounds **3.2** and **3.7** (data not shown). In the case of carbonitrile **3.6** however, no cyclized form was observed (100 % abundance of the specific acidic proton) (data in supporting information). To gain further insight into the tautomeric preferences for molecules containing a 1,2-carbaldehyde-acylsulfonamide functionalization, an additional NMR study was carried out using fragment-sized probes **3.24** and **3.28** (**Scheme 3.5**). Choosing these compounds has the advantage of avoiding any compound-specific biases in the experiments (*e.g.*, interference with cyclization by the peptide tail of the inhibitors). In addition, interpretation and integration of NMR spectra is easier for fragments than in the inhibitor series: there, cyclization creates an additional stereocenter, leading to diastereomerization and resulting in peak splitting. In case of overlaps with other peaks in the spectra, this would complicate peak integration. The first fragment, succinic semialdehyde (**3.24**) was prepared according to a procedure by Wermuth.⁴⁰ To obtain the isosteric acylsulfonamide fragment **3.29**, the terminal nitro group in **3.25** was first transformed into an acetal via a modified Nef protocol.⁴¹ After

deprotection of the methyl ester, coupling with methanesulfonamide was performed. Lastly, acidic hydrolysis of the acetal led to fragment **3.28**.



Scheme 3.5. Reagents and conditions: a) NaOMe, MeOH, 0 °C, 30 min, followed by H₂SO₄, MeOH, 0 °C, 45 min, 81 %; b) 1 M NaOH (aq), MeOH, RT, overnight, 90 %; c) CH₃SO₂NH₂, DMAP, EDC.HCl, overnight, RT; d) TFA, H₂O, RT, 18 h, 32 % over 2 steps.

Both fragments were analyzed with ¹H- and ¹³C-NMR spectroscopy in protic and aprotic solvents. Identification of the individual tautomers/derivatives occurring in solution was done based on the chemical shifts of the circled hydrogen and carbon atoms in **Figure 3.3**. In aprotic solvents, such as dimethyl sulfoxide or chloroform, reference **3.24** was found to be present in a 2:1 aldehyde:cyclic hemiacetal equilibrium (**Table 3.3**). In methanol and water, only the acyclic methyl hemiacetal (**3.29a**) and the hydrated aldehyde (**3.29b**), respectively, were observed. In case of acylsulfonamide fragment **3.28** however, the equilibrium was totally shifted to the cyclic acyl hemiaminal form in CDCl₃ and D₂O (**Table 3.4**). Only in MeOD-*d*₄ a small fraction (12 %) was observed in the acyclic methyl hemiacetal tautomer (**3.30a**). In none of these cases an aldehyde proton/carbon was detected.

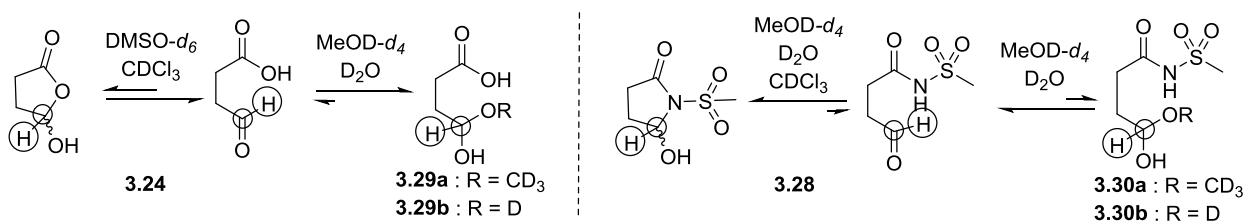


Figure 3.3. Overview of tautomers and derivatives of **3.24** and **3.28** observed in the ¹H and ¹³C NMR study. Chemical shifts of circled atoms were used as diagnostic for structure assignment.

Table 3.3. ^1H and ^{13}C NMR chemical shifts of aldehyde hydrogen and carbon atoms of **3.24** (circled in **Figure 3.3**) in different solvents.

| Solvent | δ (^1H NMR) | | δ (^{13}C NMR) | Occurrence | Ratio |
|-------------|------------------------------|---|---------------------------------|------------------------|-------|
| MeOD- d_4 | 4.58 | t | 97.34 | methyl hemiacetal | 100 % |
| D $_2$ O | 4.99 | t | 90.00 | hydrate | 100 % |
| DMSO- d_6 | 9.67 | s | 202.52 | aldehyde | 66 % |
| | 5.80 | m | 99.79 | cyclic acyl hemiacetal | 33 % |
| CDCl $_3$ | 9.83 | s | 199.96 | aldehyde | 66 % |
| | 5.95 | m | 98.91 | cyclic acyl hemiacetal | 33 % |

Table 3.4. ^1H and ^{13}C NMR chemical shifts of aldehyde hydrogen and carbon atoms of **3.28** (circled in **Figure 3.3**) in different solvents.

| Solvent | δ (^1H NMR) | | δ (^{13}C NMR) | Occurrence | Ratio |
|-------------|------------------------------|----|---------------------------------|------------------------|-------|
| MeOD- d_4 | 4.58 | t | 98.55 | methyl hemiacetal | 12 % |
| | 5.82 | dd | 84.81 | cyclic acyl hemiaminal | 88 % |
| D $_2$ O | 5.93 | dd | 84.90 | cyclic acyl hemiaminal | 100 % |
| CDCl $_3$ | 5.91 | dd | 83.38 | cyclic acyl hemiaminal | 100 % |

The data in **Table 3.3** and **3.4** seem to be in general agreement with the preliminary observations for peptide-based inhibitors in this study. Notably in water, the relative stabilities of the aldehyde tautomers of both **3.24** and **3.28** are lower than that of the corresponding hydrate and the cyclic acyl hemiaminal, respectively: this is directly reflected by the product distributions in solution. The absence of a hydrated derivative for **3.28** furthermore seems to indicate that the cyclized acyl hemiaminal tautomer is particularly stable in water. This observation could be relevant for interpreting caspase binding data for inhibitors containing fragment **3.28**, since strong intramolecular stabilization generally implies a significant penalty for the thermodynamic target affinity of compounds. More specifically, thermodynamic affinity correlates with the overall Gibbs free energy difference (ΔG) for the target binding process, starting with unbound inhibitor and target caspase, and ending with the formed [inhibitor-target] complex. Intramolecular stabilization (lowering the inhibitor's initial Gibbs free energy), will therefore reduce the overall ΔG -value (ΔG_1) compared to the situation where a ring-opened form of the inhibitor would be mainly present in solution (ΔG_2) (**Figure 3.4**). Theoretically, an inhibitor with improved affinity could be obtained by selecting a suitable warhead functionality that does not engage in intramolecular adduct formation with the acylsulfonamide. The potency data obtained for carbonitrile-based compound **3.6** nonetheless demonstrate that suitable warhead identification is not a trivial task in caspase inhibitor design.

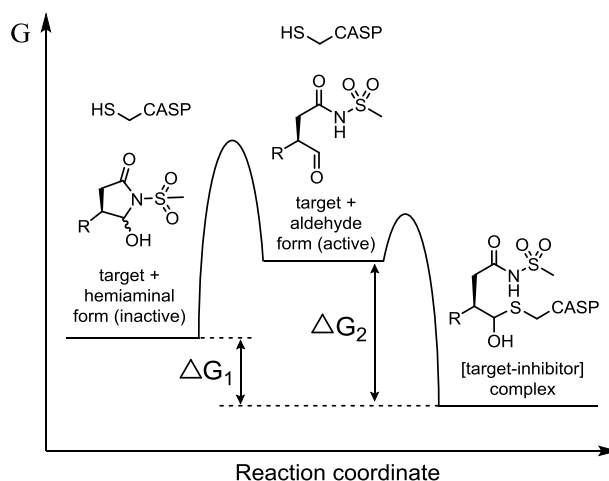


Figure 3.4. Hypothetical reaction diagram for formation of enzyme-inhibitor complex with inhibitors containing fragment **3.28**.

Finally, we used an experimental approach to qualitatively probe the dynamics of the equilibrium between the stable acyl hemiaminal tautomer and the ring-opened form of the inhibitor that is required for target binding. If the activation energy barrier to tautomerization would be significantly higher than in the carboxylate case, the acylsulfonamide inhibitors would be characterized by a very slow target binding process. This in turn would call for extending the pre-incubation time between enzyme and inhibitor in the enzymatic assays in order to obtain realistic potency data. As a proxy for equilibrium kinetics, the rate of hydrazone formation of **3.28** with phenylhydrazine in aqueous media was investigated (**Figure 3.5**). Hydrazone formation requires the presence of a reactive aldehyde function, implying tautomerization from the acyl hemiaminal to the ring-opened tautomer. As a reference, the same reaction with **3.24** was taken.

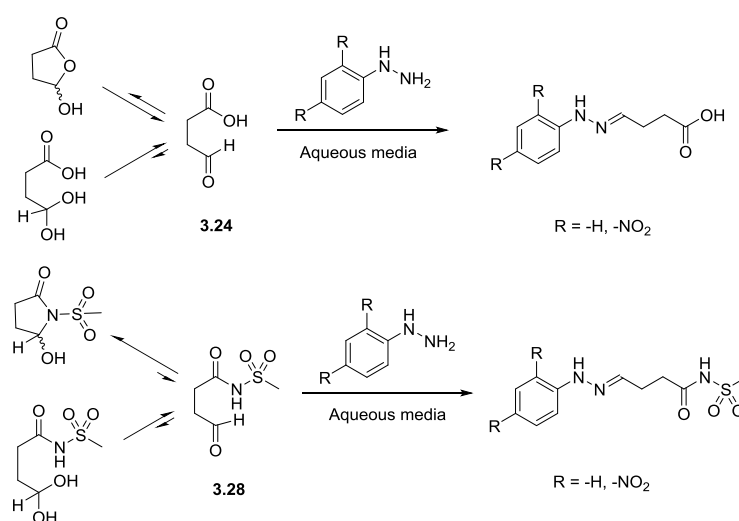


Figure 3.5. Determination of the equilibrium kinetics of **3.24** and **3.28** by hydrazone formation. Quantification of the corresponding hydrazone was carried out with LC-MS.

In both cases, full conversion to the corresponding hydrazone was observed after 5 minutes (quantification was carried out with LC-MS). Furthermore, experiments with the less reactive (2,4-dinitrophenyl)hydrazine had an identical outcome. These findings indicate that the tautomerization process is sufficiently fast to not interfere with the potency assay protocols used.

3.4.4 Stability measurements

The chemical stability of all studied compounds in buffered aqueous conditions (pH 4 and 7.4) was quantified over a period of 24 hours (**Figure 3.6**). All reference and acylsulfonamide inhibitors displayed satisfactory chemical stability at pH 4. At physiological pH however, acylsulfonamides **3.3**, **3.4** and **3.8** (possessing an aldehyde warhead) degraded relatively quickly, with half-lives around 1 hour. Identical results were obtained in metabolic stability tests with human and murine liver microsomes, indicating that eventual specific metabolization processes for these compounds are subordinate to the non-enzymatic breakdown process taking place at physiological pH. Closer inspection learned that in all conditions, a clean hydrolysis of **3.3**, **3.4** and **3.8** into the corresponding carboxylates **3.2** and **3.7** was the only degradation pathway present (data in supporting information). Noteworthy, the nitrile containing acylsulfonamide **3.6** was found to be stable under all conditions.

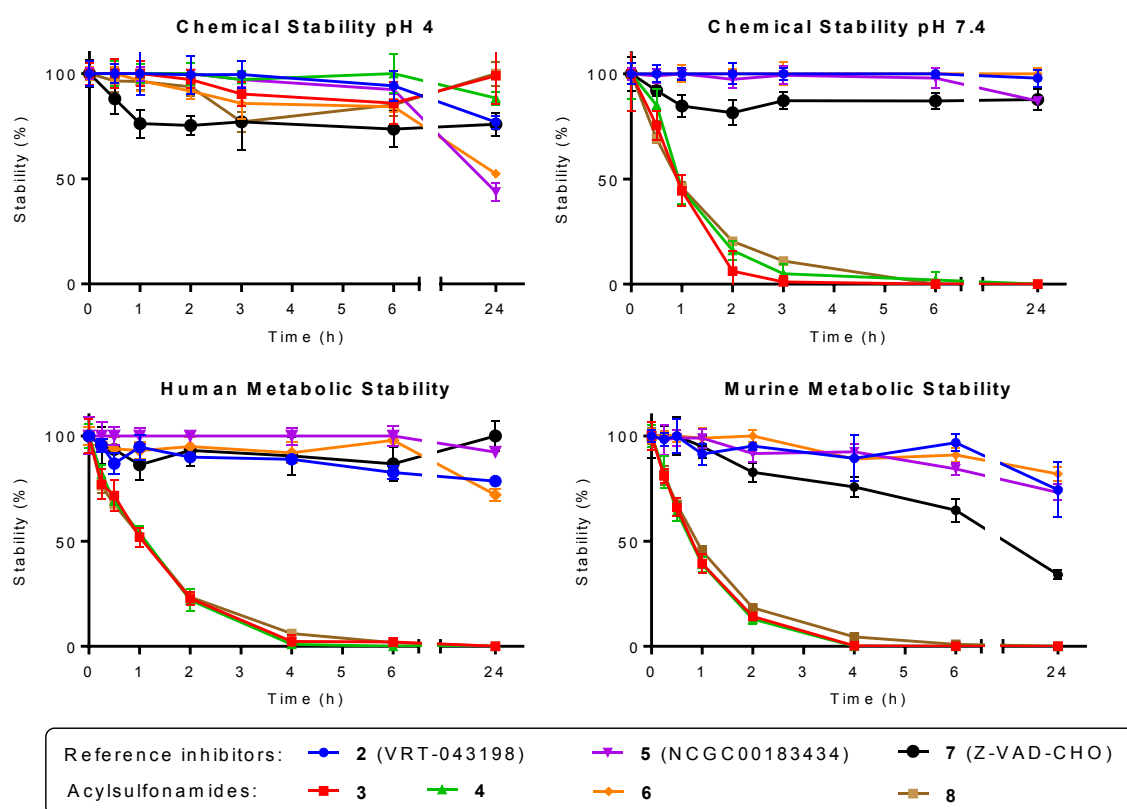


Figure 3.6. Stability profiles of all inhibitors. Measurements were carried out for 24 hours.

As a rationale for the selective hydrolysis of the aldehyde containing inhibitors, their ability to engage in cyclic acyl hemiaminal formation seems highly likely. Functionalization of the acylsulfonamide NH (*e.g.*, by alkylation, or in this case, via acyl hemiaminal formation) is well known to destabilize the functional group and to make it more sensitive to nucleophilic attack. This principle is, for example, applied in the reversed Kenner safety-catch linker used in solid-phase peptide synthesis. (**Figure 3.7**).⁴² Nonetheless, to the best of our knowledge we are the first to report instability for this type of inhibitors.

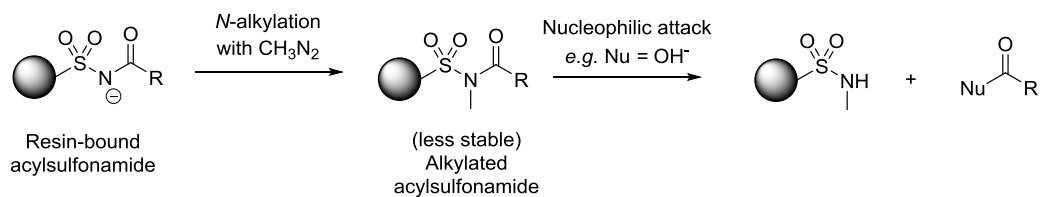


Figure 3.7. Principle of the reversed Kenner safety-catch linker. Figure was derived from ref [42].

Regardless, the stability issue is highly relevant, since it implies that IC₅₀ values for **3.3**, **3.4** and **3.8** (**Tables 3.1** and **3.2**) could be flawed, and rather represent the affinities of the corresponding carboxylate-containing parent compounds **3.2** and **3.7** (formed upon hydrolysis). Close inspection however demonstrated that the results obtained for **3.3**, **3.4** and **3.8** correctly reflected enzyme potencies of the acylsulfonamides. More specifically, all experiments were terminated within a timeframe of 35 minutes following dilution of the inhibitors from freshly prepared DMSO stocks. In addition, all inhibitors were found not to degrade in DMSO. Although **3.3**, **3.4** and **3.8** can be expected to partially hydrolyze (up to 30% at the end point) during the 35 minutes of the assay, the progress curves for these compounds clearly showed a constant degree of inhibition throughout the measurement. Hypothetically speaking, significant progress curve flattening or steepening would be visible in case the starting acylsulfonamides would have different potencies than the carboxylate analogues into which they are gradually transformed. Nonetheless, curve profiles clearly indicate that the intrinsic IC₅₀-values for **3.3**, **3.4** and **3.8** are comparable to those for **3.2** and **3.7**.

Since the acylsulfonamide inhibitors with an aldehyde warhead combine 1) stability at lower pH, 2) higher reported gastro-intestinal permeability than the corresponding carboxylates and 3) gradual conversion into the latter upon elevation of the pH, they can be considered potential prodrug candidates. In this view, the acylsulfonamides would start releasing the carboxylate inhibitors once in circulation, after diffusing through the gastro-intestinal epithelium. Esters, as in VX-765, are the most commonly used prodrugs for pharmacophoric carboxylate functions. However, inter-individual differences in plasma/liver esterase activity can lead to unpredictable bioconversion of esters. Likewise, low levels of plasma esterase activity are known to result in incomplete bioconversion and

lower than predicted bioavailability.⁴³ The non-enzymatic hydrolysis at physiological pH observed for the acylsulfonamide function in **3.3**, **3.4** and **3.8** could therefore constitute an efficient alternative for the use of ester prodrugs. Several acylsulfonamide prodrugs have been reported in literature, including the recently approved prostacyclin receptor agonist selexipag.⁴⁴⁻⁴⁹ Generally lacking intramolecular cyclization/derivatization potential, these compounds also mostly rely on slow, metabolic activation of the acylsulfonamide function to release a physiologically active carboxylate or sulfonamide drug.

3.4.5 Biological assays

Finally, VRT-043198 (**3.2**), its carbonitrile analogue **3.5** and the acylsulfonamide derivatives of both (**3.3**, **3.4** and **3.6**) were investigated as inhibitors of caspase-1 and caspase-11 mediated inflammatory responses in mouse macrophages. As described earlier, combined stimulation of mouse macrophages with lipopolysaccharide (LPS) and the ionophore nigericin results in caspase-1-dependent pyroptosis and secretion of mature IL-1 β and IL-18 through the 'canonical Nlrp3 inflammasome'. In contrast cytosolic delivery of LPS provokes caspase-11-mediated pyroptosis, with secretion of IL-1 β and IL-18 requiring both caspases 1 and 11 in the 'non-canonical' Nlrp3 inflammasome pathway.^{4,50} Both cell death (quantified based on lactate dehydrogenase (LDH) release in the medium) and IL-1 β and -18 levels were monitored as read-outs of the experiments (**Figure 3.8** and **3.9**). All inhibitors were evaluated at 50 mM concentration. In line with published results, the highly potent but poorly selective irreversible fluoromethylketone (fmk) inhibitors Z-VAD-fmk and Z-WEHD-fmk served as positive controls.

VRT-043198 (**3.2**) and its direct acylsulfonamide analogues (**3.3** and **3.4**) reduced cell death counts and secreted IL-1 β and -18 levels with comparable potency in both assay types. As can be anticipated by the significantly higher caspase-1 affinity (compared to caspase-11 affinity) of all compounds, the strongest effect was seen on interleukin maturation levels, while the impact on cell death was considerably smaller. These observations roughly reflect the comparable potencies of the inhibitors in the IC₅₀-assays. At the same time, the data suggest that the acylsulfonamide containing inhibitors do not benefit from a significantly higher cellular permeability at this concentration. Furthermore, **3.3** and **3.4** can be expected to hydrolyze to a significant extent during the experiment (read-out takes place 105 minutes after inhibitor dosing). Notwithstanding this, the eventual presence of a permeability advantage for the acylsulfonamides would still be anticipated to translate in significantly higher cellular potencies: hydrolysis taking place after compound permeation can reasonably be expected to lead to entrapment and accumulation of a potent inhibitor in the cytoplasm. This finding contrasts with earlier data by Okamoto *et al.*, who reported cellular permeabilities that were an order of magnitude higher for an acylsulfonamide inhibitor compared to a carboxylate reference.²³ Noteworthy, Okamoto *et al.* also did not report stability data for their acylsulfonamide inhibitor. Structural considerations however,

would also lead to the conclusion that this literature compound has similar limited stability as **3.3** and **3.4**.

In case of the carbonitrile-based inhibitors, carboxylate **3.5** showed a less pronounced effect on caspase-1 and -11 dependent cell death and interleukin levels compared to reference inhibitor **3.2**. Again, this is reflected by the relative potencies of both compounds in the IC₅₀-assays. Finally, acylsulfonamide **3.6** does not cause a significant decrease of the inflammatory response. Also for this molecule, the results in the cellular assay roughly correspond to the IC₅₀ values for murine caspases-1 and -11.

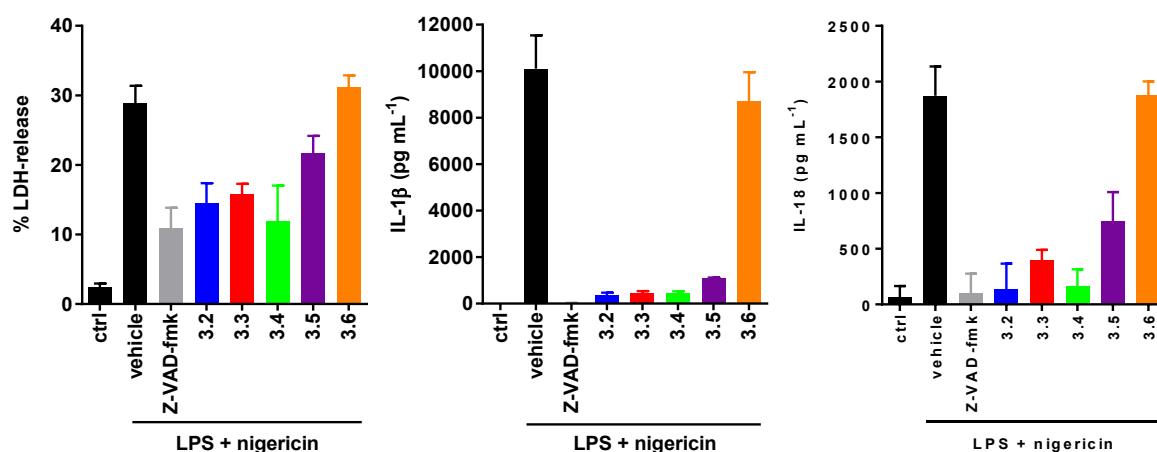


Figure 3.8. Canonical Nlrp3 inflammasome-mediated pyroptosis and secreted IL-1 β and -18 levels of stimulated macrophages after treatment with inhibitors **3.2-3.6**. The inhibitor concentration used was 50 μ M for all compounds. The blank experiment (“ctrl”) corresponds to cells that were left untreated. “Vehicle” represents cells that were only treated with the inhibitor vehicle, DMSO, prior to nigericin challenge. “Z-VAD-fmk” represents a positive control experiment. Data represent mean \pm s.d. of one out of three biological replicates, with three technical replicates each.

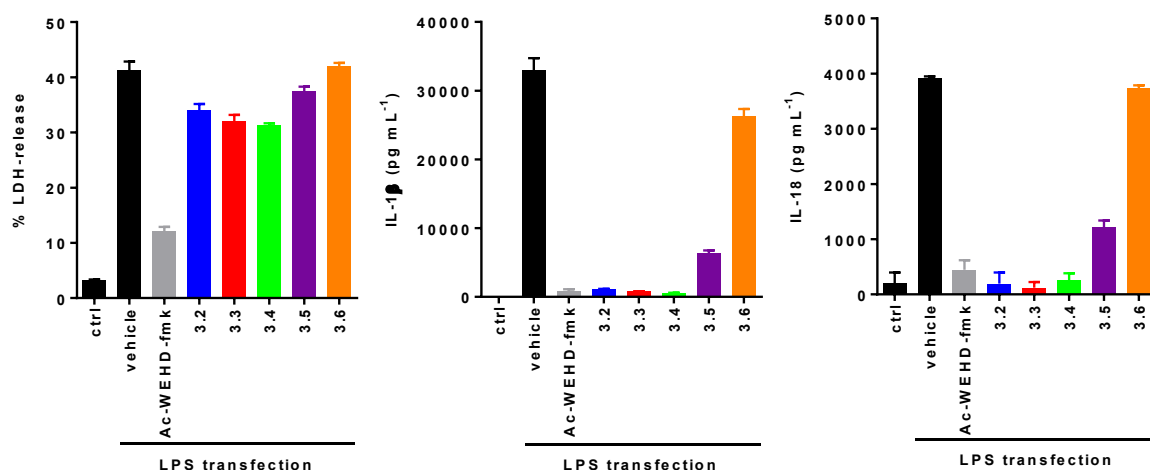


Figure 3.9. Non-canonical Nlrp3 inflammasome-mediated pyroptosis and secreted IL-1 β and -18 levels of stimulated macrophages after treatment with inhibitors **3.2-3.6**. The inhibitor concentration used was 50 μ M for all compounds. The blank experiment (“ctrl”) corresponds to cells that were left untreated. “Vehicle” represents cells that were only treated with the inhibitor vehicle, DMSO, prior to LPS transfection. “Ac-WEHD-fmk” represents a positive control experiment. Data represent mean \pm s.d. of one out of three biological replicates, with three technical replicates each.

3.5 Conclusions

Acylsulfonamides were explored as carboxylate isosteres in caspase inhibitors. Analogues of the clinically investigated caspase-1 inhibitor VRT-043198 and of the *pan*-caspase inhibitor Z-VAD-CHO were synthesized. The isostere-containing analogues with an aldehyde warhead were found to display inhibitory potencies comparable to the carboxylate reference. In addition, a ^1H - and ^{13}C -based NMR study was carried out to study conformational and tautomeric characteristics of these compounds. The propensity of acylsulfonamides with an aldehyde warhead to occur in a ring-closed conformation at physiological pH, was found to significantly increase hydrolysis of the acylsulfonamide moiety, yielding the parent carboxylate containing inhibitors. These results indicate that the acylsulfonamide analogues of the aldehyde-based inhibitor VRT-043198 might have potential as a novel type of prodrug for the latter. Finally, caspase-1 and -11 mediated cellular inflammation experiments were carried out. Obtained data were found to be in line with the potency data in the enzymatic assays. At the inhibitor concentrations used with the stimulated macrophages, a clear cellular permeability advantage was absent for the acylsulfonamides. Nonetheless, in depth evaluation of the gastro-intestinal absorption profile of these molecules could be interesting to further assess their prodrug potential.

3.6 Experimental

3.6.1 Chemistry

Reagents were obtained from Sigma-Aldrich, Acros, Fluorochem or Apollo Scientific and were used without further purification. Synthesized compounds were characterized by ^1H NMR, ^{13}C NMR and mass spectrometry. ^1H NMR and ^{13}C NMR spectra were recorded with a 400 MHz Bruker Avance DRX 400 spectrometer. and analyzed by use of MestReNova analytical chemistry software. Purities were determined with a Waters Acquity UPLC system coupled to a Waters TUV detector. ESI source and a Waters Acquity Qda Mass Detector. ADME measurements (UPLC-MS/MS) were carried out on a Waters Acquity UPLC system coupled to a Waters TUV detector, ESI source and a Waters Acquity TQ Mass Detector. HRMS involved 10 μL injection of a 10 μM sample solution using the CapLC system (Waters) and electrospray using a standard electrospray source. Positive ion mode accurate mass spectra were acquired using a Q-TOF II instrument (Waters). The mass spectrometer was calibrated prior to use with a 0.2% H_3PO_4 solution. The spectra were lock mass-corrected using the known mass of the nearest H_3PO_4 cluster. Where necessary, flash purification was performed with a Biotage ISOLERA One flash system equipped with an internal variable dual-wavelength diode array detector (200–400 nm).

(S)-tert-Butyl 3-(((benzyloxy)carbonyl)amino)-4-hydroxybutanoate (3.10)

To a cold (-5°C) solution of Z-Asp-(OtBu)-OH (**3.9**, 2 g, 6.19 mmol) in anhydrous DME (50 mL), were successively added triethylamine (0.95 mL, 6.80 mmol) and isobutylchloroformate (1.05 mL, 8.04 mmol). After 5 min the reaction mixture was filtered, and the precipitate was washed with additional DME (2 x 20 mL). The filtrate and the washings were combined and cooled to -5°C. A solution of Sodiumborohydride (702 mg, 18.56 mmol) in water (10 mL) was added in several portions, producing a strong evolution of gas, which ceased rapidly. After 5 min, additional water (60 mL) was added to the mixture and stirring was continued for 1 h. The mixture was extracted with EtOAc (2 x 60 mL). The organic layers were combined, dried (Na₂SO₄) and concentrated *in vacuo*. A transparent oil was obtained (1.80 g, 94 %). ¹H NMR (400 MHz, CDCl₃) δ 1.43 (s, 9H), 2.52 (m, 2H), 3.15 (s, 1H), 3.66 (d, *J* = 4.8 Hz, 2H), 3.98 - 4.12 (m, 1H), 5.09 (m, 2H), 5.70 (d, *J* = 8.2 Hz, 1H), 7.34 ppm (m, 5H); ¹³C NMR (101 MHz, CDCl₃) δ 28.01, 37.25, 50.0, 64.19, 66.79, 81.33, 128.00-128.20 (2 signals), 128.50, 136.39, 156.32, 171.06 ppm; UPLC-MS *m/z*: 310.4 [M+H]⁺.

(S)-3-(((Benzyloxy)carbonyl)amino)-4-((tert-butyldiphenylsilyl)oxy)butanoic acid (3.11)

tert-Butyl chlorodiphenylsilane (1.720 mL, 6.61 mmol), imidazole (0.614 g, 9.02 mmol) and 4-dimethylaminopyridine (0.110 g, 0.902 mmol) was added to a solution of **3.10** (1.86 g, 6.01 mmol) in DCM (25 mL) at 0 °C. A white precipitate formed. The solution was allowed to warm to room temperature and was stirred overnight under nitrogen atmosphere. The reaction mixture was quenched with water (50 mL). The mixture was extracted with DCM (2 x 50 mL). The combined organic layers were washed with saturated ammonium chloride solution (30 mL) and brine (30 mL), dried (Na₂SO₄) and concentrated *in vacuo*. Flash chromatography was performed (90:10 Hex:EtOAc) to give protected alcohol (3.8 g) *R*_f = 0.25 (1:1 Hex:EtOAc, visualization by UV); ¹H NMR (400 MHz, CDCl₃) δ 1.11 (m, 19H (impured)), 1.44 (s, 9H), 2.56 - 2.67 (m, 2H), 3.75 (m, 2H), 4.16 (m, 1H), 5.12 (s, 2H), 5.33 (d, *J* = 8.5 Hz, 1H), 7.42 (m, 17H), 7.63 - 7.69 (m, 4H), 7.73 - 7.78 ppm (m, 4H); ¹³C NMR (101 MHz, CDCl₃) δ 26.60, 28.05, 31.61, 37.14, 49.64, 64.87, 66.66, 81.02, 127.62 - 127.90 (m), 128.05, 128.49, 129.53 - 129.93 (m), 133.06, 133.17, 134.82, 135.29, 135.52, 135.54, 136.58, 155.69, 170.65 ppm. 3.2 g of the intermediate was dissolved in DCM (20 mL) and stirred at room temperature. Slowly TFA (20 mL) was added. After 30 min the reaction was stopped. DCM (200 mL) and H₂O (200 mL) were added to the mixture. Extraction was done. The aqueous phase was washed with DCM (200 mL). The organic layers were combined, dried (Na₂SO₄) and concentrated *in vacuo*. The residue was purified using flash chromatography (+ 0.5% FA) to give compound **3.11** (1.1 g, 46 % over steps). *R*_f = 0.67 (1:1 Hex:EtOAc, visualization by UV); ¹H NMR (400 MHz, CDCl₃) δ 1.08 (s, 8H), 1.10 (s, 3H), 2.74 (d, *J* = 5.7 Hz, 2H), 3.76 (s, 2H), 4.15 (m, impured, 1H), 5.11 (s, 2H), 5.35 (m, impured, 3H), 7.30 - 7.48 (m, 12H), 7.60 - 7.67 (m,

3H), 7.72 - 7.77 ppm (m, 1H); ^{13}C NMR (101 MHz, CDCl_3) δ 26.57, 26.85, 35.51, 49.20, 49.36, 64.75, 66.95, 127.74, 127.83, 128.20, 128.55, 129.68, 129.92, 132.80, 132.86, 134.81, 135.13, 135.53, 153.55, 155.90, 176.22 ppm; UPLC-MS m/z : 492.4 $[\text{M}+\text{H}]^+$.

Benzyl (S)-(1-((*tert*-butyldiphenylsilyl)oxy)-4-(methylsulfonamido)-4-oxobutan-2-yl)carbamate (3.12a)

Carbonyldiimidazole (0.660 g, 4.07 mmol) was added to a solution of **3.5** (1g, 2.034 mmol) in THF (10 mL) under an atmosphere of nitrogen. The reaction mixture was stirred for 3 h at room temperature. Methanesulfonamide (0.387 g, 4.07 mmol) was added followed by the addition of 1,8-diazabicyclo[5.4.0]undec-7-ene (0.608 mL, 4.07 mmol). The resulting mixture was stirred at room temperature overnight. The reaction mixture was diluted with EtOAc, washed with 1 N HCl, water, brine, dried (Na_2SO_4) and concentrated *in vacuo* to give a white foam (1.24 g, quant.). R_f = 0.56 (1:1 EtOAc:Hex + 0.1% FA, visualization by UV); ^1H NMR (400 MHz, CDCl_3) δ 1.08 (s, 9H), 2.66 (m, 2H), 3.16 (s, 3H), 3.74 (d, J = 3.7 Hz, 2H), 5.10 (d, J = 2.0 Hz, 2H), 5.37 (s, 1H), 7.30 - 7.49 (m, 12H), 7.58 - 7.68 (m, 4H), 9.48 ppm (s, 1H). ^{13}C NMR (101 MHz, CDCl_3) δ 19.28, 26.90, 41.23, 64.95, 67.26, 127.97, 128.14, 128.33, 128.61, 130.12, 132.51, 132.62, 135.49, 135.52, 136.00, 156.52, 169.85 ppm; UPLC-MS m/z : 567.6 $[\text{M}-\text{H}]^-$.

(S)-3-Amino-4-((*tert*-butyldiphenylsilyl)oxy)-N-(methylsulfonyl)butanamide (3.13a)

10% Palladium on carbon (49 mg, 0.459 mmol) was added to a solution of **3.6** (870 mg, 1.530 mmol) in dry MeOH (40 mL). The solution was flushed with nitrogen and the mixture was stirred under several balloons of hydrogen gas for 18 h. The reaction mixture was filtered through Celite and eluted with EtOAc and MeOH. The filtrate was concentrated *in vacuo*. Amine **3.13a** was obtained (630 mg, 95 %). UPLC-MS m/z : 435.2 $[\text{M}+\text{H}]^+$.

Benzyl (S)-(1-((*tert*-butyldiphenylsilyl)oxy)-4-(ethylsulfonamido)-4-oxobutan-2-yl)carbamate (3.12b)

The title compound was prepared from **3.11** (1 g, 2.034 mmol) and ethanesulfonamide (0.444 g, 4.07 mmol) in the same manner as described for the synthesis of **3.12a**. Compound **3.12b** was obtained as a white foam (0.96 g, 81 %). R_f = 0.56 (1:1 EtOAc:Hex + 0.1% FA, visualization by UV); ^1H NMR (400 MHz, CDCl_3) δ 1.08 (s, 9H), 1.20 - 1.37 (m, 3H), 2.69 (m, 2H), 3.36 (q, J = 7.4 Hz, 2H), 3.67 - 3.80 (m, 2H), 4.15 (m, 2H), 5.09 (s, 2H), 5.35 - 5.48 (d, J = 6.14 Hz, 1H), 7.30 - 7.49 (m, 11H), 7.59 - 7.68 (m, 4H), 9.46 ppm (s, 1H); ^{13}C NMR (101 MHz, CDCl_3) δ 7.63, 19.28, 26.90, 38.83, 47.80, 49.70, 64.93, 67.18, 127.93, 127.94, 128.08, 128.27, 128.58, 130.04, 130.07, 132.61, 132.74, 135.49, 135.52, 136.05, 156.41, 170.04 ppm; UPLC-MS m/z : 583.6 $[\text{M}+\text{H}]^+$.

(S)-3-Amino-4-((tert-butylidiphenylsilyloxy)-N-(ethylsulfonyl)butanamide (3.13b)

The title compound was prepared from **3.12b** (1.07 g, 1.836 mmol) in the same manner as described for the synthesis of **3.13a**. Amine **3.13b** was obtained (0.86 g, quant.). UPLC-MS m/z : 449.3 [M+H]⁺.

(S)-tert-Butyl 1-((S)-2-(((9H-fluoren-9-yl)methoxy)carbonyl)amino)-3,3-dimethylbutanoyl)pyrrolidine-2-carboxylate (3.15)

A solution of *N,N*-di-iso-propylethylamine (2.96 mL, 16.98 mmol) and H-Pro-OtBu-HCl (3.05 g, 14.68 mmol) in DMF (15 mL) was added to a solution of Fmoc-Tle-OH (5 g, 14.15 mmol), EDC·HCl (3.25 g, 16.98 mmol) and 1-hydroxybenzotriazole hydrate (2.60 g, 16.98 mmol) in DMF (35 mL). The mixture was stirred at room temperature overnight. The reaction mixture was diluted with EtOAc (250 mL), washed with 1 M HCl (200 mL), 5 % aqueous NaHCO₃ (200 mL) and brine (150 mL). The organic layer was dried over Na₂SO₄ and concentrated *in vacuo*. Dipeptide **3.15** was obtained (7.3 g, 100 %). R_f = 0.61 (1:1 Hex:EtOAc, visualization by UV); UPLC-MS m/z : 507.3 [M+H]⁺.

Diethylammonium (S)-1-((S)-2-amino-3,3-dimethylbutanoyl)pyrrolidine-2-carboxylate (3.16)

Dipeptide **3.15** was dissolved in DCM (25 mL) and TFA (25 mL) was added. The reaction mixture was stirred for 1 h and concentrated *in vacuo*, after addition of toluene (50 mL). Diethyl ether was added to the crude and concentrated to dryness. The outcome was dissolved in THF (20 mL) and diethylamine (20.58 mL, 200 mmol) was added. The reaction mixture was left stirring for 1.5 h at room temperature. The volatiles were removed *in vacuo*, EtOAc was added and concentrated again. Water + 10 % ACN (50 mL) was added and extraction with heptane (3 x 100 mL) was done. The aqueous layer was concentrated *in vacuo*. Compound **3.16** was obtained in the form of a salt with diethylamine (2.9 g, quant.) ¹H NMR (400 MHz, DMSO-*d*₆) δ 0.95 (s, 3H), 0.97 (s, 2H), 1.15 (t, J = 7.3 Hz, 3H), 1.56 - 1.75 (m, 1H), 1.75 - 1.95 (m, 1H), 1.98 - 2.18 (m, 1H), 2.88 (q, J = 7.3 Hz, 2H), 3.21 - 3.31 (m, 1H), 3.37 - 3.55 (m, 1H), 3.65 - 3.75 (m, 1H), 4.17 - 4.34 ppm (m, 2H); ¹³C NMR (101 MHz, DMSO-*d*₆) δ 11.60, 22.81, 25.17, 26.61, 26.73, 29.39, 31.52, 34.03, 35.30, 41.63, 46.39, 47.91, 58.98, 59.39, 59.94, 62.70, 171.31, 174.58, 175.15 ppm; UPLC-MS m/z : 229.2 [M+H]⁺.

(S)-1-((S)-2-(4-((tert-Butoxycarbonyl)amino)-3-chlorobenzamido)-3,3-dimethylbutanoyl)pyrrolidine-2-carboxylic acid (3.18)

A solution of **3.16** (salt with diethylamine, 719 mg, 2.385 mmol) and *N,N*-di-iso-propylethylamine (0.415 mL, 2.385 mmol) in DMF (15 mL) was added to a preactivated (30 min) solution of 4-(Boc-amino)-3-chlorobenzoic acid (**3.17**) (540 mg, 1.988 mmol), EDC·HCl (457 mg, 2.385 mmol) and 1-hydroxybenzotriazole hydrate (365 mg, 2.385 mmol) in DMF (8 mL). The mixture was stirred overnight at room temperature. EtOAc (100 mL) was added and extraction was done with 1 M HCl (3 x 50 mL),

brine (50 mL), dried (Na₂SO₄) and concentrated *in vacuo*. Flash chromatography (DCM:MeOH) was done to afford compound **3.18** (850 mg, 51 %) with a purity of 57% (by UV). R_f = 0.30 (95:5 DCM:MeOH, visualization by UV); UPLC-MS *m/z*: 480.1 [M-H]⁻.

***tert*-Butyl (4-(((*S*)-1-((*S*)-2-(((*S*)-1-((*tert*-butyldiphenylsilyl)oxy)-4-(methylsulfonamido)-4-oxobutan-2-yl)carbamoyl)pyrrolidin-1-yl)-3,3-dimethyl-1-oxobutan-2-yl)carbamoyl)-2-chlorophenyl)carbamate (**3.19a**)**

To a solution of **3.18** (400 mg, 0.830 mmol) in DMF (10 mL) was added **3.13a** (433 mg, 0.996 mmol), *N,N*-di-*iso*-propylethylamine (0.361 mL, 2.075 mmol), 1-hydroxybenzotriazole hydrate (153 mg, 0.996 mmol) and EDC-HCl (191 mg, 0.996 mmol). The reaction mixture was stirred for 3 h at room temperature. EtOAc (70 mL) was added and extraction was done with 1 M HCl (2 x 60 mL), water (70 mL) and brine (70 mL). The organic layer was concentrated *in vacuo* and flash chromatography was done. Compound **3.19a** was obtained (300 mg, 40 %). R_f = 0.40 (1:3 Hex:EtOAc, visualization by UV); UPLC-MS *m/z*: 895.8 [M-H]⁻.

***tert*-Butyl (4-(((*S*)-1-((*S*)-2-(((*S*)-1-((*tert*-butyldiphenylsilyl)oxy)-4-(ethylsulfonamido)-4-oxobutan-2-yl)carbamoyl)pyrrolidin-1-yl)-3,3-dimethyl-1-oxobutan-2-yl)carbamoyl)-2-chlorophenyl)carbamate (**3.19b**)**

The title compound was prepared from **3.18** (400 mg, 0.830 mmol) and **3.13b** (559 mg, 1.245 mmol) in the same manner as described for the synthesis of **3.19a**. Compound **3.19b** was obtained (370 mg, 40 %) with a purity of 86 % (UV). R_f = 0.56 (1:1 EtOAc:Hex + 0.1 %); UPLC-MS *m/z*: 910.1 [M-H]⁻.

(*S*)-1-((*S*)-2-(4-Amino-3-chlorobenzamido)-3,3-dimethylbutanoyl)-*N*-((*S*)-4-(methylsulfonamido)-1,4-dioxobutan-2-yl)pyrrolidine-2-carboxamide (3.3**)**

Compound **3.19a** was dissolved in THF (6 mL). Tetrabutylammonium fluoride (1 M in THF, 0.501 mL, 0.501 mmol) was added and the reaction mixture was left stirring overnight. Additional TBAF (1M, 250 μL) was added to the solution and after stirring 24 h the reaction was finished. The reaction mixture was diluted with EtOAc (50 mL) and extracted with 0.5 M HCl (2 x 40 mL) and brine (40 mL). The organic layer was dried (Na₂SO₄) and concentrated *in vacuo*. Flash chromatography was done to afford the alcohol (170 mg, 73%). R_f = 0.50 (90:10 EtOAc:MeOH, visualization by UV); UPLC-MS *m/z*: 658.1 [M-H]⁻. The alcohol was dissolved in dry DCM (5 mL) and DMF (2 mL) and Dess-Martin periodinane (142 mg, 0.335 mmol) was added. The reaction mixture was stirred for 7 h at room temperature. EtOAc (20 mL) was added and extraction was done with saturated NH₄Cl (20 mL) and 1 M HCl (20 mL). The organic layer was concentrated *in vacuo*. Flash chromatography was done to afford the aldehyde (150 mg, 89%). R_f = 0.29 (95:5 DCM:MeOH, visualization by UV); UPLC-MS *m/z*: 656.1 [M-H]⁻. The aldehyde (120

mg, 0.182 mmol) was dissolved in DCM (2 mL) and TFA (0.4 mL, 3.04 mmol) was added. The reaction mixture was left stirring for 30 min. DCM (10 mL) and toluene (10 mL) were added and the mixture was concentrated *in vacuo*. Flash chromatography was done and the final crude was lyophilized to afford final compound **3.3** as a white powder (70 mg, 69%). $R_f = 0.19$ (100 % EtOAc, visualization by UV); $^1\text{H NMR}$ (400 MHz, $\text{DMSO-}d_6$) δ 0.95 (s, 2H), 1.02 (s, 8H), 1.65 - 2.15 (m, 5H), 2.32 (d, $J = 18.0$ Hz, 1H), 3.13 (dd, $J = 18.1, 7.4$ Hz, 1H), 3.17 - 3.28 (m, 3H), 3.55 - 3.67 (m, 1H), 3.74 - 3.84 (m, 1H), 3.93 (t, $J = 6.8$ Hz, 1H), 4.22 (t, $J = 7.0$ Hz, 1H), 4.33 - 4.45 (m, 1H), 4.68 (d, $J = 8.8$ Hz, 1H), 5.29 (d, $J = 6.6$ Hz, 1H), 5.91 (s, 2H), 6.76 (d, $J = 8.5$ Hz, 1H), 7.23 (d, $J = 6.6$ Hz, 2H), 7.56 - 7.70 (m, 2H), 7.81 (d, $J = 2.0$ Hz, 1H), 8.53 ppm (d, $J = 6.2$ Hz, 1H); $^{13}\text{C NMR}$ (101 MHz, $\text{DMSO-}d_6$) δ 24.81, 26.68, 29.54, 31.34, 34.92, 34.99, 35.99, 41.36, 47.90, 50.89, 57.39, 59.44, 87.37, 114.03, 116.01, 121.70, 127.79, 129.00, 147.61, 165.44, 169.40, 172.12, 172.74 ppm; HRMS (ESI): calcd for $\text{C}_{23}\text{H}_{33}\text{N}_5\text{O}_7\text{SCl}^+$ $[\text{M}+\text{H}]^+$: 558.1784, found: 558.1766.

(S)-1-((S)-2-(4-Amino-3-chlorobenzamido)-3,3-dimethylbutanoyl)-N-((S)-4-(ethylsulfonamido)-1,4-dioxobutan-2-yl)pyrrolidine-2-carboxamide (3.4)

The title compound was prepared from **3.19b** (370 mg, 0.405 mmol) in the same manner as described for the synthesis of **3.3**. Firstly, intermediate alcohol was obtained (210 mg, 77 %); $R_f = 0.36$ (95:5 EtOAc:MeOH, visualization by UV); UPLC-MS m/z : 672.1 $[\text{M}-\text{H}]^-$. Secondly, intermediate aldehyde was obtained (170 mg, 81 %); $R_f = 0.33$ (95:5 EtOAc:MeOH, visualization by UV); UPLC-MS m/z : 670.1 $[\text{M}-\text{H}]^-$. Finally, **3.4** was obtained as a white powder (72 mg, 71 %). $R_f = 0.32$ (100 % EtOAc, visualization by UV); $^1\text{H NMR}$ (400 MHz, $\text{DMSO-}d_6$) δ 1.02 (s, 9H), 1.24 (t, $J = 7.4$ Hz, 3H), 1.63 - 1.76 (m, 1H), 1.76 - 2.15 (m, 4H), 2.33 (d, $J = 18.0$ Hz, 1H), 3.10 - 3.21 (m, 1H), 3.27 - 3.47 (m, under water peak), 3.56 - 3.68 (m, 1H), 3.74 - 3.85 (m, 1H), 3.89 - 3.96 (m, 0.6H), 4.23 (dd, $J = 8.0, 6.1$ Hz, 0.6H), 4.35 - 4.44 (m, 0.5H), 4.64 - 4.73 (m, 1H), 5.28 (d, $J = 6.4$ Hz, 0.6H), 5.89 (d, $J = 7.1$ Hz, 1H), 6.76 (d, $J = 8.5$ Hz, 1H), 7.14 - 7.25 (m, 0.6H), 7.54 - 7.68 (m, 1.6H), 7.81 ppm (d, $J = 2.0$ Hz, 1H); $^{13}\text{C NMR}$ (101 MHz, $\text{DMSO-}d_6$) δ 7.1, 24.77, 26.64, 29.52, 34.93, 35.69, 47.41, 47.71, 51.18, 57.38, 59.31, 87.22, 114.02, 116.01, 121.74, 127.74, 128.97, 147.59, 165.4, 169.37, 172.11, 172.66 ppm; HRMS (ESI): calcd for $\text{C}_{24}\text{H}_{35}\text{N}_5\text{O}_7\text{SCl}^+$ $[\text{M}+\text{H}]^+$: 572.1940, found: 572.1936.

(S)-1-((S)-2-(4-Amino-3-chlorobenzamido)-3,3-dimethylbutanoyl)-N-((S)-1-cyano-3-(methylsulfonamido)-3-oxopropyl)pyrrolidine-2-carboxamide (3.6)

Methanesulfonamide (19.90 mg, 0.209 mmol), 4-dimethylaminopyridine (19.17 mg, 0.157 mmol) and EDC-HCl (30.1 mg, 0.157 mmol) were added to a solution of **3.5** (50 mg, 0.105 mmol) in DCM (2.5 mL) and DMF (0.5 mL) under an atmosphere of nitrogen. The reaction mixture was stirred for 1 day at room temperature. The solution was diluted with EtOAc (20 mL), washed with 1 M HCl (15 mL), water (20

mL), brine (20 mL), dried (Na_2SO_4) and concentrated *in vacuo*. The crude was lyophilized to afford final compound **3.6** as a white powder (52 mg, 90 %). $R_f = 0.31$ (100 % EtOAc, visualization by UV); ^1H NMR (400 MHz, $\text{DMSO}-d_6$) δ 1.02 (s, 9H), 1.68 - 2.01 (m, 3H), 2.01 - 2.16 (m, 1H), 2.77 - 3.01 (m, 2H), 3.21 (m, 3H), 3.56 - 3.70 (m, 1H), 3.70 - 3.83 (m, 1H), 4.27 (dd, $J = 8.2, 5.6$ Hz, 1H), 4.67 (d, $J = 8.7$ Hz, 1H), 4.93 (q, $J = 7.2$ Hz, 1H), 5.92 (s, 2H), 6.76 (d, $J = 8.5$ Hz, 1H), 7.59 (dd, $J = 8.5, 2.0$ Hz, 1H), 7.68 (d, $J = 8.7$ Hz, 1H), 7.81 (d, $J = 2.0$ Hz, 1H), 8.79 (d, $J = 7.5$ Hz, 1H), 12.02 ppm (s, 1H); ^{13}C NMR (101 MHz, $\text{MeOD}-d_4$) δ 26.20, 27.11, 30.52, 36.61, 37.97, 39.12, 41.46, 49.88, 59.33, 59.43, 61.51, 115.49, 118.68, 118.81, 123.30, 123.33, 128.36, 130.09, 149.38, 168.87, 168.94, 170.01, 172.23, 173.81 ppm; HRMS (ESI): calcd for $\text{C}_{23}\text{H}_{32}\text{N}_6\text{O}_6\text{SCl}^+$ $[\text{M}+\text{H}]^+$: 555.1787, found: 555.1758.

(S)-2-((S)-2-(((Benzyloxy)carbonyl)amino)-3-methylbutanamido)propanoic acid (3.22)

N-Carbobenzyloxy-L-valine (4 g, 15.92 mmol), 1-hydroxybenzotriazole hydrate (2.68 g, 17.51 mmol), EDC.HCl (3.36 g, 17.51 mmol) were dissolved in dry DCM (80 mL) at 0 °C and left stirring 20 min at the same temperature. L-Alanine methyl ester hydrochloride (2.444 g, 17.51 mmol) and *N,N*-di-isopropylethylamine (6.93 ml, 39.8 mmol) were added to the mixture. The reaction mixture was allowed to warm up to room temperature and was left stirring overnight. The reaction mixture was diluted with DCM (50 mL), quenched with water (100 mL), extracted and washed with saturated NaHCO_3 (2 x 100 mL), 0.5 M HCl (100 mL) and brine (100 mL). The organic layer was dried (Na_2SO_4) and concentrated *in vacuo*. A back-extraction was done with the first aqueous phase. The organic phase was then extracted with the same washing solvents and combined with the previous crude after concentrating *in vacuo*. The resulting crude was dissolved in MeOH (42 mL) and a solution of LiOH (600 mg, 25.06 mmol) in water (14 mL) was. The reaction mixture was left stirring overnight at room temperature, followed by quenching with a 10% aqueous solution of citric acid (180 mL). This was left stirring for 15 min and the formed precipitate was filtered. Flash chromatography of the crude was performed to afford **3.22** (1.47 g, 28%). $R_f = 0.27$ (1:1 EtOAc:Hex + 0.1 % FA, visualization by PMA); ^1H NMR (400 MHz, $\text{DMSO}-d_6$) δ 0.84 (d, $J = 6.7$ Hz, 3H), 0.89 (d, $J = 6.8$ Hz, 3H), 1.27 (d, $J = 7.3$ Hz, 3H), 1.93 - 1.94 (m, 1H), 3.90 (dd, $J = 8.9, 7.0$ Hz, 1H), 4.19 (p, $J = 7.1$ Hz, 1H), 5.03 (s, 2H), 7.24 (d, $J = 9.1$ Hz, 1H), 7.27-7.41 (M, 5H), 8.20 (d, $J = 6.9$ Hz, 1H), 12.49 ppm (s, 1H); UPLC-MS m/z : 323.1 $[\text{M}+\text{H}]^+$.

Benzyl ((S)-1-(((S)-1-(((S)-1-hydroxy-4-(methylsulfonamido)-4-oxobutan-2-yl)amino)-1-oxopropan-2-yl)amino)-3-methyl-1-oxobutan-2-yl)carbamate (3.23)

4-Methylmorpholine (0.101 ml, 0.920 mmol) was added to a solution of acid **3.22** (270 mg, 0.837 mmol) in THF (15 mL), followed by addition of isobutyl chloroformate (0.119 ml, 0.920 mmol) at -20 °C. The reaction mixture was stirred at -20 °C for 20 min, followed by addition of amine **3.13a** (400 mg, 0.920 mmol). The resulting mixture was stirred at -20 °C for 3 h, quenched with 1M HCl (60 mL)

and extracted with EtOAc (2 x 60 mL). The combined organic layers were washed with water (60 mL), brine (50 mL), dried (Na_2SO_4) and concentrated *in vacuo*. The crude was dissolved in dry THF (10 mL), tetrabutylammonium fluoride (1 M in THF, 5.68 mL, 5.68 mmol) was added and the reaction mixture was left stirring overnight. The reaction mixture was diluted with EtOAc (100 mL) and extracted with water (100 mL). The aqueous phase was washed with EtOAc (100 mL). The combined organic layers were dried (Na_2SO_4), concentrated *in vacuo* and purified by flash chromatography to afford alcohol **3.23** (350 mg, 83 %). $R_f = 0.07$ (EtOAc + 0.1 % FA, visualization by UV/PMA); ^1H NMR (400 MHz, $\text{MeOD-}d_4$) δ 0.98 (dd, $J = 14.4, 6.8$ Hz, 6H), 1.38 (d, $J = 7.1$ Hz, 3H), 2.05 - 2.16 (m, 1H), 2.48 - 2.68 (m, 2H), 3.22 (s, 3H), 3.54 - 3.67 (m, 2H), 3.91 - 3.98 (m, 1H), 4.25 (p, $J = 5.8$ Hz, 1H), 4.34 (q, $J = 7.1$ Hz, 1H), 5.08 - 5.20 (m, 2H), 7.17 (d, $J = 7.2$ Hz, 0.2H), 7.29 - 7.43 ppm (m, 5H); ^{13}C NMR (101 MHz, $\text{MeOD-}d_4$) δ 16.63, 17.06, 18.35, 30.36, 37.23, 39.88, 49.19, 60.94, 62.57, 66.50, 127.52, 127.66, 128.09, 136.71, 157.55, 170.95, 172.71, 173.14 ppm; UPLC-MS m/z : 501.3 $[\text{M}+\text{H}]^+$.

Benzyl ((S)-3-methyl-1-(((S)-1-(((S)-4-(methylsulfonamido)-1,4-dioxobutan-2-yl)amino)-1-oxopropan-2-yl)amino)-1-oxobutan-2-yl)carbamate (3.8)

Alcohol **3.23** was dissolved in dry DCM (5 mL) and DMF (1.5 mL) and Dess-Martin periodinane (99 mg, 0.234 mmol) was added. This reaction mixture was stirred at room temperature for 2 h. EtOAc (20 mL) was added and extraction was done with saturated NH_4Cl (20 mL) and 1M HCl (20 mL). The organic layer was concentrated *in vacuo*. Flash chromatography was done and the final crude was lyophilized to afford the final compound **3.8** as a white powder (35 mg, 39 %). $R_f = 0.22$ (95:5 DCM:MeOH, visualization by UV/PMA); ^1H NMR (400 MHz, $\text{MeOD-}d_4$) δ 0.90 - 1.03 (m, 6H), 1.38 (t, $J = 6.7$ Hz, 3H), 2.06 (m, 1H), 2.42 (d, $J = 18.2$ Hz, 0.6H), 2.70 - 2.77 (m, 0.7H), 3.15 (dd, $J = 18.2, 7.5$ Hz, 0.6H), 3.26 (s, 1.8H), 3.27 (s, 1.2H), 3.82 - 4.03 (m, 1H), 4.16 (d, $J = 7.3$ Hz, 0.6H), 4.38 (dq, $J = 46.9, 8.9$ Hz, 2H), 4.48 - 4.58 (m, 0.5H), 5.06 - 5.19 (m, 2H), 5.53 (s, 0.6H), 5.76 (d, $J = 5.0$ Hz, 0.4H), 7.10 - 7.21 (m, 0.6H), 7.28 - 7.42 (m, 5H), 8.24 ppm (t, $J = 5.6$ Hz, 0.5H); ^1H NMR (400 MHz, $\text{DMSO-}d_6$) δ 0.85 (dd, $J = 16.8, 6.8$ Hz, 6H), 1.22 (t, $J = 6.2$ Hz, 3H), 1.96 (td, $J = 13.6, 6.9$ Hz, 1H), 2.31 (d, $J = 17.9$ Hz, 0.7H), 2.57 - 2.73 (m, 0.7H), 3.14 (dd, $J = 18.1, 7.3$ Hz, 0.7H), 3.24 (s, 2H), 3.27 (s, 1H), 3.79 - 4.04 (m, 2H), 4.16 - 4.28 (m, 0.8H), 4.28 - 4.47 (m, 0.7H), 4.97 - 5.10 (m, 2H), 5.29 (d, $J = 5.6$ Hz, 0.6H), 5.53 (s, 0.3H), 7.18 (d, $J = 6.3$ Hz, 0.3H), 7.22 - 7.48 (m, 6H), 7.99 - 8.14 (m, 1.5H), 8.47 ppm (d, $J = 6.0$ Hz, 0.7H); ^{13}C NMR (101 MHz, $\text{MeOD-}d_4$) δ 16.44, 16.74, 17.14, 17.27, 18.27, 18.38, 30.34, 30.56, 34.48, 35.35, 40.51, 40.64, 46.54, 48.73, 49.10, 51.08, 60.65, 61.07, 66.39, 66.49, 81.68, 87.62, 127.40, 127.44, 127.65, 128.12, 136.76, 171.99, 172.66, 172.73, 172.93, 173.53, 173.71 ppm; ^{13}C NMR (101 MHz, $\text{DMSO-}d_6$) δ 18.08, 18.27, 19.16, 30.29, 31.30, 34.38, 35.83, 41.33, 41.41, 46.24, 48.02, 50.69, 59.95, 65.38, 81.49, 87.37, 127.63, 127.76, 128.33, 137.05, 156.17, 170.81, 171.45, 172.52 ppm; HRMS (ESI): calcd for $\text{C}_{21}\text{H}_{31}\text{N}_4\text{O}_8\text{S}^+$ $[\text{M}+\text{H}]^+$: 499.1857, found: 499.1870.

5-Hydroxydihydrofuran-2(3H)-one or 4-oxobutanoic acid (3.24)

Compound **3.24** was prepared according to a procedure by Wermuth.⁴⁰ Additional characterization was done by ¹H and ¹³C NMR in different solvents (spectra included in the supporting information): ¹H NMR (400 MHz, DMSO-*d*₆) δ 1.88 (m, 0.5H), 2.26 - 2.38 (m, 0.6H), 2.46 - 2.53 (m, under solvent), 2.66 (t, *J* = 6.5 Hz, 2H), 5.79 (q, *J* = 5.7 Hz, 0.5H), 7.50 (d, *J* = 6.0 Hz, 0.5H), 9.67 (s, 1H), 12.21 (s, 1H); ¹³C NMR (101 MHz, DMSO-*d*₆) δ 26.84, 27.80, 30.02, 38.50, 99.79, 174.04, 176.89, 202.52. ¹H NMR (400 MHz, MeOD-*d*₄) δ 1.85 (dd, *J* = 7.5, 5.5 Hz, 2H), 2.40 (t, *J* = 7.5 Hz, 2H), 4.58 (t, *J* = 5.5 Hz, 1H); ¹³C NMR (101 MHz, MeOD-*d*₄) δ 28.77, 31.62, 97.34, 175.78; ¹H NMR (400 MHz, CDCl₃) δ 2.09 – 2.28 (m, 0.6H), 2.28 – 2.60 (m, 1.5H), 2.71 (m, 2.5H), 2.82 (m, 2H), 5.95 (s, 0.5H), 9.83 (s, 1H); ¹³C NMR (101 MHz, CDCl₃) δ 26.30, 27.02, 29.46, 38.23, 98.91, 177.08, 177.75, 199.96; ¹H NMR (400 MHz, D₂O) δ 1.81 (td, *J* = 7.5, 5.7 Hz, 2H), 2.39 (t, *J* = 7.5 Hz, 2H), 4.99 (t, *J* = 5.6 Hz, 1H); ¹³C NMR (101 MHz, D₂O) δ 29.25, 32.13, 90.00, 177.95.

Methyl 4,4-dimethoxybutanoate (3.26)

To a solution of sodium methoxide (29.4 g, 136 mmol) in MeOH (90 mL) was added methyl 4-nitrobutanoate (**3.25**, 8.70 mL, 68.0 mmol) at 0 °C over 30 min through an additional funnel. The resulting suspension was added dropwise via another addition funnel, over 15 min, to a round-bottom flask equipped with methanol (100 mL) and conc. sulfuric acid (21.06 mL, 394 mmol, 96% solution in water), held at 0 °C. Stirring continued for 30 min. The reaction mixture was poured into DCM (250 mL) and water (250 mL). Extraction was done and the aqueous layer was washed with DCM (100 mL). The organic layers were combined, washed with 1 % aqueous NaOH (100 mL), ice water (100 mL) and brine (100 mL), dried (Na₂SO₄) and concentrated *in vacuo* to afford the acetal **3.26** (8.96 g, 81 %) as a slightly yellow liquid. *R*_f = 0.25 (4:1 Hex:EtOAc, visualization by KMnO₄); ¹H NMR (400 MHz, CDCl₃) δ 1.91 (td, *J* = 5.6, 7.5 Hz, 8H), 2.37 (t, *J* = 7.5 Hz, 8H), 3.31 (s, 6H), 3.66 (s, 3H), 4.38 ppm (t, *J* = 5.6 Hz, 1H); ¹³C NMR (101 MHz, CDCl₃) δ 27.92, 29.19, 51.74, 53.27, 103.71, 173.82 ppm.

4,4-Dimethoxybutanoic acid (3.27)

To a solution of methyl 4,4-dimethoxybutanoate (**3.26**, 5 g, 30.8 mmol) in MeOH (45 mL) was added dropwise 1 M NaOH (35.5 mL, 35.5 mmol) at 0 °C. After stirring overnight at room temperature, the mixture was acidified to pH = 2 by addition of 1 M HCl at 0 °C. The mixture was extracted with EtOAc (3 × 100 mL). The combined organic layers were washed with brine (100 mL), dried (Na₂SO₄) and concentrated *in vacuo* to afford the acid **3.27** (4.11 g, 90 %). *R*_f = 0.24 (1:1 Hex:EtOAc, visualization by KMnO₄); ¹H NMR (400 MHz, CDCl₃) δ 1.93 (td, *J* = 7.4, 5.6 Hz, 2H), 2.43 (t, *J* = 7.4 Hz, 2H), 3.33 (s, 6H), 4.42 ppm (t, *J* = 5.6 Hz, 1H); ¹³C NMR (101 MHz, CDCl₃) δ 26.87, 28.82, 53.4, 56.83, 105.32, 176.82 ppm.

5-Hydroxy-1-(methylsulfonyl)pyrrolidin-2-one (**3.28**)

Methanesulfonamide (1.118 g, 11.76 mmol), 4-dimethylaminopyridine (1.436 g, 11.76 mmol) and EDC.HCl (2.253 g, 11.76 mmol) were added to a solution of 4,4-dimethoxybutanoic acid (**3.27**, 1 g, 5.88 mmol) in DCM (50 mL) under an atmosphere of nitrogen and the reaction mixture was stirred overnight at room temperature. The mixture was diluted with water (100 mL) and acidified with 1 M citric acid till pH 2 was obtained. The aqueous layer was extracted with EtOAc (2 x 100 mL). The organic layers were combined, washed with brine (100 mL), dried (Na₂SO₄) and concentrated *in vacuo*. Flash chromatography was done. The outcome was dissolved in CHCl₃ (10 mL), set at 0°C and a mixture of 1:1 water:TFA (5 mL) was added. The reaction mixture was stirred for 90 min at the same temperature, followed by stirring for 18 h at room temperature. The mixture was co-evaporated with toluene. Flash chromatography was performed to obtain final compound **3.28** (340 mg, 32 %). R_f = 0.24 (3:1 EtOAc:Hex, visualization by KMnO₄); ¹H NMR (400 MHz, CDCl₃) δ 2.03 - 2.14 (m, 1H), 2.32 - 2.44 (m, 1H), 2.47 - 2.57 (m, 1H), 2.76 - 2.89 (m, 1H), 3.30 (s, 3H), 4.92 (s, 1H), 5.91 ppm (dd, *J* = 6.3, 1.6 Hz, 1H); ¹H NMR (400 MHz, D₂O) δ 2.02 - 2.11 (m, 1H), 2.43 - 2.57 (m, 1H), 2.59 - 2.69 (m, 1H), 2.85 - 2.96 (m, 1H), 3.38 (s, 3H), 5.93 ppm (dd, *J* = 6.2, 1.0 Hz, 1H); ¹H NMR (400 MHz, MeOD-*d*₄) δ 1.78 - 1.92 (m, 0.5H), 1.92 - 2.02 (m, 1H), 2.39 (m, 1.5H), 2.53 (m, 1H), 2.81 (m, 1H), 3.25 (s, 0.3H), 3.26 (s, 2.7H), 4.58 (t, *J* = 5.5 Hz, partly under waterpeak), 5.82 (dd, *J* = 5.9, 0.7 Hz, 1H), 6.51 ppm (s, 0.25H); ¹³C NMR (101 MHz, CDCl₃) δ 27.22, 30.02, 42.01, 83.38, 174.22 ppm; ¹³C NMR (101 MHz, D₂O) δ 28.16, 30.74, 42.07, 84.90, 178.34 ppm; ¹³C NMR (101 MHz, MeOD-*d*₄) δ 28.88, 30.01, 30.74, 32.73, 41.86, 43.24, 84.81, 98.55, 176.46, 177.04 ppm (¹H and ¹³C spectra are included in the supporting information); UPLC-MS *m/z*: 178,1 [M-H].

3.6.2 Phenylhydrazine kinetic study

Colorless 2-phenylhydrazin-1-ium chloride (84 mg, 0.581 mmol) and sodium acetate (130 mg, 1.585 mmol) were dissolved in water (3 mL). The aldehyde (0.490 mmol), dissolved in a little ethanol (free from aldehydes and ketones), was added. The mixture was shaken until a clear solution was obtained (1-2 min). Follow-up was directly done by UPLC-UV-MS and showed full conversion into (*E*)-4-(2-phenylhydrazono)butanoic acid in the case of **3.24** (UPLC-MS *m/z* 191.1 [M-H]⁻, t_R = 1.45 min) and (*E*)-*N*-(methylsulfonyl)-4-(2-phenylhydrazono)butanamide (UPLC-MS *m/z* 268.1 [M-H]⁻, t_R = 1.43 min) in the case of **3.28**. The reaction of **3.28** with (2,4-dinitrophenyl)hydrazine was also set up; a clear solution was prepared by warming a solution of 2,4-dinitro-phenylhydrazine, 1 mL of concentrated hydrochloric acid (37 %) and 9 mL of ethanol. 10 mg of **3.28** was added to 400 μL of the previous solution, followed by 1.5 mL EtOH. The mixture was shaken until the solution became clear (1-5 min). Full conversion of **3.28** into (*E*)-4-(2-(2,4-dinitrophenyl)hydrazono)-*N*-(methylsulfonyl)butanamide was detected by

UPLC-UV-MS (UPLC-MS m/z 358.1 [M-H]⁻, t_R = 1.55 min). The UPLC-UV-MS system consisted of a Waters Acquity UPLC system coupled to a Waters TUV detector, ESI source and a Waters Acquity QDa Mass Detector. A Waters Acquity UPLC BEH C₁₈ 1.7 μ m 2.1 x 50 mm column was used, set at a temperature of 40 °C. Solvent A: water with 0.1 % formic acid, solvent B: acetonitrile with 0.1 % formic acid. The gradient used started with a flow rate of 0.7 mL/min at 95 % A, 5 % B for 0.15 min then in 1.85 min from 95 % A, 5 % B to 100 % B, isocratically at the same percentage for 0.25 min and finally 0.75 min (0.350 mL/min), 95 % A, 5 % B. The wavelength for UV detection was 254 nm.

3.6.3 Biochemical evaluation: IC₅₀ determination

In a 96 well plate, caspases and inhibitors were incubated for 15 minutes at 37 °C before substrate hydrolysis was monitored at 37 °C for 20 minutes in 2-minute intervals. Assays were run in two technical duplicates and all experiments were performed in at least two independent repeats. Total volume per well was 50 μ L. A positive control for caspase activity has been included in all of the assays (caspase + substrate + DMSO). Substrates were Ac-WEHD-AMC for m casp-11 and h casp-1,-4,-5; Ac-ATAD-AFC for m casp-12; Ac-DEVD-AMC for h casp-3; Ac-IETD-AMC for h casp-8 and Ac-LEHD-AMC for h casp-9. All the assays have been performed at 100 μ M substrate concentration. IC₅₀-values were calculated using at least 7 inhibitor concentrations giving between 10 and 90% inhibition. IC₅₀-values were obtained by fitting the data using the 4-parameter logistics function with background correction. Buffer composition was 20 mM PIPES, 100 mM NaCl, 1 mM EDTA, 0.1% (w/v) CHAPS, 10% sucrose and adjusted till pH 7.5. DTT was added just before filling the wells to obtain a 10 mM final concentration. FLx800, a fluorescent microplate reader (Bio-Tek) was used to measure fluorescence after caspase activation. Excitation and emission wavelengths for AMC and AFC substrates are 360 nm (AMC), 400 nm (AFC) and 460 nm (AMC), 528 nm (AFC) respectively.

3.6.4 Chemical stability protocol

A 10 mM stock compound solution in DMSO was prepared. The stock solution was diluted to a 500 nM solution with the specific buffer. The mixture was gently shaken at 37 °C. At different time points (0 min - 30 min - 60 min - 120 min - 180 min - 360 min – 24 h) 100 μ L was withdrawn which was analyzed with UPLC-MS/MS. Samples were prepared in duplicate and measured in triplicate. The percentage of parent compound remaining at each time point relative to the 0 min sample was then calculated from UPLC-MS/MS peak area ratios. A set of 5 dilutions (in the solution buffer) of the compound were prepared from a 10 μ M solution to give final test concentrations between 31 nM and 500 nM. A calibration line was made to evaluate the accuracy of the test method and to calculate the concentration. 10 mM PBS buffer was used for pH 7.4 and 10 mM acetic acid buffer for pH 4.0.

3.6.5 Metabolic stability protocol

Liver microsomes (20 mg protein/mL), NADPH regenerating system solutions A & B and 5 mM stock compound solution (100% DMSO) were prepared. The reaction mixture finally contained 713 μ L purified water, 200 μ L 0.5 M potassium phosphate pH 7.4, 50 μ L NADPH regenerating system solution A (BD Biosciences Cat. No. 451220), 10 μ L NADPH regenerating system solution B (BD Biosciences Cat. No. 451200) and 2 μ L of the compound stock solution (10 μ M final concentration). The reaction mixture was warmed to 37 °C for 5 minutes and the reaction was initiated by addition of 25 μ L of liver microsomes (0.5 mg protein/mL final concentration). At different time points (0 min – 15 min – 30 min – 60 min – 120 min – 240 min – 360 min – 24h), 20 μ L was withdrawn and 80 μ L cold acetonitrile was added on ice for 10 minutes. Then the mixtures were centrifuged at 13 000 rpm for 5 min at 4 °C. The supernatant was further diluted in 90 % water/acetonitrile. At each time point, the compound was analyzed using UPLC-MS/MS. The calculation of parent percentage and the calibration line were the same as in the chemical stability measurements. Verapamil was used as a positive control. Samples were prepared in duplicate and measured in triplicate.

3.6.6 Macrophage differentiation, stimulation and evaluation

Bone marrow-derived macrophages (BMDMs) were prepared as described previously.⁵⁰ BMDMs were left untreated or stimulated with ultrapure LPS (0.5 μ g ml⁻¹) (Invivogen) for 3 h. Cells were treated with the indicated inhibitors (50 μ M, 45 min) prior to the addition of 20 μ M nigericin (Sigma-Aldrich) for 1 h. In other setups, cells were left untreated or stimulated with Pam3CSK4 (1 μ g ml⁻¹) (Invivogen) for 5 h. Cells were treated with the indicated inhibitors (50 μ M, 45 min) prior to transfection with LPS (2 μ g ml⁻¹) (Invivogen) for 7 h. Cytokine levels in culture medium were evaluated using Luminex technology (Bio-Rad). Cell death was measured using the LDH assay from Promega.

References

1. U. Fischer, R. U. Janicke and K. Schulze-Osthoff, *Cell Death Differ.*, 2003, **10**, 76-100.
2. P. Fuentes-Prior and G. S. Salvesen, *Biochem. J.*, 2004, **384**, 201-232.
3. U. Fischer and K. Schulze-Osthoff, *Pharmacol. Rev.*, 2005, **57**, 187-215.
4. D. J. Fernandez and M. Lamkanfi, *Biol. Chem.*, 2015, **396**, 193-203.
5. S. Winkler and A. Rosen-Wolff, *Semin. Immunopathol.*, 2015, **37**, 419-427.
6. S. H. MacKenzie, J. L. Schipper and A. C. Clark, *Curr. Opin. Drug Discovery Dev.*, 2010, **13**, 568-576.
7. P. Galatsis, B. Caprathe, J. Gilmore, A. Thomas, K. Linn, S. Sheehan, W. Harter, C. Kostlan, E. Lunney, C. Stankovic, J. Rubin, K. Brady, H. Allen and R. Talanian, *Bioorg. Med. Chem. Lett.*, 2010, **20**, 5184-5190.
8. J. C. R. Randle, M. W. Harding, G. Ku, M. Schonharting and R. Kurrle, *Expert Opin. Invest. Drugs*, 2001, **10**, 1207-1209.
9. J. H. Stack, K. Beaumont, P. D. Larsen, K. S. Straley, G. W. Henkel, J. C. R. Randle and H. M. Hoffman, *J. Immunol.*, 2005, **175**, 2630-2634.
10. M. Maroso, S. Balosso, T. Ravizza, V. Iori, C. I. Wright, J. French and A. Vezzani, *Neurotherapeutics*, 2011, **8**, 304-315.
11. G. Doitsh, N. L. K. Galloway, X. Geng, Z. Y. Yang, K. M. Monroe, O. Zepeda, P. W. Hunt, H. Hatano, S. Sowinski, I. Munoz-Arias and W. C. Greene, *Nature*, 2014, **505**, 509+.
12. N. L. K. Galloway, G. Doitsh, K. M. Monroe, Z. Y. Yang, I. Munoz-Arias, D. N. Levy and W. C. Greene, *Cell Rep.*, 2015, **12**, 1555-1563.
13. Y. Zhang and Y. Zheng, *Clin. Exp. Rheumatol.*, 2016, **34**, 111-118.
14. M. Poreba, A. Szalek, P. Kasperkiewicz, W. Rut, G. S. Salvesen and M. Drag, *Chem. Rev.*, 2015, **115**, 12546-12629.
15. C. J. Vickers, G. E. Gonzalez-Paez, K. M. Litwin, J. C. Umotoy, E. A. Coutsiias and D. W. Wolan, *ACS Chem. Biol.*, 2014, **9**, 2194-2198.
16. C. J. Vickers, G. E. Gonzalez-Paez and D. W. Wolan, *ACS Chem. Biol.*, 2013, **8**, 1558-1566.
17. C. J. Vickers, G. E. Gonzalez-Paez and D. W. Wolan, *J. Am. Chem. Soc.*, 2013, **135**, 12869-12876.
18. R. Ganesan, S. Jelakovic, A. J. Campbell, Z. Z. Li, J. L. Asgian, J. C. Powers and M. G. Grutter, *Biochemistry*, 2006, **45**, 9059-9067.
19. N. A. Meanwell, *J. Med. Chem.*, 2011, **54**, 2529-2591.
20. C. Ballatore, D. M. Huryn and A. B. Smith, *ChemMedChem*, 2013, **8**, 385-395.
21. C. V. C. Prasad, C. P. Prouty, D. Hoyer, T. M. Ross, J. M. Salvino, M. Awad, T. L. Graybill, S. J. Schmidt, I. Kelly Osifo, R. E. Dolle, C. T. Helaszek, R. E. Miller and M. A. Ator, *Bioorg. Med. Chem. Lett.*, 1995, **5**, 315-318.
22. M. B. Boxer, A. M. Quinn, M. Shen, A. Jadhav, W. Leister, A. Simeonov, D. S. Auld and C. J. Thomas, *ChemMedChem*, 2010, **5**, 730-738.

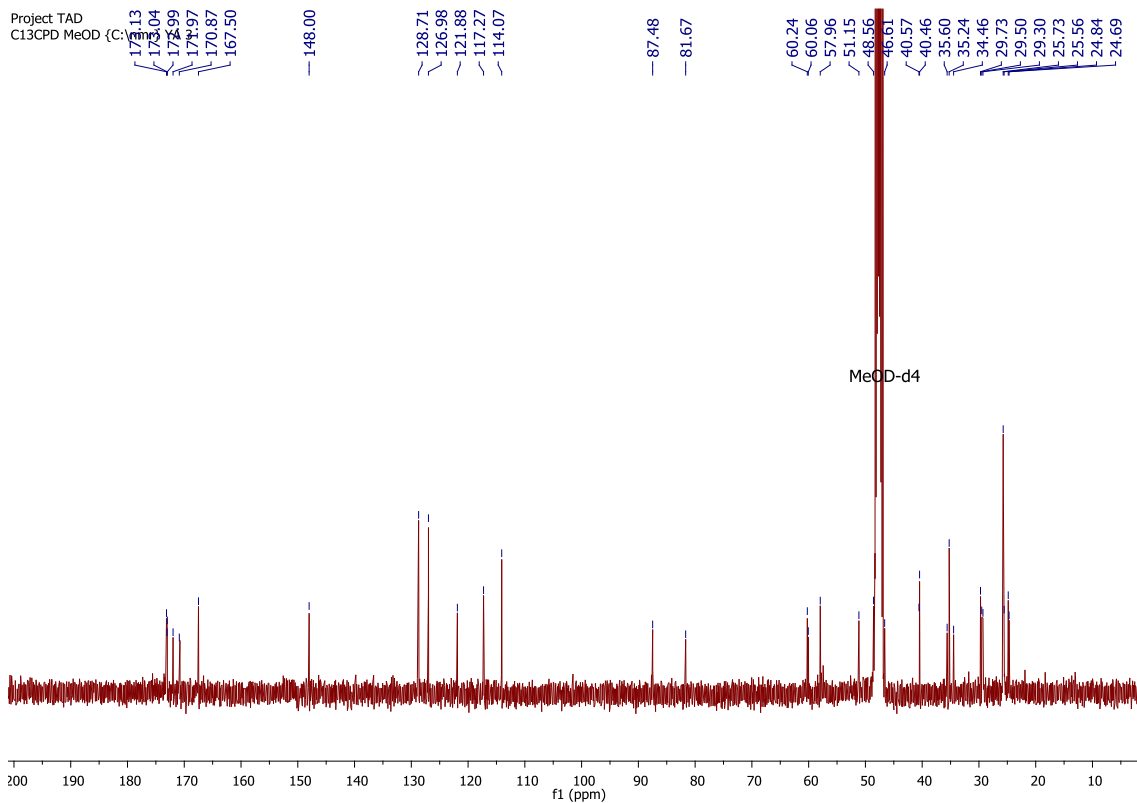
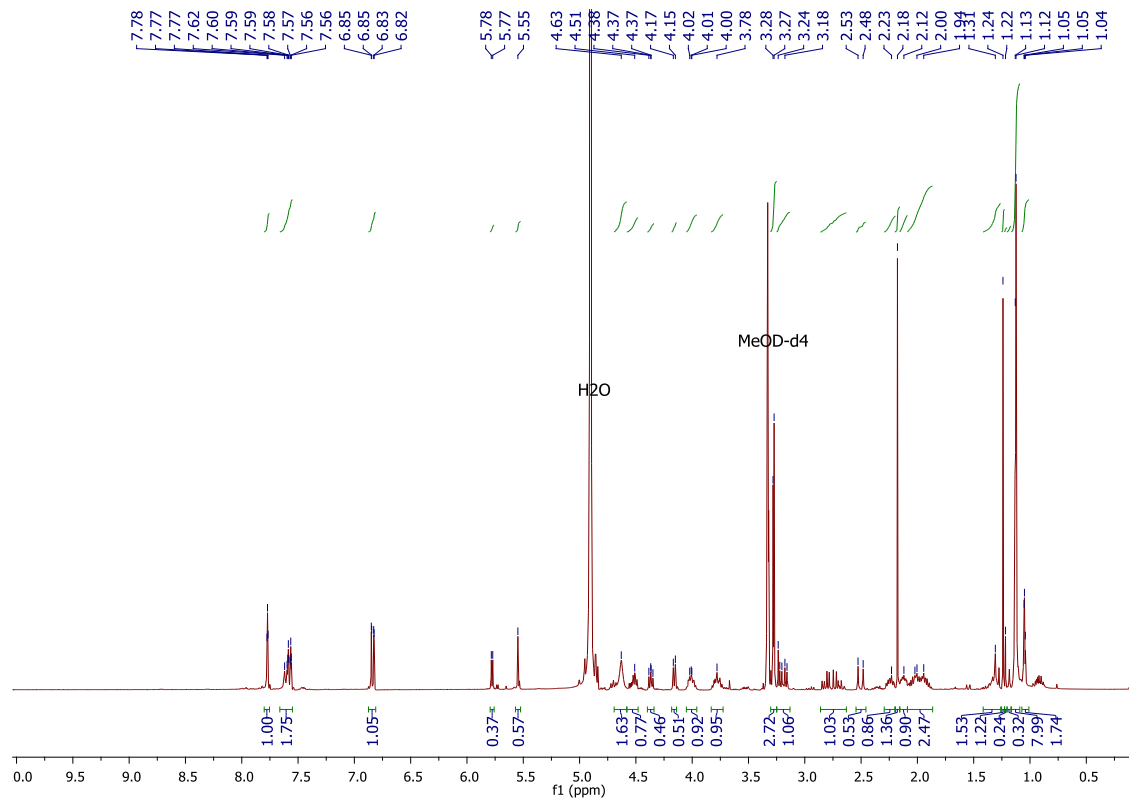
23. Y. Okamoto, H. Anan, E. Nakai, K. Morihira, Y. Yonetoku, H. Kurihara, H. Sakashita, Y. Terai, M. Takeuchi, T. Shibanuma and Y. Isomura, *Chem. Pharm. Bull.*, 1999, **47**, 11-21.
24. Y. K. Yee, P. R. Bernstein, E. J. Adams, F. J. Brown, L. A. Cronk, K. C. Hebbel, E. P. Vacek, R. D. Krell and D. W. Snyder, *J. Med. Chem.*, 1990, **33**, 2437-2451.
25. D. E. Uehling, K. H. Donaldson, D. N. Deaton, C. E. Hyman, E. E. Sugg, D. G. Barrett, R. G. Hughes, B. Reitter, K. K. Adkison, M. E. Lancaster, F. Lee, R. Hart, M. A. Paulik, B. W. Sherman, T. True and C. Cowan, *J. Med. Chem.*, 2002, **45**, 567-583.
26. P. W. Glunz, X. J. Zhang, Y. Zou, I. Delucca, A. H. Nirschl, X. H. Cheng, C. A. Weigelt, D. L. Cheney, A. Z. Wei, R. Anumula, J. M. Luetzgen, A. R. Rendina, M. Harpel, G. Luo, R. Knabb, P. C. Wong, R. R. Wexler and E. S. Priestley, *Bioorg. Med. Chem. Lett.*, 2013, **23**, 5244-5248.
27. N. F. Pelz, Z. G. Bian, B. Zhao, S. Shaw, J. C. Tarr, J. Belmar, C. Gregg, D. V. Camper, C. M. Goodwin, A. L. Arnold, J. L. Sensintaffar, A. Friberg, O. W. Rossanese, T. Lee, E. T. Olejniczak and S. W. Fesik, *J. Med. Chem.*, 2016, **59**, 2054-2066.
28. S. M. Zhenodarova, *Russ. Chem. Rev.*, 2010, **79**, 119-143.
29. F. F. Fleming, L. H. Yao, P. C. Ravikumar, L. Funk and B. C. Shook, *J. Med. Chem.*, 2010, **53**, 7902-7917.
30. L. J. Scott, *Drugs*, 2011, **71**, 611-624.
31. H. G. Bone, D. W. Dempster, J. A. Eisman, S. L. Greenspan, M. R. McClung, T. Nakamura, S. Papapoulos, W. J. Shih, A. Rybak-Feiglin, A. C. Santora, N. Verbruggen, A. T. Leung and A. Lombardi, *Osteoporosis Int.*, 2015, **26**, 699-712.
32. B. T. Fahr, T. O'Brien, P. Pham, N. D. Waal, S. Baskaran, B. C. Raimundo, J. W. Lam, M. M. Sopko, H. E. Purkey and M. J. Romanowski, *Bioorg. Med. Chem. Lett.*, 2006, **16**, 559-562.
33. *US Pat.*, US 2002/0137686 A1, 2002.
34. T. L. Graybill, R. E. Dolle, C. T. Helaszek, R. E. Miller and M. A. Ator, *Int. J. Pept. Protein Res.*, 1994, **44**, 173-182.
35. H. Roschitzki-Voser, T. Schroeder, E. D. Lenherr, F. Frolich, A. Schweizer, M. Donepudi, R. Ganesan, P. R. E. Mittl, A. Baici and M. G. Grutter, *Protein Expression Purif.*, 2012, **84**, 236-246.
36. W. Wannamaker, R. Davies, M. Namchuk, J. Pollard, P. Ford, G. Ku, C. Decker, P. Charifson, P. Weber, U. A. Germann, K. Kuida and J. C. Randle, *J. Pharmacol. Exp. Ther.*, 2007, **321**, 509-516.
37. D. S. Karanewsky, X. Bai, S. D. Linton, J. F. Krebs, J. Wu, B. Pham and K. J. Tomaselli, *Bioorg. Med. Chem. Lett.*, 1998, **8**, 2757-2762.
38. M. Poreba, A. Strozyk, G. S. Salvesen and M. Drag, *Cold Spring Harbor Perspect. Biol.*, 2013, **5**, a008680.
39. S. Roy, J. R. Sharom, C. Houde, T. P. Loisel, J. P. Vaillancourt, W. Shao, M. Saleh and D. W. Nicholson, *Proc. Natl. Acad. Sci. U. S. A.*, 2008, **105**, 4133-4138.
40. C. G. Wermuth, *J. Org. Chem.*, 1979, **44**, 2406-2408.
41. B. Simoneau and P. Brassard, *Tetrahedron*, 1988, **44**, 1015-1022.
42. D. Maclean, R. Hale and M. Y. Chen, *Org. Lett.*, 2001, **3**, 2977-2980.
43. K. Beaumont, K. Dack, L. Gardner, R. Webster and D. Smith, *Drug Metab. Rev.*, 2003, **35**, 58-58.

44. J. D. Larsen and H. Bundgaard, *Int. J. Pharm.*, 1987, **37**, 87-95.
45. J. J. Talley, S. R. Bertenshaw, D. L. Brown, J. S. Carter, M. J. Graneto, M. S. Kellogg, C. M. Koboldt, J. H. Yuan, Y. Y. Zhang and K. Seibert, *J. Med. Chem.*, 2000, **43**, 1661-1663.
46. J. D. Larsen, H. Bundgaard and V. H. L. Lee, *Int. J. Pharm.*, 1988, **47**, 103-110.
47. S. L. Huang, P. J. Connolly, R. H. Lin, S. Emanuel and S. A. Middleton, *Bioorg. Med. Chem. Lett.*, 2006, **16**, 3639-3641.
48. L. J. Scott, *Drugs*, 2016, **76**, 413-418.
49. T. Asaki, K. Kuwano, K. Morrison, J. Gatfield, T. Hamamoto and M. Clozel, *J. Med. Chem.*, 2015, **58**, 7128-7137.
50. L. Vande Walle, N. Van Opdenbosch, P. Jacques, A. Fossoul, E. Verheugen, P. Vogel, R. Beyaert, D. Elewaut, T. D. Kanneganti, G. van Loo and M. Lamkanfi, *Nature*, 2014, **512**, 69-73.

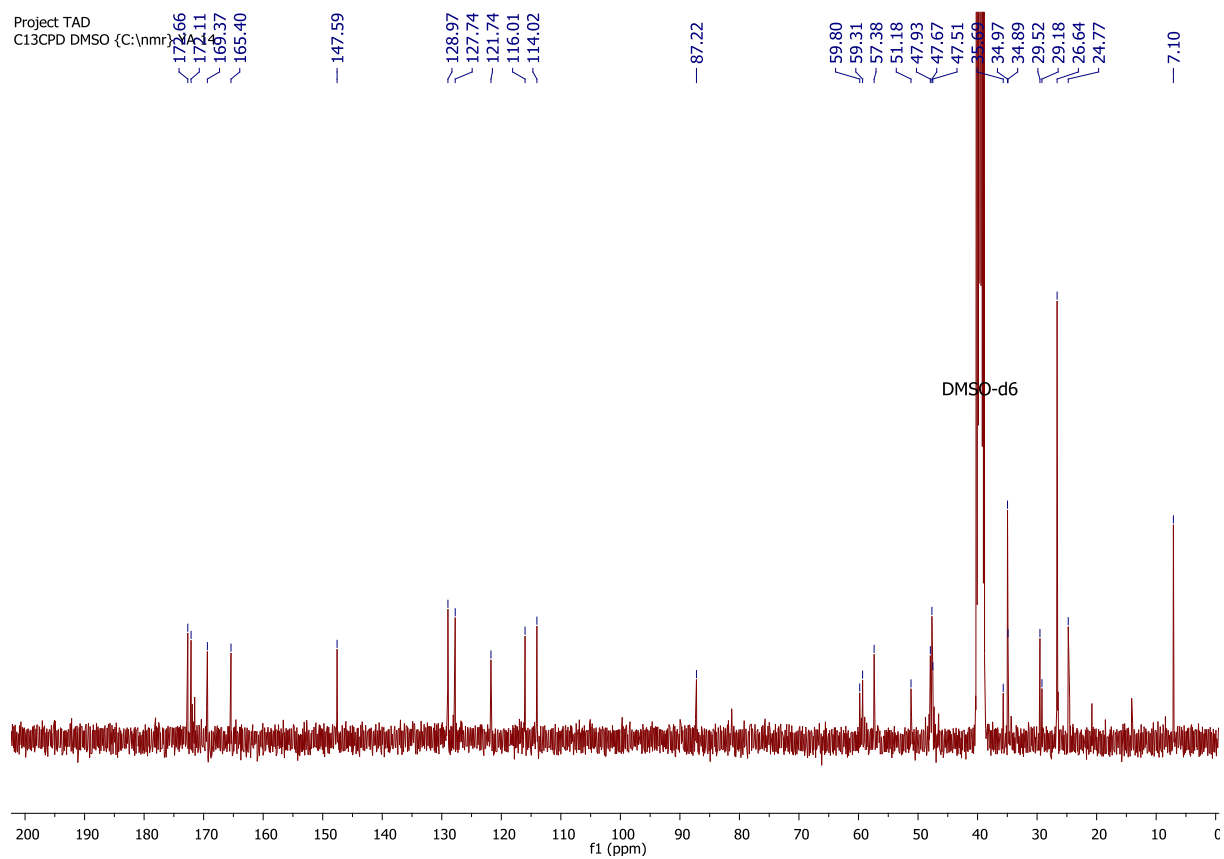
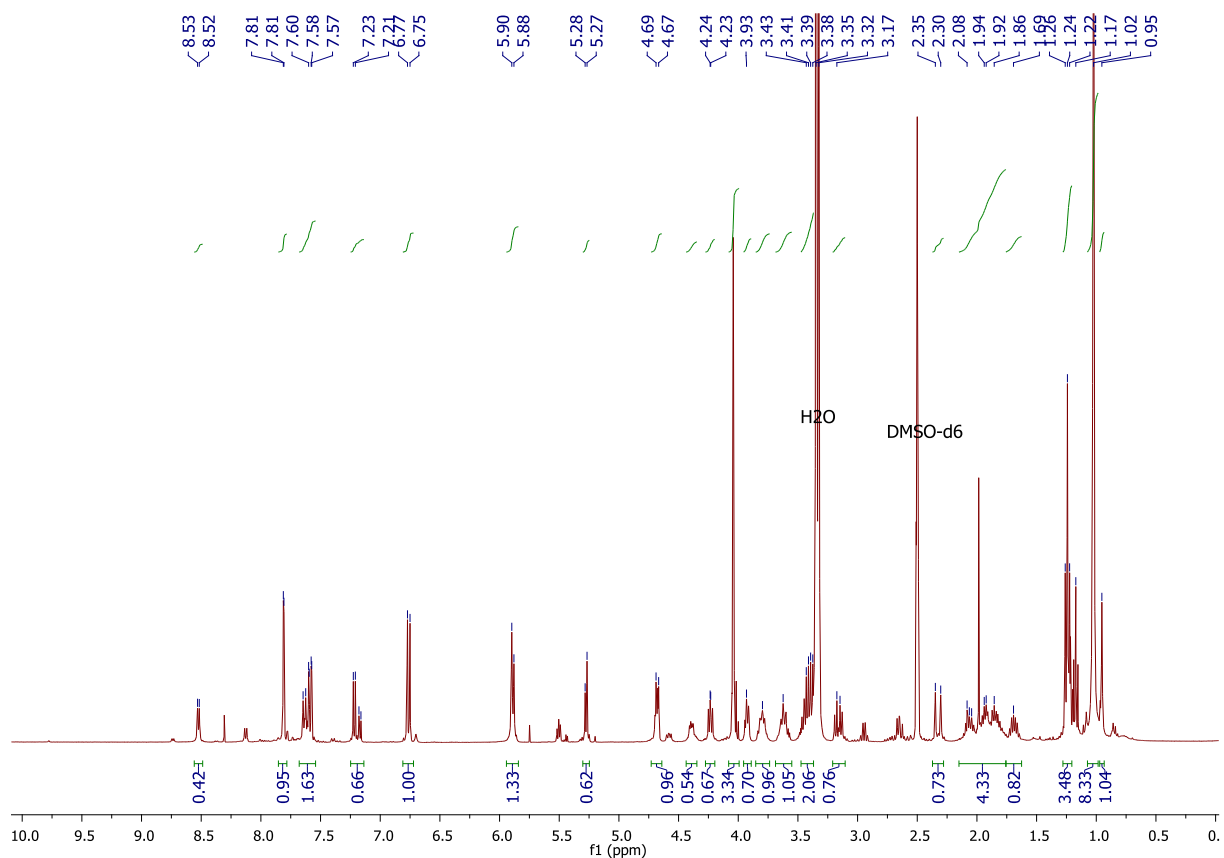
Supporting information

NMR spectroscopy

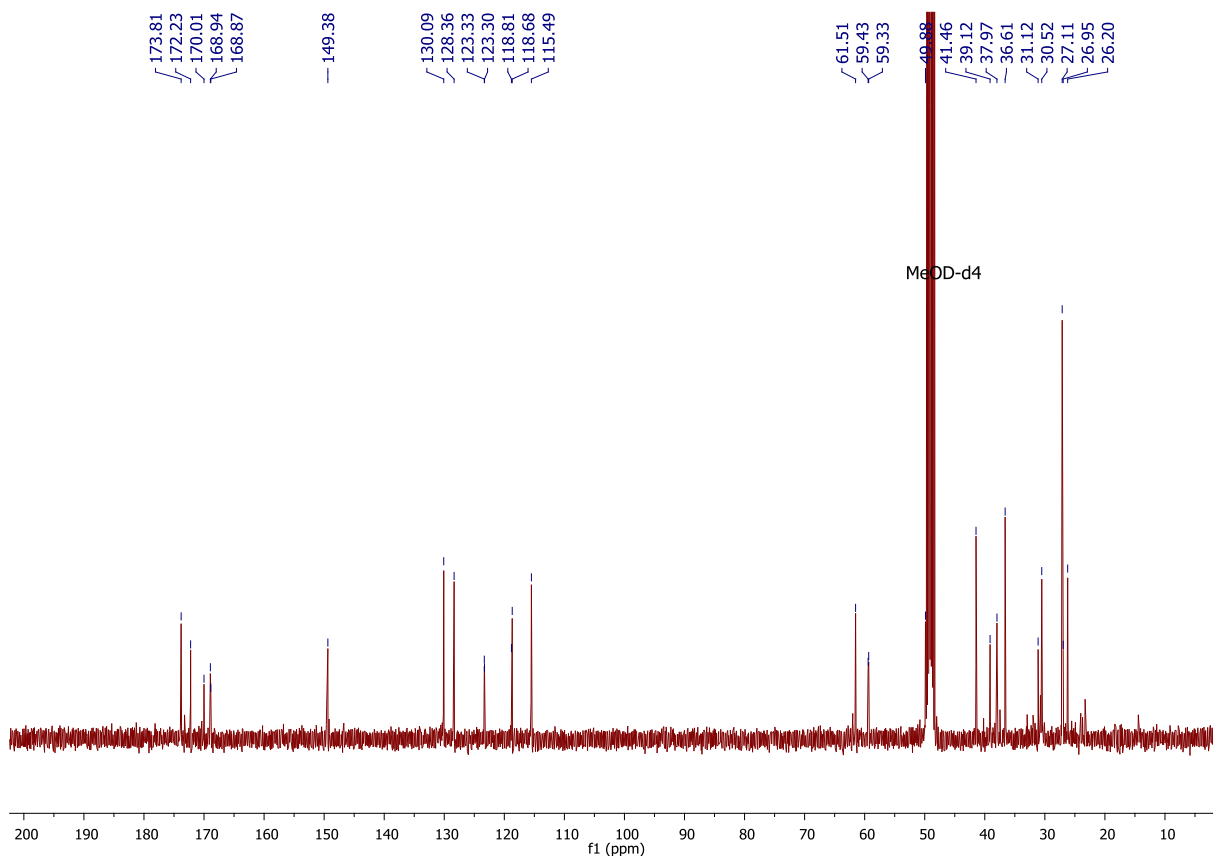
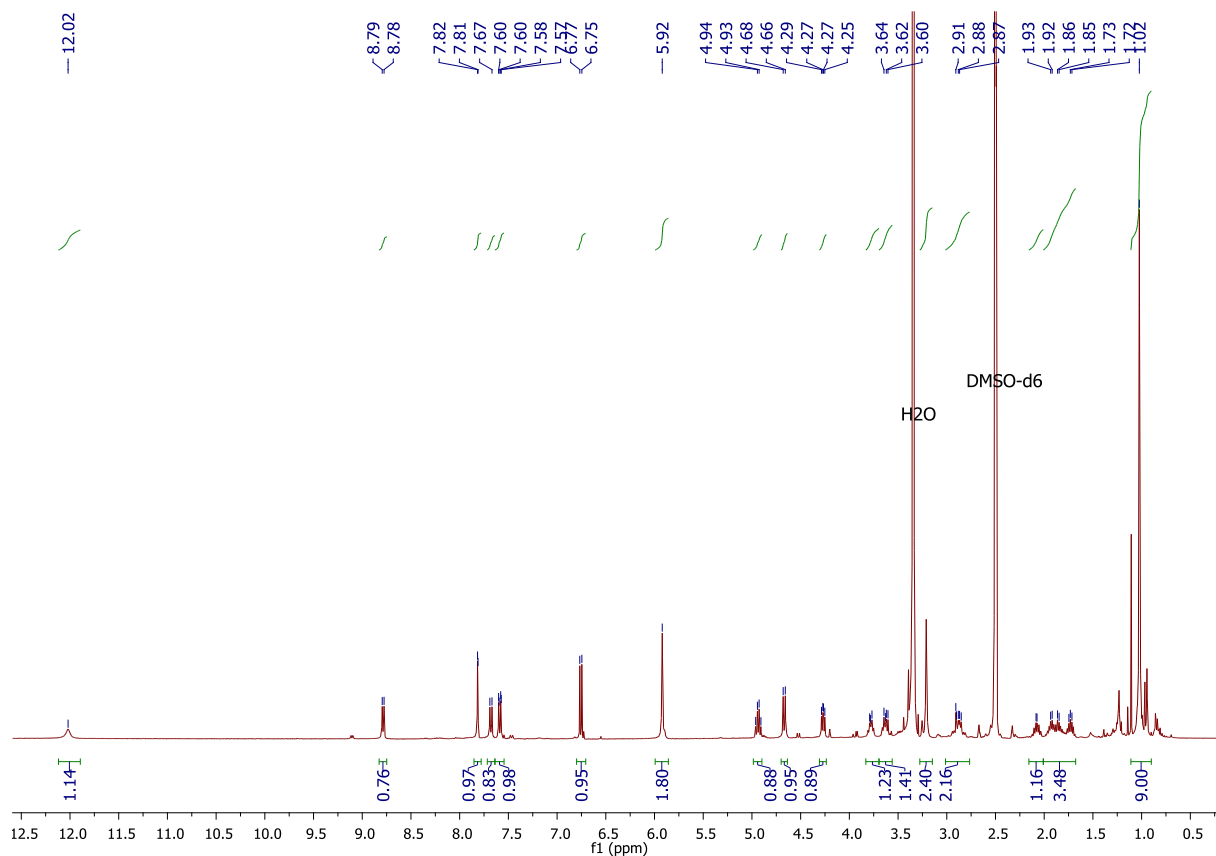
1. Compound 3.3

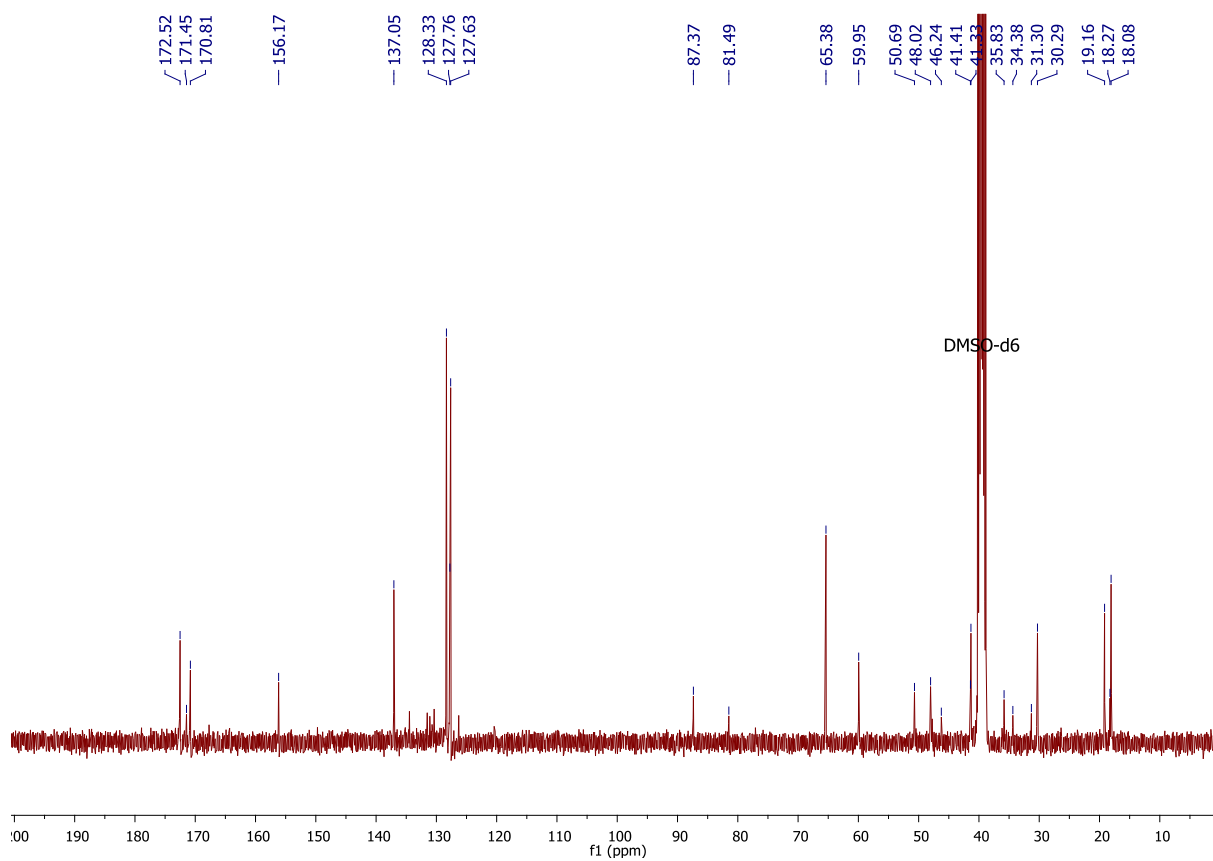
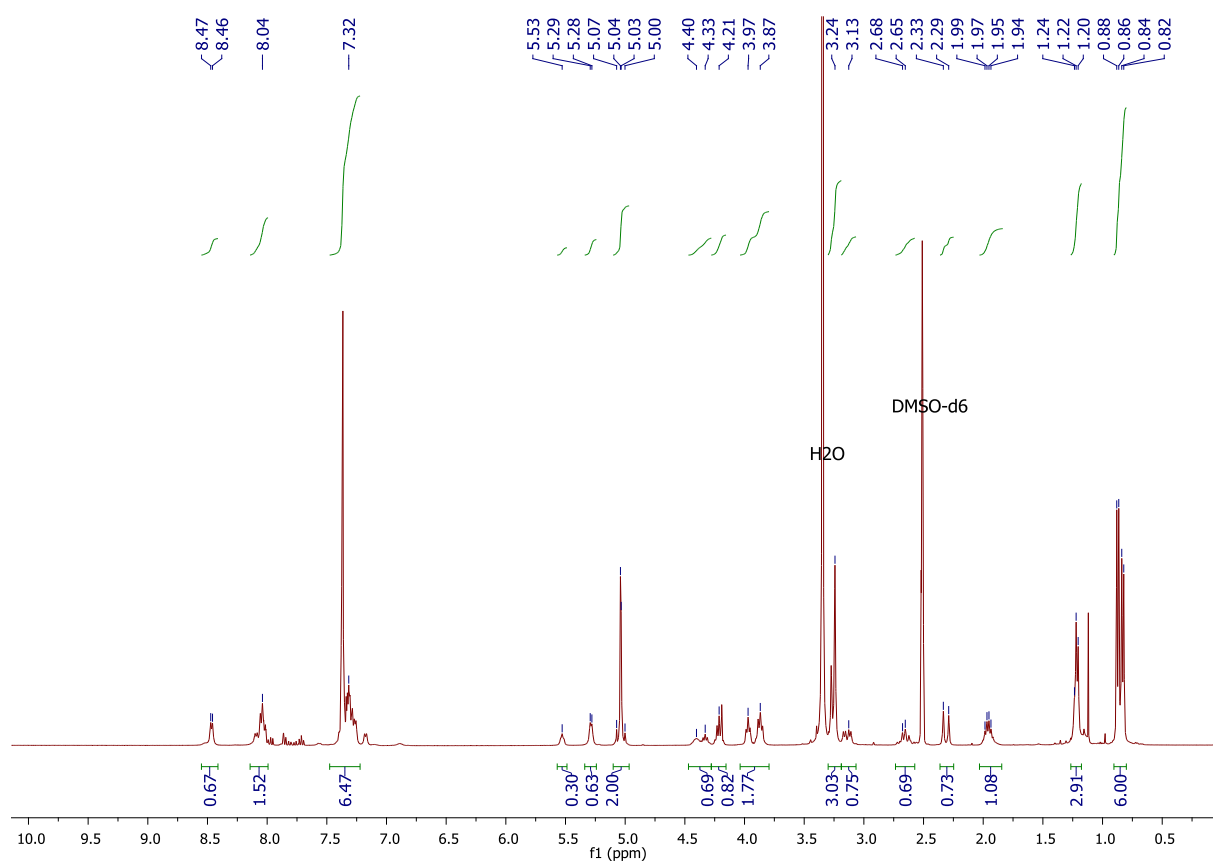


2. Comound 3.4

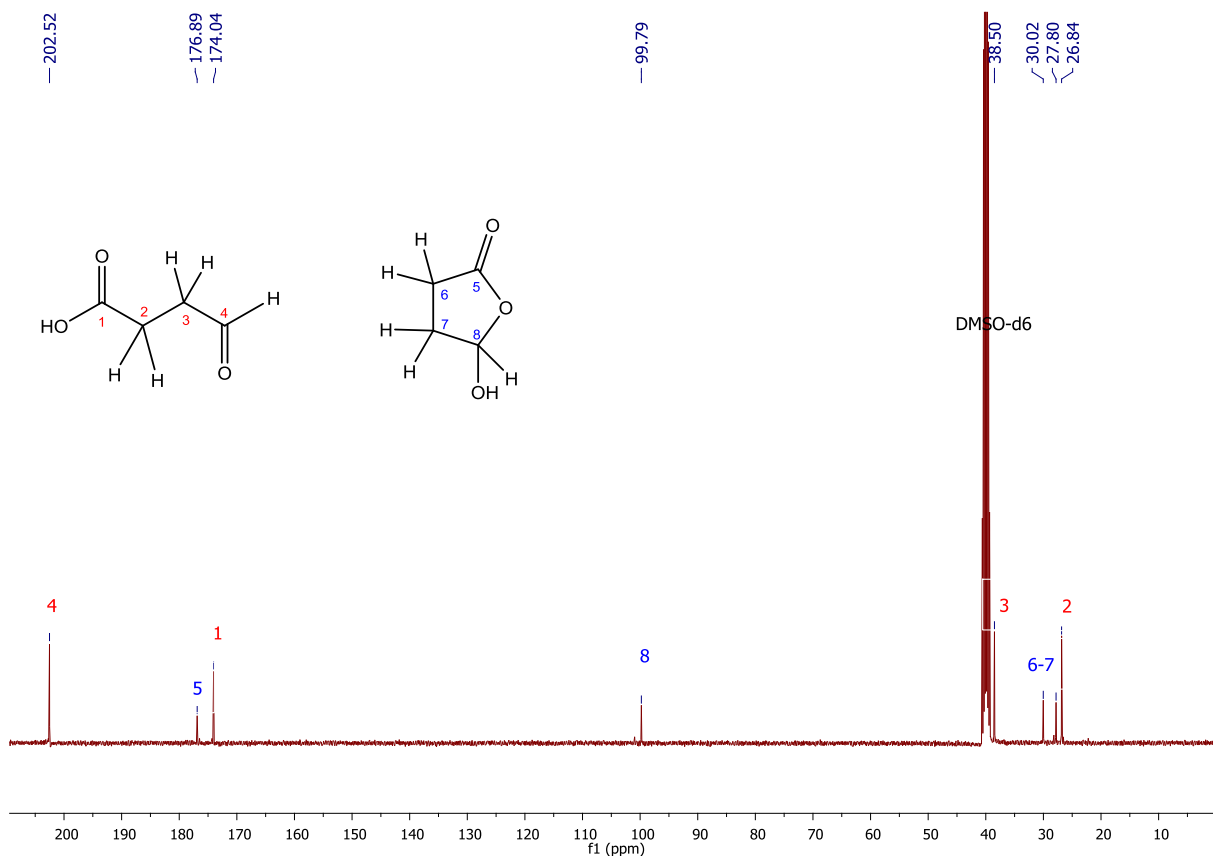
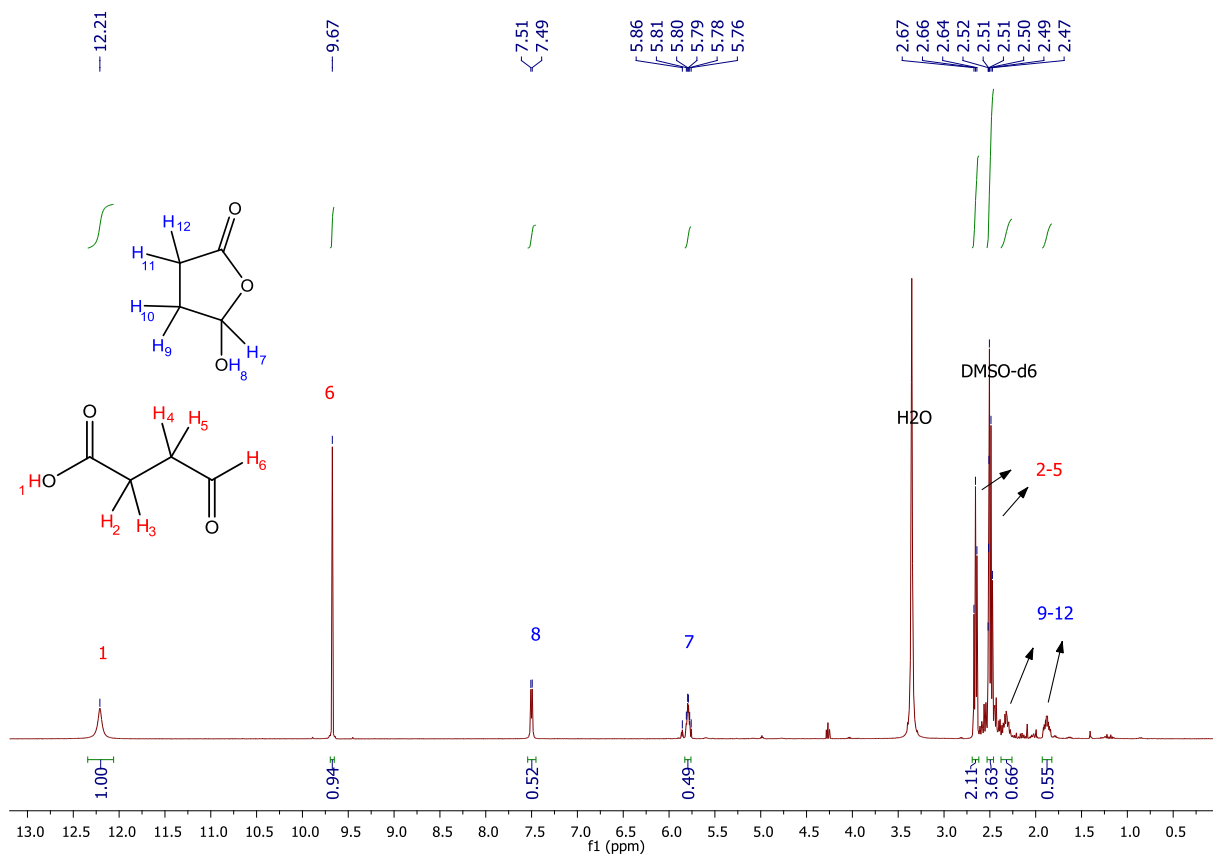


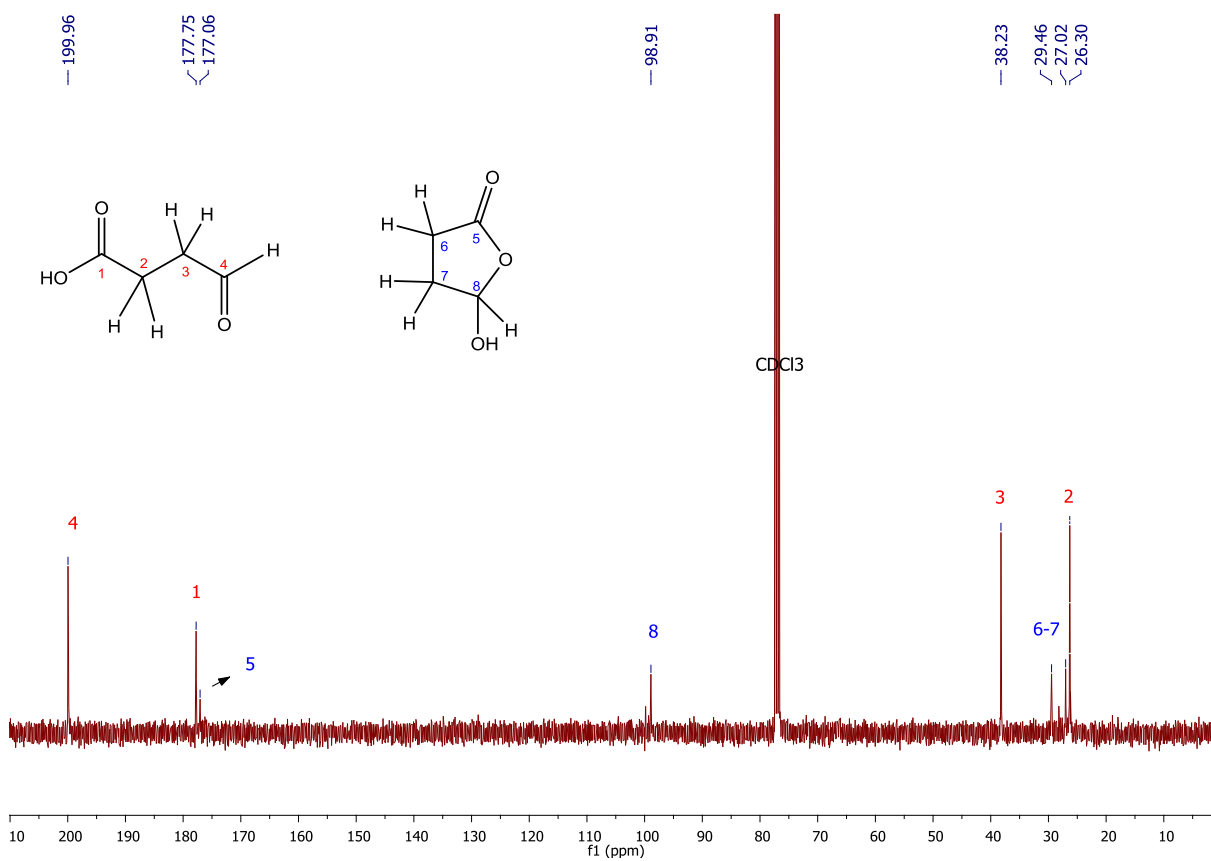
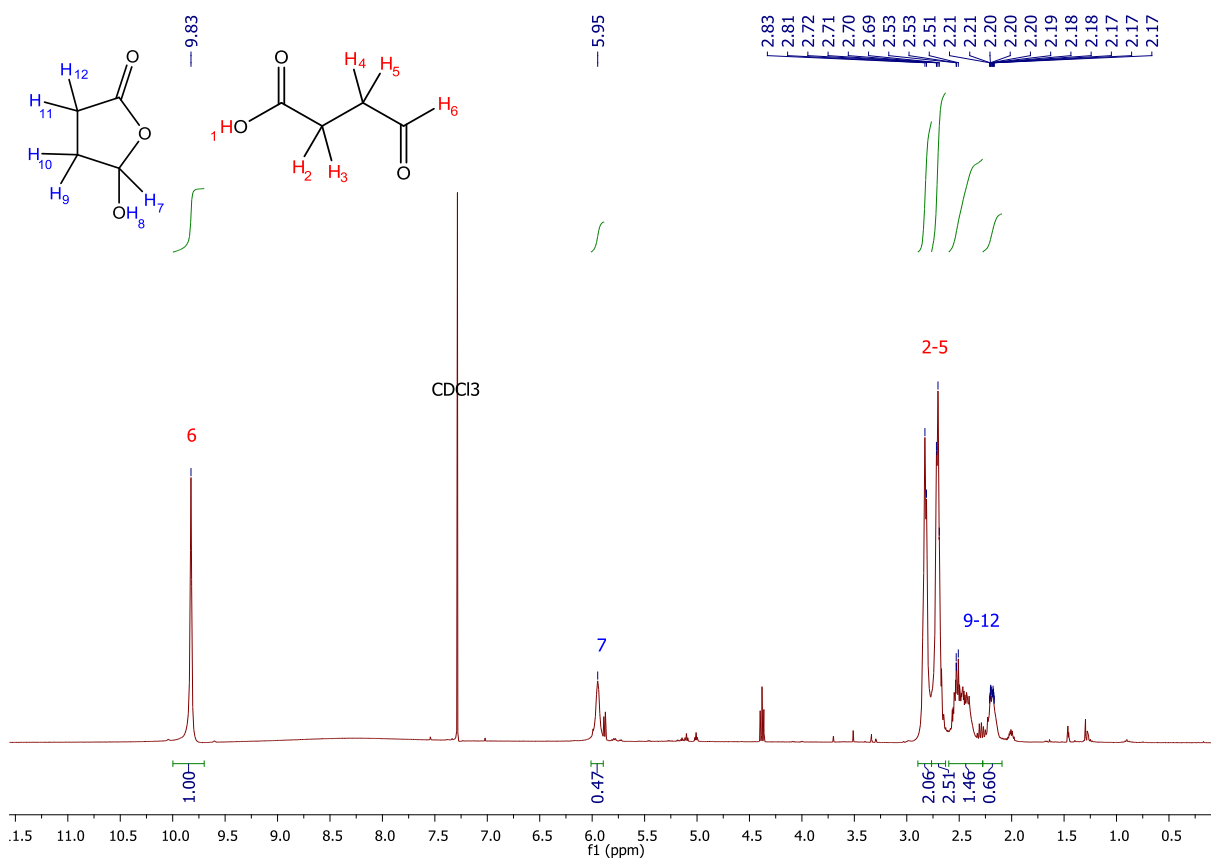
3. Compound 3.6



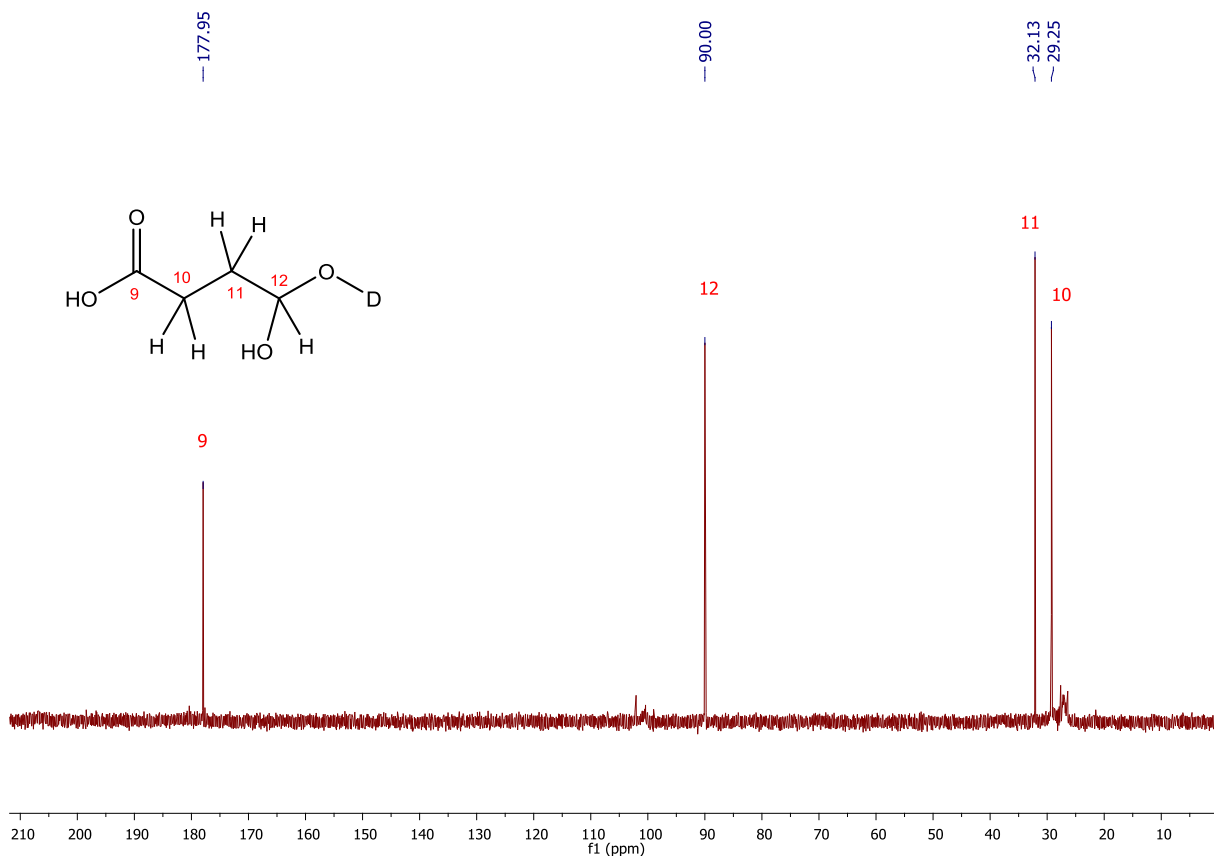
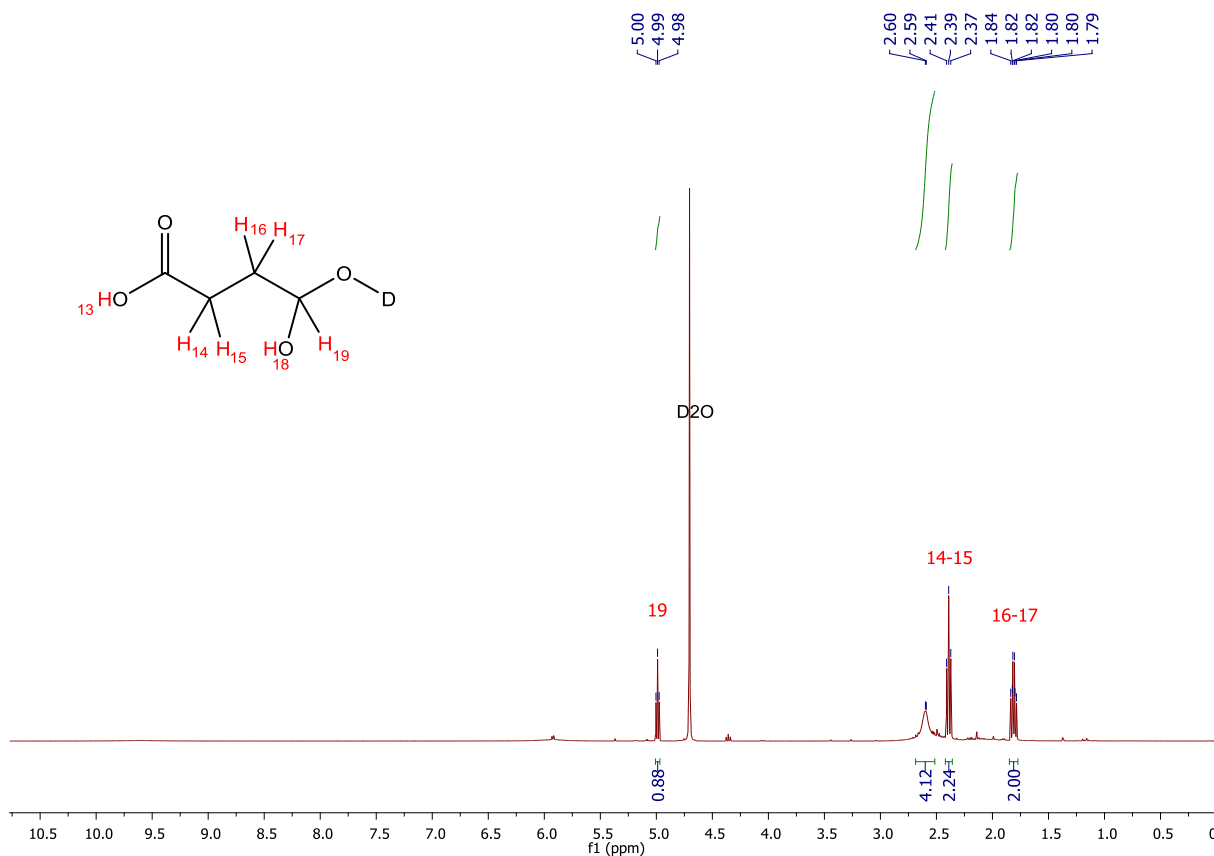
4. Compound **3.8**

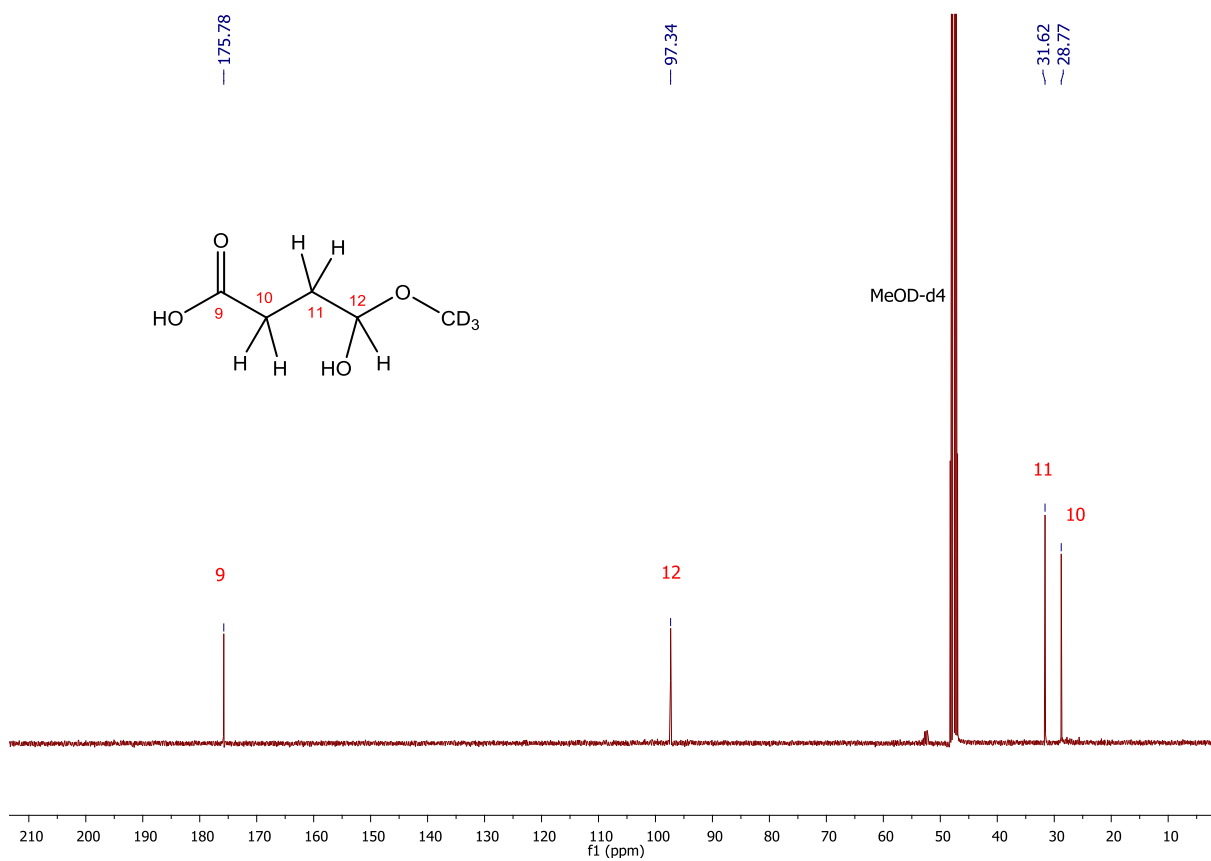
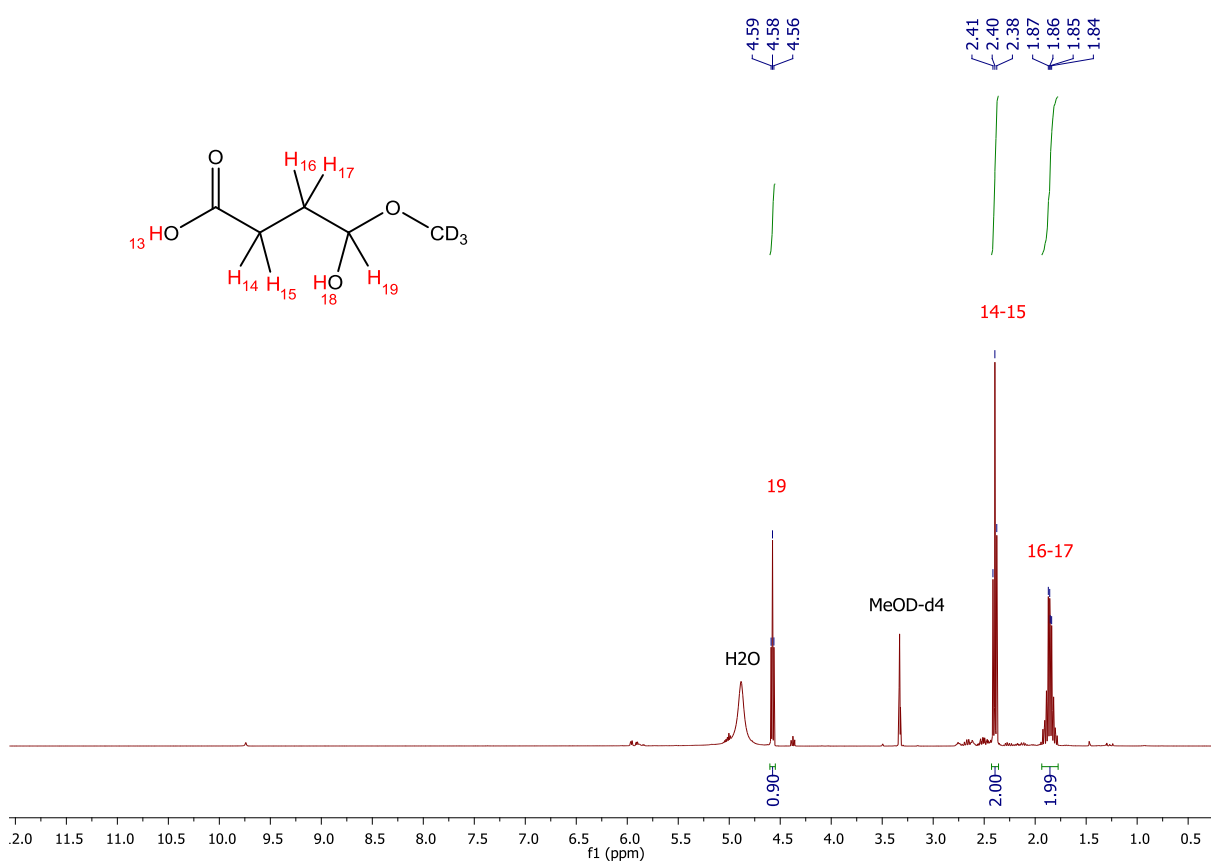
5. Compound **3.24**, **3.29a** or **3.29b** (in DMSO-d₆)



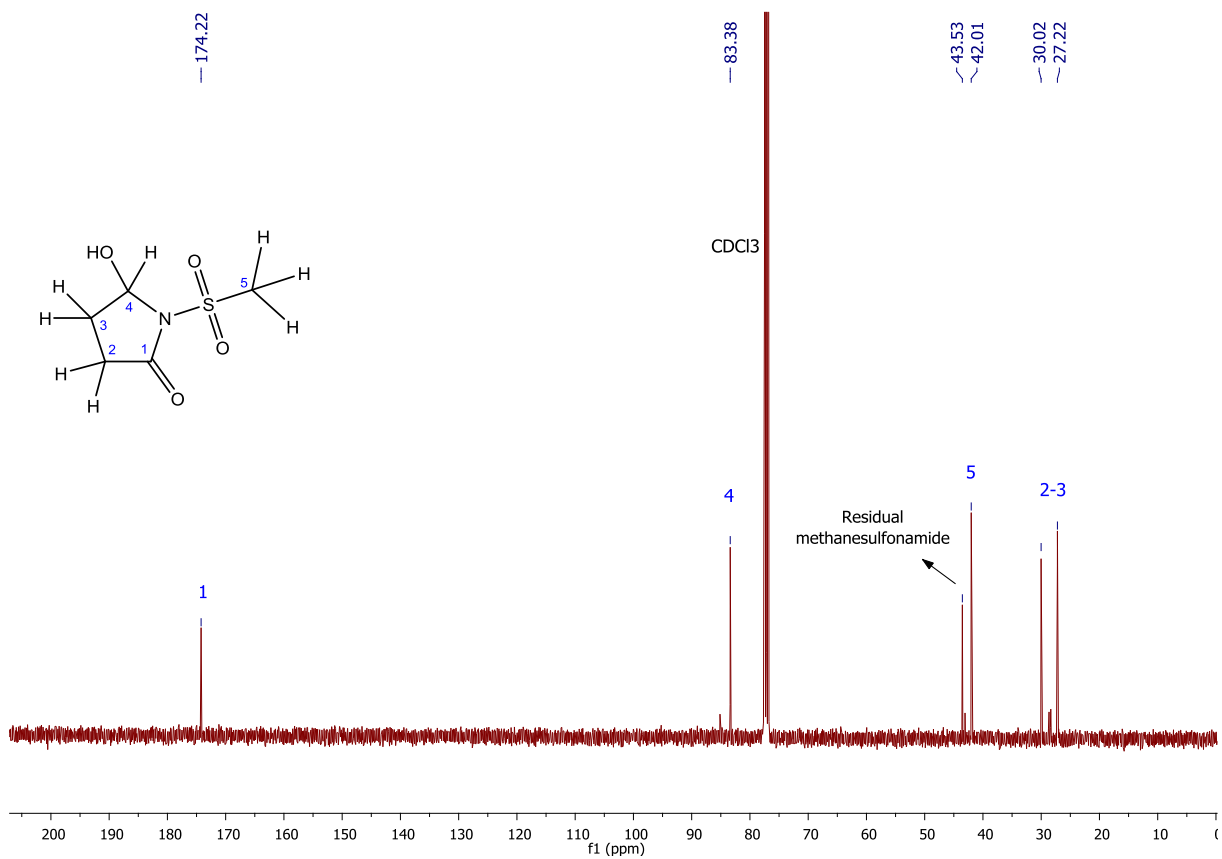
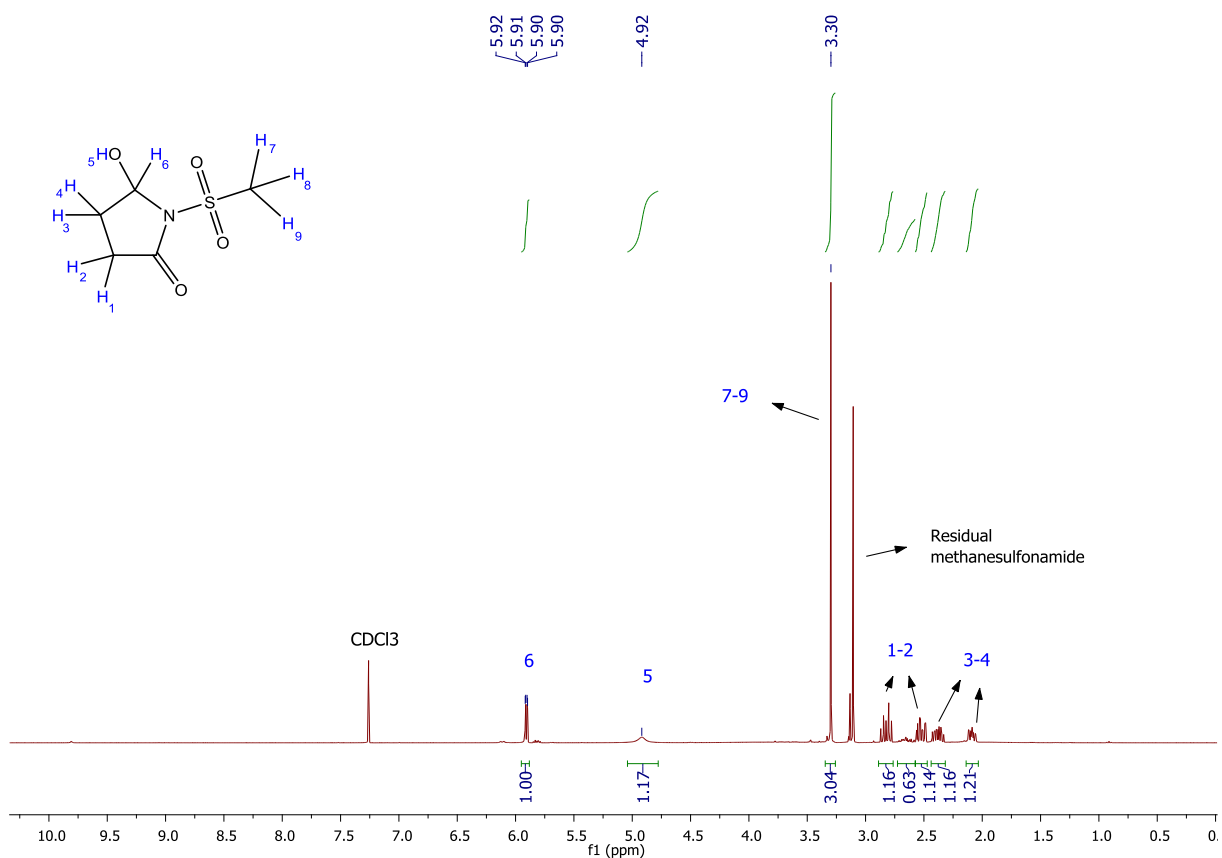
6. Compound **3.24**, **3.29a** or **3.29b** (in CDCl₃)

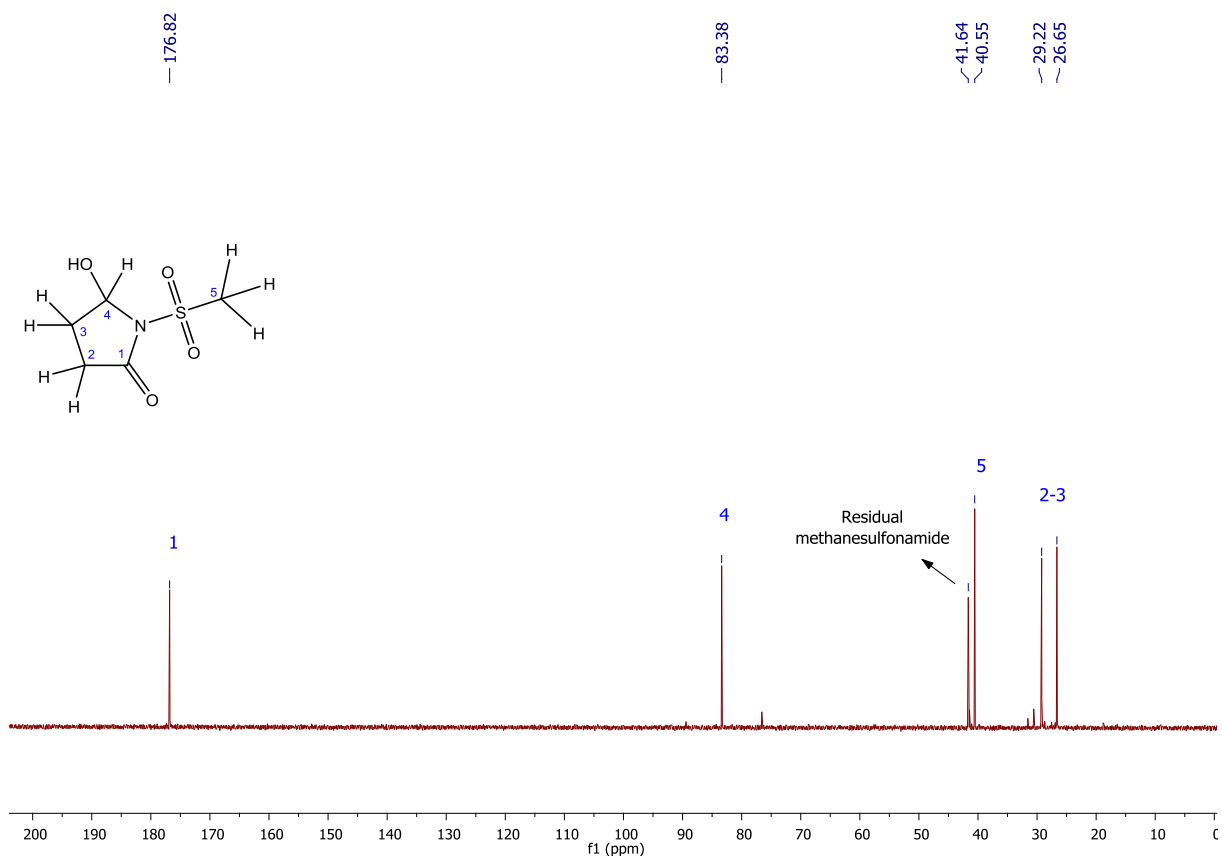
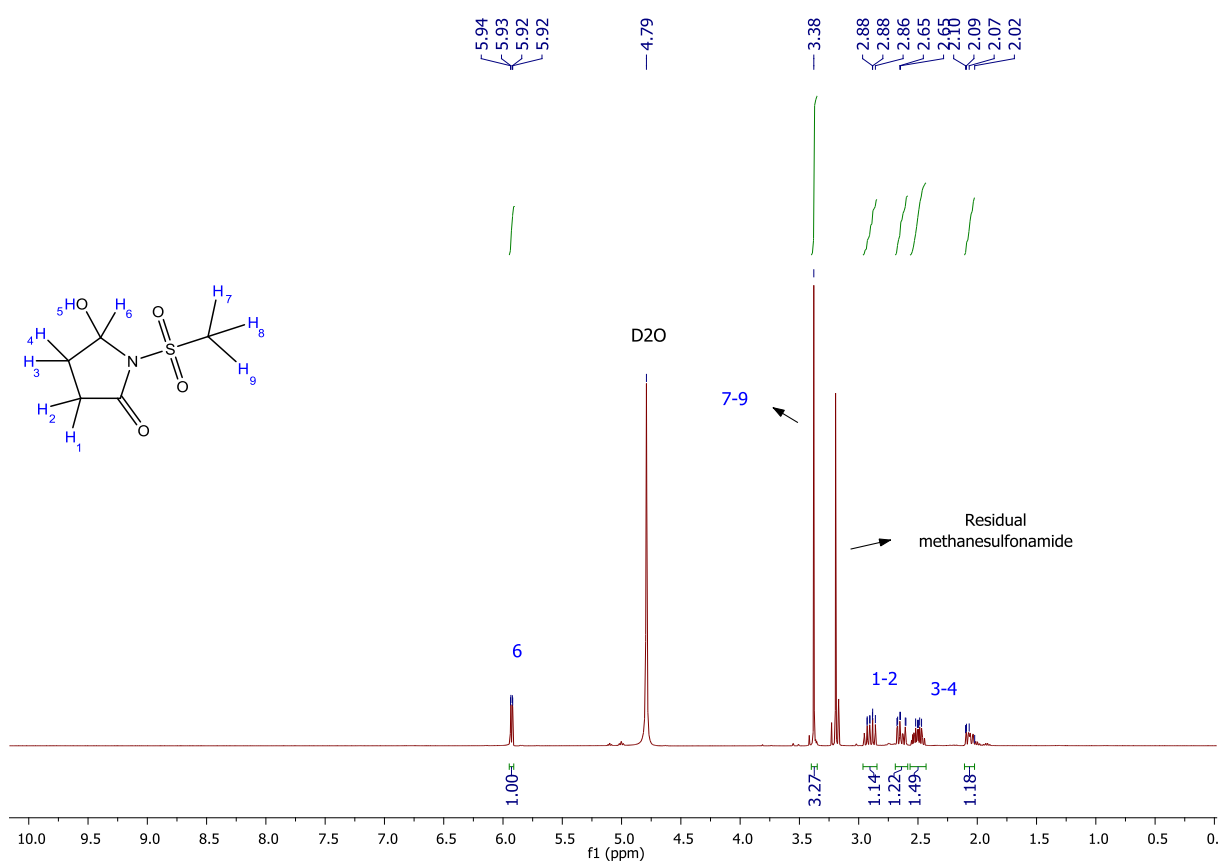
7. Compound **3.24**, **3.29a** or **3.29b** (in D₂O)



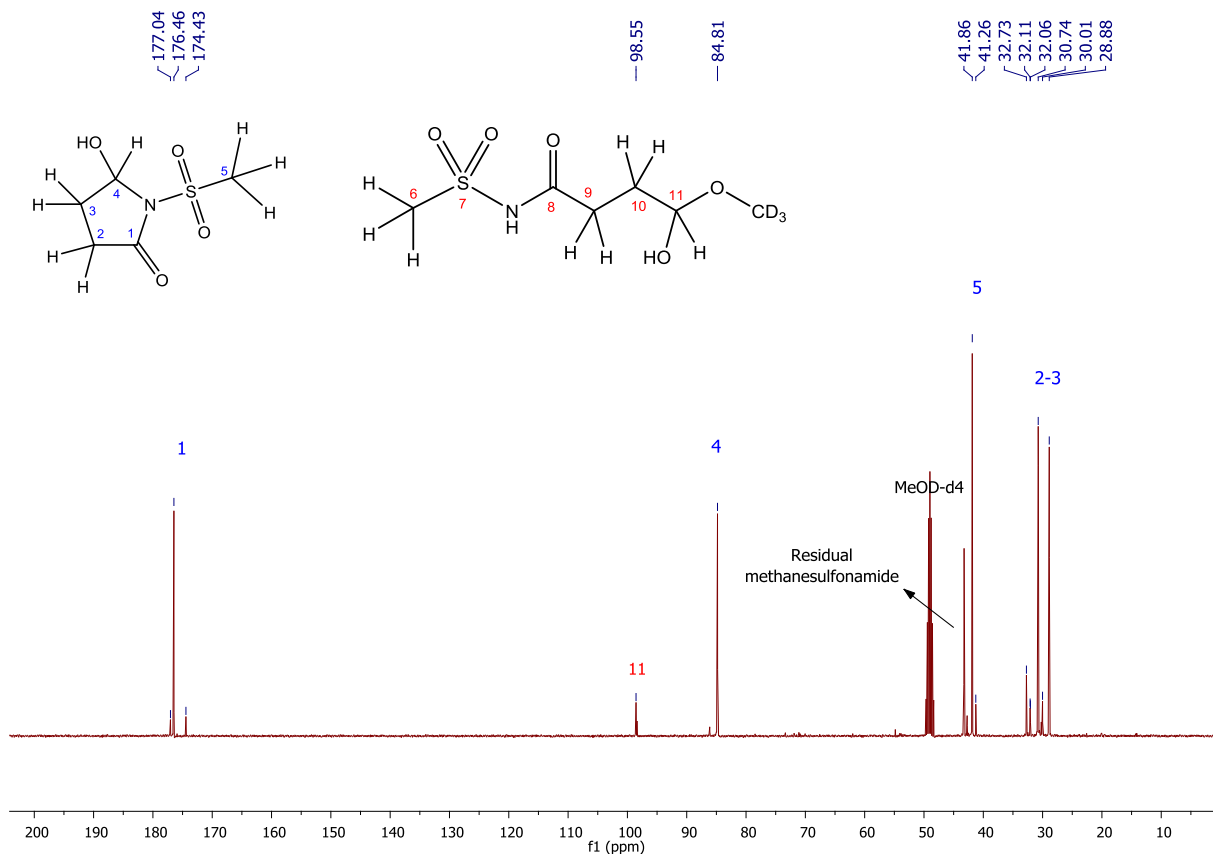
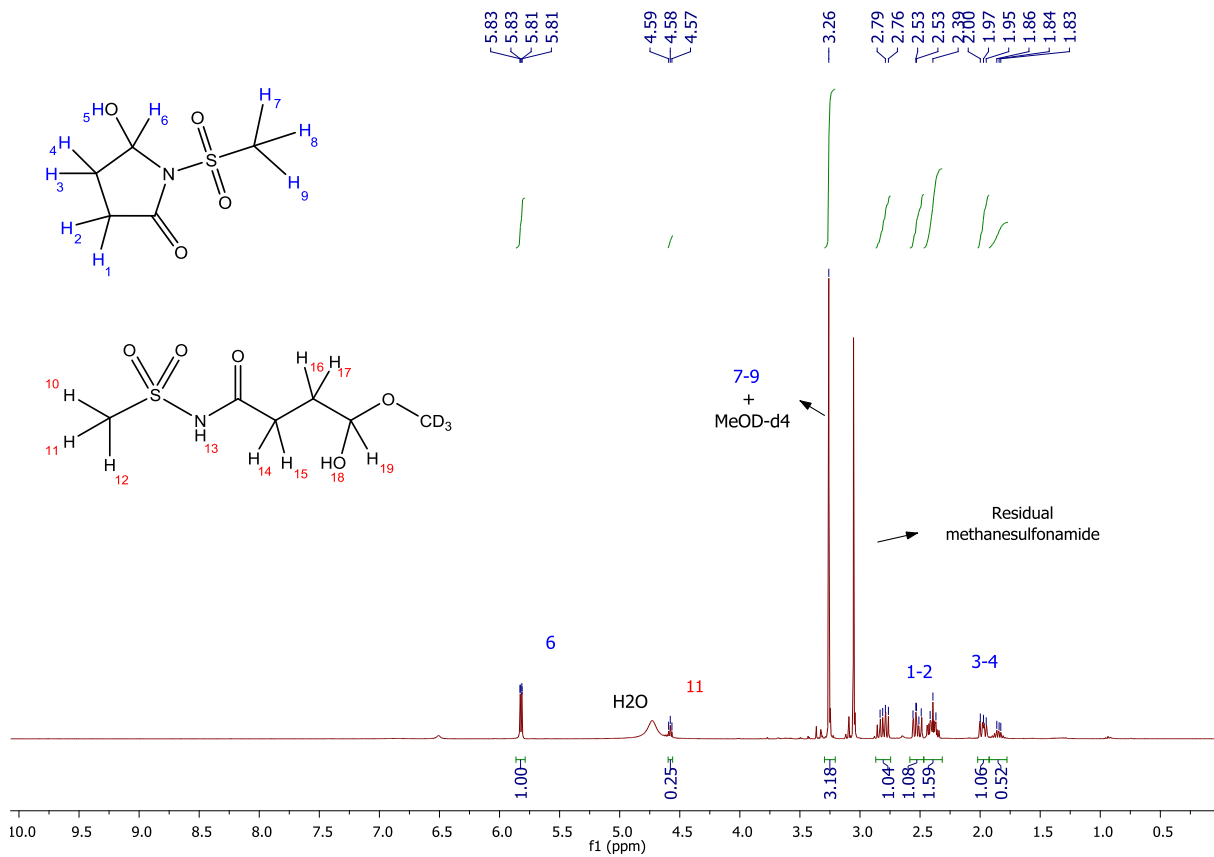
8. Compound **3.24**, **3.29a** or **3.29b** (in MeOD- d_4)

9. Compound **3.28**, **3.30a** or **3.30b** (in CDCl₃)



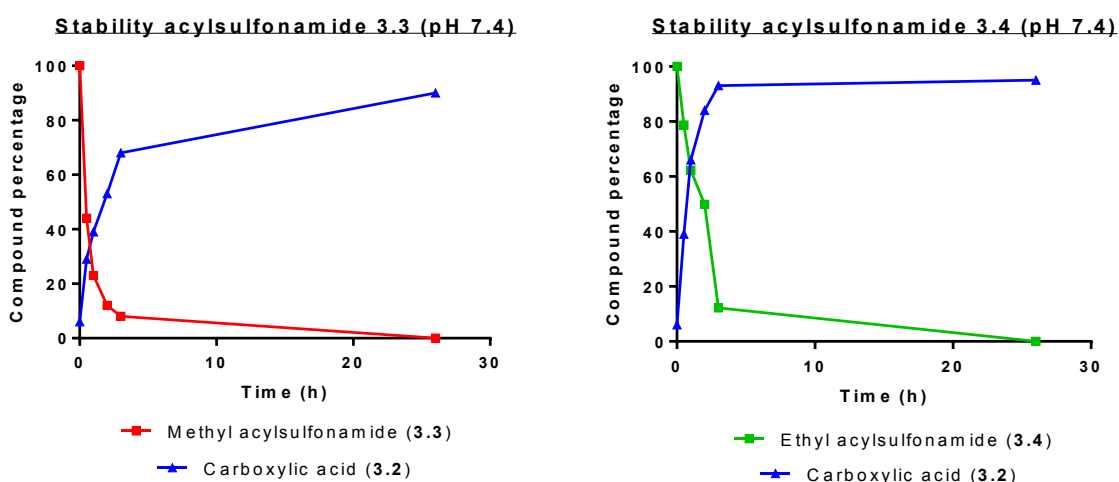
10. Compound **3.28**, **3.30a** or **3.30b** (in D₂O)

11. Compound **3.28**, **3.30a** or **3.30b** (in MeOD-d₄)

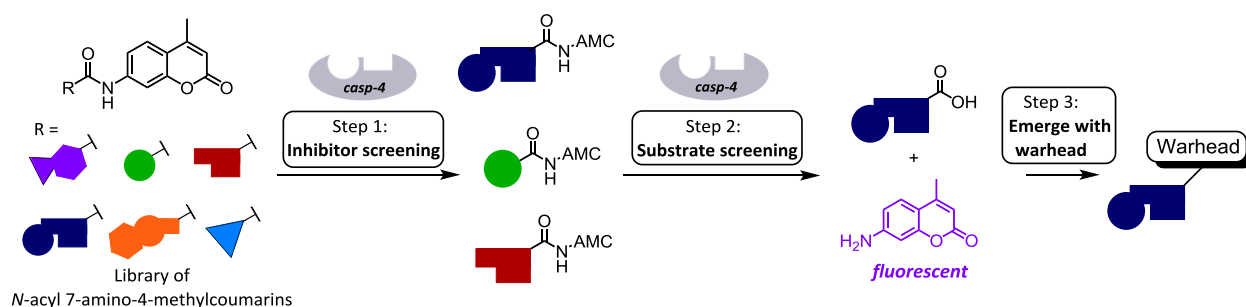


Stability: Hydrolysis of acyl sulfonamide-aldehyde, into carboxylic acid-aldehyde

10 mM stock solutions in DMSO of compounds **3.3** and **3.4** were prepared. The stock solutions were diluted to a 50 μ M solution with 10 mM PBS buffer (pH 7.4). The mixture was gently shaken at 37 $^{\circ}$ C for 9 days. At different time points (0 min, 30 min, 1 h, 2 h, 3 h and 26 h) 100 μ L was withdrawn which was analyzed with UPLC-MS. The percentage of parent acyl sulfonamide (**3.3**, **3.4**) remaining at each time point relative to the 0 min sample was then calculated from UPLC-MS peak area ratios. An additional measurement was done after 9 days, which was considered the time point for 100 % conversion. The percentage of carboxylate-based inhibitor (**3.2**) at each time point was calculated relative to the peak area at the 9 days time point. The samples were prepared in duplicate. UPLC-MS measurements were carried out on a Waters Acquity UPLC system coupled to a Waters TUV detector, ESI source and a Waters Acquity TQ Mass detector.



The identification of isosteric replacements for carboxylic acids in caspase inhibitors, determined by the Modified Substrate Activity Screening (MSAS)



The content of this chapter is based on:

The identification of isosteric replacements for carboxylic acids in caspase inhibitors, determined by the Modified Substrate Activity Screening (MSAS); **Adriaenssens, Y.**; Zonnekeijn, L.; Gladysz, R.; Peeraer, A.; Cleenewerck, M.; Elvas, F.; Joossens, J.; Lambeir, A.; Augustyns, K.; Van der Veken, P., *in preparation*.

4 The identification of isosteric replacements for carboxylic acids in caspase inhibitors, determined by the Modified Substrate Activity Screening (MSAS)

4.1 Introduction

4.1.1 Caspases

Caspases, a family of cysteine-dependent aspartate-specific proteases, fulfill critical roles in mammalian apoptosis and proteolytic activation of cytokines.¹ Depending on their biological functions as well as their sequence homology, they are typically classified into two subfamilies.^{2, 3} The first subfamily consists of caspases with key roles in the initiation (caspase-2, -8, -9, -10) and execution (caspase-3, -6, -7) of programmed cell death, or apoptosis, in a variety of cell types.⁴ The second subfamily is called the inflammatory caspases (-1, -4, -5, -11, -12) which are key modulators of inflammatory and host defense responses through the secretion of pro-inflammatory cytokines and the induction of pyroptosis, a pro-inflammatory cell death mode.^{5, 6} Caspase-1 (interleukin-1 β -converting enzyme, ICE) has been the most extensively studied member of the inflammatory group to date. Upon dysregulation of caspase-1, it is involved in the pathogenesis of many inflammatory diseases such as atherosclerosis, type-2 diabetes, gout and rare autoinflammatory disorders.⁷ Other members of this subfamily include human caspases-4, -5 and -12. Caspase-4 and -5 are poorly characterized, partly due to the fact that mice only express three inflammatory caspases (caspase-1, -11, -12). In that point of view it is not clear whether human caspase-4 and -5 represent functional orthologs of murine caspase-11.⁸ Although caspase-4 and -5 have shown to mediate inflammasome activation^{8, 9}, the amino acid identity between caspase-11 and caspase-4 or -5 is only 60%, consistent with the possibility that they may carry out unique functions.^{10, 11}

4.1.2 Overcoming selectivity problems with respect to caspase inhibitors

Selectively inhibiting one member of the caspase family remains a huge obstacle. Though some caspase-1 inhibitors have entered clinical trials, cross-reactivity with other inflammatory caspases remains relatively large.^{12, 13} In addition, despite substantial effort, only a few caspase-4 inhibitors have been reported that, to our regret, simultaneously target inflammatory caspases-1 and -5 as well, all of which are based on the tetrapeptide sequence WEHD.^{14, 15} In that perspective, we are convinced that further investigation towards higher levels of selectivity is essential in the investigation of caspase drug design.

Overcoming obstacles in regard to selectivity in the development of synthetic substrates and inhibitors has been comprehensively summarized by Drag and co-workers.¹⁶ Interestingly, limited effort has been described on the alteration of the P1-aspartate residue in caspases substrates. As generally

acknowledged, caspases have a strong preference for aspartate in the P1-substrate position and alteration of this amino acid mostly leads to dramatic loss of substrate or inhibitory activity.¹⁷ For this reason, most reported caspase inhibitors also incorporate a carboxylate that mimics the aspartate residue and acts as an affinity-enhancing structural element. Nonetheless, we hypothesize that isosteric modification of the carboxylate function can have a considerable impact on the selectivity towards individual members of the caspase family. Moreover, the use of another acidic group with distinctive size or electronic properties, could overcome drawbacks of carboxylates, such as toxic metabolite formation and low cellular permeability. Any improvement regarding these factors would clearly provide biopharmaceutical advancements for caspase-targeting compounds.^{18,19}

So far, the number of reports on the use of carboxylate isosteres in caspase-targeting compounds has been limited. The most promising isosteric replacement was the use of *N*-acylsulfonamides, firstly investigated by Okamoto *et al.* and further elaborated by our group.^{20,21} We demonstrated a twofold conclusion depending on the warhead functionality next to the acylsulfonamide. First, the combination of the isostere with an aldehyde warhead proved to lead to unstable compounds acting as prodrugs for the carboxylate-based parent inhibitors. Second, analogues with a carbonitrile warhead were found to be stable, but had a decreased caspase potency. Concerning the latter, it is important to consider that optimal positioning of the isostere inside the enzymatic pocket is essential to allow the warhead to adapt an ideal conformation for covalent bond formation with the caspases' catalytic cysteine residue.

4.1.3 Methodology: the Modified Substrate Activity Screening (MSAS)

This study focused on the search for an optimal isosteric fit for caspase-1, followed by the translation into inhibitors, which was performed by a fragment-based drug design approach, called the Modified Substrate Activity Screening (MSAS). This methodology comprises the enzymatic identification of building blocks that bind to the S1 region of the target protease. Up to now, this approach has already been validated in enzyme inhibitor discovery for urokinase plasminogen activator (uPA), a trypsin-like serine protease that is overexpressed in metastasizing solid tumors,^{22, 23} and ATG4B, a cysteine hydrolase that plays a key role in autophagy.²⁴ The MSAS methodology was described in response to the Substrate Activity Screening (SAS), devised by Ellman and co-workers.²⁵ While in the latter a library of fragments is only tested for substrates of a target enzyme, an additional preceding step involving a screening of the library for inhibitors has been included. As a result, false negatives are avoided, i.e. fragments with high potential for inhibitor discovery that are not identified in a SAS assay. Furthermore, MSAS also avoids false positives that can surface during a regular SAS assay, and runs

with better cost and time efficiency. A review that extensively documents the comparison between different variations of SAS-based methodologies has been recently reported by Gladysz *et al.*²⁶

MSAS includes three main steps, as visualized in **Figure 4.1**.²³ First, a particular library is screened for inhibitory fragments (step 1), providing SAR data for the interesting fragment types present within the library. The latter is considered very useful in contribution to fragment-based drug design (FBDD) applications. The set of hits identified during this phase is selected for the second step, consisting of a substrate screening (step 2). Optionally, a substrate optimization could be performed on the most promising fragments. Finally, the (optimized) substrates showing the highest efficiency are transformed into competitive, mechanism-based inhibitors, by replacing the processable bond with a mechanism-based warhead or a non-processable surrogate (step 3).

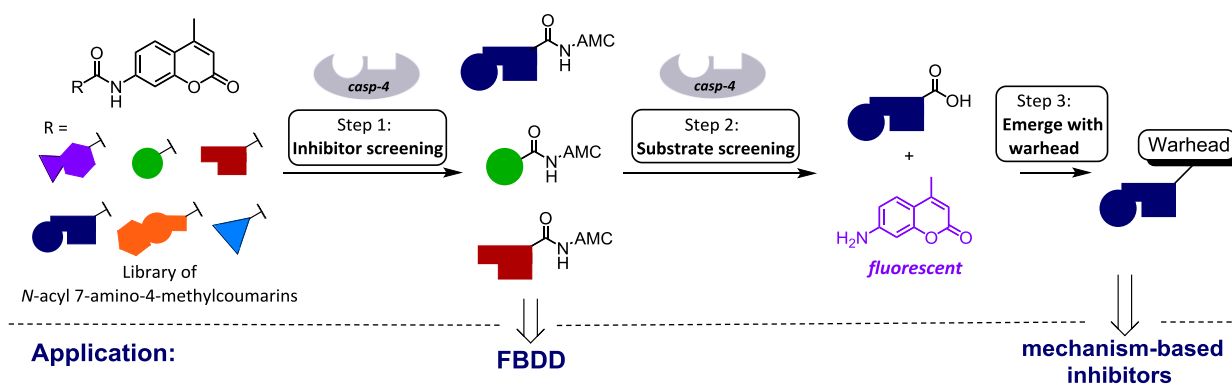


Figure 4.1. Outline of the MSAS approach. Figure was taken from ref [23].

4.2 Objectives of this chapter

The intention of this study is to identify isosteric replacements for carboxylic acids that nicely accommodate in the active site of caspase-1. Promising isosteres will then serve as the basis for the design of new inhibitors by linking them to warhead functionalities. Isosteric replacements will not only be able to provide improved physicochemical properties but are also presumed to lead to better selectivity towards certain caspases. To achieve this objective, a systematic approach will be applied that has recently been developed in our lab: the Modified Substrate Activity Screening.

4.3 Results and discussion

4.3.1 Library synthesis

A library consisting of *N*-acyl 7-amino-4-methylcoumarins with non-peptidic, low molecular-weight *N*-acyl groups (MW < 150) was produced. The main part of this library comprised a subset of isosteres and carboxylate derivatives to mimic the preferred P1 Asp-residue in the peptide substrates of the caspases. Specific carboxylate surrogates were selected, taken into account their acidity (pK_a), size,

shape, charge distribution and lipophilicity (**Figure 4.2**). Also the distance between the isostere and the potentially scissile *N*-acylcoumaride bond was varied to maximize the hit rate.

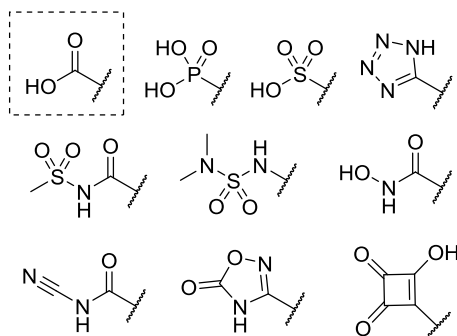
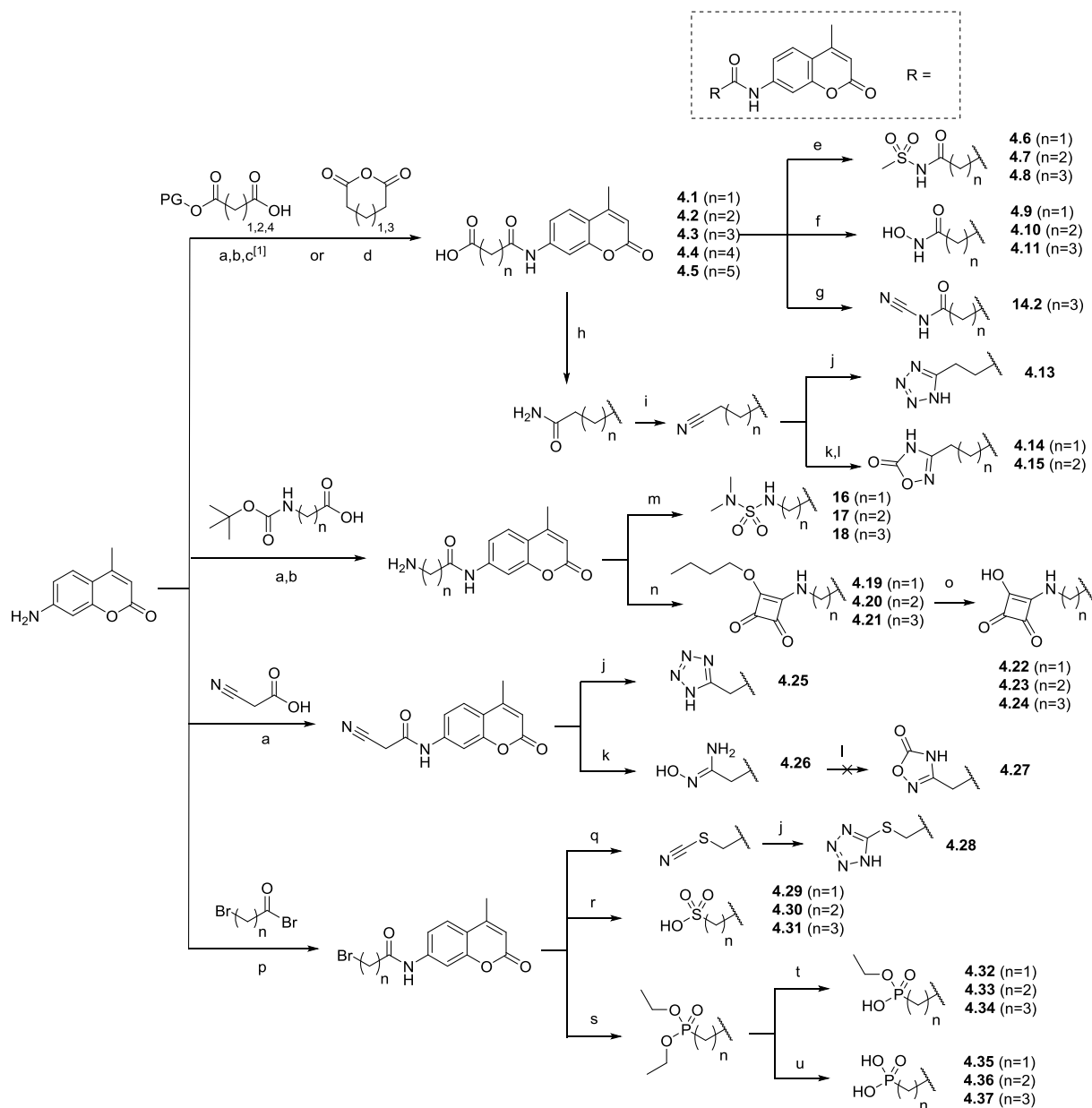


Figure 4.2. Examples of carboxylic acid isosteres used in this MSAS study.

The amide bond, connecting the isostere with 7-amino-4-methylcoumarin (AMC), was installed, generally according to a one-pot procedure with Ghosez's reagent (**Scheme 4.1**, reaction a). This required a readily available carboxylic acid on the opposite side of the main (protected) carboxylic acid or its isostere. Depending on the availability, carboxylic acids **4.1-4.5** were produced starting from the corresponding cyclic anhydride or ester protecting group. In case of the latter, an additional deprotection step was required, either in acidic (*tert*-butyl ester) or basic media (ethyl ester). Some of these reference molecules also served as intermediates for the transformation into the following isostere-containing final products: acylsulfonamides **4.6-4.8**, hydroxamic acids **4.9-4.11** and acylcyanamide **4.12**. Next, two carboxylic acids were selected to undergo amide coupling and dehydration in order to obtain carbonitriles. A [2+3] cycloaddition with sodium azide resulted in tetrazole **4.13**, while addition of hydroxylamine, followed by ring closure with 1,1'-carbonyldiimidazole led to the formation of 4*H*-[1,2,4]-oxadiazol-5-one ring isosteres **4.14-4.15**. The synthesis of AMC-based amines followed a similar route as the carboxylic acid analogues; consisting of coupling and acidolytic deprotection. These compounds were then readily converted into aminosulfonamides (**4.16-4.18**) and squaric acid derivatives (**4.19-4.21**). Acidolytic hydrolysis of the latter afforded fully deprotected squaric acid (**4.22-4.24**). Coupling of AMC and 2-cyanoacetic acid, followed by identical heterocycle formation procedures as mentioned above, afforded tetrazole **4.25** and amidoxime intermediate **4.26**. Obtaining oxadiazolone **4.27** with this synthetic pathway was found to be unsuccessful.

A comparable sulphur-linked tetrazole (**4.28**) was created after bromo-acetylation of AMC, followed by nucleophilic addition of a thiocyanate anion and cycloaddition with sodium azide. Also sulfonic and phosphonic acid derivatives were synthesized from bromo-acylated AMCs. The first isostere (**4.29-4.31**) was directly obtained after treatment with sodium sulfite, while the second after treatment with triethyl phosphite. The latter required deprotection with lithium bromide and trimethylsilyl bromide

in order to afford the monoprotected (**4.32-4.34**) and completely deprotected phosphonic acids (**4.35-4.37**), respectively.



Scheme 4.1. First part of the subset of the fragment library containing carboxylic acids and its isosteres. *Reagents and conditions*^[2]: a) Ghosez's reagent, TEA, DCM, THF, RT, overnight; b) TFA, DCM, RT, 30 min; c) K₂CO₃, H₂O, MeOH, reflux, 2 h; d) toluene, reflux, 1 h; e) CH₃SO₂NH₂, DBU, CDI, DMF, RT, 5 d; f) NH₂OH.HCl, imidazole, CDI, DMF, RT, overnight; g) cyanamide, TEA, HATU, RT, 5 h; h) CDI, DMF, 1h, RT, followed by bubbling NH₃, RT, 20 min; i) TFAA, DMF, RT, 1 h; j) NaN₃, NH₄Cl, DMF, 110°C, overnight; k) NH₂OH.HCl, DIPEA, EtOH, reflux, overnight; l) CDI, DBU, 1,4-dioxane, reflux, 2 h; m) *N,N*-dimethylsulfamoyl chloride, TEA, DMF, RT, 3-7 h; n) squaric acid dibutyl ester; TEA, DMF, 4 h; o) 2 M HCl, EtOH, 90 °C, 1 h; p) TEA, DCM, acetone, RT, 3 h; q) KSCN, KI, DMF, RT, 2 h; r) Na₂SO₃, DMF, H₂O, RT, 3 d; s) triethylphosphite, ACN, reflux, 2-5 d; t) LiBr, ACN, reflux, 5 d; u) TMSBr, ACN, RT, 2 d. [1] PG = protecting groups: *tert*-butyl ester (deprotection by b) or ethyl ester (deprotection by c); [2] Yields are reported in the experimental section.

Additionally, fragments **4.38-4.52** were included in the library, containing carboxylic acids or isosteres and a conjugated, fluorinated, amino acid, heterocyclic or aromatic core (**Figure 4.3**). These compounds were synthesized through a combination of previously described pathways which are documented in the supporting information.

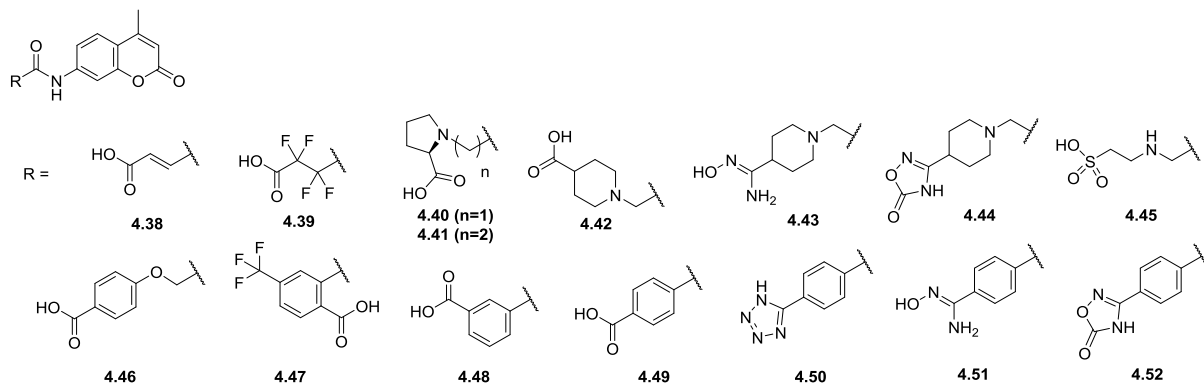


Figure 4.3. Second part of the subset of the fragment library containing carboxylic acids and its isosteres. Synthesis of these compounds was similar as their analogues in Scheme 1, which is specified in the supporting information.

Finally, the library was enriched with subsets (171 compounds) that had already been produced by our group during earlier exploration of the MSAS methodology. A first subset included around 98 *N*-acyl groups, selected in a non-target-biased manner, aiming to cover as much of “drug-like” chemical space as possible in terms of steric, electronic and electrostatic parameters. Furthermore, two target-biased subsets were present, containing moieties that were reasonably expected to bind to the active centers of uPA and ATG4B.^{23, 24}

4.3.2 Inhibitor screening (step 1)

4.3.2.1 *N*-Acyl aminomethylcoumarins

The first part, i.e. the isosteric subset, was tested for their inhibitory capacity against caspase-1, -3 and -4. The latter two were included in order to create a first impression of the caspase selectivity of the different isosteres. Caspase-3 represents an abundant executioner caspase, while the less investigated caspase-4 is added in order to map the selectivity within the inflammatory caspase subfamily. All compounds were tested at their highest concentration depending on their solubility in HEPES buffer (pH 7.0), up to 500 μ M. Optimal buffer conditions were chosen based on earlier experimental optimization by Garcia-Calvo *et al.*²⁷ The readout consisted of quantifying the percentage inhibition of substrate cleavage at a given compound concentration. The results for the subset of carboxylates and isosteres are summarized in **Table 4.1**. A standard threshold percentage of 10 % was chosen. Except for the carboxylic acid reference molecules, *N*-acyl AMCs with lower inhibition capacities are not displayed.

compound **4.2** has an optimal carbon length between its amide bound and the functional group, therefore nicely mimicking the aspartate functionality in the preferred substrates of caspases. Only one carboxylic acid-containing AMC was identified with an inhibition percentage higher than 50 %; aromatic derivative **4.46**.

Concerning the isosteres, four replacements appeared to be worthy alternatives for lowering caspase substrate turnover; *N*-acylsulfonamides, oxadiazolones, tetrazoles and squaric acids. Depending on the linker, each of these isosteres showed examples with inhibition values above 75%. Moreover, the inhibition values for oxadiazolones **4.44** and **4.52** and acylsulfonamide **4.6** were found to exceed the detection limit for precise inhibition determination at a compound concentration of 500 μ M. In general, due to the higher inhibition percentages of caspase-4, it seems that this enzyme has a bigger tolerance of allowing isosteric replacements than the other two caspases. Also, the linker between the isosteric functional group and the amide bound does not necessarily need to resemble the linker of an aspartate moiety. In contrast, multiple examples, such as oxadiazolones **4.15**, **4.44** and **4.52**, show that other linkers provide higher inhibition levels.

In case of the tetrazole moieties, **4.28** and **4.13** were identified. Interestingly, they both possess a 2-atom linker, but it appeared that replacement of the tetrazole α -carbon by sulfur has a beneficial effect on the inhibitory potency of this compound towards caspase-4. Furthermore, this molecule indicates that an enhanced preference towards one member of the inflammatory subfamily, besides caspase-1, is possible. Other tetrazoles with a longer carbon spacer or phenyl-type linker were not recognized as worthy inhibitors. Finally, while most of the identified isosteres were found with a preference for caspase-4, the sulfonic acid surrogates (**4.29**, **4.31**) appeared the only replacements that were more likely to favor inhibition of caspase-3.

In addition to the potency determination, an exploratory study based on the Michaelis-Menten model was performed to investigate the competitive character of these inhibitors. A fixed concentration of inhibitor **4.6** was incubated with varying concentrations of substrate (Ac-WEHD-pNA, 100 μ M - 2 mM) in a spectroscopic assay with caspase-4. After mapping the cleavage rate versus the substrate concentration, the model describes that a comparison of the saturation curves of the inhibitor and a blank (without inhibitor) should indicate the competitive behavior of the inhibitor.²⁸ Preliminary results illustrated that inhibitor **4.6** has a significantly lower V_{\max} than the blank series while maintaining a similar Michaelis constant (K_M), therefore suggesting that the inhibition of caspase-4 occurs in a non-competitive way (**Figure 4.4**). However, since we are convinced that the isosteric fragments accommodate in the S1 subsite of caspases (as in **Chapter 3**), we believe that this model fails in recognizing a more complicated mechanism of inhibition. For example, if the formation of the

tetrahedral thiohemiacetal complex would initiate a beneficial energetic complex and the rate of hydrolysis is low, this would resemble an irreversible type of inhibition and consequently influence the Michaelis-Menten model. Moreover, the poor fitting of the curves indicate that this model is not successful. Additional and various experiments are therefore essential in order to verify the correct type of inhibition. Unfortunately, due to a lack of time the continuation of these experiments was not included in the scope of this thesis.

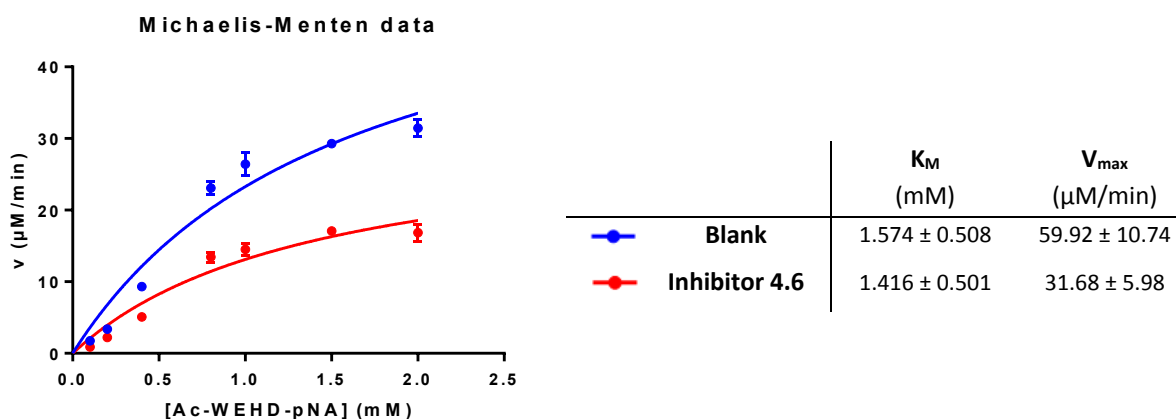
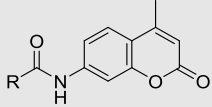
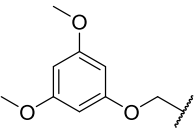
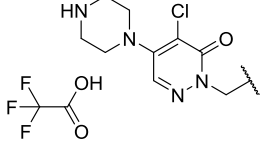
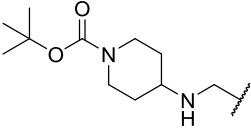
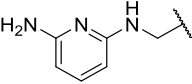
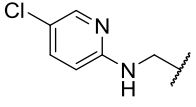
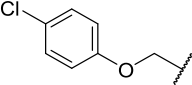
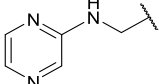
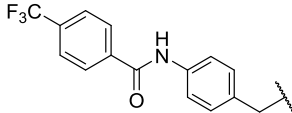
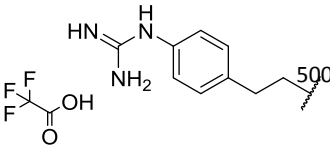
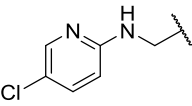
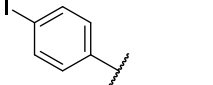
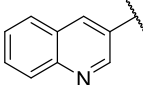
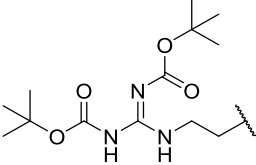


Figure 4.4. Determination of the type of inhibition for caspase-4 by the Michaelis-Menten model. The cleavage rate (v) is visualized versus the substrate concentration ($[\text{Ac-WEHD-pNA}]$) at fixed concentrations of inhibitor **4.6** ($150 \mu\text{M}$) or without inhibitor (blank). K_M and V_{max} were determined by the best fit-values according to the software of GraphPad Prism.

The second part of the library, consisting of the non-biased set of AMC-based compounds as well as specific molecules produced to fit other enzymatic pockets, was tested in a similar inhibition screening, specifically for caspase-4. The results are displayed in **Table 4.2**. At first sight, it seemed that the hit rate of this subset is significantly larger than the isosteric subset. However, the probability that these compounds establish competitive inhibition with caspase-4 is limited. The high lipophilicity of these compounds can reasonably be assumed to be responsible for close binding to many subsites of the enzyme, other than the active site.

With respect to this matter, some of these compounds could serve as starting points for the discovery of allosteric inhibitors. Nonetheless, it is important to acknowledge that the lipophilic character of the identified fragments makes binding to many other enzymes possible, therefore implying selectivity issues towards one target. The non-selectivity was confirmed after comparison with results from the inhibitor screening for enzymes uPA and ATG4B. Compounds **4.60** and **4.62** for example, have also demonstrated inhibition of uPA, while **4.58** inhibited uPA and ATG4B. Remarkably, guanidine **4.57**, an expected and confirmed inhibitor for uPA, was also identified as a hit for caspase-4. No effort was put in the further investigation of this finding, since positively charged molecules are very unlikely to fit the S1 active site of caspases.

Table 4.2. Hits obtained after inhibitor screening of the unbiased subset of *N*-acyl AMC_s against human caspase-4.

| | |  | | | | | |
|------|---|---|----------------------------------|------|--|-------------------|----------------------------------|
| Cpd | Structure R = | [I] (μ M) | Inhibition (%) ^[a] | Cpd | Structure R = | [I] (μ M) | Inhibition (%) ^[a] |
| 4.53 |  | 125 | 71.7 | 4.60 |  | 500 | 39.8 |
| 4.54 |  | 500 | 65.4 | 4.61 |  | 250 | 38.5 |
| 4.55 |  | 500 | 54.3 | 4.62 |  | 100 | 34.9 |
| 4.56 |  | 500 | 52.6 | 4.63 |  | 100 | 34.1 |
| 4.57 |  | 500 | 47.0 | 4.64 |  | 500 | 32.8 |
| 4.58 |  | 100 | 40.9 | 4.65 |  | 125 | 32.6 |
| 4.59 |  | 50 | 39.9 | | | | |

[a] Inhibition is defined as the percent decrease in the processing rate of reference caspase-4 substrate Ac-WEHD-pNA. Substrate concentration in the assay was 200 μ M. A standard threshold percentage of 30% was chosen. The buffer consisted of 0.1 M HEPES, pH 7.0, 10% Glycerol (v/v), 0.1% CHAPS (m/m), 100mM NaCl, 1mM EDTA and 10 mM DTT.

It is worth mentioning that two compounds were found to facilitate substrate turnover of caspase-4, instead of inhibiting this enzyme. The structures of these so-called activators are shown in **Table 4.3**. The protected squaric acid-containing compound **4.66** was found to double the substrate turnover at a concentration of 100 μ M. Though the more lipophilic aminomethylcoumarin **4.67** multiplied the turnover by 2.5 times at 25 μ M, it seemed that this trend was not proportional with the concentration. The cause of this potential artefact could be precipitation, though this was not observed during the experiments. With respect to the identification of direct caspase activators, it is worth emphasizing the versatility of the MSAS methodology. This technique can easily be extended to the search of

activators for different sorts of enzymes. However, this study did not further elaborate on the development of caspase activators.

Table 4.3. Activators identified in the inhibitor screening of human caspase-4.

| Compound | Structure | Concentration | Substrate turnover increase |
|----------|-----------|---------------|-----------------------------|
| 4.66 | | 50 μ M | x 1.5 |
| | | 100 μ M | x 2 |
| 4.67 | | 25 μ M | x 2.5 |
| | | 50 μ M | x 2.1 |

4.3.2.2 Acetic acid isosteres

Intrigued by the screening results of the isosteric subset of aminomethylcoumarins and aiming at the further validation of the MSAS approach, the inhibitory potencies of all isosteres were evaluated again but without the AMC moiety and linker. More specifically, a set of nine isosteric fragments was selected, mimicking acetic acid as shown in **Figure 4.5**. Although many types of fragment-identification techniques have been reported in fragment-based drug discovery, direct activity-based methods utilizing such small fragments have so far not been employed in a similar inhibition assay. The commercial availability and convenient synthesis of these fragments facilitate the preparation of this small library and could therefore play an important role in future applications of MSAS on other target enzymes.²⁹⁻³¹

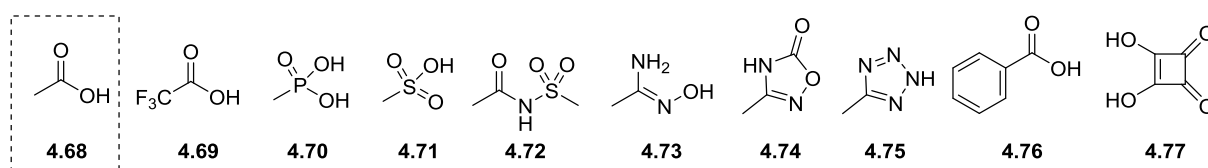
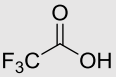
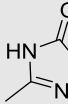


Figure 4.5. Fragments that isosterically mimic acetic acid, tested in this exploratory MSAS extension.

A full IC_{50} analysis was performed for each of these fragments on caspase-1, -3 and -4. However, since the caspase affinities of such small fragments are rather limited, elevated concentrations were required. The latter implied two complications: 1) amidoxime **4.73** and squaric acid **4.76** were not sufficiently soluble in the buffer and 2) in some cases, the buffer was unable to compensate the high concentrations of acid. Since caspase activity is highly sensitive to pH changes, inhibition can easily be mistaken with enzyme instability.²⁷ The buffer's capacity was verified after the addition of two fragments with distinct pK_a values (**Table 4.4**). In both cases, acceptable pHs (>7) were detected as long as the concentration was not exceeding 10 mM. Nevertheless, the data points at inhibitor

concentrations 12.5 mM and 25 mM were essential in order to calculate the IC_{50} values of these fragments. Moreover, all fragments were found to have IC_{50} values between 5 and 15 mM (**Table 4.5**). It was therefore recommended to include an alternative criterion for the analysis of these results: the S-shape of the graph. A strong analogy was present between the shape of the IC_{50} graphs and the previously mentioned pH influence, which is illustrated in **Figure 4.6**. Graphs that drop abruptly (e.g. of **4.69**) are more likely to be pH-dependent, while smooth S-graphs (e.g. of **4.74**) are expected to be related to the inhibitory potency of this fragment. IC_{50} results determined by drastic drops were given a red color in **Table 4.5**, while nicely S-shaped results were displayed green. In this perspective, it is worth highlighting that the oxadiazolone-containing fragment **4.74** has the highest potency ($IC_{50} = 5.2$ mM against caspase-1) and is characterized by a clearly shaped S-graph (**Figure 4.6**). The modest identification of this fragment confirms that oxadiazolone heterocycles have a promising impact on inhibiting caspase-1. In addition, to our knowledge, this is the first time that a fragment of considerable small size has been enzymatically identified with respect to the discovery of caspase inhibitors, without the use of expensive and time-consuming equipment such as X-ray crystallography.³² It should be stressed that the experimental set-up of this approach requires further optimization in order to fully valorize its results. It is however doubtful if solutions with higher buffering capacities could provide a more distinct effect between pH dependency and inhibitory response, because not only do caspases demand stringent conditions to establish sufficient activity, other (or more concentrated) buffer solutions can also impair the reliability of the inhibitory experiments.

Table 4.4. Determination of the pH after dissolving following compounds in buffer at different concentrations

| | pK_a | Concentration in buffer | | | |
|--|---------------------|-------------------------|--------|-------|-------|
| | | 1 mM | 2.5 mM | 10 mM | 25 mM |
| 4.69  | -0.25 | 7.44 | 7.18 | 6.48 | 4.33 |
| 4.74  | 6.56 ^[a] | 7.35 | 7.21 | 6.68 | 6.19 |

[a] predicted.

Table 4.5. IC₅₀ values (in mM) of fragments containing isosteric replacements against a panel of caspases^{[a][b]}

| | 4.68 | 4.69 | 4.70 | 4.71 | 4.72 | 4.73 | 4.74 | 4.75 | 4.76 | 4.77 |
|--------------------------------|---------------------|-------|--------------|------|------|---------------------|------|-----------------------|------|------------|
| pK _a ^[c] | 4.7 | -0.25 | 2.12 7.29 | -1.9 | 4.8 | 7.48 | 6.56 | 5.11 | 4.2 | 1.5 3.4 |
| Casp-1 | n.p. ^[d] | 7.1 | 11.0 | n.p. | 11.3 | n.s. ^[e] | 5.2 | n.i.a. ^[f] | n.p. | n.s. |
| Casp-3 | 10.3 | 11.7 | 8.5 | 9.4 | 8.2 | n.s. | 9.5 | 10.1 | 7.4 | n.s. |
| Casp-4 | 8.4 | 8.6 | 6.7 | 12.1 | 10.1 | n.s. | 14.9 | 12.6 | 12.3 | n.s. |

[a] Substrates tested were Ac-WEHD-AMC for h casp-1 and -4, and Ac-DEVD-AMC for h casp-3. [b] The colors refer to the graph shape and therefore likelihood of the inhibitory relevance of these results: green for nicely S-shaped graphs and red for drastic drops in the graphs. [c] If experimental data was not available, the pK_a value was predicted. [d] n.p.: not possible to determine the S-shaped curve due to incorrect data points. [e] n.s.: compound was not sufficiently soluble to determine its IC₅₀ value. [f] n.a.: no inhibitory activity in this concentration range.

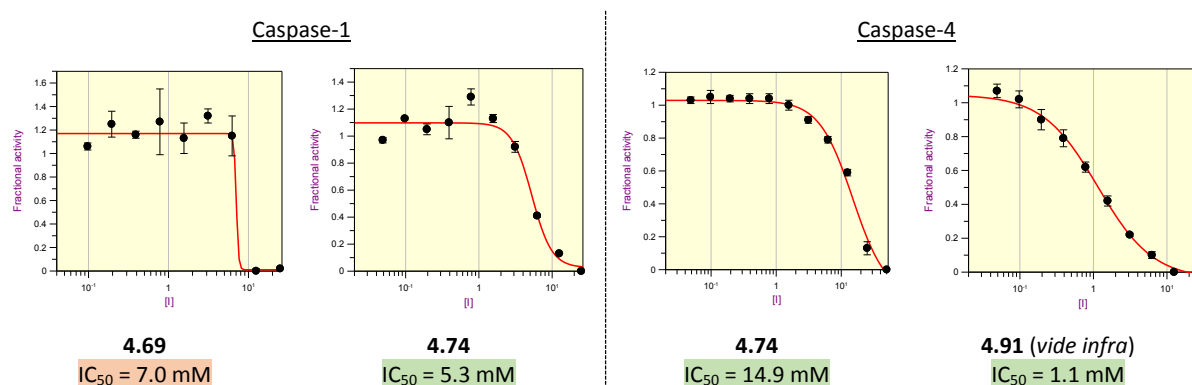


Figure 4.6. Examples of several graphs, determining the IC₅₀ values for caspase-1 and -4 in Table 4.4. The graph of 4.69 shows a drastic drop (red) while the others show nicely S-shaped graphs (green).

4.3.3 Substrate screening (step 2)

While the inhibitor screening was based on competition with a known chromogenic substrate, the substrate screening will focus on the use of the *N*-acyl AMCs to serve as substrates. Building blocks that display sufficient affinity and simultaneously position its amide bond in close proximity of the target protease's nucleophilic cysteine residue, will trigger the proteolytic release of fluorescent AMC. Though the substrate screening consists of a simple fluorescence-based assay, it is rather time- and money-consuming. We therefore focused on identifying S1 region binding fragments for only one enzyme: caspase-4. As demonstrated earlier for uPA and ATG4B, only library members with measurable enzyme affinity (i.e. hits during inhibitor screening) will be processed as substrates. Therefore, only the identified fragments from Table 4.1 and 4.2 were submitted to the caspase-4 substrate screening. As a result, no substrates were identified. It is extremely important that optimal fitting of the substrate in the S1 region of caspase-4 is achieved, in order to generate enzymatic cleavage of the amide bond. Moreover, when the aspartate-mimicking *N*-acyl AMC 4.2 was included in additional substrate testing, no fluorescence was detected either. As observed by Benkova and co-

workers, caspase-4 is characterized by low substrate hydrolysis rates.³³ Nevertheless, after increasing the amount of enzymatic units up to 50 times, still no substrate cleavage was observed. It is worth mentioning that a positive control with substrate Ac-WEHD-AMC was carried out in the original assay conditions, which resulted in a strong fluorescent response. With respect to this matter, we want to highlight the importance of the inhibitor screening as an additional step to the original SAS methodology of Ellman *et al.* This first step is not only crucial for the identification of promising fragments without optimal positioning of the amide bond towards the target protease's nucleophilic center, but also for the identification of sets of fragments that are characterized by less distinct enzyme affinity profiles.

4.3.4 Validation through emerging with warhead (step 3)

4.3.4.1 Replacement of the amide bond by a warhead

Since no substrates were identified, the most promising results from the inhibitor screening were considered the main starting point for the validation. Since oxadiazolone-containing *N*-acyl AMCs (and fragments) generally displayed the highest inhibitory potency, their amide bonds were replaced by aldehyde warheads. Aldehydes have shown to preserve their selectivity pattern in caspase inhibitor design and are therefore considered excellent warhead functionalities in this part of our project.³⁴ Since *N*-acyl AMCs **4.44** and **4.52** were the most potent compounds carrying the oxadiazolone isostere, they were considered the starting points for this part of the study (**Figure 4.7**).

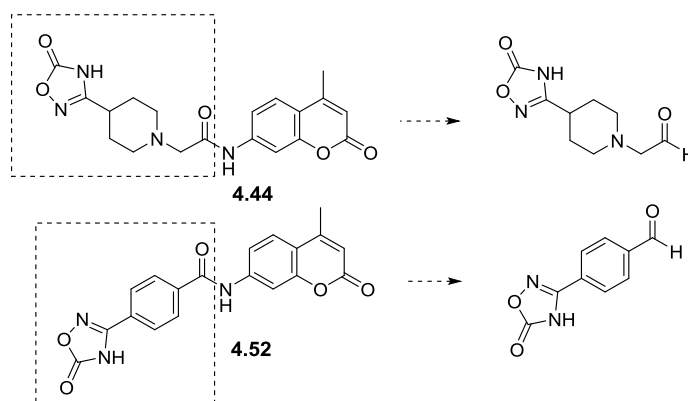
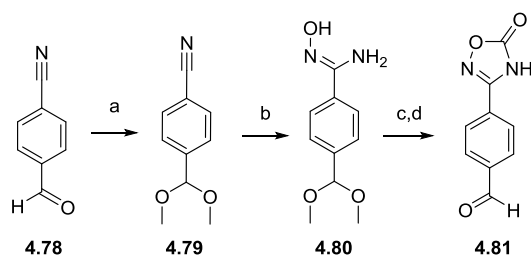


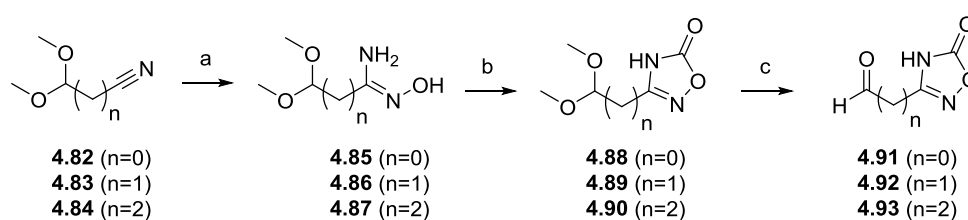
Figure 4.7. Transformation of the amide bond in *N*-acyl AMCs **4.44** and **4.52** into an aldehyde bond.

To produce the warhead analogue of fragment **4.52** (**Scheme 4.2**), an acetal protection was first performed on 4-cyanobenzaldehyde (**4.78**). The next two steps to install the heterocycle were identical to the preparation of the corresponding *N*-acyl AMCs. In the end, the aldehyde functionality was restored under acidolytic conditions to afford **4.81**. The produced aldehyde was subjected to an inhibitor assay similar to step 1 of this methodology, but did not show any inhibitory activity against caspase-1, -3 or -4.



Scheme 4.2. Reagents and conditions: a) trimethoxymethane, *p*TsOH, H₂O, MeOH, 45 °C, overnight, 89%; b) NH₂OH.HCl, NaHCO₃, MeOH, 70 °C, overnight, >99%; c) CDI, DBU, 1,4-dioxane, 110 °C, 2 h; d) formic acid, H₂O, EtOAc, 40 °C, 1 h, 67% over 2 steps.

The synthesis of the aldehyde equivalent of *N*-acyl AMC **4.44** was unsuccessful. The final step to obtain a 1-piperidineacetaldehyde derivative seemed to produce an unstable outcome (data not shown). To explore further aspects of the inhibiting capacity of this isostere, the connection of the aldehyde warhead via a regular saturated carbon linker was achieved, consisting of 0-2 carbons (**Scheme 4.3**). The commercially available carbonitriles **4.82-4.84** were transformed in inhibitor-like compounds **4.91-4.93** in using a similar synthetic pathway as for the production of oxadiazolone **4.81**. The results from the biochemical evaluation of these inhibitors are summarized in **Table 4.6**. Similar to the evaluation of the acetic acid isosteres, the shape of the graphs determined the correctness of the resulting IC₅₀ values (red or green). Most of the graphs were found to be reasonably shaped (example in **Figure 4.5**, *vide supra*) and therefore providing trustworthy IC₅₀ values. Because of the resemblance of its ethyl-linker to the favored aspartic acid, oxadiazolone **4.93** was expected to have the highest affinity. On the contrary, the inhibitory potencies of this compound are much smaller than the other two oxadiazolones. Regarding the latter, oxadiazolone **4.91** has an IC₅₀ of 1.2 mM against caspase-4, which is found to be significantly lower than the other values.



Scheme 4.3. Reagents and conditions^[1]: a) NH₂OH.HCl, NaHCO₃, MeOH, reflux, overnight; b) CDI, DBU, 1,4-dioxane, reflux, 2 h; c) 6 M HCl, 2 h, 50 °C. [1] Yields are reported in experimental section.

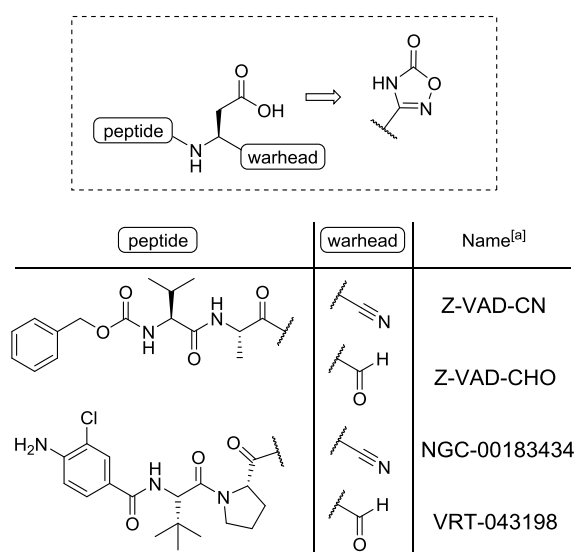
Table 4.6. IC₅₀ values of fragments containing isosteric replacements against a panel of caspases^{[a][b]}

| (in mM) | 4.91 | 4.92 | 4.93 |
|---------|------|------|------|
| Casp-1 | 6.7 | 9.6 | 17.1 |
| Casp-3 | 8.6 | 9.4 | >50 |
| Casp-4 | 1.2 | 6.1 | 62.4 |

[a] Substrates tested were Ac-WEHD-AMC for h casp-1 and -4, and Ac-DEVD-AMC for h casp-3. [b] The colors refer to the graph shape and therefore likelihood of the inhibitory relevance of these results: green for nicely S-shaped graphs and red for drastic drops in the graphs.

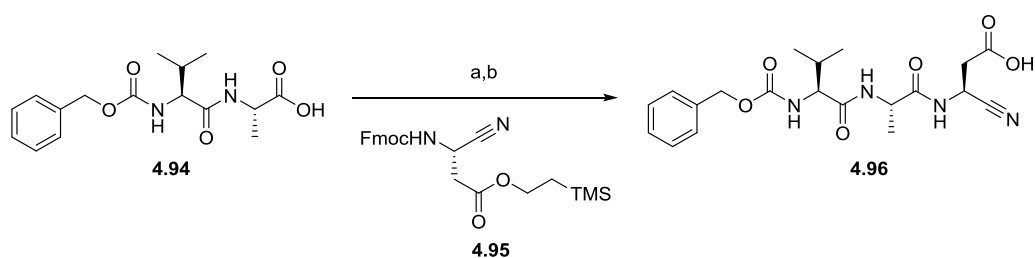
4.3.4.2 Incorporation of identified isosteres in existing caspase inhibitors

Besides oxadiazolone replacements, also acylsulfonamides were found to be worthy carboxylic acid isosteres in the first step of this MSAS approach. These findings are in line with Chapter 3, in which acylsulfonamides have been incorporated into existing caspase inhibitors.²¹ Similarly, we intend to test the influence of replacing the carboxylic acid moieties in caspase inhibitors VRT-043198, NCGC-00183434, Z-VAD-CHO and Z-VAD-CN, by oxadiazolone heterocycles (**Figure 4.8**). We believe that the incorporation of an oxadiazolone could be a powerful tool to upgrade the selectivity towards specific caspases. Due to the preference of these isosteres for inflammatory caspases, two specific caspase-1 inhibitors have been selected: VRT-043198 and NCGC-00183434. VRT-043198 is the active form of belnacasan (or VX-765), an orally absorbed ethyl-hemiacetal prodrug that has been tested in the treatment for chronic epilepsy and psoriasis,³⁵⁻³⁷ and more recently for HIV-1 infection and rheumatoid arthritis.³⁸⁻⁴⁰ NCGC-00183434, a carbonitrile-containing analogue of the previous inhibitor, has been appointed as the most selective caspase-1 inhibitor up to date and is therefore subject of many caspase drug trials.^{12, 21} The final inhibitors consist of the Z-VAD peptide core and therefore considered *pan*-caspase inhibitors.

**Figure 4.8.** Isosteric replacement for the carboxylic acid functional group, by an oxadiazolone. [a] in case of the carboxylate.

Besides the potential advantages of improving selectivity, this heterocycle displays geometrically different protomers, charge delocalization upon ionization and slightly different physicochemical properties, so compounds bearing this heterocycle have a greater lipophilicity that may translate into improved bioavailability with respect to their carboxylic analogues. Moreover, their efficient absorption upon oral administration potentially avoids the need for prodrug formation.⁴¹ The use of oxadiazolones as (bio)isosteres was first reported by Kohora *et al.* in angiotensin II receptor antagonists.⁴² More recently, it has also been successfully implemented in retinoids⁴³, phospholipase A₂-II inhibitors^{44, 45} and inhibitors of hepatitis C virus NS5B polymerase⁴⁶.

To serve as a reference for the oxadiazolone subseries, VRT-043198, NCGC-00183434 and Z-VAD-CHO have been synthesized according to earlier described procedures.^{12, 47} In addition, we produced a carbonitrile-containing analogue of Z-VAD, through a similar protocol as described by Boxer *et al.* (**Scheme 4.4**).¹² The aspartic acid derived building block **4.95** was first amine-protected employing DBU as a non-nucleophilic base, followed by coupling with dipeptide **4.94** and TBAF-mediated deprotection of the carboxylic acid in order to afford reference molecule **4.96**. However, since final purification by preparative LC was required to obtain this compound with >95% purity, it has not yet been submitted to the biochemical evaluation.

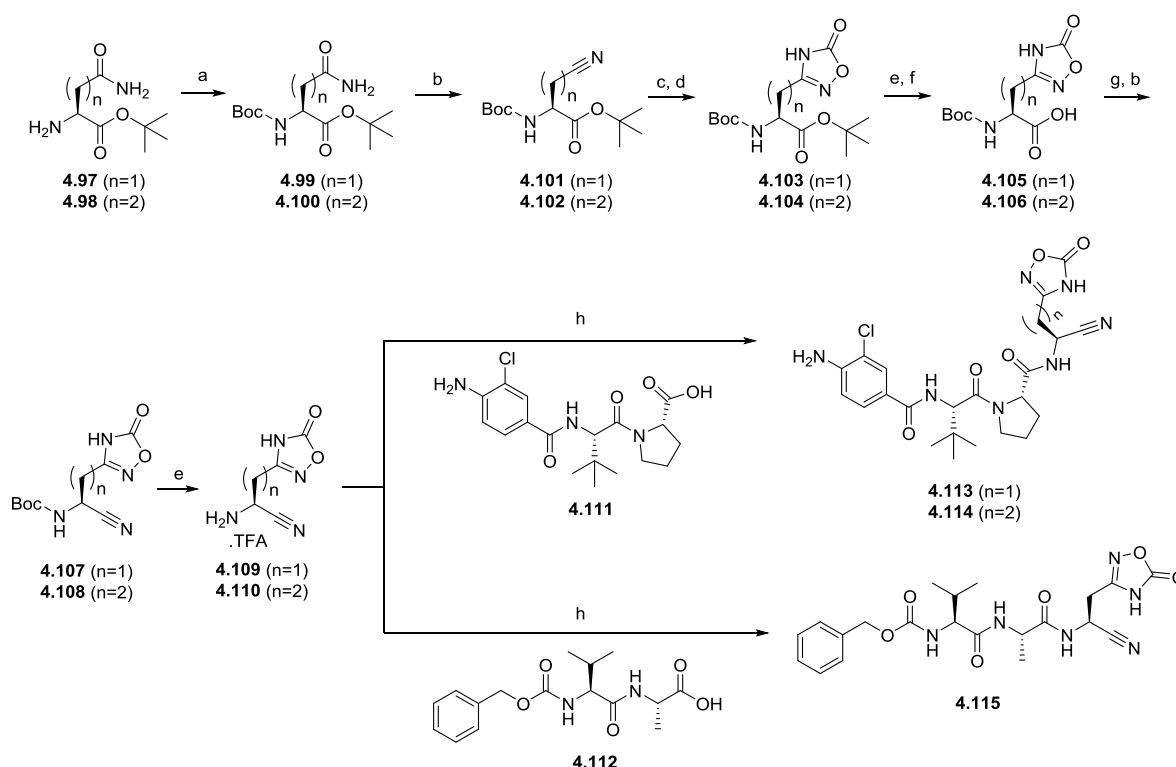


Scheme 4.4. Reagents and conditions: a) i. **4.95**, DBU, DMF, RT, 10 min; ii. **4.94**, HATU, 0 °C, 10 min; iii. 2 solutions together, DIPEA, RT, 2 h; b) TBAF, THF, 0 °C -> RT, overnight, purification in progress.

With respect to the oxadiazolone analogues of NCGC-00183434, two carbon chain lengths were selected to cover the distance between the warhead and the heterocycle. Glutamic acid and aspartic acid derivatives were intended to be incorporated in the peptidomimetic chain to maximize the possibility of a good fit for the caspases. The production of these analogues as well as an oxadiazolone-isosteric form of Z-VAD-CN is presented in **Scheme 4.5**. Commercially available asparagine - and glutamine *tert*-butyl esters (**4.97-4.98**), were Boc-protected on the amine. Next, dehydration of the amide function was performed with trifluoroacetic anhydride. The afforded carbonitriles **4.101-4.102** were converted into oxadiazolone heterocycles (**4.103-4.104**) through a similar two-step procedure as described above. Since selective deprotection of a *tert*-butyl ester in the proximity of a Boc-protecting group is tricky, full deprotection was achieved in acid media, which allowed a new Boc-protection of the amine. It is worth mentioning that 2-(trimethylsilyl)ethoxycarbonyl (Teoc) was not a suitable amine

protecting group alternative since it did not survive *tert*-butyl deprotection either. The carboxylic acid in **4.105-4.106** was converted into an amide by coupling with aqueous ammonia. Consecutive hydration led to carbonitriles **4.107-4.108** which underwent TFA-mediated deprotection. The afforded amines **4.109-4.110** were coupled to peptide chain **4.111** to obtain potential inhibitors **4.113-4.114**. The amino acid derivative **4.109**, where $n = 1$, was also allowed to react with dipeptide Z-VA-OH (**4.112**) to afford inhibitor **4.115**.

It is worth mentioning that the aldehyde-containing subset of this series is currently in preparation. In the meanwhile, the carbonitrile-based set of compounds was evaluated for their inhibitory potency against a panel of human caspases (**Table 4.7**). The panel was composed of inflammatory caspase-1, -4 and -5, supplemented with the most relevant representatives of the initiator and executioner subgroups. Compared to our previous study (*cf.* Chapter 3), it appears that the high selectivity of reference compound NCGC-00183434 towards caspase-1 was preserved. Replacing the carboxylic acid in this compound by an oxadiazolone heterocycle, such as in **4.113**, led to a higher IC_{50} value. The interpretation of the selectivity towards caspase-1 is however hindered, since no exact determination of the IC_{50} values against the other enzymes was done. Further biochemical tests are planned in order to complete this table.



Scheme 4.5. Reagents and conditions^[1]: a) Boc_2O , K_2CO_3 , 1,4-dioxane:water (1:1), RT, 3 h; b) TFAA, pyridine, 1,4-dioxane, RT, 5 h; c) $NH_2OH.HCl$, $NaHCO_3$, MeOH, reflux, overnight; d) CDI, DBU, 1,4-dioxane, reflux, 2 h; e) TFA, DCM, RT, 2 h; f) Boc_2O , TEA, 1,4-dioxane:water (1:1), RT, 5 h; g) isobutyl chloroformate, 4-methylmorpholine, NH_4OH , THF, $-10\text{ }^\circ\text{C} \rightarrow 25\text{ }^\circ\text{C}$, overnight; h) HATU, DIPEA, DMF, RT, 2 h. [1] Yields are reported in the experimental section.

Table 4.7. IC₅₀ values (in μM) for the given set of inhibitors versus a human caspase panel^[a]

| | Inflammatory caspases | | | Apoptotic caspases | | |
|------------------------|-----------------------|-----------------|-----------------|--------------------|-----------------|-----------------|
| | casp-1 | casp-4 | casp-5 | casp-3 | casp-8 | casp-9 |
| NCGC-00183434 | 0.14 \pm 0.01 | 7.39 \pm 2.99 | 1.01 \pm 0.09 | > 25 | 6.23 \pm 1.21 | 0.66 \pm 0.08 |
| 4.113 | 4.30 \pm 1.49 | > 250 | > 25 | n.d. | > 25 | > 25 |
| 4.114 | > 25 | > 250 | > 25 | > 25 | > 25 | > 25 |
| Z-VAD-CN (4.96) | n.d. | n.d. | n.d. | n.d. | n.d. | n.d. |
| 4.115 | > 25 | > 250 | > 25 | > 25 | > 25 | > 25 |

[a] Substrates tested were Ac-WEHD-AMC for h casp-1,-4,-5; Ac-DEVD-AMC for h casp-3; Ac-IETD-AMC for h casp-8 and Ac-LEHD-AMC for h casp-9. [b] n.d.: not determined.

Implementation of an oxadiazolone-containing glutamic acid derivative, as in **4.114**, was not beneficial in terms of inhibitory capacity. Also, the Z-VAD-based compound **4.115** was not found to sufficiently inhibit any of the caspases. With respect to the latter, data from its analogue Z-VAD-CN (**4.96**) is still missing in order to have a better comparison.

4.3.4.3 Physicochemical profile

In addition to the inhibitory potency, stability measurements were carried out in order to obtain a physicochemical profile of the set of inhibitors. The chemical stability at pH 4 and 7.4, as well as the human and murine metabolic stability were quantified over a period of 24 hours and displayed in **Figure 4.9**. All compounds showed sufficient stability in these conditions over a short period of time (~6 hours). Interestingly, the carbonitrile in reference compound NCGC-00183434 underwent partial hydrolysis at pH 4 after 24 hours, while the oxadiazolone-containing compounds were resistant to this phenomenon. On the other hand, **4.113** and **4.114** were the only compounds found to slowly degrade after prolonged times in the human metabolic stability assay.

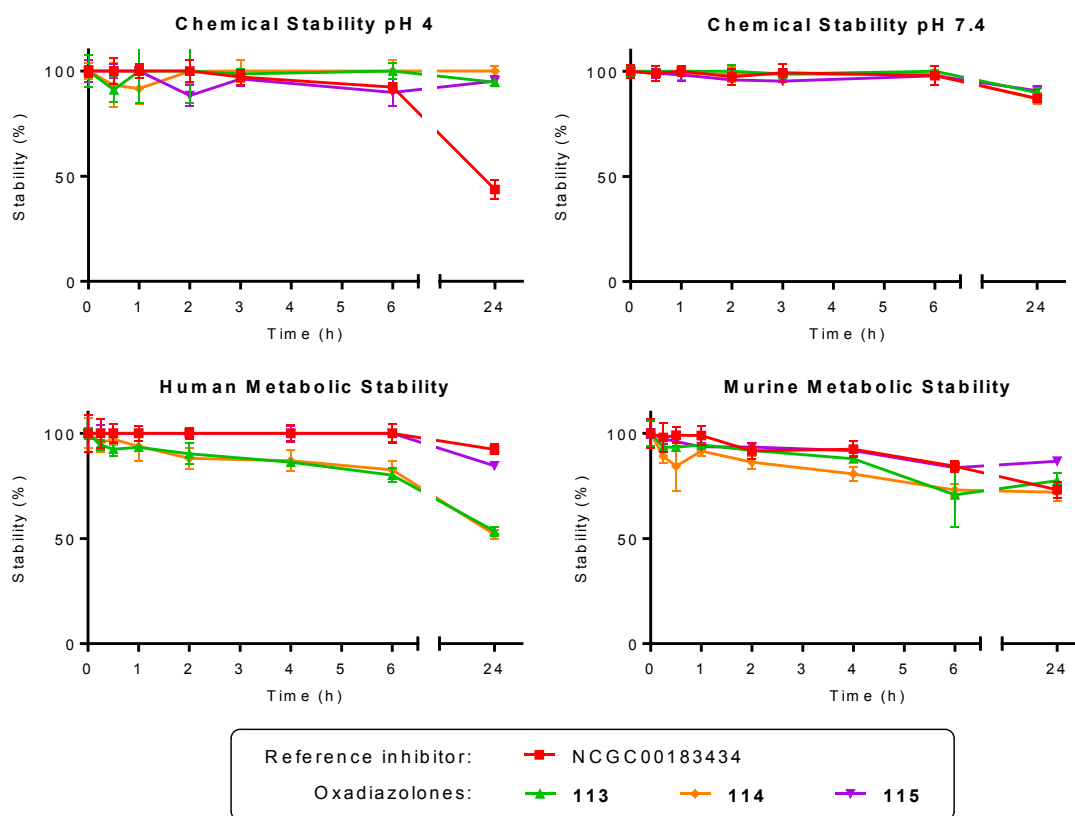


Figure 4.9. Physicochemical profile of the specified set of inhibitors. Measurements were carried out for 24 hours.

4.4 Conclusions

This study comprised the application of the MSAS methodology for the discovery of caspase inhibitors with improved selectivities toward caspase-1 and/or -4. A library of *N*-acyl aminomethylcoumarins was produced, containing carboxylic acids and many different isosteres thereof. The inhibitor screening of the library resulted in the identification of two main isosteric groups that are believed to fit the S1 subsite of caspase-1 and -4: acylsulfonamides and oxadiazolones. Moreover, the versatility of the MSAS methodology was enlarged by performing the inhibitor screening on commercially available or easy synthesized small isosteric analogues of acetic acid, which also pointed oxadiazolones out as promising replacements. Since the substrate screening, the second step in MSAS, did not provide any substrates for caspase-4, focus was set on the incorporation of oxadiazolone heterocycles in existing caspase inhibitors. Despite the difference in potency of **4.113** in comparison to its carboxylic acid analogue, the selectivity towards caspase-1 was mostly preserved. In addition, its improved physicochemical properties at low pH and assumed enhanced ability to pass cell membranes because of its heterocyclic structure, support oxadiazolones to remain subject of further investigation towards improved caspase inhibitors.

4.5 Outlook

As shown in the inhibitor screening, caspases have the ability to accommodate isosteric replacements of carboxylic acid. A perfect fit in the S1 subsite is however essential, including optimal positioning of the warhead towards the caspase's nucleophilic center. In that perspective, we believe that other warhead functionalities should be tested in order to achieve that optimal positioning. Aldehydes, for example, have proven to be worthy warheads in terms of caspase inhibitor design. In addition, the investigation of different linkers between isostere and warhead should provide further understanding about binding in the S1 region of caspases. Currently, our lab is in progress with the development of these adaptations, as displayed in **Figure 4.10**.

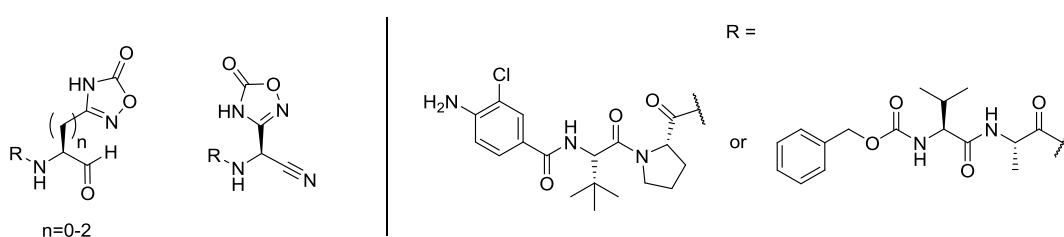


Figure 4.10. Potential inhibitors that could provide improved inhibitory potencies against caspases.

Besides focusing on peptidic or peptidomimetic inhibitors containing warhead functionalities, it would be highly recommended to also investigate the possibility of combining these promising isosteres with a heterocyclic scaffold. However, this field is much underestimated; so far only few caspase inhibitors exist with such a structure. The absence of a warhead would allow easier adaptation in the enzyme's pocket in order to provide a good fit of the negatively charged isostere towards the caspase arginines. Such a validation has been performed during the MSAS investigation towards potent and druglike uPA inhibitors, and could therefore be considered for caspase inhibitors as well.²² Due to their straightforward synthesis and easy substituent decoration, pyrimidines are considered excellent scaffolds for the transformation of identified *N*-acyl aminomethylcoumarins into scaffold-based inhibitors (**Figure 4.11**). Moreover, besides the isosteres, also additional scaffold substituents could contribute to higher levels of caspase selectivity.

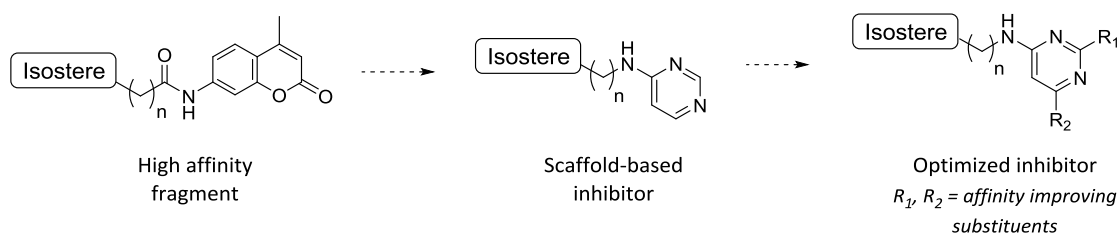


Figure 4.11. Transformation of a high affinity fragment into a scaffold-based inhibitor.

4.6 Experimental section

4.6.1 Chemistry

Reagents were obtained from Sigma-Aldrich, Acros, Fluorochem or Apollo Scientific and were used without further purification. Synthesized compounds were characterized by ^1H NMR, ^{13}C NMR and mass spectrometry. ^1H NMR and ^{13}C NMR spectra were recorded with a 400 MHz Bruker Avance DRX 400 spectrometer, and analyzed by use of MestReNova analytical chemistry software. Purities were determined with a Waters Acquity UPLC system coupled to a Waters TUV detector, ESI source and a Waters Acquity Qda Mass Detector. A Waters Acquity UPLC BEH C18 1.7 μm 2.1 x 50 mm column was used. Solvent A: water with 0.1% formic acid, solvent B: acetonitrile with 0.1% formic acid. The gradient used started with a flow rate of 0.7 mL/min at 95% A, 5% B for 0.15 min then in 1.85 min from 95% A, 5% B to 95% B, 5% A, isocratically at the same percentage for 0.25 min and finally 0.75 min (0.350 mL/min), 95% A, 5% B. The wavelength for UV detection was 254 nm. ADME measurements (UPLC-MS/MS) were carried out on a Waters Acquity UPLC system coupled to a Waters TUV detector, ESI source and a Waters Acquity TQ Mass Detector. Where necessary, flash purification was performed with a Biotage ISOLERA One flash system equipped with an internal variable dual-wavelength diode array detector (200–400 nm). HRMS measurements involved 10 μL injection of a 10 μM sample solution using the CapLC system (Waters) and electrospray using a standard electrospray source. Positive ion mode accurate mass spectra were acquired using a Q-TOF II instrument (Waters). The mass spectrometer was calibrated prior to use with a 0.2% H_3PO_4 solution. The spectra were lock mass-corrected using the known mass of the nearest H_3PO_4 cluster.

Library of *N*-acyl aminomethylcoumarins:

General procedure A (amide bond formation using 'Ghosez's reagent' in a one-pot coupling reaction)

The respective carboxylic acid (1.4 eq) was dissolved in a 1/1 mixture of dry DCM/THF (5 mL). Ghosez's reagent (1.4 eq) was added and the reaction mixture was left stirring for 30 min at room temperature. 7-amino-4-methylcoumarin (1 eq) and triethylamine (1.2 eq) were added and the reaction mixture was allowed to stir overnight at room temperature. Volatiles were evaporated and the crude product was washed with small amounts of acetone and water to obtain pure target compound. If needed, the obtained compound was chromatographed.

General procedure B (deprotection using TFA)

A *tert*-butyl protected acid or Boc-protected amine was dissolved in equal amounts of trifluoroacetic acid and DCM (0.15 M) and the reaction mixture was left stirring for 40 min. The volatiles were

evaporated and for the precipitation diethyl ether was added. After decantation a solid product was obtained.

General procedure C (methyl/ethyl ester deprotection)

The methyl or ethyl ester was dissolved in 3:1 methanol:water (0.05 M) and K_2CO_3 (10 eq) was added. The reaction mixture was heated to 70 °C and left stirring 2 h. The volatiles were evaporated and 2 M HCl was added to acidify the solution. Upon addition of EtOAc a precipitate was formed. Filtration of the crude afforded solid target compound.

General procedure D (anhydride ring opening)

7-amino-4-methylcoumarin (1 eq) was dissolved in toluene (0.2 M) and the appropriate anhydride (1.3 eq) was added. The reaction mixture was heated at reflux (120°C) for 1 h, cooled and filtered to give the crude acid. The crude product was toluene (3 times) and decantation with Et_2O afforded pure carboxylic acid.

General procedure E (preparation of acylsulfonamide derivatives)

The specific carboxylic acid (1 eq) was dissolved in DMF (0.2 M) and 1,1'-carbonyldiimidazole (2 eq) was added. This reaction mixture was left stirring for 1 h. A solution of methanesulfonamide (2 eq) and 1,8-diazabicyclo[5.4.0]undec-7-ene (2 eq) in DMF (0.2 M) was prepared. The first solution was added dropwise, in a time range of 15 min, to the latter mixture and the solution was left stirring for 6 d under nitrogen atmosphere. The reaction mixture was added to a large volume of water and 2 M HCl was added until a pH of 1 was reached. This mixture was left stirring for 10 min and the formed precipitate was filtered. If required, flash chromatography (EtOAc:MeOH) was performed to obtain pure acylsulfonamide.

General procedure F (preparation of hydroxamic acid derivatives)

The specific carboxylic acid (1 eq) was dissolved in DMF (0.24 M) and 1,1'-carbonyldiimidazole- (1.5 eq) was added. This reaction mixture was left stirring for 2 h. A solution of imidazole (4 eq) and hydroxylammonium chloride (5 eq) were dissolved in DMF (0.24 M). The first solution was added dropwise to the latter mixture and was left stirring for 1 d. The reaction mixture was poured into a large volume of 0.5 M HCl. The formed precipitate was filtered and if required, reversed phase flash chromatography (H_2O :MeOH) was performed to obtain pure hydroxamic acid.

General procedure G (preparation of acylcyanamide derivatives)

The specific carboxylic acid (1 eq) was dissolved in DMF (0.075 M). HATU (1.1 eq) and triethylamine (1 eq) were added and the reaction mixture was left stirring for 30 min. Next, a solution of cyanamide

(1.5 eq, freeze-dried before adding because very hygroscopic) and trimethylamine (1.5 eq) in DMF (0.2 M) was added and the reaction mixture was stirred overnight. The mixture was added drop by drop to icecold 2 M HCl. The formed precipitate was filtered and dried to obtain pure acylcyanamide derivative.

General procedure H (preparation of amides from carboxylic acids)

The specific carboxylic acid (1 eq) was dissolved in DMF (0.07 M) and 1,1'-carbonyldiimidazole (1.2 eq) was added. This mixture was left stirring for 1 h. In another flask, aqueous ammonia was heated to 70 °C and the formed gas was bubbled through the first reaction mixture, via a wash bottle. Also two balloons were added to release overpressure. The reaction mixture was left stirring until the bubbling stopped. The mixture was dropped in a large volume of water. The formed precipitate was filtered and washed with little portions of water. After drying, pure amide was obtained as a solid.

General procedure I (preparation of nitriles from amides)

The specific amide from procedure H (1 eq) was dissolved in DMF (0.25 M) and set at 0 °C under nitrogen atmosphere. Triethylamine (4 eq) was added, followed by dropwise addition of trifluoroacetic anhydride (2.1 eq). After stirring for 5 minutes, the mixture was allowed to warm up to room temperature and stirring was continued for 1h. The mixture was dropped in a large volume of water. The formed precipitate was filtered and washed with little portions of water. After drying, pure nitrile was obtained as a solid.

General procedure J (preparation of tetrazole derivatives)

The specific nitrile (1 eq) was dissolved in DMF (0.08 M). Sodiumazide (1.5 eq) and ammonium chloride (1.5 eq) were added. This mixture was heated to 110 °C and left stirring overnight. The mixture was cooled down, mixed with H₂O and left stirring for 30 min. The formed precipitate was filtered, was washed with small portions of H₂O and left drying. Reversed phase flash chromatography (H₂O:MeOH) was performed to afford pure tetrazole as a solid.

General procedure K (preparation of amidoxime derivatives)

The specific nitrile (1 eq), *N,N*-di-isopropylethylamine (3 eq) and hydroxylammonium chloride (1.5 eq) were added to EtOH (0.1 M). The resulting mixture was left stirring at 90 °C for 5 d. The reaction mixture was cooled down, filtered, washed with ethanol (3 times) and with water (3 times). After drying pure amidoxime was obtained.

General procedure L (preparation of 5-oxo-1,2,4-oxadiazole derivatives)

The specific hydroxyl-amidine (1 eq) from procedure K was added to dioxane, followed by 1,1'-carbonyldiimidazole (1.5 eq) and 1,8-diazabicyclo[5.4.0]undec-7-ene (1.1 eq) . The resulting mixture

was stirred at 110 °C for 2 h. The mixture was cooled down, filtered and washed with little portions of 2 M HCl. If necessary, reversed phase flash chromatography (H₂O:MeOH) was performed to afford a pure 5-oxo-1,2,4-oxadiazole derivative.

General procedure M (preparation of aminosulfonamide derivatives)

The specific amine (TFA salt, 1 eq) was dissolved in DMF (0.2 M) and triethylamine (3 eq) was added. The solution was set at 0 °C under nitrogen atmosphere and dimethylsulfamoylchloride (2 eq) was added. The reaction mixture was allowed to warm up to room temperature and was left stirring for 3 h. The mixture was added to a large volume of water. The formed precipitate was filtered and dried to obtain pure aminosulfonamide.

General procedure N (preparation protected squaric acid derivatives)

The specific amine (1 eq) was dissolved in DMF (0.2 M) and triethylamine (2 eq) and 3,4-dibutoxycyclobut-3-ene-1,2-dione (1.2 eq) were added. The reaction mixture was stirred for 4 h at room temperature. The mixture was dropped in a large volume of water. The formed precipitate was filtered and washed with little portions of water and subsequently with Et₂O. After drying, pure protected squaric acid was obtained as a solid.

General procedure O (deprotection of squaric acid derivatives)

To protected squaric acid from procedure N (1 eq) was added a 2:1 mixture of EtOH and 2 M HCl. The reaction mixture was heated up to 90 °C and stirred for 1 h. The volatiles were removed and reversed phase flash chromatography (H₂O:MeOH) was performed. A pure squaric acid derivative was obtained as a solid.

General procedure P (preparation of bromo-*N*-acyl AMC derivatives)

To a solution of bromoacetyl bromide (**P1**; 1.3 eq), 3-bromopropionyl chloride (**P2**, 1.5 eq) or 4-bromobutanoyl chloride (**P3**, 1.4 eq) in dry DCM (0.1 M) a solution of 7-amino-4-methylcoumarin (1 eq) and triethylamine (1.5 eq) in acetone (0.1 M) was added. The reaction was stirred for 2 h at room temperature. The reaction mixture was filtered and washed with small portions of acetone and water to obtain the bromo-*N*-acyl AMC derivative as a solid.

General procedure Q (nucleophilic substitution of bromo-*N*-acyl AMC derivatives)

The product of procedure P was dissolved in DMF (0.1 M) and an amine, alcohol or thiol (1 eq) was added, followed by *N,N*-di-isopropylethylamine (1.2 eq). (In case of potassium thiocyanate (4 eq) no base was used.) The reaction mixture was left stirring for 1 h at room temperature. The reaction

mixture was added to a large volume of water. The formed precipitate was filtered and washed with a little amount of water and left drying. Target compound was obtained as a solid.

General procedure R (preparation of sulfonic acid derivatives)

The product of procedure P (1 eq) was dissolved in DMF (0.02 M). Sodium sulfite (3 eq) was dissolved in water (0.02 M) and added to the previous solution. The reaction mixture was left stirring overnight at room temperature. Water was removed by rota-evaporation. The precipitate was filtered, added to methanol and filtered again after 10 min stirring. If required, reversed phase flash chromatography (H₂O:MeOH) was performed with this crude in order to afford pure sulfonic acid.

General procedure S (preparation of phosphonic acid derivatives)

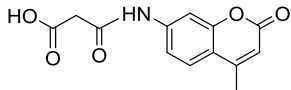
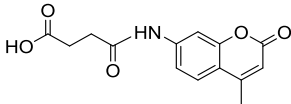
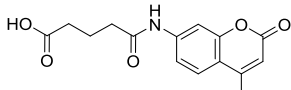
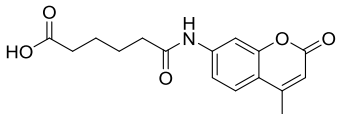
The product of procedure P (1 eq) was dissolved in acetonitrile (0.08 M) and triethoxyphosphine (5 eq) was added. This reaction mixture was refluxed, varying from 5 h to 2 days. The volatiles were evaporated and decantation with Et₂O was done. If needed, flash chromatography was performed. Pure protected phosphonic acid was obtained as a solid.

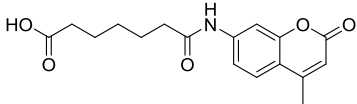
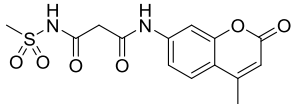
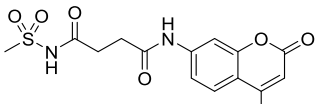
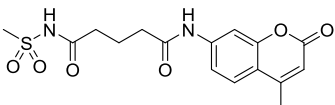
General procedure T (monodeprotection of phosphonic acid derivatives)

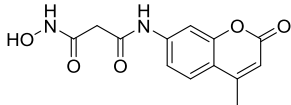
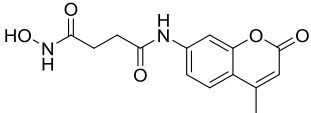
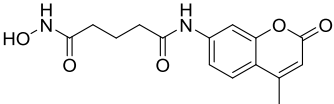
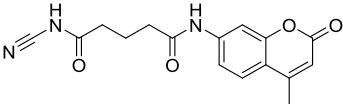
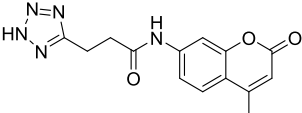
The protected phosphonic acid (1 eq) from procedure S was dissolved in acetonitrile (0.08 M) and lithium bromide (5 eq) was added. The reaction mixture was refluxed overnight. The mixture was cooled, filtered and washed with a little amount of acetone (3 times). The crude product was dissolved in water and 2 M HCl was added to obtain pH 1. The formed precipitate was filtered to afford pure mono-protected phosphonic acid.

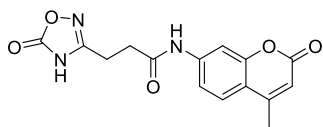
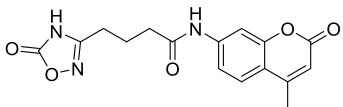
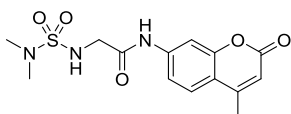
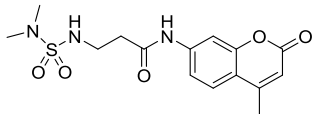
General procedure U (full deprotection of phosphonic acid derivatives)

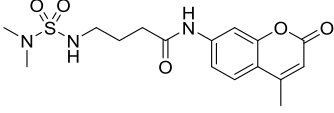
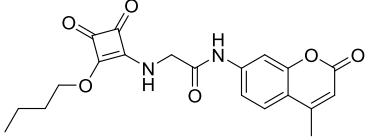
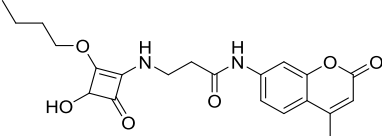
The protected phosphonic acid (1 eq) from procedure S was dissolved in acetonitrile (0.08 M) and bromotrimethylsilane (5 eq) was added. The reaction mixture was left stirring for 3 days. The volatiles were evaporated. The crude product was dissolved in methanol and was left stirring for 1 h. If precipitate was present, filtration was done to obtain pure phosphonic acid. In case no precipitate was formed, evaporation of the volatiles was done, 2 M HCl was added and next filtration of the precipitate was performed to obtain pure phosphonic acid.

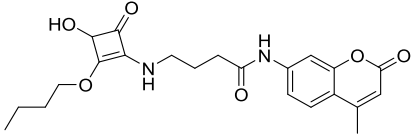
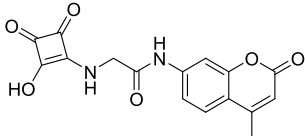
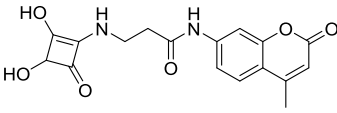
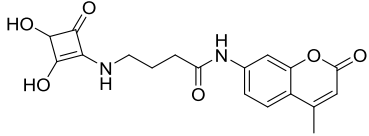
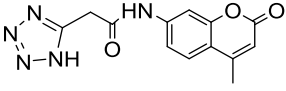
| Cpd | Structure | Procedure | Analytical data |
|-----|---|-----------|--|
| 4.1 |  | A,B | <p>$R_f = 0.60$ (1:1 H₂O:MeOH, visualization by UV); ¹H NMR (400 MHz, DMSO-<i>d</i>₆) δ 2.40 (d, $J = 1.3$ Hz, 3H), 3.41 (s, 2H), 6.28 (d, $J = 1.3$ Hz, 1H), 7.46 (dd, $J = 8.7, 2.1$ Hz, 1H), 7.71 - 7.77 (m, 2H), 10.57 (s, 1H), 12.75 ppm (s, 1H); ¹³C NMR (101 MHz, DMSO-<i>d</i>₆) δ 18.45, 44.63, 106.00, 112.85, 115.54, 115.66, 126.50, 142.63, 153.55, 154.13, 160.46, 165.78, 169.42 ppm; MS (ESI) m/z 259.8 [M-H]⁻, 520.9 [2M-H]⁻, UPLC $t_r = 1.25$ min; yield: 87%.</p> |
| 4.2 |  | A,B | <p>¹H NMR (400 MHz, DMSO-<i>d</i>₆) δ 2.40 (d, $J = 1.2$ Hz, 3H), 2.55 (d, $J = 6.5$ Hz, 2H), 2.62 (d, $J = 6.2$ Hz, 2H), 6.25 (d, $J = 1.3$ Hz, 1H), 7.48 (dd, $J = 8.7, 2.1$ Hz, 1H), 7.70 - 7.75 (m, 2H), 10.43 (s, 1H), 12.17 ppm (s, 1H); MS (ESI) m/z 273.9 [M-H]⁺ m/z 549.0 [2M-H]⁻, UPLC $t_r = 1.27$ min; yield: 85%.</p> |
| 4.3 |  | D | <p>¹H NMR (400 MHz, DMSO-<i>d</i>₆) δ 1.83 (p, $J = 7.4$ Hz, 2H), 2.30 (t, $J = 7.3$ Hz, 2H), 2.36 - 2.46 (m, 5H), 6.26 (d, $J = 1.2$ Hz, 1H), 7.48 (dd, $J = 8.7, 2.1$ Hz, 1H), 7.71 (d, $J = 8.7$ Hz, 1H), 7.76 (d, $J = 2.0$ Hz, 1H), 10.34 (s, 1H), 12.11 ppm (s, 1H); ¹³C NMR (101 MHz, DMSO-<i>d</i>₆) δ 18.45, 20.64, 33.37, 35.98, 105.91, 112.60, 115.28, 115.53, 126.35, 143.03, 153.59, 154.15, 160.52, 172.01, 174.59 ppm; MS (ESI) m/z 287.8 [M-H]⁻, 576.8 [2M-H]⁻, UPLC $t_r = 1.34$ min; yield: 72%.</p> |
| 4.4 |  | A,C | <p>$R_f = 0.28$ (3:1 EtOAc:Hex, visualization by UV); ¹H NMR (400 MHz, DMSO-<i>d</i>₆) δ 1.49 - 1.68 (m, 4H), 2.25 (t, $J = 7.2$ Hz, 2H), 2.34 - 2.44 (m, 5H), 6.26 (d, $J = 1.2$ Hz, 1H), 7.49 (dd, $J = 8.7, 2.0$ Hz, 1H), 7.71 (d, $J = 8.7$ Hz, 1H), 7.78 (d, $J = 2.0$ Hz, 1H), 10.37 ppm (s, 1H); ¹³C NMR (101 MHz, DMSO-<i>d</i>₆) δ 18.45, 24.60, 24.91, 33.95, 36.70, 105.88, 112.58, 115.27, 115.52, 126.36, 143.08, 153.60, 154.16, 160.53, 172.34, 174.87 ppm; MS (ESI) m/z 304.2 [M+H]⁺; UPLC $t_r = 1.61$ min; yield: 28%.</p> |

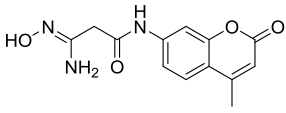
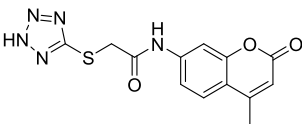
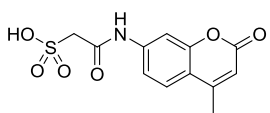
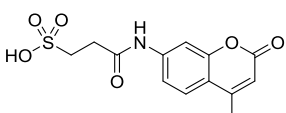
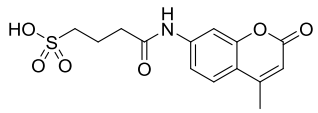
| | | | |
|-----|---|-------|--|
| 4.5 |  | D | <p>$R_f = 0.28$ (3:1 EtOAc:Hex, visualization by UV); $^1\text{H NMR}$ (400 MHz, DMSO-d_6) δ 1.24 - 1.38 (m, 2H), 1.55 (m, 4H), 2.22 (t, $J = 7.2$ Hz, 2H), 2.36 (t, $J = 7.4$ Hz, 2H), 2.40 (d, $J = 1.2$ Hz, 3H), 6.25 (d, $J = 1.2$ Hz, 1H), 7.48 (dd, $J = 8.7, 2.0$ Hz, 1H), 7.70 (d, $J = 8.7$ Hz, 1H), 7.77 (d, $J = 2.0$ Hz, 1H), 10.34 (s, 1H), 12.00 (s, 1H) ppm; $^{13}\text{C NMR}$ (101 MHz, DMSO-d_6) δ 18.45, 24.73, 25.08, 28.64, 34.01, 36.85, 105.87, 112.57, 115.26, 115.51, 126.36, 143.09, 153.61, 154.16, 160.54, 172.46, 174.91 ppm; MS (ESI) m/z 318.2 [M+H]$^+$; UPLC $t_r = 1.71$ min; yield: 8%.</p> |
| 4.6 |  | A,B,E | <p>$R_f = 0.35$ (1:1 H$_2$O:MeOH, visualization by UV); $^1\text{H NMR}$ (400 MHz, DMSO-d_6) δ 2.41 (d, $J = 0.99$ Hz, 3H), 2.89 (s, 3H), 3.20 (s, 2H), 6.26 (d, $J = 1.09$ Hz, 1H), 7.45 (dd, $J = 9.0, 1.9$ Hz, 1H), 7.73 (d, $J = 8.6$ Hz, 1H), 7.79 (d, $J = 2.0$ Hz, 1H), 10.85 (s, 1H) ppm; $^{13}\text{C NMR}$ (101 MHz, DMSO-d_6) δ 18.46, 40.83, 48.11, 105.78, 112.56, 115.31, 115.49, 126.42, 142.94, 151.33, 153.64, 154.20, 160.55, 167.70 ppm; MS (ESI) m/z 339.4 [M+H]$^+$; UPLC $t_r = 1.34$ min; yield: 10%.</p> |
| 4.7 |  | A,B,E | <p>$^1\text{H NMR}$ (400 MHz, DMSO-d_6) δ 2.40 (s, 3H), 2.65 (m, 4H), 3.22 (s, 3H), 6.26 (s, 1H), 7.47 (dd, $J = 8.5, 2.0$ Hz, 1H), 7.72 (d, $J = 8.6$ Hz, 1H), 7.75 (d, $J = 2.1$ Hz, 1H), 10.46 (s, 1H), 11.80 ppm (s, 1H); $^{13}\text{C NMR}$ (101 MHz, DMSO-d_6) δ 18.46, 30.66, 30.83, 41.45, 105.82, 112.62, 115.30, 115.43, 126.44, 142.95, 153.60, 154.18, 160.51, 171.16, 172.33 ppm; MS (ESI) m/z 353.4 [M+H]$^+$; UPLC: $t_r = 1.29$ min; yield: 77%.</p> |
| 4.8 |  | D,E | <p>$^1\text{H NMR}$ (400 MHz, DMSO-d_6) δ 1.85 (m, 2H), 2.32 - 2.46 (m, 7H), 3.24 (s, 3H), 6.26 (d, $J = 1.6$ Hz, 1H), 7.48 (dd, $J = 8.6, 2.1$ Hz, 1H), 7.72 (d, $J = 8.6$ Hz, 1H), 7.77 (d, $J = 2.0$ Hz, 1H), 10.36 (s, 1H), 11.70 ppm (s, 1H); $^{13}\text{C NMR}$ (101 MHz, DMSO-d_6) δ 18.45, 19.99, 35.00, 35.71, 41.49, 105.93, 112.62, 115.31, 115.54, 126.38, 143.00, 153.59, 154.15, 160.52, 171.87, 172.69 ppm; MS (ESI) m/z 367.4 [M+H]$^+$; UPLC $t_r = 1.36$ min; yield: 36%.</p> |

| | | | |
|------|---|-----------|---|
| 4.9 |  | A,B,F | <p>$R_f = 0.39$ (RP, 1:1 H₂O:MeOH, visualization by UV); ¹H NMR (400 MHz, DMSO-<i>d</i>₆) δ 2.41 (s, 3H), 3.17 (s, 2H), 6.28 (d, $J = 0.93$ Hz, 1H), 7.47 (dd, $J = 8.6, 1.7$ Hz, 1H), 7.73 (d, $J = 8.7$ Hz, 1H), 7.78 (d, $J = 1.7$ Hz, 1H), 10.70 ppm (s br, 2H); ¹³C NMR (101 MHz, DMSO-<i>d</i>₆) δ 18.46, 42.71, 106.02, 112.80, 115.59, 126.47, 142.66, 153.57, 154.12, 160.47, 163.48, 166.69 ppm; MS (ESI) m/z 277.1 [M+H]⁺; UPLC $t_r = 1.15$ min; yield: 11%.</p> |
| 4.10 |  | A,B,F | <p>¹H NMR (400 MHz, DMSO-<i>d</i>₆) δ 2.31 (t, $J = 7.1$ Hz, 2H), 2.40 (d, $J = 1.3$ Hz, 3H), 2.63 (t, $J = 7.1$ Hz, 2H), 6.26 (d, $J = 1.3$ Hz, 1H), 7.47 (dd, $J = 8.7, 2.1$ Hz, 1H), 7.71 (d, $J = 8.7$ Hz, 1H), 7.77 (d, $J = 2.0$ Hz, 1H), 8.73 (s, 1H), 10.43 (s, 1H), 10.45 ppm (s, 1H); ¹³C NMR (101 MHz, DMSO-<i>d</i>₆) δ 18.45, 27.56, 32.02, 105.78, 112.58, 115.24, 115.43, 126.39, 143.06, 153.61, 154.18, 160.54, 168.68, 171.56 ppm; MS (ESI) m/z 291.4 [M+H]⁺; UPLC: $t_r = 1.16$ min; yield: 26%.</p> |
| 4.11 |  | D,F | <p>¹H NMR (400 MHz, DMSO-<i>d</i>₆) δ 1.83 (q, $J = 7.3$ Hz, 2H), 2.03 (t, $J = 7.4$ Hz, 2H), 2.35 - 2.43 (m, 5H), 6.26 (d, $J = 1.3$ Hz, 1H), 7.49 (dd, $J = 8.7, 2.0$ Hz, 1H), 7.71 (d, $J = 8.7$ Hz, 1H), 7.78 (d, $J = 2.0$ Hz, 1H), 10.37 (s, 1H), 10.40 ppm (s, 1H); ¹³C NMR (101 MHz, DMSO-<i>d</i>₆) δ 18.46, 21.33, 31.98, 36.16, 105.91, 112.59, 115.27, 115.54, 126.36, 143.08, 153.60, 154.16, 160.53, 169.08, 172.04 ppm; MS (ESI) m/z 305.4 [M+H]⁺; UPLC $t_r = 1.18$ min; yield: 86%.</p> |
| 4.12 |  | D,G | <p>¹H NMR (400 MHz, DMSO-<i>d</i>₆) δ 1.86 (p, $J = 6.6$ Hz, 2H), 2.41 (m, 7H), 6.26 (s, 1H), 7.47 (d, $J = 8.4$ Hz, 1H), 7.62 - 7.91 (m, 2H), 10.37 (s, 1H), 11.77 ppm (s br, 1H); ¹³C NMR (101 MHz, DMSO-<i>d</i>₆) δ 18.45, 20.03, 34.21, 35.58, 105.94, 109.11, 112.62, 115.32, 115.54, 126.36, 142.97, 153.58, 154.14, 160.51, 171.80, 173.89 ppm; MS (ESI) m/z 314.2 [M+H]⁺; UPLC $t_r = 1.64$ min; yield: 47%.</p> |
| 4.13 |  | A,B,H,I,J | <p>¹H NMR (400 MHz, DMSO-<i>d</i>₆) δ 2.40 (d, $J = 1.0$ Hz, 3H), 2.94 (t, $J = 7.2$ Hz, 2H), 3.19 (t, $J = 7.2$ Hz, 2H), 6.26 (d, $J = 1.1$ Hz, 1H), 7.46 (dd, $J = 8.7, 2.0$ Hz, 1H), 7.71 (d, $J = 8.7$ Hz, 1H), 7.74 (d, $J = 1.9$ Hz, 1H), 10.52 ppm (s, 1H); ¹³C NMR</p> |

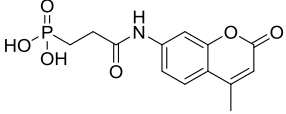
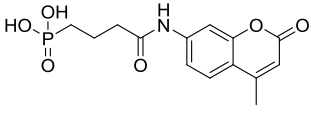
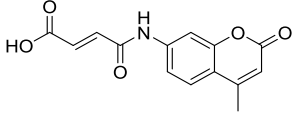
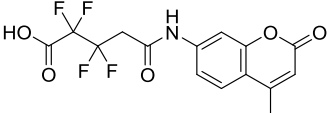
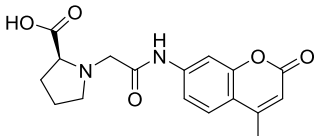
| | | | |
|------|---|-------------|--|
| | | | (101 MHz, DMSO- <i>d</i> ₆) δ 18.45, 18.93, 33.85, 105.92, 112.67, 115.38, 115.50, 126.42, 142.84, 153.57, 154.14, 156.12, 160.49, 170.71 ppm; MS (ESI) <i>m/z</i> 300.3 [M+H] ⁺ ; UPLC <i>t_r</i> = 1.26 min; yield: 6%; purity (UV): 81%. |
| 4.14 |  | A,B,H,I,K,L | <i>R_f</i> = 0.20 (100% EtOAc, visualization by UV); ¹ H NMR (400 MHz, DMSO- <i>d</i> ₆) δ 2.39 (d, <i>J</i> = 0.77 Hz, 3H), 2.74 - 2.87 (m, 4H), 6.25 (d, <i>J</i> = 0.9 Hz, 1H), 7.49 (dd, <i>J</i> = 8.7, 2.0 Hz, 1H), 7.71 (d, <i>J</i> = 8.7 Hz, 1H), 7.76 (d, <i>J</i> = 2.0 Hz, 1H), 10.61 ppm (s, 1H); ¹³ C NMR (101 MHz, DMSO- <i>d</i> ₆) δ 18.45, 20.76, 31.72, 105.93, 112.66, 115.38, 115.52, 126.39, 142.85, 153.58, 154.12, 160.50, 161.14, 170.43 ppm; MS (ESI) <i>m/z</i> 316.3 [M+H] ⁺ ; UPLC: <i>t_r</i> = 1.28 min; yield: 21%. |
| 4.15 |  | D,H,I,K,L | <i>R_f</i> = 0.35 (100% EtOAc, visualization by UV); ¹ H NMR (400 MHz, DMSO- <i>d</i> ₆) δ 1.84 (m, 3H), 2.23 (t, <i>J</i> = 7.1 Hz, 2H), 2.35 - 2.45 (m, 5H), 6.27 (d, <i>J</i> = 1.1 Hz, 1H), 7.50 (dd, <i>J</i> = 8.7, 2.0 Hz, 1H), 7.71 (d, <i>J</i> = 8.7 Hz, 1H), 7.78 (d, <i>J</i> = 1.9 Hz, 1H), 10.56 ppm (s, 1H); ¹³ C NMR (101 MHz, DMSO- <i>d</i> ₆) δ 18.46, 22.97, 27.01, 36.37, 105.82, 112.50, 115.19, 115.51, 126.34, 143.19, 153.63, 154.17, 160.56, 169.66, 172.42 ppm; MS (ESI) <i>m/z</i> 328.0 [M-H] ⁻ ; UPLC <i>t_r</i> = 1.37 min; yield: 6%. |
| 4.16 |  | A,B,M | ¹ H NMR (400 MHz, DMSO- <i>d</i> ₆) δ 2.41 (d, <i>J</i> = 1.3 Hz, 3H), 2.69 (s, 6H), 3.84 (d, <i>J</i> = 5.6 Hz, 2H), 6.28 (q, <i>J</i> = 1.3 Hz, 1H), 7.49 (dd, <i>J</i> = 8.6, 2.1 Hz, 1H), 7.63 (t, <i>J</i> = 6.0 Hz, 1H), 7.72 - 7.79 (m, 2H), 10.43 ppm (s, 1H); ¹³ C NMR (101 MHz, DMSO- <i>d</i> ₆) δ 18.45, 38.04, 46.73, 106.15, 112.85, 115.65-115.69 (m, 2 signals), 126.54, 142.46, 153.55, 154.13, 160.44, 168.73 ppm; MS (ESI) <i>m/z</i> 340.4 [M+H] ⁺ ; UPLC <i>t_r</i> = 1.46 min; yield: 41%. |
| 4.17 |  | A,B,M | ¹ H NMR (400 MHz, DMSO- <i>d</i> ₆) δ 2.40 (d, <i>J</i> = 1.3 Hz, 3H), 2.61 (t, <i>J</i> = 7.0 Hz, 2H), 2.67 (s, 6H), 3.23 (q, <i>J</i> = 6.8 Hz, 2H), 6.26 (d, <i>J</i> = 1.3 Hz, 1H), 7.26 (t, <i>J</i> = 5.8 Hz, 1H), 7.48 (dd, <i>J</i> = 8.7, 2.0 Hz, 1H), 7.72 (d, <i>J</i> = 8.7 Hz, 1H), 7.78 (d, <i>J</i> = 2.0 Hz, 1H), 10.43 ppm (s, 1H); ¹³ C NMR (101 MHz, DMSO- <i>d</i> ₆) δ 18.45, 37.28, 38.08, 39.36, 106.03, 112.67, 115.41, 115.61, 126.41, |

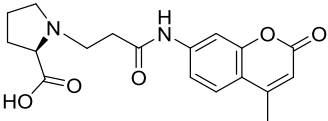
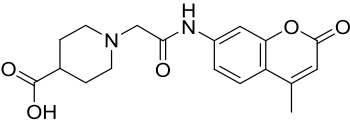
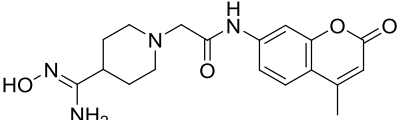
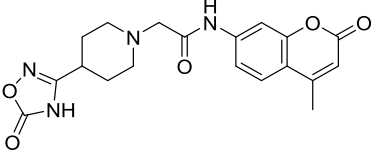
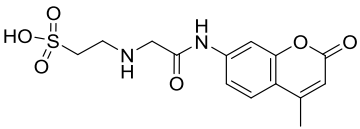
| | | | |
|------|---|-------|--|
| | | | 142.87, 153.64, 154.12, 160.54, 170.31; MS (ESI) m/z 354.4 [M+H] ⁺ ; UPLC t_r = 1.47min; yield: 54%. |
| 4.18 |  | A,B,M | ¹ H NMR (400 MHz, DMSO- <i>d</i> ₆) δ 1.73 - 1.85 (m, 2H), 2.40 (d, <i>J</i> = 1.3 Hz, 3H), 2.44 (t, <i>J</i> = 7.4 Hz, 2H), 2.66 (s, 6H), 2.96 (q, <i>J</i> = 6.8 Hz, 2H), 6.26 (d, <i>J</i> = 1.3 Hz, 1H), 7.20 (t, <i>J</i> = 5.9 Hz, 1H), 7.48 (dd, <i>J</i> = 8.7, 2.1 Hz, 1H), 7.71 (d, <i>J</i> = 8.7 Hz, 1H), 7.77 (d, <i>J</i> = 2.0 Hz, 1H), 10.36 ppm (s, 1H); ¹³ C NMR (101 MHz, DMSO- <i>d</i> ₆) δ 18.45, 25.46, 33.96, 38.10, 42.77, 105.91, 112.60, 115.30, 115.54, 126.38, 143.02, 153.62, 154.15, 160.54, 172.01 ppm; MS (ESI) m/z 368.4 [M+H] ⁺ ; UPLC t_r = 1.50 min; yield: 41%. |
| 4.19 |  | A,B,N | ¹ H NMR (400 MHz, DMSO- <i>d</i> ₆) δ 0.67 - 1.00 (dt, <i>J</i> = 82.1, 7.4 Hz, 3H), 1.26 (q, <i>J</i> = 7.3 Hz, 1H), 1.41 (p, <i>J</i> = 7.6 Hz, 1H), 1.58 (p, <i>J</i> = 6.6 Hz, 1H), 1.74 (p, <i>J</i> = 8.5 Hz, 1H), 2.41 (d, <i>J</i> = 1.3 Hz, 3H), 4.18 (d, <i>J</i> = 6.1 Hz, 1H), 4.37 (d, <i>J</i> = 6.0 Hz, 1H), 4.62 (dt, <i>J</i> = 35.2, 6.4 Hz, 2H), 6.29 (q, <i>J</i> = 1.2 Hz, 1H), 7.48 (dd, <i>J</i> = 8.6, 2.1 Hz, 1H), 7.71 - 7.78 (m, 2H), 8.93 (dt, <i>J</i> = 73.4, 5.5 Hz, 1H), 10.57 ppm (d, <i>J</i> = 12.7 Hz, 1H); ¹³ C NMR (101 MHz, DMSO- <i>d</i> ₆) δ 13.82, 18.45, 18.54, 31.91, 46.78, 47.10, 72.97, 106.19, 112.91, 115.66, 115.71, 126.56, 142.36, 153.55, 154.12, 160.42, 167.81, 168.17, 178.40 ppm; MS (ESI) m/z 385.4 [M+H] ⁺ ; UPLC t_r = 1.61 min; yield: 49%. |
| 4.20 |  | A,B,N | ¹ H NMR (400 MHz, DMSO- <i>d</i> ₆) δ 0.90 (t, <i>J</i> = 7.4 Hz, 3H), 1.40 (m, 2H), 1.72 (m, 2H), 2.40 (d, <i>J</i> = 1.3 Hz, 3H), 2.69 (m, 2H), 3.59 - 3.85 (m, 2H), 4.57 - 4.66 (dq, <i>J</i> = 66.4, 6.3 Hz, 2H), 6.27 (d, <i>J</i> = 1.3 Hz, 1H), 7.47 (dd, <i>J</i> = 8.7, 2.1 Hz, 1H), 7.72 (d, <i>J</i> = 8.6 Hz, 1H), 7.75 (d, <i>J</i> = 2.0 Hz, 1H), 8.77 (dt, <i>J</i> = 68.3, 5.6 Hz, 1H), 10.44 ppm (s, 1H); ¹³ C NMR (101 MHz, DMSO- <i>d</i> ₆) δ 14.00, 18.45, 18.54, 31.96, 37.32, 37.96, 72.91, 106.02, 112.72, 115.44, 115.58, 126.42, 142.80, 153.58, 154.13, 160.48, 169.97, 173.08, 177.63, 182.80, 189.62 ppm; MS (ESI) m/z 399.4 [M+H] ⁺ ; UPLC t_r = 1.65 min; yield: 60%. |

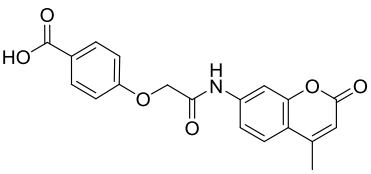
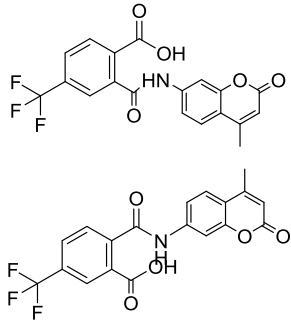
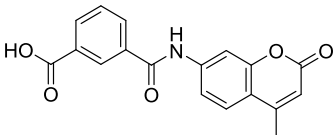
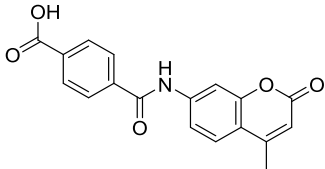
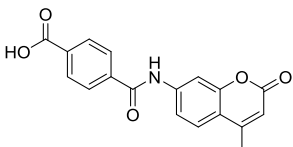
| | | | |
|------|---|---------|--|
| 4.21 |  | A,B,N | $^1\text{H NMR}$ (400 MHz, $\text{DMSO-}d_6$) δ 0.86 (dt, $J = 30.0$, 7.3 Hz, 3H), 1.32 (dsex, $J = 30.0$, 7.5 Hz, 2H), 1.64 (dp, $J = 29.0$, 6.8 Hz, 2H), 1.81 - 1.93 (m, 2H), 2.36 - 2.46 (m, 5H), 3.56 (q, $J = 6.4$ Hz, 1H), 4.55 (dt, $J = 18.1$, 6.6 Hz, 2H), 6.26 (d, $J = 1.5$ Hz, 1H), 7.45 (dd, $J = 8.7$, 2.0 Hz, 1H), 7.75 (m, 2H), 8.70 (dt, $J = 82.0$, 5.8 Hz, 1H), 10.35 ppm (s, 1H); MS (ESI) m/z 413.4 $[\text{M}+\text{H}]^+$; UPLC $t_r = 1.67$ min; yield: 63%. |
| 4.22 |  | A,B,N,O | $R_f = 0.66$ (RP, 1:1 $\text{H}_2\text{O}:\text{MeOH}$, visualization by UV); $^1\text{H NMR}$ (400 MHz, $\text{DMSO-}d_6$) δ 2.40 (d, $J = 1.4$ Hz, 3H), 4.30 (d, $J = 5.7$ Hz, 2H), 6.28 (d, $J = 1.5$ Hz, 1H), 7.49 (dd, $J = 8.7$, 2.1 Hz, 1H), 7.71 - 7.77 (m, 2H), 8.35 (t, $J = 6.3$ Hz, 1H), 10.60 ppm (s, 1H); $^{13}\text{C NMR}$ (101 MHz, $\text{DMSO-}d_6$) δ 18.46, 46.94, 106.14, 112.86, 115.64, 115.67, 126.56, 142.42, 153.56, 154.12, 160.44, 168.45, 175.63, 186.94 ppm; MS (ESI) m/z 329.4 $[\text{M}+\text{H}]^+$; UPLC: $t_r = 1.09$ min; yield: 13%. |
| 4.23 |  | A,B,N,O | $R_f = 0.61$ (RP, 1:1 $\text{H}_2\text{O}:\text{MeOH}$, visualization by UV); $^1\text{H NMR}$ (400 MHz, $\text{DMSO-}d_6$) δ 2.39 (s, 3H), 2.69 (s, 2H), 3.80 (m, 2H), 6.25 (s, 1H), 7.48 (d, $J = 8.8$ Hz, 1H), 7.66 - 7.86 (m, 3H), 10.54 ppm (s, 1H); $^{13}\text{C NMR}$ (101 MHz, $\text{DMSO-}d_6$) δ 18.46, 38.52, 39.85, 105.99, 112.63, 115.36, 115.60, 126.36, 142.89, 153.62, 154.11, 160.53, 170.39, 177.66, 186.74 ppm; MS (ESI) m/z 343.5 $[\text{M}+\text{H}]^+$; UPLC $t_r = 1.16$ min; yield: 19%. |
| 4.24 |  | A,B,N,O | $R_f = 0.61$ (RP, 1:1 $\text{H}_2\text{O}:\text{MeOH}$, visualization by UV); $^1\text{H NMR}$ (400 MHz, $\text{DMSO-}d_6$) δ 1.86 (p, $J = 6.9$ Hz, 2H), 2.41 (m, 5H), 3.47 (q, $J = 6.5$ Hz, 2H), 6.26 (d, $J = 1.6$ Hz, 1H), 7.47 (dd, $J = 8.9$, 2.0 Hz, 1H), 7.70 (d, $J = 8.7$ Hz, 1H), 7.76 (d, $J = 1.7$ Hz, 1H), 8.28 (t, $J = 6.0$ Hz, 1H), 10.38 ppm (s, 1H); $^{13}\text{C NMR}$ (101 MHz, $\text{DMSO-}d_6$) δ 18.45, 26.52, 33.77, 43.39, 105.97, 112.59, 115.29, 115.58, 126.33, 143.01, 153.60, 154.14, 160.53, 171.83, 175.09, 186.40 ppm; MS (ESI) m/z 357.4 $[\text{M}+\text{H}]^+$; UPLC $t_r = 1.17$ min; yield: 7%. |
| 4.25 |  | A,J | $^1\text{H NMR}$ (400 MHz, $\text{DMSO-}d_6$) δ 2.41 (s, 3H), 4.23 (s, 2H), 6.29 (s, 1H), 7.50 (d, $J = 2.2$ Hz, 1H), 7.70 - 7.82 (m, 2H), 10.88 ppm (s, 1H); |

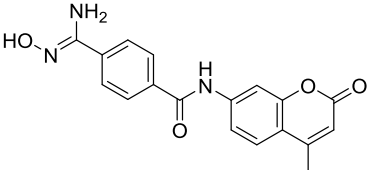
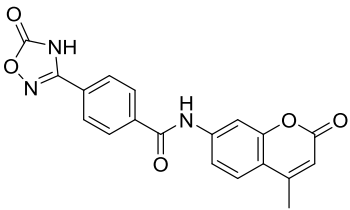
| | | | |
|------|---|--------|---|
| | | | MS (ESI) m/z 283.9 [M-H] ⁻ ; UPLC t_r = 1.40 min; yield: 10.2% |
| 4.26 |  | A,K | ¹ H NMR (400 MHz, DMSO- <i>d</i> ₆) δ 2.41 (d, <i>J</i> = 1.3 Hz, 3H), 3.12 (s, 2H), 5.55 (s, 2H), 6.27 (d, <i>J</i> = 1.2 Hz, 1H), 7.73 (d, <i>J</i> = 8.7 Hz, 1H), 7.76 (d, <i>J</i> = 2.0 Hz, 1H), 9.10 (s, 1H), 10.49 ppm (s, 1H); ¹³ C NMR (101 MHz, DMSO- <i>d</i> ₆) δ 18.46, 40.02, 105.91, 112.71, 115.45, 115.52, 126.42, 142.90, 148.76, 153.59, 154.14, 160.50, 168.04 ppm; MS (ESI) m/z 276.4 [M+H] ⁺ ; UPLC t_r = 0.89 min; yield: 65%. |
| 4.28 |  | P1,Q,J | ¹ H NMR (400 MHz, DMSO- <i>d</i> ₆) δ 2.40 (d, <i>J</i> = 0.96 Hz, 3H), 4.18 (s, 2H), 6.25 - 6.29 (d, <i>J</i> = 1.09 Hz, 1H), 7.46 (dd, <i>J</i> = 8.6, 2.0 Hz, 1H), 7.74 (m, 3H), 11.00 ppm (s, 1H); ¹³ C NMR (101 MHz, DMSO- <i>d</i> ₆) δ 18.45, 37.40, 106.05, 112.85, 115.58, 115.69, 126.54, 142.55, 153.57, 154.11, 154.92, 160.46, 167.31 ppm; MS (ESI) m/z 318.1 [M+H] ⁺ ; UPLC t_r = 1.58 min, yield: 26%. |
| 4.29 |  | P1,R | R_f = 0.70 (RP, 1:1 H ₂ O:MeOH, visualization by UV); ¹ H NMR (400 MHz, DMSO- <i>d</i> ₆) δ 2.40 (s, 3H), 3.58 (s, 2H), 6.26 (s, 1H), 7.44 (dd, <i>J</i> = 8.7, 2.2 Hz, 1H), 7.71 (d, <i>J</i> = 8.6 Hz, 1H), 7.82 (d, <i>J</i> = 2.2 Hz, 1H), 10.41 ppm (s, 1H); ¹³ C NMR (101 MHz, DMSO- <i>d</i> ₆) δ 18.46, 59.68, 105.86, 112.60, 115.33, 115.56, 126.33, 142.93, 153.63, 154.16, 160.55, 165.63 ppm; MS (ESI) m/z 296.4 [M-H] ⁻ ; UPLC: t_r = 1.08 min; yield: 47%. |
| 4.30 |  | P2,R | R_f = 0.64 (RP, 1:1 H ₂ O:MeOH, visualization by UV); ¹ H NMR (400 MHz, DMSO- <i>d</i> ₆) δ 2.39 (s, 3H), 2.67 - 2.83 (m, 4H), 6.23 (d, <i>J</i> = 1.4 Hz, 1H), 7.46 (dd, <i>J</i> = 8.7, 2.2 Hz, 1H), 7.68 (d, <i>J</i> = 8.6 Hz, 1H), 7.77 (d, <i>J</i> = 2.1 Hz, 1H), 10.52 ppm (s, 1H); ¹³ C NMR (101 MHz, DMSO- <i>d</i> ₆) δ 18.44, 33.75, 47.32, 105.89, 112.51, 115.21, 115.56, 126.26, 143.13, 153.63, 154.12, 160.57, 171.49 ppm; MS (ESI) m/z 310.4 [M-H] ⁻ ; UPLC t_r = 1.12 min; yield: 25%. |
| 4.31 |  | P3,R | ¹ H NMR (400 MHz, DMSO- <i>d</i> ₆) δ 1.91 (p, <i>J</i> = 7.6 Hz, 2H), 2.39 (d, <i>J</i> = 1.4 Hz, 3H), 2.51 (m, under solvent peak) 6.24 (d, <i>J</i> = 1.7 Hz, 1H), 7.49 (dd, <i>J</i> = 8.7, 2.1 Hz, 1H), 7.70 (d, <i>J</i> = 8.7 Hz, 1H), 7.78 (d, <i>J</i> = 2.1 Hz, 1H), 10.40 ppm (s, 1H); ¹³ C |

| | | | |
|------|--|--------|--|
| | | | NMR (101 MHz, DMSO- d_6) δ 18.44, 21.66, 36.08, 50.98, 105.86, 112.50, 115.19, 115.55, 126.31, 143.15, 153.64, 154.15, 160.57, 172.52 ppm; MS (ESI) m/z 324.4 [M-H] ⁻ ; UPLC: t_r = 1.15 min; yield: 6%. |
| 4.32 | | P1,S,T | ¹ H NMR (MeOD- d_4 , 400 MHz) δ 1.35 (t, J = 7.0 Hz, 3H), 2.47 (s, 3H), 3.11 (d, J = 21.6 Hz, 2H), 4.10 - 4.24 (m, 2H), 6.25 (s, 1H), 7.42 - 7.58 (m, 1H), 7.73 (d, J = 8.7 Hz, 1H), 7.82 ppm (s, 1H); MS (ESI) m/z 324.4 [M-H] ⁻ , UPLC t_r = 1.10 min; yield: 27.6% |
| 4.33 | | P2,S,T | ¹ H NMR (400 MHz, DMSO- d_6) δ 1.21 (t, J = 7.0 Hz, 3H), 1.79 - 2.02 (m, 2H), 2.40 (s, 3H), 2.58 (qt, J = 8.2, 3.1 Hz, 2H), 3.95 (p, J = 7.2 Hz, 2H), 6.26 (d, J = 1.2 Hz, 1H), 7.48 (dd, J = 8.6, 2.1 Hz, 1H), 7.71 (dd, J = 8.6, 2.2 Hz, 1H), 7.76 (d, J = 2.1 Hz, 1H), 10.47 ppm (s, 1H); ¹³ C NMR (101 MHz, DMSO- d_6) δ 16.83, 16.89, 18.45, 21.06, 22.45, 30.45, 30.48, 60.61, 60.67; 65.39, 105.92 (d, J = 2.3 Hz), 112.63, 115.34, 115.51, 115.54, 126.38, 142.97, 153.59, 154.14, 160.51, 171.03, 171.19, 171.39, 171.57 ppm; MS (ESI) m/z 338.4 [M-H] ⁻ ; UPLC t_r = 1.20 min; yield: 29%; purity: 66% (impured with double deprotected phosphonic acid). |
| 4.34 | | P3,S,T | ¹ H NMR (400 MHz, DMSO- d_6) δ 1.22 (t, J = 7.0 Hz, 3H), 1.67 (m, 2H), 1.80 (m, 2H), 2.39 (s, 3H), 2.44 - 2.54 (m, under solvent peak), 3.93 (p, J = 7.1 Hz, 2H), 6.22 - 6.26 (d, J = 0.97 Hz, 2H), 7.49 (dd, J = 8.7, 1.9 Hz, 1H), 7.69 (d, J = 8.7 Hz, 1H), 7.77 (d, J = 1.9 Hz, 1H), 10.45 ppm (s, 1H); ¹³ C NMR (101 MHz, DMSO- d_6) δ 16.86, 16.91, 18.44, 18.91, 18.95, 25.04, 26.41, 37.09, 37.25, 60.39, 60.42, 105.90, 112.57, 115.26, 115.53, 126.31, 143.04, 153.58, 154.13, 160.53, 171.98 ppm; MS (ESI) m/z 352.2 [M-H] ⁻ ; UPLC t_r = 1.85 min; yield: 80%. |
| 4.35 | | P1,S,U | ¹ H NMR (DMSO- d_6 , 400 MHz) δ 2.40 (d, J = 1.3 Hz, 3H), 3.18 (s, 2H), 6.27 (d, J = 1.3 Hz, 1H), 7.46 (dd, J = 8.7, 2.0 Hz, 1H), 7.72 (d, J = 8.7 Hz, 1H), 7.78 (d, J = 2.0 Hz, 1H), 10.41 ppm (s, 1H); MS (ESI) m/z 296.4 [M-H] ⁻ , UPLC t_r = 0.33 min; yield: 62.1% |

| | | | |
|------|---|--------|---|
| 4.36 |  | P2,S,U | ^1H NMR (400 MHz, DMSO- d_6) δ 1.80 - 1.91 (m, 2H), 2.40 (d, J = 1.3 Hz, 3H), 2.53 - 2.62 (m, 2H), 3.17, 6.26 (d, J = 1.3 Hz, 1H), 7.48 (dd, J = 8.7, 2.1 Hz, 1H), 7.72 (d, J = 8.7 Hz, 1H), 7.76 (d, J = 2.0 Hz, 1H), 10.45 ppm (s, 1H); ^{13}C NMR (101 MHz, DMSO- d_6) δ 18.45, 22.91, 24.29, 105.94, 112.63, 115.32, 115.55, 126.37, 143.02, 153.60, 154.15, 160.51, 171.39, 171.57 ppm; MS (ESI) m/z 310.4 [M-H] ⁻ ; UPLC t_r = 1.07 min; yield: 71%. |
| 4.37 |  | P3,S,U | ^1H NMR (400 MHz, DMSO- d_6) δ 1.57 (s, 2H), 1.81 (s, 2H), 2.39 (s, 4H), 6.25 (s, 1H), 7.50 (d, J = 7.9 Hz, 1H), 7.71 (d, J = 8.3 Hz, 1H), 7.78 (s, 1H), 10.45 ppm (s, 1H); MS (ESI) m/z 324.1 [M-H] ⁻ ; UPLC t_r = 1.67 min; yield: 87%. |
| 4.38 |  | A,C | ^1H NMR (DMSO- d_6 , 400 MHz) δ 2.41 (s, 3H), 6.30 (s, 1H), 6.71 (d, J = 15.4 Hz, 1H), 7.14 (d, J = 15.4 Hz, 1H), 7.55 (d, J = 8.7 Hz, 1H), 7.74 - 7.87 (m, 2H), 10.92 ppm (s, 1H); MS (ESI) m/z 271.9 [M-H] ⁻ ; UPLC t_r = 1.37 min; yield: 44.1%. |
| 4.39 |  | D | R_f = 0.61 (RP, 1:1 H ₂ O:MeOH, visualization by UV); ^1H NMR (400 MHz, DMSO- d_6) δ 2.42 (d, J = 1.2 Hz, 3H), 6.33 (d, J = 1.2 Hz, 1H), 7.56 (dd, J = 8.7, 2.1 Hz, 1H), 7.75 - 7.83 (m, 2H), 12.76 (s, 1H) ppm; ^{13}C NMR (101 MHz, DMSO- d_6) δ 18.47, 107.29, 113.47, 116.55, 116.63, 126.62, 141.22, 153.48, 153.94, 159.12 (t, J = 23.67 Hz), 160.33, 160.62 ppm (t, J = 27.76 Hz); MS (ESI) m/z 348.0 [M+H] ⁺ ; UPLC t_r = 1.27 min; yield: 18%. |
| 4.40 |  | P1,Q,B | ^1H NMR (400 MHz, DMSO- d_6) δ 1.70 - 1.86 (m, 2H), 1.91 (m, 1H), 2.10 - 2.24 (m, 1H), 2.41 (d, J = 1.3 Hz, 3H), 2.72 (m, 1H), 3.16 (m, 1H), 3.42 - 3.69 (m, 3H), 6.28 (d, J = 1.3 Hz, 1H), 7.52 (dd, J = 8.7, 2.1 Hz, 1H), 7.74 (d, J = 8.7 Hz, 1H), 7.78 (d, J = 2.0 Hz, 1H), 10.50 ppm (s, 1H); ^{13}C NMR (101 MHz, DMSO- d_6) δ 18.47, 24.42, 30.05, 54.43, 58.30, 65.71, 106.06, 112.79, 115.61, 115.67, 126.45, 142.31, 153.58, 154.15, 160.46, 170.46, 176.03 ppm; MS (ESI) m/z 331.4 [M+H] ⁺ ; UPLC t_r = 1.06 min; yield: 97%. |

| | | | |
|------|---|----------|--|
| 4.41 |  | P2,Q,B | ^1H NMR (400 MHz, DMSO- d_6) δ 1.65 - 1.80 (m, 1H), 1.83 - 2.00 (m, 2H), 2.11 - 2.26 (m, 1H), 2.41 (d, J = 1.3 Hz, 3H), 2.70 - 2.86 (m, 3H), 3.05 - 3.17 (m, 2H), 3.55 - 3.66 (m, 2H), 6.27 (d, J = 1.5 Hz, 1H), 7.49 (dd, J = 8.7, 2.1 Hz, 1H), 7.73 (d, J = 8.7 Hz, 1H), 7.76 (d, J = 2.0 Hz, 1H), 10.67 ppm (s, 1H); ^{13}C NMR (101 MHz, DMSO- d_6) δ 18.46, 23.63, 29.24, 34.00, 50.27, 54.10, 67.57, 106.10, 112.74, 115.47, 115.65, 126.42, 142.75, 153.58, 154.19, 160.49, 170.01, 171.83 ppm; MS (ESI) m/z 345.2 [M+H] $^+$; UPLC t_r = 1.06 min; yield: 6%. |
| 4.42 |  | P1,Q,C | ^1H NMR (400 MHz, DMSO- d_6) δ 1.79 - 2.16 (m, 4H), 2.42 (d, J = 1.4 Hz, 3H), 3.17 (m, 2H), 3.57 (m, 2H), 4.23 (s, 2H), 6.32 (d, J = 1.4 Hz, 1H), 7.54 (dd, J = 8.5, 2.1 Hz, 1H), 7.76 - 7.84 (m, 2H), 10.08 (s, 1H), 11.39 (s, 1H), 12.55 ppm (s, 1H); ^{13}C NMR (101 MHz, DMSO- d_6) δ 18.47, 25.61, 31.17, 49.05, 52.46, 106.56, 113.22, 115.89, 116.19, 126.64, 141.71, 153.52, 154.01, 160.35, 175.02, 206.96 ppm; MS (ESI) m/z 345.5 [M+H] $^+$; UPLC t_r = 1.01 min; yield: 44%. |
| 4.43 |  | P1,Q,K | MS (ESI) m/z 359.5 [M+H] $^+$; UPLC t_r = 0.24 min; yield: 47%. |
| 4.44 |  | P1,Q,K,L | ^1H NMR (400 MHz, DMSO- d_6) δ 1.63 (s, 1H), 2.00 (s, 2H), 2.16 (s, 2H), 2.42 (s, 3H), 2.68 (s, 1H), 2.96 (s, 1H), 3.25 (s, 2H), 3.64 (s, 2H), 4.24 (s, 2H), 6.33 (s, 1H), 7.52 (d, J = 8.6 Hz, 1H), 7.79 (m, 2H), 10.16 (s, 1H), 11.26 (s, 1H), 12.41 - 12.53 ppm (s, 1H); MS (ESI) m/z 385.4 [M+H] $^+$; UPLC t_r = 1.10 min; yield: 6%. |
| 4.45 |  | P1,Q | ^1H NMR (400 MHz, DMSO- d_6) δ 2.42 (d, J = 1.3 Hz, 3H), 2.88 (t, J = 6.7 Hz, 2H), 3.37 (s, 3H), 4.08 (s, 2H), 6.31 (d, J = 1.3 Hz, 1H), 7.48 (dd, J = 8.7, 2.1 Hz, 1H), 7.73 (d, J = 2.0 Hz, 1H), 7.78 (d, J = 8.7 Hz, 1H), 8.88 (s, 1H), 10.89 ppm (s, 1H); ^{13}C NMR (101 MHz, DMSO- d_6) δ 18.46, 44.52, 47.06, 49.11, 106.37, 113.20, 115.71, 116.14, 126.79, 141.66, 153.50, 154.08, 160.35, 165.32 ppm; MS (ESI) m/z 339.4 [M-H] $^-$; UPLC t_r = 0.76 min; yield: 19.7% |

| | | | |
|------|---|--------|--|
| 4.46 |  | P1,Q,C | $^1\text{H NMR}$ (400 MHz, $\text{DMSO-}d_6$) δ 2.42 (d, $J = 1.3$ Hz, 3H), 4.87 (s, 2H), 6.30 (d, $J = 1.6$ Hz, 1H), 7.10 (dd, $J = 9.3, 2.3$ Hz, 2H), 7.59 (dd, $J = 8.6, 2.1$ Hz, 1H), 7.74 - 7.84 (m, 2H), 7.89 - 7.97 (m, 2H), 10.59 (s, 1H), 12.69 ppm (s, 1H); MS (ESI) m/z 354.3 $[\text{M}+\text{H}]^+$; UPLC $t_r = 1.52$ min; yield: 14%. |
| 4.47 |  | A | $^1\text{H NMR}$ (400 MHz, $\text{MeOD-}d_4$) δ 2.50 (d, $J = 1.3$ Hz, 6H), 6.28 (d, $J = 1.3$ Hz, 2H), 7.59 (ddd, $J = 8.6, 4.5, 2.1$ Hz, 2H), 7.79 (m, 3H), 7.89 (t, $J = 2.2$ Hz, 2H), 7.91 - 7.97 (m, 2H), 8.03 (dt, $J = 8.0, 1.0$ Hz, 1H), 8.23 (dt, $J = 8.0, 0.7$ Hz, 1H), 8.33 ppm (d, $J = 1.9$ Hz, 1H); MS (ESI) m/z 389.9 $[\text{M}-\text{H}]^-$, 781.9 $[2\text{M}-\text{H}]^-$; UPLC $t_r = 1.70, 1.74$ min; yield: 5.8%. |
| 4.48 |  | A,C | $^1\text{H NMR}$ (400 MHz, $\text{DMSO-}d_6$) δ 2.43 (d, $J = 1.3$ Hz, 3H), 6.30 (d, $J = 1.3$ Hz, 1H), 7.69 (dd, $J = 7.7$ Hz, 1H), 7.78 (d, $J = 1.2$ Hz, 2H), 7.95 (s, 1H), 8.20 (ddd, $J = 22.6, 7.9, 1.4$ Hz, 2H), 8.55 (dd, $J = 1.8$ Hz, 1H), 10.84 ppm (s, 1H); $^{13}\text{C NMR}$ (101 MHz, $\text{DMSO-}d_6$) δ 18.05, 48.62, 106.84, 112.59, 115.52, 116.31, 125.84, 128.60, 129.04, 131.14, 132.22, 132.61, 134.78, 142.43, 153.17, 153.52, 160.08, 165.34, 166.78 ppm; MS (ESI) m/z 322.0 $[\text{M}-\text{H}]^-$; UPLC $t_r = 1.66$ min; yield: 94.0%. |
| 4.49 |  | A,C | $^1\text{H NMR}$ (400 MHz, $\text{DMSO-}d_6$) δ 2.43 (d, $J = 1.3$ Hz, 3H), 6.31 (d, $J = 1.3$ Hz, 1H), 7.74 - 7.81 (m, 2H), 7.95 (d, $J = 1.6$ Hz, 1H), 8.08 (d, $J = 1.9$ Hz, 4H), 10.80 ppm (s, 1H); MS (ESI) m/z 322.6 $[\text{M}-\text{H}]^-$, 645.1 $[2\text{M}-\text{H}]^-$; UPLC $t_r = 1.60$ min; yield: 6.1%. |
| 4.50 |  | A,J | $R_f = 0.24$ (RP, 1:1 $\text{H}_2\text{O}:\text{MeOH}$, visualization by UV); $^1\text{H NMR}$ (400 MHz, $\text{DMSO-}d_6$) δ 2.43 (d, $J = 1.3$ Hz, 3H), 6.29 (d, $J = 1.4$ Hz, 1H), 7.74 - 7.84 (m, 2H), 7.92 - 8.05 (m, 3H), 8.13 (d, $J = 8.4$ Hz, 2H), 8.54 (s, 1H), 10.63 ppm (s, 1H); MS (ESI) m/z 346.5 $[\text{M}-\text{H}]^-$; UPLC $t_r = 1.60$ min; yield: 20%. |

| | | |
|------|---|--|
| 4.51 |  | <p>¹H NMR (400 MHz, DMSO-<i>d</i>₆) δ 2.43 (d, <i>J</i> = 1.3 Hz, 3H), 5.96 (s, 2H), 6.30 (d, <i>J</i> = 1.3 Hz, 1H), 7.78 (d, <i>J</i> = 1.2 Hz, 2H), 7.83 - 7.90 (m, 2H), 7.94 - 8.02 (m, 3H), 8.04 (d, <i>J</i> = 2.1 Hz, 1H), 9.88 (s, 1H), 10.66 ppm (s, 1H); ¹³C NMR (101 MHz, DMSO-<i>d</i>₆) δ 18.49, 107.09, 112.95, 115.84, 116.64, 125.72, 126.28, 128.17, 134.85, 137.04, 143.02, 150.52, 153.62, 154.00, 160.53, 166.10 ppm; MS (ESI) <i>m/z</i> 338.1 [M+H]⁺; UPLC <i>t</i>_r = 1.19 min; yield: 96%.</p> |
| 4.52 |  | <p>¹H NMR (400 MHz, DMSO-<i>d</i>₆) δ 2.42 (s, 3H), 6.29 (s, 1H), 7.76 (m, 2H), 7.90 - 8.03 (m, 3H), 8.15 (m, 2H), 10.83 ppm (s, 1H); ¹³C NMR (101 MHz, DMSO-<i>d</i>₆) δ 18.48, 107.23, 113.09, 116.04, 116.70, 126.32, 126.67, 126.71, 129.21, 137.85, 142.76, 153.57, 153.97, 157.32, 160.32, 160.48, 165.51 ppm; MS (ESI) <i>m/z</i> 364.5 [M+H]⁺; UPLC <i>t</i>_r = 1.55 min; yield: 69%.</p> |

General procedure V (formation of amidoxime)

Hydroxylammonium chloride (1.1 eq.) was dissolved in methanol (0.35 M), NaHCO₃ (1.1 eq.) was added and stirred for 30 min at room temperature. Carbonitrile (1 eq.) dissolved in methanol (0.35 M) was added and refluxed overnight. The reaction mixture was cooled to room temperature and salt was removed by filtration. The solution was concentrated under reduced pressure. Acetone was added and filtration was repeated. Intermediate amidoxime was obtained as a white solid.

General procedure W (cyclization to 1,2,4-oxadiazol-5-one)

In a round-bottom flask intermediate amidoxime (1 eq.), 1,1'-carbonylbis-1H-imidazole (1.5 eq.), 1,8-diazabicyclo[5.4.0]undec-7-ene (1.1 eq.) and dioxane (0.2 M) were added. The resulting mixture was refluxed for 2 h. The reaction mixture was cooled down and concentrated *in vacuo*. 1 M HCl and EtOAc were added and extraction was done. The aqueous layer was washed EtOAc. The combined organic layers were dried (Na₂SO₄) and concentrated *in vacuo*. If necessary, flash chromatography (Hex:EtOAc + 0.5% FA) was performed.

General procedure X (acetal deprotection)

6 M HCl (0.25 M) was added to the acetal and the solution was left stirring in a closed vial for 3 h at 50 °C. The solvent was removed under reduced pressure to obtain final compound as a solide.

4-(Dimethoxymethyl)benzotrile (4.79)

4-Formyl-benzotrile (**4.78**, 3 g, 22.88 mmol) was dissolved in dry methanol (40 mL) and trimethoxymethane (15,02 mL, 137 mmol) and p-toluenesulfonic acid monohydrate (1,306 g, 6,86 mmol) were added and the mixture was heated overnight at 45 °C. The mixture was concentrated *in vacuo*, diluted with MeOH (20 mL) and hexanes (150 mL). The combined organic layers were washed with saturated Na₂CO₃ solution. The aqueous layer was back-extracted with hexanes (2 x 100 mL). The combined organic layers were washed with brine (100 mL), dried over Na₂SO₄ and concentrated *in vacuo* to afford the acetal **4.79** with purity (UV) = 89 % (4 g, 89%). R_f = 0.59 (1:1 Hex:EtOAc, visualization by UV); ¹H NMR (400 MHz, CDCl₃) δ 3.34 (s, 6H), 5.45 (s, 1H), 7.59 (dd, *J* = 8.6, 0.6 Hz, 2H), 7.68 ppm (d, *J* = 8.5 Hz, 2H); ¹³C NMR (101 MHz, CDCl₃) δ 52.72, 101.76, 112.32, 118.70, 127.59, 132.09, 143.21 ppm; UPLC-MS *m/z*: 176.2 [M-H]⁻.

(Z)-4-(Dimethoxymethyl)-N'-hydroxybenzimidamide (4.80)

4-(dimethoxymethyl)benzotrile (**4.79**, 4 g, 22.57 mmol) was used for the synthesis of amidoxime **4.80** (5.1 g, >99%) according to general procedure V. R_f = 0.44 (100% EtOAc, visualization by UV); ¹H NMR (400 MHz, CDCl₃) δ 3.33 (s, 6H), 5.17 (s, 2H), 5.41 (s, 1H), 6.81 - 7.38 (m, 1H), 7.47 (d, *J* = 8.1 Hz, 2H), 7.60 - 7.66 ppm (m, 2H); UPLC-MS *m/z*: 211.1 [M+H]⁺.

4-(5-Oxo-4,5-dihydro-1,2,4-oxadiazol-3-yl)benzaldehyde (4.81)

Amidoxime **4.80** (2 g, 9.51 mmol) was used for the synthesis of 3-(4-(dimethoxymethyl)phenyl)-1,2,4-oxadiazol-5(4H)-one according to general procedure W. The outcome was dissolved in EtOAc (100 mL) and a mixture of water (10 mL) and formic acid (5 mL) was added. This reaction mixture was slowly rota-evaporated at 40 °C to afford aldehyde **4.81** (1.22 g, 67%). R_f = 0.46 (3:1 EtOAc:Hex + 0.1% FA, visualization by UV); ¹H NMR (400 MHz, DMSO-*d*₆) δ 8.00 - 8.13 (m, 4H), 10.10 (s, 1H), 13.17 ppm (s, 1H); ¹³C NMR (101 MHz, DMSO-*d*₆) δ 127.28, 128.76, 130.59, 138.79, 157.28, 160.32, 193.11 ppm; UPLC-MS *m/z*: 189.1 [M-H]⁻.

(Z)-N'-Hydroxy-2,2-dimethoxyacetimidamide (4.85)

Carbonitrile **4.82** (1.88 g, 18.59 mmol) was used for the synthesis of amidoxime **4.85** (1.83 g, 73%) according to general procedure V. R_f = 0.40 (100% EtOAc, visualization by KMnO₄); ¹H NMR (400 MHz, CDCl₃) δ 3.40 (s, 6H), 4.66 (s, 1H), 4.77 - 4.96 (s br, 2H), 7.43 - 7.92 ppm (s br, 1H); ¹³C NMR (101 MHz, CDCl₃) δ 54.34, 100.46, 150.73 ppm.

3-(Dimethoxymethyl)-1,2,4-oxadiazol-5(4H)-one (4.88)

Amidoxime **4.85** (1.83 g, 13.64 mmol) was used for the synthesis of 1,2,4-oxadiazol-5-one **4.88** (1.90 g, 87%) according to general procedure W. $R_f = 0.42$ (1:1 EtOAc:Hex+0.1% FA, visualization by KMnO_4); $^1\text{H NMR}$ (400 MHz, CDCl_3) δ 3.50 (s, 6H), 5.29 (s, 1H), 10.17 ppm (s, 1H); $^{13}\text{C NMR}$ (101 MHz, CDCl_3) δ 54.64, 96.06, 156.21, 160.09 ppm; UPLC-MS m/z : 159.3 [M-H] $^-$.

5-Oxo-4,5-dihydro-1,2,4-oxadiazole-3-carbaldehyde (4.91)

Acetal **4.88** (4 g, 22.57 mmol) was used for the synthesis of aldehyde **91** (150 mg, >99%) according to general procedure X. $^1\text{H NMR}$ (400 MHz, D_2O) δ 5.90 ppm (s, 1H); $^1\text{H NMR}$ (400 MHz, $\text{DMSO-}d_6$) δ 5.66 (s, 2H), 12.38 ppm (s, 2H); $^{13}\text{C NMR}$ (101 MHz, D_2O) δ 82.90, 160.40, 161.48 ppm; $^{13}\text{C NMR}$ (101 MHz, $\text{DMSO-}d_6$) δ 83.60, 160.20, 161.59 ppm; UPLC-MS m/z : 113.2 [M-H] $^-$.

(Z)-N'-Hydroxy-3,3-dimethoxypropanimidamide (4.86)

Carbonitrile **4.83** (2 g, 17.37 mmol) was used for the synthesis of amidoxime **4.86** (2.18 g, 85%) according to general procedure V. $R_f = 0.36$ (95:5 EtOAc:MeOH, visualization by KMnO_4); $^1\text{H NMR}$ (400 MHz, CDCl_3) δ 2.46 (d, $J = 5.2$ Hz, 2H), 3.40 (s, 6H), 4.54 (t, $J = 5.2$ Hz, 1H), 5.00 (s, 2H), 6.67 ppm (s, 1H); $^{13}\text{C NMR}$ (101 MHz, CDCl_3) δ 34.86, 53.95, 103.20, 151.35 ppm.

3-(2,2-Dimethoxyethyl)-1,2,4-oxadiazol-5(4H)-one (4.89)

Amidoxime **4.86** (2.09 g, 14.11 mmol) was used for the synthesis of 1,2,4-oxadiazol-5-one **4.89** (2.26 g, 94%) according to general procedure W. $R_f = 0.42$ (3:1 EtOAc:Hex + 0.1% FA, visualization by KMnO_4); $^1\text{H NMR}$ (400 MHz, CDCl_3) δ 2.91 (d, $J = 4.6$ Hz, 2H), 3.45 (s, 6H), 3.72 (s, 1H), 4.64 (t, $J = 4.6$ Hz, 1H), 9.88 ppm (s, 1H); $^{13}\text{C NMR}$ (101 MHz, CDCl_3) δ 29.72, 54.75, 101.37, 155.55, 160.45 ppm; UPLC-MS m/z : 173.3 [M-H] $^-$.

2-(5-Oxo-4,5-dihydro-1,2,4-oxadiazol-3-yl)acetaldehyde (4.92)

Acetal **4.89** (0.5 g, 2.87 mmol) was used for the synthesis of aldehyde **4.92** (61.8 mg, 17%) according to general procedure X. $^1\text{H NMR}$ (400 MHz, $\text{MeOD-}d_4$) δ 2.81 (d, $J = 5.2$ Hz, 2H), 4.86 ppm (t, $J = 5.2$ Hz, 1H); $^{13}\text{C NMR}$ (101 MHz, $\text{MeOD-}d_4$) δ 32.74, 94.47, 156.52, 160.82 ppm; UPLC-MS m/z : 127.2 [M-H] $^-$.

(Z)-N'-Hydroxy-4,4-dimethoxybutanimidamide (4.87)

Carbonitrile **4.84** (1 g, 7.74 mmol) was used for the synthesis of amidoxime **4.87** (0.92 g, 73%) according to general procedure V. $R_f = 0.2$ (100% EtOAc, visualization by KMnO_4); $^1\text{H NMR}$ (400 MHz, CDCl_3) δ 1.84 - 1.93 (m, 2H), 2.22 (t, $J = 7.6$ Hz, 2H), 3.35 (s, 6H), 4.42 (t, $J = 5.6$ Hz, 1H), 4.75 (s, 2H), 7.91 ppm

(s, 1H); ^{13}C NMR (101 MHz, CDCl_3) δ 26.22, 29.56, 53.26, 103.84, 153.70 ppm; UPLC-MS m/z : 163.3 $[\text{M}+\text{H}]^+$.

3-(5-Oxo-4,5-dihydro-1,2,4-oxadiazol-3-yl)propanal (4.93)

Amidoxime **4.87** (910 mg, 5.61 mmol) was used for the synthesis of 1,2,4-oxadiazol-5-one **4.90** according to general procedure W. Subsequently, flash chromatography was performed (Hex:EtOAc + 0.5% FA). After concentrating *in vacuo* at 40 °C full deprotection of the acetal occurred to afford aldehyde **4.93** (580 mg, 72%). R_f = 0.3 (3:1 EtOAc:Hex + FA, visualization by KMnO_4); ^1H NMR (400 MHz, CDCl_3) δ 2.89 (t, J = 6.5 Hz, 2H), 3.03 (t, J = 6.5 Hz, 2H), 9.64 (s, 1H), 9.86 ppm (s, 1H); ^{13}C NMR (101 MHz, CDCl_3) δ 17.91, 39.45, 157.68, 160.03, 162.97, 200.09 ppm; UPLC-MS m/z : 141.3 $[\text{M}-\text{H}]^-$.

(5S,8S,11S)-2-(trimethylsilyl)ethyl 11-cyano-5-isopropyl-8-methyl-3,6,9-trioxo-1-phenyl-2-oxa-4,7,10-triazatridecan-13-oate (4.96)

Fmoc-protected amine **4.95** was dissolved in 1 mL DMF and 1,8-diazabicyclo[5.4.0]undec-7-ene (0.034 mL, 0.229 mmol) was added. This reaction mixture was left stirring 10 min. Parallel, carboxylic acid **4.94** (0.074 g, 0.229 mmol) was dissolved in DMF (1 mL) and set at 0 °C. To this solution was added HATU (0.105 g, 0.275 mmol) and also left stirring for 10 min. After this period *N,N*-diisopropylethylamine (0.050 mL, 0.286 mmol) was added to the first solution, followed by adding this solution to the second. The reaction mixture was allowed to warm up to room temperature and left stirring 2 h, after which water (10 mL) was added. Extraction was done with EtOAc (2 x 12 mL). The organic layers were combined and extracted with 1 M HCl (10 mL) and brine (10 mL) and dried over Na_2SO_4 . The volatiles were removed and flash chromatography was done (heptane:EtOAc), to yield protected carboxylic acid (0.10 g) as a white solid. This crude product was dissolved in THF (2.5 mL) and set at 0 °C. Tetrabutylammonium fluoride (1 M in THF, 0.212 mmol) was added and the reaction mixture was left stirring 4 h at room temperature. Additional TBAF (100 μL) was added and the mixture was left stirring overnight. The reaction mixture was diluted with EtOAc (10 mL), washed with 0.5 N HCl (2 x 10 mL), dried (Na_2SO_4) and concentrated *in vacuo* to give a yellow oil. *Preparative LC is still required to obtain pure compound 4.96.*

(S)-tert-Butyl 4-amino-2-((tert-butoxycarbonyl)amino)-4-oxobutanoate (4.99)

(S)-tert-Butyl 2,4-diamino-4-oxobutanoate hydrochloride (**4.97**, 4.98 g, 22.16 mmol), di-*t*-butyldicarbonate (5.80 g, 26.6 mmol), and potassium carbonate (6.13 g, 44.3 mmol) were dissolved in dioxane:water (1:1, 60 mL). The solution was stirred at room temperature for 3 h. Next, the formed precipitate was filtered, washed with a little water and the volatiles were evaporated. The filtrate was extracted EtOAc (3 times). The solid was redissolved in EtOAc (200 mL) and washed with water (2 x

150 mL). The organic phases were combined, dried with anhydrous Na_2SO_4 and evaporated under reduced pressure. The extract was joined with the solid to give Boc-protected **4.99** (6.24 g, 98 %) as a white solid. ^1H NMR (400 MHz, acetone- d_6) δ 1.41 (s, 9H), 1.43 (s, 9H), 2.69 (ddd, $J = 20.5, 15.7, 5.4$ Hz, 2H), 4.31 (dt, $J = 8.9, 5.6$ Hz, 1H), 6.12 (d, $J = 8.4$ Hz, 1H), 6.65 (d, $J = 221.4$ Hz, 2H); UPLC-MS m/z : 311.2 $[\text{M}+\text{Na}]^+$.

(S)-tert-Butyl 2-((tert-butoxycarbonyl)amino)-3-cyanopropanoate (4.101)

(S)-tert-Butyl 4-amino-2-((tert-butoxycarbonyl)amino)-4-oxobutanoate (**4.99**, 5.96 g, 20.67 mmol) was dissolved directly in 1,4-dioxane (345 mL) containing pyridine (5.51 mL, 68.2 mmol), and the solution was cooled in ice. Trifluoroacetic anhydride (4.15 mL, 22.74 mmol) was added dropwise over 25 min at 0 °C. The mixture was stirred for 1 h at 0 °C, and then stirred 4 h at room temperature. A yellow solution was obtained. A few chips of ice were added and the reaction mixture was concentrated under reduced pressure to approximately half of the initial volume. Next, ethyl acetate (150 mL) was added and the organic layer was washed with brine, dried with anhydrous Na_2SO_4 , and evaporated under reduced pressure to give the crude product as a yellow oil. The crude product was purified by flash chromatography (heptane:EtOAc) to give carbonitrile **4.101** (5.23 g, 94%) as a white solid. $R_f = 0.23$ (1:4 EtOAc:heptane, visualization by ninhydrin and PMA); ^1H NMR (400 MHz, CDCl_3) δ 1.42 (s, 9H), 1.48 (s, 9H), 2.85 (dd, $J = 16.8, 4.6$ Hz, 1H), 2.93 (dd, $J = 16.8, 5.3$ Hz, 1H), 4.34 (dd, $J = 11.3, 5.1$ Hz, 1H), 5.44 ppm (d, $J = 6.0$ Hz, 1H); UPLC-MS m/z : 293.1 $[\text{M}+\text{Na}]^+$.

(S)-tert-Butyl 2-((tert-butoxycarbonyl)amino)-3-(5-oxo-4,5-dihydro-1,2,4-oxadiazol-3-yl)propanoate (4.103)

Hydroxylammonium chloride (1.381 g, 19.88 mmol) was dissolved in MeOH (25 mL), sodium bicarbonate (1.670 g, 19.88 mmol) was added and the mixture was stirred for 20 min at room temperature. Next, carbonitrile **4.101** in MeOH (10 mL) was added, the mixture was refluxed for 26 h and then cooled to room temperature. Formed salt was filtered and removed. The filtrate was concentrated under reduced pressure. Acetone was added and the mixture was filtered again. The filtrate was concentrated under reduced pressure to give the crude product as a green oil. The crude product was purified by flash chromatography (heptane:EtOAc). Hydroxamic acid was obtained as a white solid. $R_f = 0.45$ (EtOAc:heptane 3:1, visualization by ninhydrin); ^1H NMR (400 MHz, CDCl_3) δ 1.43 (s, 9H), 1.45 (s, 9H), 2.60 (d, $J = 5.5$ Hz, 2H), 4.38 (d, $J = 6.5$ Hz, 1H), 4.79 (s, 2H), 5.59 ppm (d, $J = 7.8$ Hz, 1H); UPLC-MS m/z : 304.2 $[\text{M}+\text{H}]^+$. The hydroxamic acid was dissolved in 1,4-dioxane (50 mL) and 1,8-diazabicyclo[5.4.0]undec-7-ene (2.021 mL, 13.53 mmol) and 1,1'-carbonyldiimidazole (2.393 g, 14.76 mmol) were added. The mixture was refluxed for 6 h at reflux. After 5 h, another 500 mg of CDI was added to make the reaction proceed. The mixture was stirred for an additional hour. An orange

solution was obtained. The reaction mixture was concentrated *in vacuo*. 1 M HCl (50 mL) was added and extraction was done with EtOAc (3 x 40 mL). The organic layers were collected, washed with brine (50 mL), dried over anhydrous Na₂SO₄ and concentrated under reduced pressure to give the crude product as a yellow solid. The crude product was purified by flash chromatography (heptane:EtOAc) to afford oxadiazolone **4.103** (3.64 g, 58%) as a white solid. *R_f* = 0.43 (EtOAc:Heptane 1:1, visualization by ninhydrin); ¹H NMR (400 MHz, CDCl₃) δ 1.44 (s, 9H), 1.47 (s, 9H), 2.95 (dd, *J* = 15.4, 6.1 Hz, 1H), 3.08 (dd, *J* = 15.4, 6.1 Hz, 1H), 4.40 (dd, *J* = 12.6, 6.2 Hz, 1H), 5.55 (s, 1H), 10.23 ppm (s, 1H); UPLC-MS *m/z*: 328.2 [M-H].

(S)-2-((tert-Butoxycarbonyl)amino)-3-(5-oxo-4,5-dihydro-1,2,4-oxadiazol-3-yl)propanoic acid (4.105)

Oxadiazolone **4.103** (3.16 g, 9.59 mmol) was dissolved in DCM (30 mL) and trifluoroacetic acid (30 mL, 9.59 mmol) was added. The mixture was left stirring under N₂ atmosphere at room temperature for 1.5 h. The reaction mixture was evaporated under reduced pressure (after addition of toluene). The crude product (1.97 g, 6.86 mmol) in 1,4-dioxane:water mixture (1:1, 40 mL) was added triethylamine (2 mL, 14.41 mmol), followed by di-*t*-butyldicarbonate (1.647 g, 7.55 mmol) in small fractions. The solution was left stirring at room temperature. After 3 hours, additional di-*t*-butylcarbonate (500 mg) and triethylamine (1 mL) were added for the reaction to proceed. After 5 hours, the reaction was complete. After evaporation of the volatiles, the mixture was dissolved in water (30 mL) and acidified with 2M HCl solution until pH 2-3 and then extracted with EtOAc (3 x 30 mL). The organic phases were combined, dried with anhydrous Na₂SO₄ and evaporated under reduced pressure to give the crude product. Reversed phase flash chromatography was performed (water:MeOH) to yield carboxylic acid **4.105** (1.48 g, 56% yield) as a transparent oil. ¹H NMR (400 MHz, acetone-*d*₆) δ 1.39 (s, 9H); 3.11 (ddd, *J* = 24.1, 15.2, 7.0 Hz, 2H), 4.60 (td, *J* = 8.7, 5.3 Hz, 1H), 6.44 ppm (d, *J* = 8.2 Hz, 1H); ¹³C NMR (101 MHz, MeOD-*d*₄) δ 28.61, 29.30, 52.24, 80.86, 157.63, 158.57, 162.20, 173.86 ppm; UPLC-MS *m/z*: 272.1 [M-H].

(S)-tert-Butyl (1-cyano-2-(5-oxo-4,5-dihydro-1,2,4-oxadiazol-3-yl)ethyl)carbamate (4.107)

To a solution of carboxylic acid **4.105** (0.300 g, 1.098 mmol) in THF (3 mL) at -10 °C in a salt/ice/water bath was added 4-methylmorpholine (0.133 mL, 1.208 mmol), followed by dropwise addition of isobutyl chloroformate (0.157 mL, 1.208 mmol) over 20 min. After 30 min of stirring, the mixture was cooled down to -10°C, and ammonium hydroxide (3 mL, 21.40 mmol) solution (25% in water) was added portionwise over 5 min. The reaction was allowed to warm up to room temperature and stirred overnight. Afterwards the solvent was evaporated. The remaining solution was diluted with water (10 mL), acidified with a 2 M HCl solution until pH 2-3 and extracted with EtOAc (3 x 10 mL). Drying over anhydrous Na₂SO₄ and removal of solvents under vacuum yielded the intermediate amide. *R_f* = 0.47

(1:1 EtOAc:heptane, visualization by PMA); UPLC-MS m/z : 271.2 [M-H]⁻. The amide was dissolved in 1,4-dioxane (18 mL) containing pyridine (0.292 mL, 3.62 mmol), and the solution was cooled in ice. Trifluoroacetic anhydride (0.220 mL, 1.208 mmol) was added dropwise over 25 min. The mixture was stirred for 1 h at 0 °C, and then kept overnight at room temperature. A few chips of ice were added, followed by ethyl acetate (10 mL). The organic layer was washed with brine, dried with anhydrous Na₂SO₄, and evaporated under reduced pressure to give the crude product as a brown oil. The crude product was purified by flash chromatography (heptane:EtOAc) to yield carbonitrile **4.107** (0.12 g, 43% yield) as a yellow oil. R_f = 0.27 (EtOAc:heptane 1:1, visualization by ninhydrin); ¹H NMR (400 MHz, CDCl₃) δ 1.46 (s, J = 8.7 Hz, 9H), 3.20 (d, J = 6.4 Hz, 2H), 5.02 (s, 1H), 5.85 (s, 1H), 10.35 ppm (s, 1H); UPLC-MS m/z : 507.2 [2M-H]⁻.

(S)-1-Cyano-2-(5-oxo-4,5-dihydro-1,2,4-oxadiazol-3-yl)ethanaminium 2,2,2-trifluoroacetate (4.109)

Boc-protected amine **4.107** (0.12 g, 0.472 mmol) was dissolved in DCM (3 mL) and the solution was cooled to 0 °C. Trifluoroacetic acid (1 mL, 13.06 mmol) was added, and the solution was stirred for 40 min at 0 °C. After completion of the reaction, toluene was added and the mixture was evaporated under reduced pressure to afford amine **4.109** as a solid (150 mg, quant.), which was used without further purification. UPLC-MS m/z : 188.1 [M+MeOH+H]⁺.

(S)-1-((S)-2-(4-Amino-3-chlorobenzamido)-3,3-dimethylbutanoyl)-N-((S)-1-cyano-2-(5-oxo-4,5-dihydro-1,2,4-oxadiazol-3-yl)ethyl)pyrrolidine-2-carboxamide (4.107)

To a solution of amine **4.109** (0.1 g, 0.373 mmol) in DMF (1 mL) were added carboxylic acid **4.111** (0.157 g, 0.410 mmol), HATU (0.156 g, 0.410 mmol) and *N,N*-di-isopropylethylamine (0.143 mL, 0.820 mmol), and the mixture was stirred 2 h under an N₂ atmosphere. Afterwards, the reaction mixture was diluted with EtOAc (50 mL) and washed with 0.5 M KHSO₄ (2 x 40 mL), 10% NaHCO₃ (2 x 40 mL) and brine (40 mL). The pH of the NaHCO₃ aqueous phase was decreased to 2 by adding dropwise concentrated HCl-solution. Backextraction was done with EtOAc (2 x 60 mL) and all organic layers were combined, dried with anhydrous Na₂SO₄ and evaporated under reduced pressure. The residue (a yellow oil) was washed with diethyl ether (3 times) to give crude product as a light brown solid. Further purification by preparative HPLC yielded final compound **4.113** (39,4 mg, 20 %), obtained as a white powder after lyophilization. R_f = 0.31 (3:1 EtOAc:heptane, visualization by UV); ¹H NMR (400 MHz, CDCl₃) δ 0.95 - 1.13 (m, 11H), 1.95 (d, J = 6.5 Hz, 2H), 2.13 (d, J = 3.1 Hz, 2H), 2.91 - 3.16 (m, 2H), 3.67 - 4.09 (m, 2H), 6.70 (d, J = 8.2 Hz, 1H), 5.14 - 5.26 (m, 1H), 4.81 (d, J = 9.1 Hz, 1H), 4.19 (s, 1H), 6.83 - 6.99 (m, 1H), 7.47 (d, J = 7.5 Hz, 1H), 7.71 (s, 1H), 8.05 (d, J = 7.1 Hz, 1H), 11.37 ppm (s, 1H); ¹³C NMR (101 MHz, CDCl₃) δ 25.63, 26.56, 26.70, 28.41, 29.21, 36.19, 39.05, 49.26, 57.81, 61.32, 114.98, 116.17, 118.73, 123.81,

127.00, 129.21, 146.32, 154.38, 160.35, 166.77, 171.48, 171.74 ppm; HRMS (ESI): calcd for $C_{23}H_{29}N_7O_5Cl^+$ $[M+H]^+$: 518.1913, found: 518.1928.

(S)-tert-Butyl 5-amino-2-((tert-butoxycarbonyl)amino)-5-oxopentanoate (4.100)

Di-tert-butyl carbonate (3.72 g, 17.05) L-glutamine tert-butyl hydrochloride (**4.98**, 3.7 g, 15.50 mmol), $NaHCO_3$ (2.99 g, 35.6 mmol) and THF (73 mL) were used in a similar procedure as for the synthesis of **4.99**. Boc-protected **4.100** was obtained as a white solid (4.72 g, >99%). $R_f = 0.42$ (1:1 Hept:EtOAc, visualization by ninhydrin); 1H NMR (400 MHz, $CDCl_3$) δ 1.43 (s, 9H), 1.46 (s, 9H), 1.77 - 1.91 (m, 2H), 2.08 - 2.20 (m, 1H), 2.22 - 2.38 (m, 2H), 4.10 - 4.24 (m, 1H), 5.30 (d, $J = 7.6$ Hz, 1H), 5.82 (d, $J = 98.9$ Hz, 1H), 6.40 ppm (s, 1H); UPLC-MS m/z : 325.2 $[M+Na]^+$.

(S)-tert-Butyl 2-((tert-butoxycarbonyl)amino)-4-cyanobutanoate (4.102)

Amide **4.100**, trifluoroacetic anhydride (3.07 mL, 16.81 mmol), pyridine (4.07 mL, 50.4 mmol) and 1,4-dioxane (260 mL) were used in a similar procedure as for the synthesis of **4.101**. Carbonitrile **4.102** was obtained (2.09 g, 47.9%). 1H NMR (400 MHz, $CDCl_3$) δ 1.43 (s, 9H), 1.47 (s, 9H), 1.96 (m, 3H), 2.33 - 2.58 (m, 2H), 4.22 ppm (s, 1H); UPLC-MS m/z : 307.1 $[M+Na]^+$.

(S)-tert-Butyl 2-((tert-butoxycarbonyl)amino)-4-(5-oxo-4,5-dihydro-1,2,4-oxadiazol-3-yl)butanoate (4.104)

Hydroxylammonium chloride (0.664 g, 9.56 mmol), sodium bicarbonate (0.803 g, 9.56 mmol), (S)-tert-butyl 2-((tert-butoxycarbonyl)amino)-4-cyanobutanoate (**4.102**, 2.09 g, 7.35 mmol) and MeOH (30 mL) were used in a similar procedure as for the first part of the synthesis of **4.103**. The hydroxamic acid intermediate was obtained. $R_f = 0.7$ (1:1 EtOAc:heptane, visualization by ninhydrin); 1H NMR (400 MHz, $CDCl_3$) δ 1.39 - 1.59 (m, 18H), 2.17 (m, 2H), 2.38 (m, 2H), 4.12 ppm (q, $J = 7.2$ Hz, 1H); UPLC-MS m/z : 318.2 $[M+H]^+$. The intermediate (1.48 g, 4.66 mmol), 1,8-diazabicyclo[5.4.0]undec-7-ene (0.766 mL, 5.13 mmol), 1,1'-carbonyldiimidazole (0.907 g, 5.60 mmol) and 1,4-dioxane (30 mL) were used in a similar procedure as for the second part of the synthesis of **4.103**. Oxadiazolone **4.104** was obtained as an oil (1.52 g, 46%). $R_f = 0.44$ (1:1EtOAc:heptane, visualization by ninhydrin). 1H NMR (400 MHz, $CDCl_3$) δ 1.40 - 1.54 (m, 18H), 2.07 - 2.17 (m, 2H), 2.44 - 2.58 (m, 1H), 2.77 (ddd, $J = 14.9, 5.4, 3.5$ Hz, 1H), 5.47 (d, $J = 7.9$ Hz, 1H), 10.93 ppm (s, 1H); UPLC-MS m/z : 342.2 $[M-H]^-$.

(S)-2-((tert-Butoxycarbonyl)amino)-4-(5-oxo-4,5-dihydro-1,2,4-oxadiazol-3-yl)butanoic acid (4.106)

Compound **4.104** (1.23 g, 3.58 mmol), trifluoroacetic acid (10 mL) and DCM (10 mL) were used in a similar procedure as for the first part of the synthesis of **4.105**. Fully deprotected intermediate was obtained as a brown solid. 1H NMR (400 MHz, $DMSO-d_6$) δ 1.97 - 2.26 (m, 2H), 2.55 - 2.81 (m, 2H), 4.01

(s, 1H), 8.34 ppm (s, 2H); UPLC-MS m/z : 188.1 [M+H]⁺. The intermediate, triethylamine (1.061 mL, 7.64 mmol), di-*t*-butyldicarbonate (0.917 g, 4.20 mmol), 1,4-dioxane:water (1:1, 38 mL) were used in a similar procedure as for the second part of the synthesis of **4.105**. Carboxylic acid **4.106** was obtained as a solid (0.72 g, 69%). ¹H NMR (400 MHz, DMSO-*d*₆) δ 1.31 - 1.41 (m, 9H), 1.78 - 1.91 (m, 1H), 2.00 - 2.10 (m, 1H), 2.64 - 2.80 (m, 1H), 3.99 - 4.07 (m, 1H), 7.20 (dd, $J = 19.7, 8.1$ Hz, 1H), 8.36 (s, 1H), 12.19 (s, 1H). UPLC-MS m/z : 286.1 [M-H]⁻.

(S)-tert-Butyl (1-amino-1-oxo-4-(5-oxo-4,5-dihydro-1,2,4-oxadiazol-3-yl)butan-2-yl)carbamate (4.108)

Carboxylic acid **4.106** (0.62 g, 2.158 mmol), 4-methylmorpholine (0.285 mL, 2.59 mmol), isobutyl chloroformate (0.336 mL, 2.59 mmol), ammonium hydroxide (6 mL, 42.8 mmol) and THF (5.5 mL) were used in a similar procedure as for the first part of the synthesis of **4.107**. Intermediate amide was obtained as a yellow oil. ¹H NMR (400 MHz, DMSO-*d*₆) δ 0.80 - 0.90 (m, 2H), 1.38 (s, 9H), 1.74 - 1.87 (m, 1H), 1.95 (dd, $J = 13.1, 5.8$ Hz, 1H), 3.86 - 3.97 (m, 1H), 6.90 (d, $J = 8.2$ Hz, 1H), 7.08 (s, 2H), 12.15 ppm (s, 1H); UPLC-MS m/z : 285.1 [M-H]⁻. The intermediate, pyridine (0.307 mL, 3.80 mmol), trifluoroacetic anhydride (0.231 mL, 1.268 mmol) and 1,4-dioxane (20 mL) were used in a similar procedure as for the second part of the synthesis of **4.107**. Carbonitrile **4.108** was obtained as a white solid (0.110 g, 19%). $R_f = 0.35$ (1:1 EtOAc:heptane, visualization by ninhydrin); ¹H NMR (400 MHz, acetone-*d*₆) δ 0.91 (d, $J = 6.7$ Hz, 1H), 1.43 (s, 9H), 2.25 - 2.39 (m, 3H), 4.69 - 4.83 (m, 1H), 6.99 ppm (s, 1H); UPLC-MS m/z : 267.1 [M-H]⁻.

(S)-1-Cyano-3-(5-oxo-4,5-dihydro-1,2,4-oxadiazol-3-yl)propan-1-aminium 2,2,2-trifluoroacetate (4.110)

Carbonitrile **4.108** (80 mg, 0.298 mmol), trifluoroacetic acid (1 mL) and DCM (1 mL) were used in a similar procedure as for the synthesis of **4.109**. The amine **4.110** was obtained as a solid (0.110 g, quant.); UPLC-MS m/z : 169.1 [M+H]⁺.

(S)-1-((S)-2-(4-Amino-3-chlorobenzamido)-3,3-dimethylbutanoyl)-N-((S)-1-cyano-3-(5-oxo-4,5-dihydro-1,2,4-oxadiazol-3-yl)propyl)pyrrolidine-2-carboxamide (4.114)

Amine **4.110** (84 mg, 0.298 mmol), carboxylic acid **4.111** (0.125 g, 0.327 mmol), HATU (0.125 g, 0.327 mmol), *N,N*-di-isopropylethylamine (0.114 mL, 0.655 mmol) and DMF (1.5 mL) were used in a similar procedure as for the synthesis of **4.113**. Final compound **4.114** was obtained as white powder (6.4 mg, 4%). ¹H NMR: (400 MHz, CDCl₃) δ 0.88 - 0.96 (m, 1H), 1.04 - 1.13 (m, 9H), 1.88 - 2.25 (m, 7H), 2.62 (ddd, $J = 14.4, 11.0, 6.5$ Hz, 1H), 2.77 (dt, $J = 16.7, 8.5$ Hz, 1H), 3.66 - 3.77 (m, 1H), 4.07 (dd, $J = 11.9, 5.1$ Hz, 1H), 4.19 (t, $J = 7.3$ Hz, 1H), 4.73 (dd, $J = 19.1, 8.4$ Hz, 1H), 6.63 - 6.73 (m, 1H), 5.02 - 5.11 (m, 1H), 6.86

(dd, $J = 17.4, 8.1$ Hz, 1H), 7.59 (ddd, $J = 19.2, 8.4, 2.0$ Hz, 1H), 7.86 - 7.73 (m, 2H), 11.80 ppm (s, 1H); ^{13}C NMR (101 MHz, CDCl_3) δ 20.11, 25.79, 26.72, 29.19, 29.37, 35.61, 39.83, 48.99, 58.61, 61.91, 114.86, 117.20, 118.71, 122.85, 127.10, 129.33, 146.76, 158.27, 160.53, 166.85, 172.01, 172.12 ppm; HRMS (ESI): calcd for $\text{C}_{24}\text{H}_{31}\text{N}_7\text{O}_5\text{Cl}^+$ $[\text{M}+\text{H}]^+$: 532.2070, found: 532.2068.

Benzyl ((S)-1-(((S)-1-(((S)-1-cyano-2-(5-oxo-4,5-dihydro-1,2,4-oxadiazol-3-yl)ethyl)amino)-1-oxopropan-2-yl)amino)-3-methyl-1-oxobutan-2-yl)carbamate (4.115)

Amine **4.109** (0.1 g, 0.373 mmol), Z-VA-OH (**4.112**, 0.132 g, 0.410 mmol), HATU (0.156 g, 0.410 mmol), *N,N*-di-isopropylethylamine (0.143 mL, 0.820 mmol) and DMF (1 mL) were used in a similar procedure as for the synthesis of product **4.113**. Final compound **4.115** was afforded as a white powder (40.5 mg, 24%). ^1H NMR (400 MHz, acetone- d_6) δ 0.97 (dd, $J = 10.4, 6.9$ Hz, 6H); 1.37 (d, $J = 7.1$ Hz, 3H), 2.10 - 2.23 (m, 1H), 3.13 - 3.29 (m, 2H), 4.05 (t, $J = 5.7$ Hz, 1H), 4.34 (dt, $J = 13.0, 6.6$ Hz, 1H), 5.09 (q, $J = 12.6$ Hz, 2H), 5.34 (dd, $J = 13.5, 7.3$ Hz, 1H), 6.61 (d, $J = 7.3$ Hz, 1H), 7.25 - 7.45 (m, 5H), 8.02 (d, $J = 5.0$ Hz, 1H), 8.38 ppm (d, $J = 7.8$ Hz, 1H); ^{13}C NMR (101 MHz, acetone- d_6) δ 17.01, 18.32, 19.58, 29.26, 31.55, 39.00, 50.39, 61.25, 66.98, 117.78, 128.63, 128.69, 129.22, 138.01, 157.62, 173.10, 206.00, 206.40, 206.59 ppm; HRMS (ESI): calcd for $\text{C}_{21}\text{H}_{27}\text{N}_6\text{O}_6^+$ $[\text{M}+\text{H}]^+$: 459.1987, found: 459.1996.

4.6.2 Biochemical assays

Inhibitor screening

In a 96 well plate (half-area, polystyrene, transparent) caspase-1, -3 or -4 and inhibitor (25 μM - 500 μM) were incubated for 15 minutes at 37 $^\circ\text{C}$ before substrate was added. Hydrolysis was monitored at 37 $^\circ\text{C}$ for 5 minutes. Assays were run in two technical duplicates (except for the results from **Table 4.2**). In each series 2 blank methods were added (caspase + substrate + DMSO). Total volume per well was 100 μL . The concentration of DMSO in the assays was 5% v/v. Substrate was Ac-WEHD-pNA in case of caspase-1 and -4, and Ac-DEVD-pNA in case of caspase-3, at a concentration of 200 μM . Substrates and enzymes were purchased at ENZO life sciences. Buffer composition was 50 mM HEPES, pH 7.4, 0.1% CHAPS, 10 mM KCl, 50 mM sucrose, 1 mM MgCl_2 , 10 mM DTT (added just before use) or 0.1 M HEPES, pH 7.0, 10% Glycerol (v/v), 0.1% CHAPS (m/m), 100mM NaCl, 1mM EDTA and 10 mM DTT (added just before use). SynergyMX, a fluorescent microplate reader (Bio-Tek) was used to measure UV-absorbance after caspase activation at 405 nm. Percentage of inhibition was calculated according to the formula:

$$\% \text{ of Inhibition} = \left(1 - \frac{v}{v_{pNA}} \right) * 100\%$$

where v is the rate of substrate turnover in solution with buffer and v_{pNA} is the rate of the substrate turnover without inhibitor.

Determination of the type of inhibition

The rate of the substrate cleavage was determined for inhibitor **4.6** at a concentration of 150 μ M with substrate concentrations varying from 100 μ M to 2 mM in a caspase-4 assay. To compare, a blank serie was added, in which DMSO without inhibitor was used. Assays were run in two technical duplicates. Buffer composition was 20 mM PIPES, pH 7.5, 100 mM NaCl, 1 mM EDTA, 0.1% (w/v) CHAPS, 10% sucrose and DTT (added just before use). Other conditions were identical to the inhibitor screening assay.

Substrate screening

In a 96 well plate (black, half area), caspase-4 (1-50 units) and substrate (25 μ M - 1000 μ M) were incubated at 37°C and fluorescence was measured for 30 minutes in 30 seconds intervals. Excitation and emission wavelengths were 380 nm and 442 nm respectively. Further assay conditions were similar as in the inhibitor screening (*cf. supra*).

Biochemical evaluation: IC₅₀ determination

In a 96 well plate (black, half area), caspases and inhibitors were incubated for 15 minutes at 37 °C before substrate hydrolysis was monitored at 37 °C for 30 minutes in 2-minute intervals. Assays were run in two technical duplicates and all experiments were performed in at least two independent repeats. Total volume per well was 50 μ L. A positive control for caspase activity was included in all of the assays (caspase + substrate + DMSO). Substrates were Ac-WEHD-AMC for h casp-1,-4,-5; Ac-DEVD-AMC for h casp -3; Ac-IETD-AMC for h casp -8 and Ac-LEHD-AMC for h casp -9. All the assays were performed at 100 μ M substrate concentration. The outcome of at least 7 inhibitor concentrations (performed in duplicate) and a comparison with the blank made calculations of the IC₅₀ value possible. Buffer composition was 20 mM PIPES, 100 mM NaCl, 1 mM EDTA, 0.1% (w/v) CHAPS, 10% sucrose and adjusted till pH 7.5. DTT was added just before filling the wells to obtain a 10mM final concentration. SynergyMX, a fluorescent microplate reader (Bio-Tek) was used to measure fluorescence after caspase activation. Excitation and emission wavelengths for AMC substrates were 360 nm and 460 nm, respectively.

Determination of the pH

The pH was determined by a pH meter Education Line EL20 from Mettler Toledi.

4.6.3 Physicochemical profile

Chemical stability protocol

A 10 mM stock compound solution in DMSO was prepared. The stock solution was diluted to a 500 nM solution with the specific buffer. The mixture was gently shaken at 37 °C. At different time points (0 min - 30 min - 60 min - 120 min - 180 min - 360 min – 24 h) 100 µL was withdrawn which was analyzed with UPLC-MS/MS. Samples were prepared in duplicate and measured in triplicate. The percentage of parent compound remaining at each time point relative to the 0 min sample was then calculated from UPLC-MS/MS peak area ratios. A set of 5 dilutions (in the solution buffer) of the compound were prepared from a 10 µM solution to give final test concentrations between 31 nM and 500 nM. A calibration line was made to evaluate the accuracy of the test method and to calculate the concentration. 10 mM PBS buffer was used for pH 7.4 and 10 mM acetic acid buffer for pH 4.0.

Metabolic stability protocol

Liver microsomes (20 mg protein/mL), NADPH regenerating system solutions A & B and 5 mM stock compound solution (100% DMSO) were prepared. The reaction mixture finally contained 713 µL purified water, 200 µL 0.5 M potassium phosphate pH 7.4, 50 µL NADPH regenerating system solution A (BD Biosciences Cat. No. 451220), 10 µL NADPH regenerating system solution B (BD Biosciences Cat. No. 451200) and 2 µL of the compound stock solution (10 µM final concentration). The reaction mixture was warmed to 37 °C for 5 minutes and the reaction was initiated by addition of 25 µL of liver microsomes (0.5 mg protein/mL final concentration). At different time points (0 min – 15 min – 30 min – 60 min – 120 min – 240 min – 360 min – 24h), 20 µL was withdrawn and 80 µL cold acetonitrile was added on ice for 10 minutes. Then the mixtures were centrifuged at 13 000 rpm for 5 min at 4 °C. The supernatant was further diluted in 90 % water/acetonitrile. At each time point, the compound was analyzed using UPLC-MS/MS. The calculation of parent percentage and the calibration line were the same as in the chemical stability measurements. Verapamil was used as a positive control. Samples were prepared in duplicate and measured in triplicate.

References

1. F. Martinon and J. Tschopp, *Cell*, 2004, **117**, 561-574.
2. U. Fischer, R. U. Janicke and K. Schulze-Osthoff, *Cell Death Differ.*, 2003, **10**, 76-100.
3. P. Fuentes-Prior and G. S. Salvesen, *Biochem. J.*, 2004, **384**, 201-232.
4. C. Pop and G. S. Salvesen, *J. Biol. Chem.*, 2009, **284**, 21777-21781.
5. U. Fischer and K. Schulze-Osthoff, *Pharmacol. Rev.*, 2005, **57**, 187-215.
6. D. J. Fernandez and M. Lamkanfi, *Biol. Chem.*, 2015, **396**, 193-203.
7. S. Winkler and A. Rosen-Wolff, *Semin. Immunopathol.*, 2015, **37**, 419-427.
8. G. Sollberger, G. E. Strittmatter, M. Kistowska, L. E. French and H. D. Beer, *J. Immunol.*, 2012, **188**, 1992-2000.
9. F. Martinon, K. Burns and J. Tschopp, *Mol Cell*, 2002, **10**, 417-426.
10. S. Y. Wang, M. Miura, Y. K. Jung, H. Zhu, V. Gagliardini, L. F. Shi, A. H. Greenberg and J. Y. Yuan, *J. Biol. Chem.*, 1996, **271**, 20580-20587.
11. Y. Kajiwarra, T. Schiff, G. Voloudakis, M. A. G. Sosa, G. Elder, O. Bozdagi and J. D. Buxbaum, *J. Immunol.*, 2014, **193**, 335-343.
12. M. B. Boxer, A. M. Quinn, M. Shen, A. Jadhav, W. Leister, A. Simeonov, D. S. Auld and C. J. Thomas, *ChemMedChem*, 2010, **5**, 730-738.
13. W. Wannamaker, R. Davies, M. Namchuk, J. Pollard, P. Ford, G. Ku, C. Decker, P. Charifson, P. Weber, U. A. Germann, K. Kuida and J. C. Randle, *J. Pharmacol. Exp. Ther.*, 2007, **321**, 509-516.
14. T. A. Rano, T. Timkey, E. P. Peterson, J. Rotonda, D. W. Nicholson, J. W. Becker, K. T. Chapman and N. A. Thornberry, *Chem. Biol.*, 1997, **4**, 149-155.
15. M. Poreba, A. Strozyk, G. S. Salvesen and M. Drag, *Cold Spring Harbor Perspect. Biol.*, 2013, **5**, a008680.
16. M. Poreba, A. Szalek, P. Kasperkiewicz, W. Rut, G. S. Salvesen and M. Drag, *Chem. Rev.*, 2015, **115**, 12546-12629.
17. C. V. C. Prasad, C. P. Prouty, D. Hoyer, T. M. Ross, J. M. Salvino, M. Awad, T. L. Graybill, S. J. Schmidt, I. Kelly Osifo, R. E. Dolle, C. T. Helaszek, R. E. Miller and M. A. Ator, *Bioorg. Med. Chem. Lett.*, 1995, **5**, 315-318.
18. N. A. Meanwell, *J. Med. Chem.*, 2011, **54**, 2529-2591.
19. C. Ballatore, D. M. Huryn and A. B. Smith, *ChemMedChem*, 2013, **8**, 385-395.
20. Y. Okamoto, H. Anan, E. Nakai, K. Morihira, Y. Yonetoku, H. Kurihara, H. Sakashita, Y. Terai, M. Takeuchi, T. Shibamura and Y. Isomura, *Chem. Pharm. Bull.*, 1999, **47**, 11-21.
21. Y. Adriaenssens, D. J. Fernández, L. Vande Walle, F. Elvas, J. Joossens, A. M. Lambeir, K. Augustyns, M. Lamkanfi and P. Van der Veken, unpublished work.

22. R. Gladysz, Y. Adriaenssens, H. De Winter, J. Joossens, A. M. Lambeir, K. Augustyns and P. Van der Veken, *J. Med. Chem.*, 2015, **58**, 9238-9257.
23. R. Gladysz, M. Cleenewerck, J. Joossens, A. M. Lambeir, K. Augustyns and P. Van der Veken, *Chembiochem*, 2014, **15**, 2238-2247.
24. M. Cleenewerck, M. O. J. Grootaert, R. Gladysz, Y. Adriaenssens, R. Roelandt, J. Joossens, A.-M. Lambeir, G. R. Y. De Meyer, W. Declercq, K. Augustyns, W. Martinet and P. Van der Veken, *Eur. J. Med. Chem.*, 2016, **123**, 631-638.
25. W. J. L. Wood, A. W. Patterson, H. Tsuruoka, R. K. Jain and J. A. Ellman, *J. Am. Chem. Soc.*, 2005, **127**, 15521-15527.
26. R. Gladysz, A. M. Lambeir, J. Joossens, K. Augustyns and P. Van der Veken, *ChemMedChem*, 2016, **11**, 467-476.
27. M. Garcia-Calvo, E. P. Peterson, D. M. Rasper, J. P. Vaillancourt, R. Zamboni, D. W. Nicholson and N. A. Thornberry, *Cell Death Differ.*, 1999, **6**, 362-369.
28. A. Cornish-Bowden, *Fundamentals of Enzyme Kinetics, 4th Edition*, Wiley-Blackwell, 2012.
29. A. E. Moormann, J. L. Wang, K. E. Palmquist, M. A. Promo, J. S. Snyder, J. A. Scholten, M. A. Massa, J. A. Sikorski and R. K. Webber, *Tetrahedron*, 2004, **60**, 10907-10914.
30. K. Seio, T. Miyashita, K. Sato and M. Sekine, *Eur. J. Org. Chem.*, 2005, DOI: 10.1002/ejoc.200500520, 5163-5170.
31. M. H. Ghasemi, E. Kowsari and S. K. Hosseini, *Tetrahedron Lett.*, 2016, **57**, 387-391.
32. M. J. Romanowski, J. M. Scheer, T. O'Brien and R. S. McDowell, *Structure*, 2004, **12**, 1361-1371.
33. B. Benkova, V. Lozanov, I. P. Ivanov and V. Mitev, *Anal. Biochem.*, 2009, **394**, 68-74.
34. N. A. Pereira and Z. W. Song, *Biochem. Biophys. Res. Commun.*, 2008, **377**, 873-877.
35. J. C. R. Randle, M. W. Harding, G. Ku, M. Schonharting and R. Kurrle, *Expert Opin. Invest. Drugs*, 2001, **10**, 1207-1209.
36. J. H. Stack, K. Beaumont, P. D. Larsen, K. S. Straley, G. W. Henkel, J. C. R. Randle and H. M. Hoffman, *J. Immunol.*, 2005, **175**, 2630-2634.
37. M. Maroso, S. Balosso, T. Ravizza, V. Iori, C. I. Wright, J. French and A. Vezzani, *Neurotherapeutics*, 2011, **8**, 304-315.
38. G. Doitsh, N. L. K. Galloway, X. Geng, Z. Y. Yang, K. M. Monroe, O. Zepeda, P. W. Hunt, H. Hatano, S. Sowinski, I. Munoz-Arias and W. C. Greene, *Nature*, 2014, **505**, 509-+.
39. N. L. K. Galloway, G. Doitsh, K. M. Monroe, Z. Y. Yang, I. Munoz-Arias, D. N. Levy and W. C. Greene, *Cell Rep.*, 2015, **12**, 1555-1563.
40. Y. Zhang and Y. Zheng, *Clin. Exp. Rheumatol.*, 2016, **34**, 111-118.
41. Y. Kohara, K. Kubo, E. Imamiya, T. Wada, Y. Inada and T. Naka, *J. Med. Chem.*, 1996, **39**, 5228-5235.

42. Y. Kohara, E. Imamiya, K. Kubo, T. Wada, Y. Inada and T. Naka, *Bioorg. Med. Chem. Lett.*, 1995, **5**, 1903-1908.
43. J. Charton, R. Deprez-Poulain, N. Hennuyer, A. Tailleux, B. Staels and B. Deprez, *Bioorg. Med. Chem. Lett.*, 2009, **19**, 489-492.
44. S. Plocki, D. Aoun, A. Ahamada-Himidi, F. Tavares-Camarinha, C. Z. Dong, F. Massicot, J. Huet, S. Adolphe-Pierre, F. Chau, J. J. Godfroid, N. Gresh, J. E. Ombetta and F. Heymans, *Eur. J. Org. Chem.*, 2005, DOI: 10.1002/ejoc.200400541, 2747-2757.
45. C. Z. Dong, A. Ahamada-Himidi, S. Plocki, D. Aoun, M. Touaibia, N. Meddad-Bel Habich, J. Huet, C. Redeuilh, J. E. Ombetta, J. J. Godfroid, F. Massicot and F. Heymans, *Bioorg. Med. Chem.*, 2005, **13**, 1989-2007.
46. I. Stansfield, M. Pompei, I. Conte, C. Ercolani, G. Migliaccio, M. Jairaj, C. Giuliano, M. Rowley and F. Narjes, *Bioorg. Med. Chem. Lett.*, 2007, **17**, 5143-5149.
47. T. L. Graybill, R. E. Dolle, C. T. Helaszek, R. E. Miller and M. A. Ator, *Int. J. Pept. Protein Res.*, 1994, **44**, 173-182.

Chapter 5

Oxadiazolones: a challenge to implement

5 Oxadiazolones: a challenge to implement

5.1 Introduction

Oxadiazolone heterocycles were discovered during the MSAS approach as valuable carboxylate replacements for the discovery of caspase inhibitors. However, implementing such isosteres in existing caspase inhibitors was found to be a real challenge. Though our group eventually succeeded at producing NCGC-00183434 analogues **5.6** and **5.7** (**Figure 5.1**), it is worth highlighting that several other synthetic pathways were investigated in an earlier stage. The explored methods focused on producing aspartate analogues **5.2-5.4**, i.e. molecules that have not yet been reported in literature. We aimed at synthesizing these analogues via an easy and reproducible method that would provide various carbon lengths (n) between the heterocycle and the α -carbon of the amino acid. Once synthesized, these aminonitriles can be easily coupled to the NCGC-00183434 peptide tail by standard peptide synthesis protocols, affording carbonitriles **5.5-5.7**. In addition, a one-step procedure to obtain the aldehyde analogues (**5.8-5.10**) would provide a powerful tool to vary the warhead functionality in a time-efficient way.

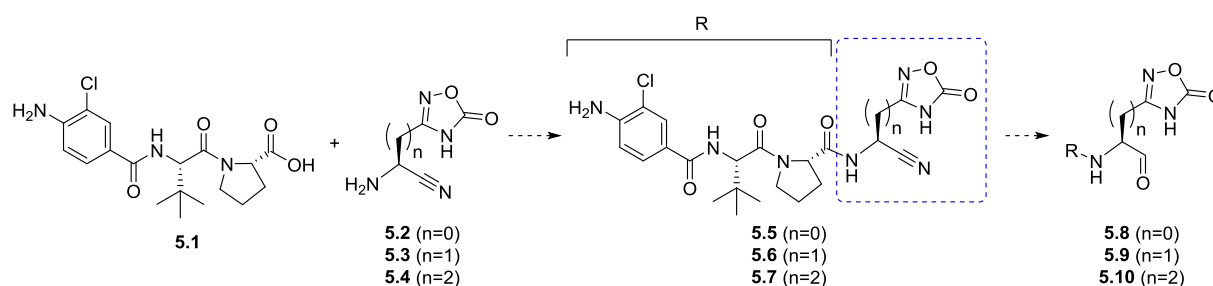


Figure 5.1. Production of oxadiazolone-containing derivatives of caspase inhibitor NCGC-00183434 and the conversion of carbonitrile warheads into aldehyde warheads.

5.1.1 General synthesis of oxadiazolones

Oxadiazolone heterocycles are generally produced starting from the corresponding carbonitriles (**Figure 5.2**). The first step consists of the nucleophilic attack of hydroxylamine, followed by a tautomerization to obtain the amidoxime.¹ The cyclization process is usually performed by two different approaches. In the first and most commonly used method a double addition-elimination reaction occurs, directly affording the oxadiazolone. Carbonyl derivatives, such as carbonyldiimidazole or diethyl carbonate, are ideal reagents for this purpose due to the presence of good leaving groups and its safe handling.²⁻⁴ The second approach is based on the use of trichloroacetyl chloride, providing the intermediate trichloromethyl oxadiazole which is transformed into the oxadiazolone in basic aqueous media.⁵ This method is however more frequently used for the substitution of primary or secondary amines onto this position.⁶

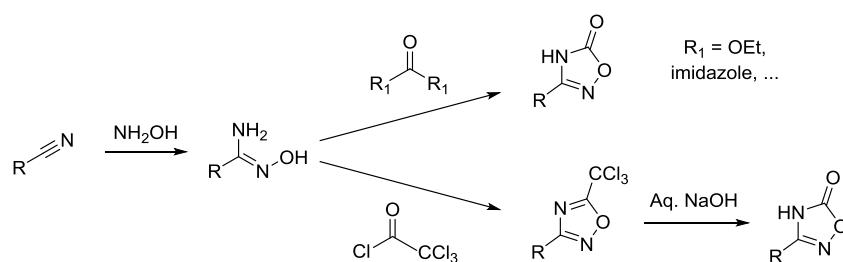


Figure 5.2. Two most common procedures for the production of oxadiazolone heterocycles.

5.2 Objectives

In order to obtain new unnatural amino acids containing an oxadiazolone moiety, two main approaches will be explored in this chapter; the acyliminium-Strecker reaction and a Schiff-base approach (Figure 5.3). A third method, which successfully led to the formation of this product, consisted of the synthetical adaptation of aspartic acid, which was presented in Chapter 4. With respect to maximizing the success of the two first approaches, also specific oxadiazolone protecting groups will be discussed.

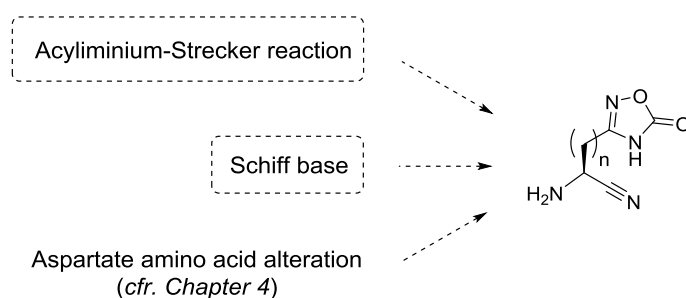


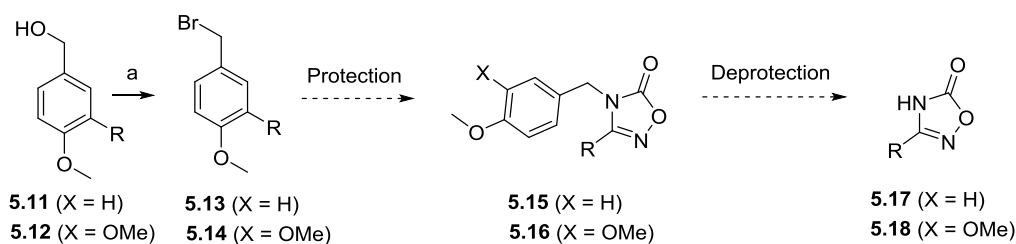
Figure 5.3. Different pathways to obtain oxadiazolone-containing aspartate analogues.

5.3 Results and discussion

5.3.1 Protecting groups

Oxadiazolone heterocycles have the ability to undergo acid-base reactions, as well as nucleophilic attacks. Moreover, the oxadiazolone moiety is easily converted into an amidine functional group after palladium-catalyzed hydrogenation.⁵ To avoid any of these side reactions, it is highly recommended to protect the oxadiazolone during long synthetic pathways. In our perspective, methoxybenzyl derivatives seemed the most promising protecting groups for the oxadiazolone. Protection included nucleophilic substitution with benzyl bromide, from which the latter was obtained after reaction of the alcohol with phosphorus tribromide (Scheme 5.1). It is worth mentioning that in our hands, protection with methoxybenzyl alcohol in acidic conditions and protection through a Mitsunobu reaction were both unsuccessful. Moreover, preliminary experiments with a *tert*-butyldiphenylsilyl protecting group did not provide heterocycle protection.

Deprotection of methoxybenzyl derivatives has been reported with Lewis acids, 2,3-dichloro-5,6-dicyano-1,4-benzoquinone (DDQ) or in acidic media.⁷⁻⁸ However, since the compatibility of the first two types of reagents with the oxadiazolone moiety is questionable, deprotection in acidic media would be preferable. Because dimethoxybenzyl derivatives require milder deprotection conditions than *para*-methoxybenzyl, we selected 3,4-dimethoxybenzyl as a suitable protecting group. 2,4-Dimethoxybenzyl bromide on the other hand, was found to be unstable upon exposure to air.



Scheme 5.1. Reagents and conditions^[a]: a) PBr₃, DCM, 0 °C, 6 h, 78-93%. [a] exact yields are appointed in experimental section.

It is worth highlighting that the oxadiazolone heterocycle has the ability to undergo tautomerization (**Figure 5.4**). Since earlier reports described the preference of the NH-tautomer, this nitrogen is expected to be alkylated in the protection mechanism.⁹ Comparison of the chemical shifts from several NMR experiments with other reports from literature confirmed *N*-alkylation, as shown in **Scheme 5.1** (data in experimental section).¹⁰

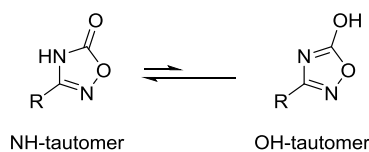
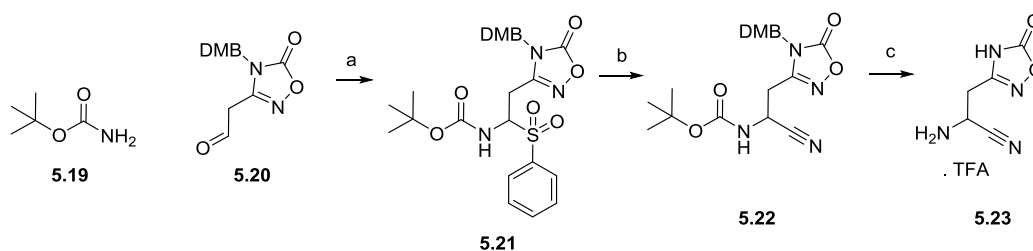


Figure 5.4. Tautomerization of the oxadiazolone heterocycle.

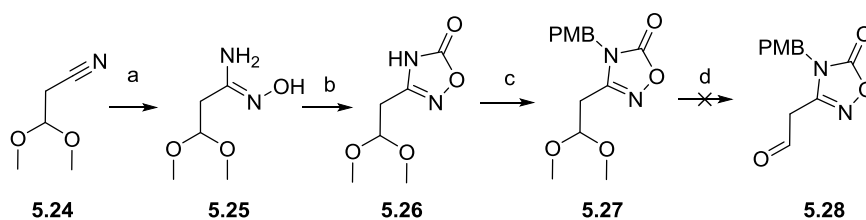
5.3.2 Via the acyliminium-Strecker reaction

The acyliminium-Strecker reaction serves as a valuable approach for the preparation of oxadiazolone-containing amino acids. A full discussion of the perspectives and optimized conditions of this type of reaction will be done in Chapter 6. Specifically, *tert*-Butyl carbamate (**5.19**) and oxadiazolone-aldehyde derivative **5.20** are expected to yield a stable sulfone in the presence of phenylsulfonic acid (**Scheme 5.2**). Subsequent acyliminium-Strecker conditions, followed by two deprotection steps would allow to afford aminonitrile **5.23**. The efficiency of the organocatalyst (quinine) to provide sufficient stereoselectivity can then be tested by using chiral column chromatography. If required, stereoisomer separation can be achieved with supercritical fluid chromatography (SFC), a state-of-the-art technique available in our lab.



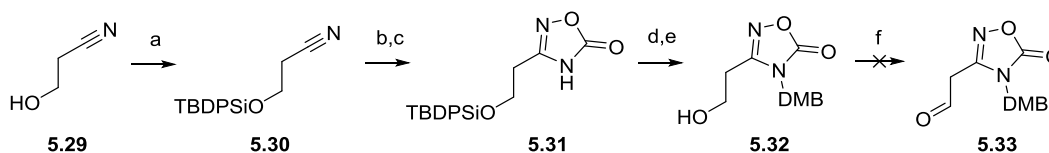
Scheme 5.2. Reagents and conditions^[a]: a) Sodium sulfinate, MeOH, H₂O, RT, 3 d; b) KCN, quinine, DCM, RT, 5 h; c) TFA, 75 °C, 2 h. [a] Predicted.

To successfully apply this strategy, the production of an aldehyde building block containing the oxadiazolone was first required (**Scheme 5.3**). The commercially available 3,3-dimethoxypropanenitrile (**5.24**) was used as starting point for the synthesis of the heterocycle (**5.26**) via a similar two-step procedure as explained before. During the early stage of this investigation, we implemented a *para*-methoxybenzyl protecting group, with sodium hydride as a suitable base. Regrettably, the acetal deprotection step to obtain **5.28** failed, employing similar conditions as during the synthesis of similar non-protected fragments (*cf.* Chapter 4).



Scheme 5.3. Reagents and conditions: a) NH₂OH.HCl, NaHCO₃, MeOH, 70 °C, overnight, 85%; b) CDI, DBU, 1,4-dioxane, 110 °C, 2 h, 72%; c) methoxybenzylbromide, NaH, DMF, RT, overnight, 95%; d) 6 M HCl, 50 °C, 3 h.

In response, a pathway was developed that set the focus on oxidizing the corresponding alcohol into the correct aldehyde (**Scheme 5.4**), instead of deprotecting acetal functional groups. The alcohol in 3-hydroxypropionitrile (**5.29**) was protected with a *tert*-butyldiphenylsilyl protecting group. Heterocycle formation followed by dimethoxybenzyl protection and TBAF-mediated silyl ether deprotection afforded alcohol **5.32**. However, attempts with Swern conditions and Dess-Martin periodinane both failed to oxidize the alcohol in order to produce aldehyde **5.33**.

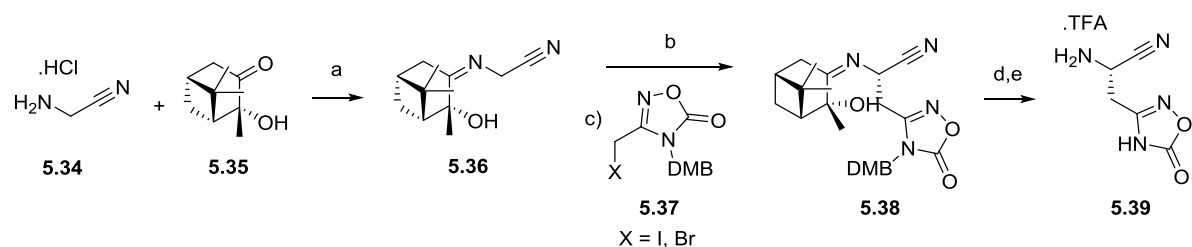


Scheme 5.4. Reagents and conditions: a) TBDPSiCl, imidazole, DMAP, DCM, RT, overnight, >99%; b) NH₂OH.HCl, NaHCO₃, MeOH, 70 °C, overnight, 85%; c) CDI, DBU, 1,4-dioxane, 110 °C, 2 h, 94%; d) dimethoxybenzyl bromide, NaH, DMF, RT, overnight, 83%; e) TBAF, THF, RT, overnight, 89%; f) Dess-Martin periodinane, DCM, RT, 1 h or oxalyl chloride, DMSO, TEA, 0 °C -> RT, 30 min.

Since we were unable to provide the aldehyde-based building blocks required for the acyliminium-Strecker synthesis, the full potential of this type of reaction to afford oxadiazolone-containing aminonitriles left undetermined.

5.3.3 Via Schiff base formation

Another approach to create unnatural amino acids is based on employing the chiral inductor (+)-(1R,2R,5R)-2-hydroxy-3-pinanone to create a Schiff base. This was first described in 1976, but has recently been repeated for the synthesis of trimethylsilylalanine and β -(5-arylthiazolyl) α -amino acids.¹¹⁻¹³ The conditions in the last two reports formed the basis for the production of oxadiazolone derivatives in this investigation (**Scheme 5.5**). However, in contrast to these reports, we started with aminoacetonitrile (**5.34**) instead of *tert*-butyl glycine. This starting material was allowed to react with the chiral inductor (**5.35**) in the presence of boron trifluoride diethyl etherate, to form imine **5.36** with a moderate yield (33%). Next, the α -proton is supposed to be subtracted by lithium diisopropylamide, followed by a nucleophilic attack to the oxadiazolone-containing building block **5.37** (which has not yet been synthesized). Because of the bulky substituents of 2-hydroxy-3-pinanone, a stereoselective reaction should appear, favoring the L-amino acid configuration. Finally, the chiral auxiliary is expected to be removed by hydrolysis with aqueous citric acid, followed by dimethoxybenzyl deprotection, affording oxadiazolone-containing aminonitrile **5.39**.

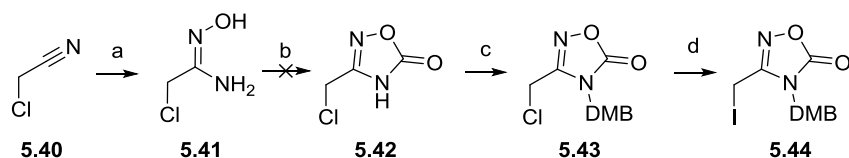


Scheme 5.5. Reagents and conditions: a) NEt_3 , toluene, followed by $\text{Et}_2\text{O} \cdot \text{BF}_3$, reflux, 4 h, 33%; b)^[a] LDA, -78°C , 30 min; c)^[a] -78°C , 8 h, then -10°C , overnight; d)^[a] citric acid (aq, 15%), THF, RT, 3 d; e)^[a] TFA, elevated temperature, 2 h. [a] predicted.

This approach seems promising in regard to the production of a variety of stereoselective inhibitors containing carbonitrile warheads. Nevertheless, the synthesis of the oxadiazolone-based building blocks (**5.37**) was considered quite challenging. Two attempts were done but, to our regret, did not give the desired products. Based on the findings from these attempts, a third potential pathway will be described.

5.3.3.1 Synthesis of the oxadiazolone building block: attempt 1

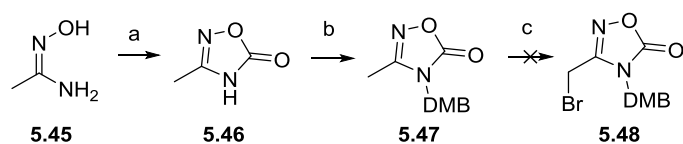
A first attempt was performed starting from chloroacetonitrile (**Scheme 5.6**). Amidoxime formation was successful but the ring closure, using standard conditions, failed. The intention was to protect the heterocycle and convert the chloride into a iodide with *n*-tetrabutylammonium iodide. This is considered an excellent leaving group, suited for the nucleophilic attack from the Schiff base.



Scheme 5.6. Reagents and conditions: a) $\text{NH}_2\text{OH}\cdot\text{HCl}$, NaOEt , EtOH , RT, 1 h, 55%. b) CDI, DBU, 1,4-dioxane, $110\text{ }^\circ\text{C}$, 2 h; c)^[a] dimethoxybenzyl bromide, NaH, DMF, RT, overnight; d)^[a] TBAI, acetone, $60\text{ }^\circ\text{C}$, 2 h. [a] predicted.

5.3.3.2 Synthesis of the oxadiazolone building block: attempt 2

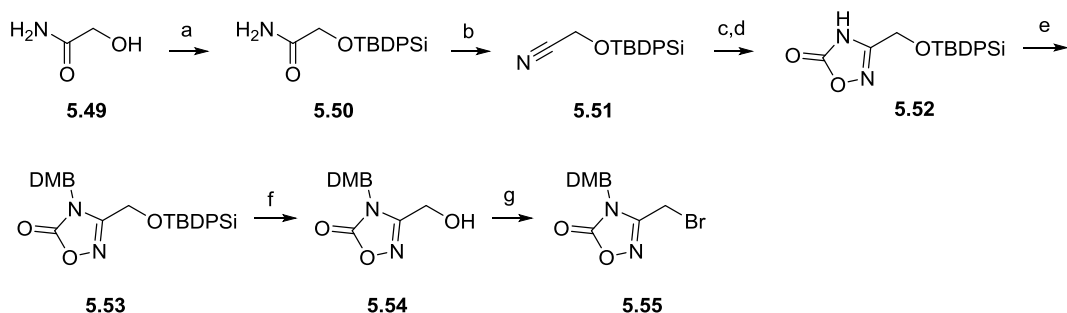
The focus in the second pathway was set on firstly producing the oxadiazolone and introducing the halogen in the last stage (**Scheme 5.7**). The produced oxadiazolone fragment **5.46** was protected to afford compound **5.47**. Optimistically, we tried to brominate the methyl-group of the fragment via a radical reaction employing *N*-bromosuccinimide, but not surprisingly, this reaction failed. The bromination is highly likely to be favored on the benzylic position of the protecting group.



Scheme 5.7. Reagents and conditions: a) CDI, DBU, 1,4-dioxane, $110\text{ }^\circ\text{C}$, 2 h, 80%; b) dimethoxybenzyl bromide, NaH, DMF, RT, overnight, 90%; c) NBS, benzoyl peroxide, CCl_4 / DCM, reflux, 3 h.

5.3.3.3 Synthesis of the oxadiazolone building block: attempt 3

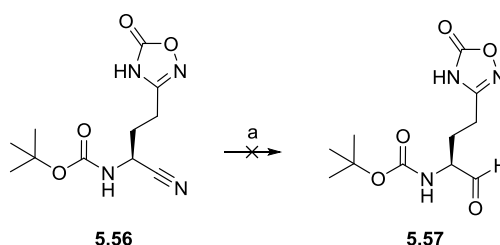
A final pathway is suggested that is similar to the previous pathway, but the implementation of the bromine leaving group should be realized by transformation of the alcohol in the last stage (**Scheme 5.8**). To obtain the alcohol, commercially available 2-hydroxyacetamide (**5.49**) should first be alcohol-protected, followed by dehydration of the amide. General oxadiazolone formation and dimethoxybenzyl protection would afford compound **5.53**. Deprotection of the alcohol would allow it to react with phosphorous tribromide, in order to obtain building block **5.55**. Though this pathway seemed highly promising, there was limited time in this PhD thesis to apply this synthesis.



Scheme 5.8. Reagents and conditions^[a]: a) TBDPSCI, imidazole, DMAP, DCM; b) TFAA, DCM; c) $\text{NH}_2\text{OH}\cdot\text{HCl}$, NaHCO_3 , MeOH; d) CDI, DBU, 1,4-dioxane; e) DMB-Br, NaH, DMF; f) TBAF, THF; g) PBr_3 , DCM. [a] predicted.

5.3.4 Transformation of aminonitriles into amino aldehydes

To avoid an additional comprehensive synthesis of aldehyde-based analogues of the previously discussed aminonitriles, the direct transformation of the carbonitrile warhead into an aldehyde warhead was investigated. Diisobutylaluminium hydride (DIBAL-H) is a versatile reducing agent, known for its ability to convert carbonitriles into aldehydes.¹⁴⁻¹⁶ In our case, it is important to consider that the reduction must occur selectively at the carbonitrile functionality in order to safeguard the oxadiazolone moiety. Transformation of carbonitrile **5.56** (which was synthesized in Chapter 4) into aldehyde **5.57** was investigated using DIBAL-H as reducing agent (**Scheme 5.9**). Though different conditions, such as temperatures up to ambient temperature and up to two equivalents of DIBAL-H, were tried, starting material was always recovered. Other reducing agents, such as titanium-based derivatives remain to be tested.



Scheme 5.9. Reagents and conditions: a) DIBAL-H, THF, -78 °C – RT, 2 h, followed by MeOH, NH₄Cl:HCl (pH 3).

5.4 Conclusions

Two main approaches were explored to obtain oxadiazolone-containing aminonitriles. Such compounds are considered of great interest due to their relevance in the discovery of potent and selective caspase inhibitors. A first approach applied the acyliminium-Strecker synthesis, while the second approach focused on the use of a Schiff base. Nonetheless, both cases required challenging synthetic pathways to obtain building blocks that were essential to succeed these approaches. Since the production of the required building blocks was hampered, the realization of these approaches to create oxadiazolone-based aminonitriles was not feasible either. In the end, transformation of a carbonitrile warhead into an aldehyde was attempted with DIBAL-H as reducing agent but appeared to be unsuccessful.

5.5 Experimental section

5.5.1 Chemistry

Reagents were obtained from Sigma-Aldrich, Acros, Fluorochem or Apollo Scientific and were used without further purification. Synthesized compounds were characterized by ¹H NMR, ¹³C NMR and mass spectrometry. ¹H NMR and ¹³C NMR spectra were recorded with a 400 MHz Bruker Avance DRX

400 spectrometer, and analyzed by use of MestReNova analytical chemistry software. Purities were determined with a Waters Acquity UPLC system coupled to a Waters TUV detector, ESI source and a Waters Acquity QDa Mass Detector. A Waters Acquity UPLC BEH C18 1.7 μm 2.1 x 50 mm column was used. Solvent A: water with 0.1% formic acid, solvent B: acetonitrile with 0.1% formic acid. The gradient used started with a flow rate of 0.7 mL/min at 95% A, 5% B for 0.15 min then in 1.85 min from 95% A, 5% B to 100% B, isocratically at the same percentage for 0.25 min and finally 0.75 min (0.350 mL/min), 95% A, 5% B. The wavelength for UV detection was 254 nm. Where necessary, flash purification was performed with a Biotage ISOLERA One flash system equipped with an internal variable dual-wavelength diode array detector (200–400 nm).

1-(Bromomethyl)-4-methoxybenzene (5.13)

A solution of phosphorus tribromide (0.952 mL, 10.13 mmol) in DCM (10 mL) was added dropwise to a solution of 4-methoxybenzyl alcohol (0.898 mL, 7.24 mmol) in DCM (10 mL) at 0 °C. The reaction mixture was stirred for 2 h then warmed to room temperature. After 4 h, the solution was poured into ice-water (40 mL) and stirred for 10 min. The organic layer was washed with water (20 mL) and aqueous NaHCO_3 (3 x 20 mL), dried over anhydrous sodium sulfate and evaporated under reduced pressure at 10–20 °C. Compound **5.13** was obtained as a white solid (1.13 g, 78%). The compound was used without any further purification/analysis. The compound is unstable at higher temperatures and on silica. Must be stored at 5 °C and used within the week.

4-(Bromomethyl)-1,2-dimethoxybenzene (5.14)

A solution of phosphorus tribromide (1.956 mL, 20.81 mmol) in DCM (20 mL) was added dropwise to a solution of (3,4-dimethoxyphenyl)methanol (2.161 mL, 14.86 mmol) in DCM (50 mL) at 0 °C. The reaction mixture was stirred for 90 min and then warmed to room temperature. After 4 h, the solution was poured into ice-water (80 mL) and stirred for 5 min. The organic layer was washed with water (50 mL) and aqueous NaHCO_3 (3 x 50 mL), dried over anhydrous sodium sulfate and evaporated under reduced pressure at ambient temperature. Compound **5.14** was obtained as a white solid (3.18 g, 93%). The compound was used without any further purification. The compound is unstable at higher temperatures and on silica. Must be stored at 5 °C and used within the week. ^1H NMR (400 MHz, CDCl_3) δ 3.87 (s, 3H), 3.89 (s, 2H), 4.50 (s, 2H), 6.80 (d, J = 8.2 Hz, 1H), 6.90 (d, J = 2.1 Hz, 2H), 6.94 ppm (dd, J = 8.2, 2.1 Hz, 2H); ^{13}C NMR (101 MHz, CDCl_3) δ 34.55, 55.96, 56.00, 111.02, 112.07, 121.62, 130.28, 149.10, 149.27 ppm.

3-(2,2-Dimethoxyethyl)-4-(4-methoxybenzyl)-1,2,4-oxadiazol-5(4H)-one (5.27)

To a suspension of sodium hydride (50.5 mg, 1.263 mmol, 60% dispersion in mineral oil) in anhydrous DMF (1 mL) at 0°C was added dropwise a solution of 3-(2,2-dimethoxyethyl)-4-(4-methoxybenzyl)-1,2,4-oxadiazol-5(4H)-one (**5.26**, synthesized in chapter 4) (320 mg, 1.087 mmol) in DMF (1 mL). After the addition was complete (20 min), the cooling bath was removed and the mixture stirred at room temperature for 30 min and a solution of 1-(bromomethyl)-4-methoxybenzene (**5.13**, 277 mg, 1.378 mmol) in DMF (0.5 mL) was added. The reaction mixture was left stirring at room temperature overnight. The reaction mixture was poured into water (10 mL) and extracted with EtOAc (3 x 10 mL). The organic phase was washed with water (2 x 8 mL), brine (8 mL), dried and concentrated in vacuo. The residue was purified by flash chromatography. Compound **5.27** was obtained as a solid (320 mg, 95%). $R_f = 0.37$ (1:1 EtOAc:hex, visualization by UV); $^1\text{H NMR}$ (400 MHz, $\text{DMSO-}d_6$) δ 2.90 (d, $J = 5.5$ Hz, 2H), 3.23 (s, 6H), 3.75 (s, 3H), 4.55 (t, $J = 5.5$ Hz, 1H), 4.80 (s, 2H), 6.93 - 6.98 (m, 2H), 7.22 - 7.26 ppm (m, 2H); UPLC-MS m/z : 121.2 [methoxybenzyl cation] $^+$.

3-((*tert*-Butyldiphenylsilyl)oxy)propanenitrile (5.30)

To a solution of 3-hydroxypropanenitrile (**5.29**, 2.383 mL, 35.2 mmol) in DCM (50 mL) was added imidazole (3.59 g, 52.8 mmol) and 4-dimethylaminopyridine (0.645 g, 5.28 mmol). The mixture was stirred for 10 min in an ice bath, before adding *tert*-butylchlorodiphenylsilane (10.06 mL, 38.7 mmol). The cold bath was removed and stirring was continued overnight. A white solid appeared after a couple of minutes. Additional DCM (70 mL) was added, followed by saturated aqueous ammonium chloride solution (100 mL) and the layers were separated. The aqueous layer was extracted with DCM (2 x 50 mL). The combined organic layers were washed with brine (100 mL), dried over Na_2SO_4 and concentrated *in vacuo* to afford pure **5.30** (12.12 g, >99%). $R_f = 0.62$ (8:2 Hex:EtOAc, visualization by UV and KMnO_4); $^1\text{H NMR}$ (400 MHz, CDCl_3) δ 1.05 - 1.14 (s, 9H), 2.55 (t, $J = 6.3$ Hz, 2H), 3.86 (t, $J = 6.3$ Hz, 2H), 7.35 - 7.51 (m, 6H), 7.66 - 7.77 ppm (m, 4H); $^{13}\text{C NMR}$ (101 MHz, CDCl_3) δ 19.25, 21.54, 26.79, 59.12, 118.07, 127.99, 130.11, 132.76, 135.62 ppm.

3-(2-((*tert*-Butyldiphenylsilyl)oxy)ethyl)-1,2,4-oxadiazol-5(4H)-one (5.31)

Hydroxylammonium chloride (2.69 g, 38.7 mmol) was dissolved in MeOH (75 mL), NaHCO_3 (3.25 g, 38.7 mmol) was added thereto and then stirred for 20 minutes at room temperature. Carbonitrile **5.30** (10.89 g, 35.2 mmol) in MeOH (10 mL) was added thereto, heated, and stirred for 16 hours at reflux temperature and then, cooled to room temperature. Formed salt was filtrated and removed. The filtrate was concentrated under reduced pressure. Acetone was added and filtered again. Flash chromatography was done to afford the amidoxime as a transparent oil (10.23 g, 85%). $R_f = 0.19$ (1:1 Hept:EtOAc, visualization by UV); $^1\text{H NMR}$ (400 MHz, CDCl_3) δ 1.06 (s, 9H), 2.38 (t, $J = 5.62$ Hz, 2H), 3.87

(t, $J = 5.62$ Hz, 2H), 5.16 (s, 2H), 6.55 (s, 1H), 7.36 - 7.47 (m, 6H), 7.63 - 7.68 ppm (m, 4H); ^{13}C NMR (101 MHz, CDCl_3) δ 19.19, 26.96, 33.54, 62.45, 127.98, 130.04, 132.94, 135.62, 154.19 ppm; UPLC-MS m/z : 343.2 $[\text{M}+\text{H}]^+$. The intermediate amidoxime (5.8 g, 16.93 mmol) was dissolved in 1,4-dioxane (50 mL), 1,8-diazabicyclo[5.4.0]undec-7-ene (2.73 mL, 18.63 mmol) and 1,1'-carbonyldiimidazole (3.29 g, 20.32 mmol) were added. The reaction mixture was left stirring 2 h at reflux. The mixture was concentrated *in vacuo*. 1 M HCl (100 mL) was added and extraction was done with EtOAc (3 x 70 mL). The organic layers were collected, washed with brine (100 mL), dried over Na_2SO_4 , filtered and concentrated under reduced pressure to give oxadiazolone **5.31** as a white solid (5.87 g, 94%). $R_f = 0.38$ (1:1 Hept:EtOAc, visualization by UV); ^1H NMR (400 MHz, CDCl_3) δ 1.01 - 1.09 (m, 9H), 2.79 (t, $J = 5.9$ Hz, 2H), 3.96 (t, $J = 5.9$ Hz, 2H), 7.36 - 7.48 (m, 6H), 7.59 - 7.67 (m, 4H), 9.85 ppm (s, 1H); ^{13}C NMR (101 MHz, CDCl_3) δ 19.19, 26.91, 28.46, 60.24, 128.08, 130.23, 132.54, 135.56, 157.59, 160.54 ppm; UPLC-MS m/z : 367.2 $[\text{M}-\text{H}]^-$.

4-(3,4-Dimethoxybenzyl)-3-(2-hydroxyethyl)-1,2,4-oxadiazol-5(4H)-one (**5.32**)

To a suspension of sodium hydride (0.179 g, 4.48 mmol, 60% dispersion in oil) in anhydrous DMF (7.5 mL) at 0 °C was added dropwise a solution of oxadiazolone **5.31** (1.76 g, 3.39 mmol) in DMF (7.5 mL). After the addition was complete (20 min), the cooling bath was removed and the mixture stirred at room temperature for 30 min and a solution of 4-(bromomethyl)-1,2-dimethoxybenzene (**5.14**, 1.129 g, 4.88 mmol) in DMF (5 mL) was added. The reaction mixture was left stirring at room temperature overnight. The reaction mixture was poured into water (70 mL) and extracted with EtOAc (3 X 70 mL). The organic phase was washed with water (2 X 60 mL), brine (1 X 60 mL), dried and concentrated *in vacuo*. The residue was purified by flash chromatography to afford the intermediate protected form as a white solid (1.76 g, 83%). $R_f = 0.48$ (1:1 EtOAc:Hex, visualization by UV); ^1H NMR (400 MHz, CDCl_3) δ 1.04 (s, 9H), 2.69 (t, $J = 6.4$ Hz, 2H), 3.83 (s, 3H), 3.86 (s, 3H), 3.91 (t, $J = 6.4$ Hz, 2H), 4.64 (s, 2H), 6.66 - 6.79 (m, 3H), 7.35 - 7.50 (m, 6H), 7.55 - 7.63 (m, 4H); ^{13}C NMR (101 MHz, CDCl_3) δ 19.26, 26.91, 28.41, 45.75, 56.05, 56.09, 60.35, 110.44, 111.27, 119.85, 126.82, 128.04, 130.2, 132.82, 135.58, 149.42, 149.72, 157.70, 159.81 ppm; UPLC-MS m/z : 151.2 $[\text{dimethoxybenzyl cation}]^+$. The intermediate was dissolved in dry THF (12 mL). Tetra-*n*-butylammonium fluoride (1 M in THF, 10.18 mL, 10.18 mmol) was added and the reaction mixture was left stirring overnight. The reaction mixture was diluted with EtOAc (150 mL) and washed with water (2 x 100 mL). The aqueous layers were washed with EtOAc (2 x 100 mL). All organic layers were combined, washed with brine (100 mL), dried (Na_2SO_4), concentrated *in vacuo* and purified by flash chromatography. Alcohol **5.32** was obtained (850 mg, 89%). $R_f = 0.29$ (3:1 EtOAc:Hex, visualization by UV); ^1H NMR (400 MHz, CDCl_3) δ 2.41 (s, 1H), 2.68 (t, $J = 5.8$ Hz, 2H), 3.84 (s, 3H), 3.85 (s, 3H), 3.91 (t, $J = 5.8$ Hz, 2H), 4.73 (s, 2H), 6.76 - 6.83 ppm (m, 3H); UPLC-MS m/z : 151.2 $[\text{dimethoxybenzyl cation}]^+$.

2-((Z)-((1R,2R,5R)-2-Hydroxy-2,6,6-trimethylbicyclo[3.1.1]heptan-3-ylidene)amino)acetonitrile (5.36)

A suspension of aminoacetonitrile hydrochloride (1.388 g, 15 mmol) in dry toluene (30 mL) was stirred in the presence of triethylamine (2.085 mL, 15.00 mmol) for 1 h. After triethylammonium chloride filtration, (+)-(1R,2R,5R)-2-hydroxy-3-pinanone (1682 mg, 10.00 mmol) was added to the amine. The mixture was heated to reflux for 4 h in the presence of borontrifluoride diethyl etherate (0.099 mL, 0.800 mmol). Water, formed during the reaction, was removed with a Dean-Stark trap. After cooling, the mixture was concentrated *in vacuo*. A brown liquid (1.67 g) was obtained, which was purified by flash chromatography (Hex:EtOAc + 1% TEA). Product **5.36** was obtained as a solid (680 mg, 33%). $R_f = 0.37$ (1:1 EtOAc:Hex + 1% TEA, visualization by KMnO_4); $^1\text{H NMR}$ (400 MHz, CDCl_3) δ 0.84 (s, 3H), 1.34 (s, 3H), 1.50 (s, 3H), 1.57 (d, $J = 10.9$ Hz, 1H), 2.05 - 2.11 (m, 2H), 2.33 - 2.41 (m, 1H), 2.52 (d, $J = 1.0$ Hz, 2H), 4.15-4.27 ppm (m, 2H); $^{13}\text{C NMR}$ (101 MHz, CDCl_3) δ 22.96, 27.27, 28.15, 28.17, 34.0, 38.14, 38.38, 38.79, 50.28, 76.77, 117.12, 183.57 ppm; UPLC-MS m/z : 207.2 $[\text{M}+\text{H}]^+$.

(Z)-2-Chloro-N'-hydroxyacetimidamide (5.41)

Sodium ethoxide (29.9 mL, 80 mmol, 21%wt in EtOH) was added dropwise to a suspension of hydroxylammonium chloride (5.56 g, 80 mmol) in EtOH (95 mL) and MeOH (5 mL) at 0 °C. Stirring was continued for 10 min, then α -chloroacetonitrile (5.06 mL, 80 mmol) was added dropwise. The reaction mixture was warmed to room temperature over 1 h, and then filtered. The filtrate was concentrated *in vacuo*. The crude was dissolved in EtOAc and purified by filtering through silica. After concentration *in vacuo* of the filtrate, the product solidified upon standing to afford compound **5.41** (4.81 g, 55%). $R_f = 0.16$ (1:1 Hex:EtOAc, visualization by KMnO_4 and UV); $^1\text{H NMR}$ (400 MHz, $\text{DMSO}-d_6$) δ 4.00 (s, 2H), 5.62 (s, 2H), 9.44 ppm (s, 1H); $^{13}\text{C NMR}$ (101 MHz, $\text{DMSO}-d_6$) δ 42.34, 149.54 ppm.

3-Methyl-1,2,4-oxadiazol-5(4H)-one (5.46)

(Z)-N'-Hydroxyacetimidamide (**5.45**, 2 g, 27.0 mmol) was dissolved in 1,4-dioxane (40 mL), 1,8-diazabicyclo[5.4.0]undec-7-ene (4.36 mL, 29.7 mmol) and 1,1'-carbonyldiimidazole (6.57 g, 40.5 mmol) were added. The reaction mixture was left stirring 2 h at reflux, and was concentrated *in vacuo*. 2 N HCl (100 mL) was added and extraction was done with EtOAc (3 x 70 mL). The organic layers were collected, dried over Na_2SO_4 , filtered and concentrated under reduced pressure to give oxadiazolone **5.46** as a light brown-red solid (2.43 g, 90%). $^1\text{H NMR}$ (400 MHz, $\text{MeOD}-d_4$) δ 2.21 (s, 3H); $^{13}\text{C NMR}$ (101 MHz, $\text{MeOD}-d_4$) δ 10.29, 158.08, 162.19 ppm.

4-(3,4-Dimethoxybenzyl)-3-methyl-1,2,4-oxadiazol-5(4H)-one (5.47)

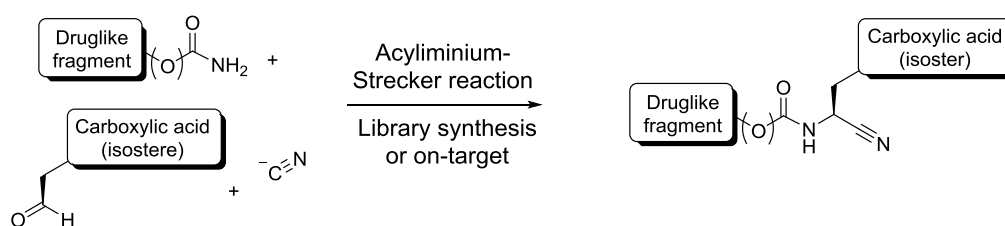
To a suspension of sodium hydride (0.220 g, 5.50 mmol) in anhydrous DMF (10 mL) at 0 °C was added dropwise a solution of oxadiazolone **5.46** (0.5 g, 5.00 mmol) in DMF (10 mL). After the addition was complete (20 min), the cooling bath was removed and the mixture stirred at room temperature for 30 min and a solution of 4-(bromomethyl)-1,2-dimethoxybenzene (**5.14**, 1.385 g, 6.00 mmol) in DMF (5 mL) was added. The reaction mixture was left stirring at room temperature overnight. The reaction mixture was poured into water (80 mL) and extracted with EtOAc (3 x 70 mL). The organic phase was washed with water (2 x 80 mL), brine (1 x 80 mL), dried and concentrated *in vacuo*. The residue was purified by reversed phase flash chromatography. Protected oxadiazolone **5.47** was obtained as a transparent oil (1.12 g, 90%). $R_f = 0.53$ (7:3 MeOH:H₂O, visualization by UV); ¹H NMR (400 MHz, CDCl₃) δ 2.15 (s, 3H), 3.86 (s, 3H), 3.87 (s, 3H), 4.68 (s, 2H), 6.81 ppm (m, 3H); ¹³C NMR (101 MHz, CDCl₃) δ 10.84, 45.89, 56.07, 56.13, 110.71, 111.39, 120.12, 126.62, 149.57, 149.79, 156.48, 159.69 ppm; UPLC-MS m/z : 151.1 [dimethoxybenzyl cation]⁺.

References

1. Kohara, Y.; Imamiya, E.; Kubo, K.; Wada, T.; Inada, Y.; Naka, T., A New Class of Angiotensin-II Receptor Antagonists with a Novel Acidic Bioisostere. *Bioorg. Med. Chem. Lett.* **1995**, *5* (17), 1903-1908.
2. Hett, R.; Krähmer, R.; Vulont, I.; Leschinsky, K.; Snyder, J. S.; Kleine, P. H., Large-Scale Preparation of 3-Methyl-4H-[1,2,4]oxadiazol-5-one, Potassium or Sodium Salt. *Organic Process Research & Development* **2002**, *6* (6), 896-897.
3. Valgeirsson, J.; Nielsen, E. O.; Peters, D.; Mathiesen, C.; Kristensen, A. S.; Madsen, U., Bioisosteric modifications of 2-arylidobenzoic acids: Selective noncompetitive antagonists for the homomeric kainate receptor subtype GluR5. *Journal of Medicinal Chemistry* **2004**, *47* (27), 6948-6957.
4. Charton, J.; Deprez-Poulain, R.; Hennuyer, N.; Tailleux, A.; Staels, B.; Deprez, B., Novel non-carboxylic acid retinoids: 1,2,4-Oxadiazol-5-one derivatives. *Bioorg. Med. Chem. Lett.* **2009**, *19* (2), 489-492.
5. Bolton, R. E.; Coote, S. J.; Finch, H.; Lowdon, A.; Pegg, N.; Vinader, M. V., 3-substituted-1,2,4-oxadiazolin-5-one; A useful amidine precursor and protecting group. *Tetrahedron Lett.* **1995**, *36* (25), 4471-4474.
6. Sheremetev, A. B.; Andrianov, V. G.; Mantseva, E. V.; Shatunova, E. V.; Aleksandrova, N. S.; Yudin, I. L.; Dmitriev, D. E.; Averkiev, B. B.; Antipin, M. Y., Synthesis of secondary and tertiary aminofurazans. *Russian Chemical Bulletin* **2004**, *53* (3), 596-614.
7. Subramanyam, C., 4-Methoxybenzyl (PMB), A Versatile Protecting Group for the Regiospecific Lithiation and Functionalization of Pyrazoles. *Synth. Commun.* **1995**, *25* (5), 761-774.
8. Watanabe, K.; Katoh, T., Effective chemoselective deprotection of 3,4-dimethoxybenzyl (3,4DMB) ethers in the presence of benzyl and p-methoxybenzyl (PMB) ethers by phenyliodine(III) bis(trifluoroacetate) (PIFA). *Tetrahedron Lett.* **2011**, *52* (41), 5395-5397.
9. Katritzky, A. R.; Wallis, B.; Brownlee, R. T.; Topsom, R. D., Tautomerism of Heteroaromatic Compounds with 5-Membered Rings .8. Hydroxy-Oxadiazoles or Oxadiazolones. *Tetrahedron* **1965**, *21* (7), 1681-+.
10. Dong, C. Z.; Ahamada-Himidi, A.; Plocki, S.; Aoun, D.; Touaibia, M.; Meddad-Bel Habich, N.; Huet, J.; Redeuilh, C.; Ombetta, J. E.; Godfroid, J. J.; Massicot, F.; Heymans, F., Inhibition of secretory phospholipase A2. 2-Synthesis and structure-activity relationship studies of 4,5-dihydro-3-(4-tetradecyloxybenzyl)-1,2,4-4H-oxadiazol-5-one (PMS1062) derivatives specific for group II enzyme. *Bioorg. Med. Chem.* **2005**, *13* (6), 1989-2007.
11. Hapău, D.; Rémond, E.; Fanelli, R.; Vivancos, M.; René, A.; Côté, J.; Besserer-Offroy, É.; Longpré, J.-M.; Martinez, J.; Zaharia, V.; Sarret, P.; Cavelier, F., Stereoselective Synthesis of β -(5-Arylthiazolyl) α -Amino Acids and Use in Neurotensin Analogues. *Eur. J. Org. Chem.* **2016**, *2016* (5), 1017-1024.
12. René, A.; Vanthuynne, N.; Martinez, J.; Cavelier, F., (L)-(Trimethylsilyl)alanine synthesis exploiting hydroxypinanoneinduced diastereoselective alkylation. *Amino Acids* **2013**, *45*, 301-307.
13. Yamada, S.-I.; Oguri, T.; Shioiri, T., Asymmetric synthesis of [small alpha]-amino-acid derivatives by alkylation of a chiral Schiff base. *J. Chem. Soc., Chem. Commun.* **1976**, (4), 136-137.

14. Nicolaou, K. C.; Yun, J.; Mandal, D.; Erande, R. D.; Klahn, P.; Jin, M.; Aujay, M.; Sandoval, J.; Gavriyuk, J.; Vourloumis, D., Total Synthesis and Biological Evaluation of Natural and Designed Tubulysins. *J. Am. Chem. Soc.* **2016**, *138* (5), 1698-1708.
15. Trofimenko, S., 1,1,2,2-Ethanetetracarboxaldehyde + Its Reactions. *J. Org. Chem.* **1964**, *29* (10), 3046-&.
16. AkzoNobel, Technical Bullitin: Total Synthesis and Biological Evaluation of Natural and Designed Tubulysins. **2006**.

Optimization of the acyliminium-Strecker reaction for convenient library synthesis and on-target experiments



Contributed to this chapter:

As part of her PhD, **Antonella Messori** joined our laboratory for 6 months. Her contribution to this chapter consisted of performing the carbamate-based experiments in this exploratory study. The results from her findings, also summarized in her PhD thesis, have been included in this chapter and formed the basis for further investigation.

6 Optimization of the acyliminium-Strecker reaction for convenient library synthesis and on-target experiments

6.1 Introduction

As explained earlier, one of the initial objectives of this PhD project was to investigate and implement target-assisted synthetic approaches for assembly of inhibitor building blocks (including carboxylate isosteres), as an efficient means to produce high-affinity caspase inhibitors. Developing target-assisted versions of multicomponent reactions that can be used in diversity-oriented drug discovery seemed highly attractive for this project, given the possibility to simultaneously assemble multiple building blocks and deliver complex, functionalized molecular structures in a single, target-catalyzed step. The Strecker reaction that typically delivers 1-aminoalkylcarbonitriles (that have proven potential as protease inhibitors) seemed particularly attractive for investigation in the context of this project.¹ An overview of hallmark features of target-assisted drug discovery, the Strecker reaction and related transformations are described in the next part. In addition, different endeavors are described to optimize this reaction towards a version that would allow efficient library synthesis and/or on-target drug discovery.

6.1.1 Target-assisted drug discovery

Target-assisted drug discovery relies on direct assistance of the drug target, which serves as a physical template that selects drug fragments with target affinity and assembles them into finalized ligands. Since each of these fragments contains a reactive moiety, assembly of the counterparts is made possible. A main tenet of the approach is that the target-aided assembly is selective for building blocks that possess affinity for the target. This leads to so-called “selective amplification” of assembled ligands with strong affinity for the target, over building block assemblies that lack target affinity. Amplified ligands can then be further optimized either using classical approaches or additional cycles of on-target investigations.

According to the type of reaction, this strategy can be divided into two categories (**Figure 6.1**). If the counterparts react in a reversible way, it is called (protein-directed) dynamic combinatorial chemistry (DCC).² In this case the target's preference leads to a shift of the thermodynamic equilibrium of the reversible reaction. Should the reaction proceed in an irreversible manner, in the so-called kinetic target-guided synthesis (KTGS), target-directed selection of the building blocks occurs first.³ Following, the stabilized configuration facilitates a proximity-induced irreversible reaction, resulting in a ligand with improved affinity compared with the affinities of each reagent. In both type of reactions, the identification of the formed equilibria or products is often performed by mass spectrometry.

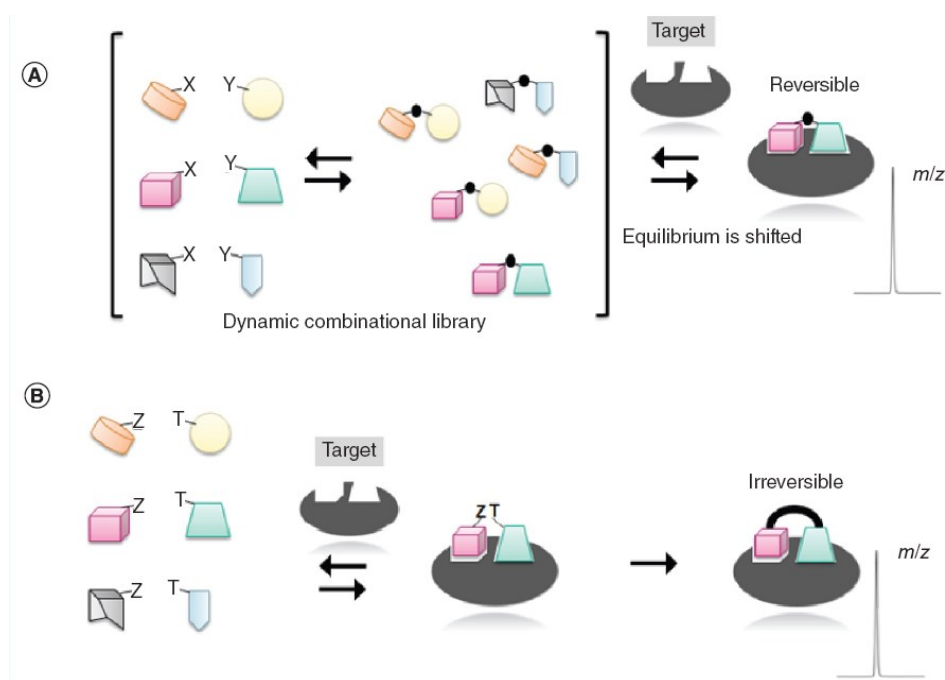


Figure 6.1. Representation of protein-directed Dynamic Combinatorial Chemistry (A) and Kinetic Target-Guided Synthesis (B). Figure was taken from ref [4].⁴

Target-assisted approaches hold significant potential for drug discovery because they circumvent the need for separate synthesis, purification/characterization and biochemical evaluation of individual compounds. Nonetheless, the domain is still in its infancy and has so far only produced convincing proof-of-concept. Several reviews comprehensively summarize all recent developments in DCC⁵⁻⁷ and KTGS.^{4,8}

An overview of reaction types that have been used in target-assisted conditions (most of them coming from the field of DCC) is shown in **Table 6.1**. It is important to consider that specific conditions are required in order to achieve successful protein-templated transformations. First, the reversible reaction should be possible in aqueous media at physiological pH, making them biocompatible. Subsequently, the different reagents should be water-soluble. A small percentage of organic co-solvent can be added to increase solubility, but only if sufficient target stability can be preserved. Next, specific reactions are selected that undergo fast equilibration. These reactions should be chemoselective to avoid cross-reactivity with functional groups of the building blocks or the target. Reactions that are characterized by these factors and have shown their applicability in target-assisted drug discovery include the reversible formation of imines, hydrazones, tioethers, disulfides and several others for DCC, and the alkyne-azide Huisgen-addition and reductive amination for KGTS.

Table 6.1. Examples of reversible and irreversible reactions used in protein-templated DCC and KGTS, respectively.

| Target-assisted approach | Type of reaction | Schematic representation | Example ref. |
|--------------------------|-------------------------------|--|--------------|
| DCC | Imine formation | $\text{R}_1\text{C}(=\text{O})\text{R}_2 + \text{H}_2\text{N}-\text{R}_3 \rightleftharpoons \text{R}_1\text{C}(\text{R}_2)=\text{N}-\text{R}_3$ | 9-10 |
| | Hydrazone formation | $\text{R}_1\text{C}(=\text{O})\text{R}_2 + \text{H}_2\text{N}-\text{N}(\text{R}_3)-\text{H} \rightleftharpoons \text{R}_1\text{C}(\text{R}_2)=\text{N}-\text{N}(\text{R}_3)-\text{H}$ | 11-12 |
| | Hemithioacetal formation | $\text{R}_1\text{C}(=\text{O})\text{H} + \text{HS}-\text{R}_2 \rightleftharpoons \text{R}_1\text{C}(\text{H})(\text{OH})\text{S}-\text{R}_2$ | 13 |
| | Disulfide formation | $\text{R}_1-\text{SH} + \text{HS}-\text{R}_2 \rightleftharpoons \text{R}_1-\text{S}-\text{S}-\text{R}_2$ | 14-15 |
| | Boronate ester formation | $\text{HO}-\text{B}(\text{R}_1)-\text{OH} + \text{HO}-\text{C}(\text{R}_2)(\text{OH})-\text{C}(\text{R}_3)(\text{OH})-\text{H} \rightleftharpoons \text{R}_1-\text{B}(\text{O})_2-\text{O}-\text{C}(\text{R}_2)(\text{OH})-\text{C}(\text{R}_3)(\text{OH})-\text{H}$ | 16 |
| KGTS | Reductive amination | $\text{R}_1\text{C}(=\text{O})\text{R}_2 + \text{H}_2\text{N}-\text{R}_3 \longrightarrow \text{R}_1\text{C}(\text{R}_2)\text{NH}-\text{R}_3$ | 17 |
| | Alkyne-azide Huisgen-addition | $\text{R}_1-\text{N}=\text{N}=\text{N}^- + \text{C}\equiv\text{C}-\text{R}_2 \longrightarrow \text{R}_1-\text{N}=\text{N}-\text{C}(\text{R}_2)=\text{N}$ | 18-19 |

Another important aspect during target-assisted experiments is that for all building block types used, the individual representatives should possess comparable reactivity. This is necessary to ensure formation of an unbiased reversible set. Finally, the post-experimental analysis of the complex mixtures that typically result under these conditions, can be challenging in its own right. Three main types of analytical techniques have been used, including HPLC^{15, 20}, native non-denaturing mass spectrometry²¹⁻²² and ligand-observed NMR spectroscopy^{13, 23}. In our perspective, HPLC-UV/MS is considered to be the most useful and straightforward. It also deserves mentioning that for DCC-experiments (performed under equilibrium conditions), reaction mixtures (and the corresponding product distributions) need to be blocked or “frozen” before analysis. This can be achieved by changing the conditions of the reversible reactions or by irreversible functionalization of the labile reaction products. Reversibly formed imines, for example, are mostly reduced to their corresponding amines using sodium cyanoborohydride.¹⁷ Reactions which are “frozen” via their conditions mostly rely on changing the pH.²⁴ Since we considered Strecker-type reactions to be essentially irreversible under

the experimental and analytical conditions that we projected (and therefore belonging to the realm of KGTS), “freezing” steps were deemed not to be required in our case.

6.1.2 The Strecker and “acyliminium-Strecker” reaction

Target-assisted drug discovery relying on Strecker or related reactions so far has not been described. As explained earlier, the typical 1-aminoalkylcarbonitrile substructures of Strecker products nonetheless are essential pharmacophores in many known protease inhibitors.²⁵⁻²⁷ In addition, caspases to date had not been studied as targets using the on-target methodology. All these considerations were decisive to set the exploration of target-assisted drug discovery on caspase-1 as an objective of the thesis. Importantly however, the basic properties of the amine function present in products of the classical Strecker protocol seemed undesirable, considering the strict endopeptidase properties of caspases. Therefore, we decided to focus on a variant of the Strecker reaction that has the potential to produce compounds with an acylated amine function, starting from the corresponding amide or carbamate building blocks. This reaction will be named the “acyliminium-Strecker” hereafter. To date, the acyliminium-Strecker synthesis has mainly focused on using carbamate building blocks, while the use of amides has largely been overlooked.²⁸⁻³⁵ Consolidating the scope of the acyliminium-Strecker synthesis by investigating the use of amide building blocks would nonetheless be highly relevant to medicinal chemistry and was one of the goals pursued in this study.

A comparison of the classical and the acyliminium-Strecker transformation is given in **Figure 6.2**. The first step in both reactions consists of the nucleophilic attack of the amine, amide or carbamate to the ketone/aldehyde, followed by a rearrangement of the protons. The next step requires acidic conditions in order to complete dehydration. The generated iminium and acyliminium ions are able to undergo tautomerization, therefore facilitating the nucleophilic attack of the cyanide ion, leading to the Strecker and acyliminium-Strecker products, respectively.³⁶⁻³⁷ Although the overall structure and mechanism of both variants are highly analogous, the number of literature antecedents for the acyliminium-Strecker is remarkably more limited.³⁸ Two inherent differences between the classical and acyliminium protocols most probably contribute to this: 1) the lower nucleophilicity of amides/carbamates when compared to the amines used in the classical protocol and 2) the limited stability/high free energy of the acyliminium intermediate compared to the iminium species of the classical variant. Both factors can reasonably be expected to translate into higher activation energy barriers in case of the acyliminium-Strecker, leading to slower and/or more sluggish performance of this variant.

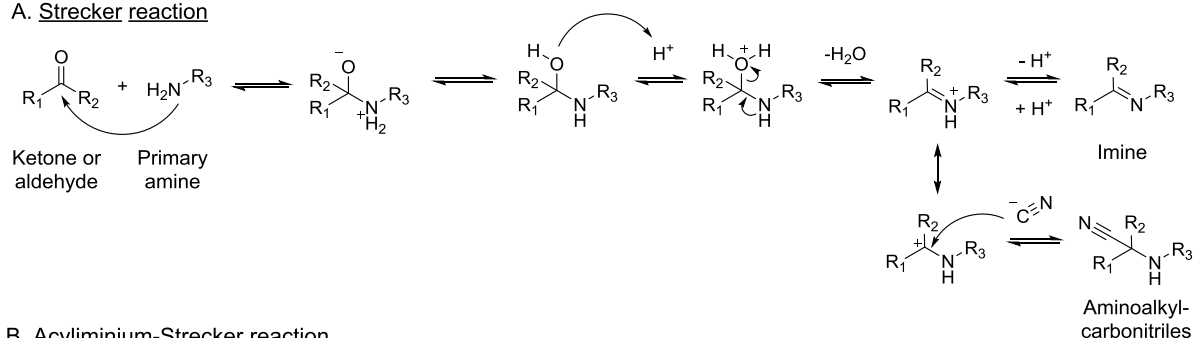
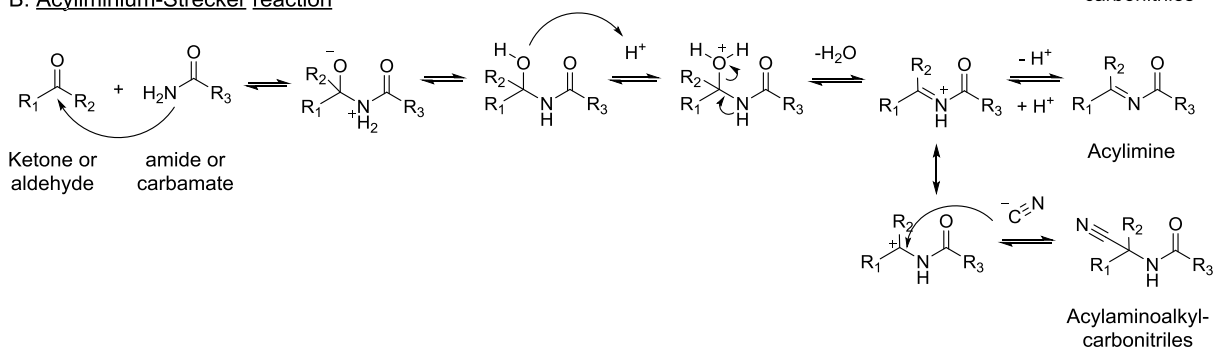
A. Strecker reactionB. Acyliminium-Strecker reaction

Figure 6.2. Mechanism of the classical Strecker reaction (A) and its variant, the acyliminium-Strecker reaction (B).

In literature, two main approaches have been followed in attempt to circumvent this problem. 1) A limited number of Lewis acids were described to promote the reaction, though the reported yields were not convincing (<10%).³⁹ 2) The most promising approach however consists of adding acyliminium-intermediate stabilizers to promote the reaction, generally in stoichiometric quantities. Well-known examples include phenylsulfonic acid (leading to the reversible formation of a 1-aminoalkylsulfone intermediate)⁴⁰ and 1H-benzotriazole (that also reversibly forms a covalent adduct).⁴¹ Interestingly, these stabilizers also seemed to be capable of adduct formation in aqueous media. Most of these literature data nonetheless had been independently reported by different groups who used differing reagent sets (aldehydes, cyanide sources, carbamates/amides) and conditions in their studies, making side-by-side comparison of all methodologies difficult. In addition, the extent to which most of the data can be extrapolated to structurally more diverse and functionalized reagents was also unclear.

1.3 Objectives of this Chapter

Starting from the state-of-the-art described above, we decided to set out on a synthetic study with which we wanted to get a clearer view on the different parameters that determine the kinetics, outcome and scope (including on the possibility to use amides) of the acyliminium-Strecker reaction. This was expected to result in two reliable and cross-optimized protocols for the reaction: 1) an “aqueous” protocol that can be used in target-guided synthesis conditions. 2) Additionally, we were interested in devising a traditional organic synthesis protocol that would allow efficient and versatile

library synthesis of protease inhibitors with an acylaminoalkylcarbonitrile basic structure. Application of both protocols would involve a diversified library of druglike amides and/or carbamates, an optimal cyanide source, and either 3-oxopropanoic acid (or a protected derivative thereof) or a suitable bioisostere of the carboxylate group equipped with an aldehyde function (**Figure 6.3**).

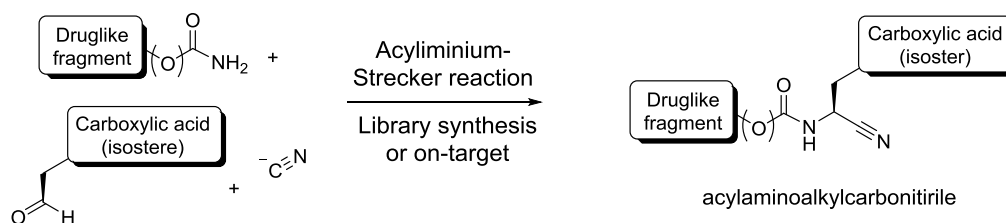


Figure 6.3. Library synthesis and target-assisted drug discovery based on the acyliminium-Strecker reaction to obtain acylaminoalkylcarbonitriles that could serve as caspase-1 inhibitors.

Noteworthy, by chemoselectively reducing the carbonitrile function in these molecules to an aldehyde group, further exploration of an alternative warhead functionality would theoretically be possible in an efficient manner (**Figure 6.4**). Finally, the acyliminium-Strecker reaction typically generates a chiral carbon. Although several papers are present that claim significant enantioselectivity by using chiral catalysts in the acyliminium-Strecker transformations, *ees* are still significantly lower than the ones attainable with the most performant enantioselective protocols for the classical Strecker reaction. Optimization of enantioselectivity nonetheless was not a direct goal of this study.

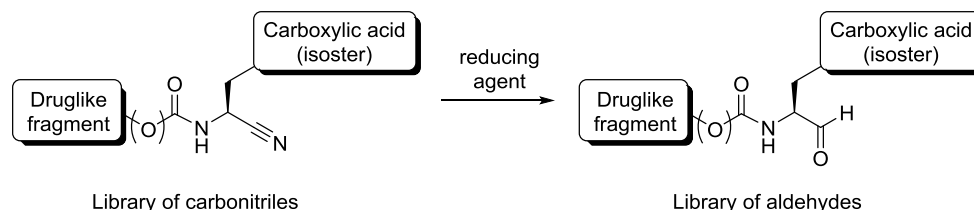


Figure 6.4. Theoretical one-step conversion of acylaminoalkylcarbonitriles into acylaminoalkylaldehydes.

6.2 Study design

Given the multitude of reaction parameters (e.g., temperature, solvent, reagent types, catalysts) that required comparison and optimization to deliver the projected protocols, it was clear that only partial achievement would be attainable during the remaining part of my PhD project. It was therefore decided to carry out mainly prospective work focused on one subgroup of approaches in the acyliminium-Strecker literature, i.e. the approaches using phenylsulfonic acid to stabilize the acyliminium intermediate as an acylaminoalkylsulfone functionality. Remarkably, the acylaminoalkylsulfone adducts are mostly synthesized separately by mixing equimolar amounts of aldehyde, carbamate (or amide) and phenylsulfonic acid.⁴² Phenylsulfonic acid's mildly acidic properties are sufficient to catalyze this condensation, although most often excess of additional acids (e.g., formic

acid) are also added for this purpose.⁴³ The resulting sulfones in many cases precipitate from the reaction mixture, allowing easy purification. In addition, these compounds are generally shelf-stable for prolonged periods of time.⁴⁴ In separate steps, the acylalkylaminosulfones can then be subjected to different types of nucleophiles, (e.g., cyanide ion, carbon nucleophiles,...) and a (Lewis) acid or base. The latter promote the *in situ* elimination of phenylsulfinate and generation of, respectively, the corresponding acyliminium or acylimine species (**Figure 6.5**). These electrophiles subsequently react with the nucleophilic partner in the reaction mixture. An extensive review by Petrini is available that comprehensively covers the chemical properties, reactivity and synthetic applications of acylaminoalkylsulfones.⁴⁵

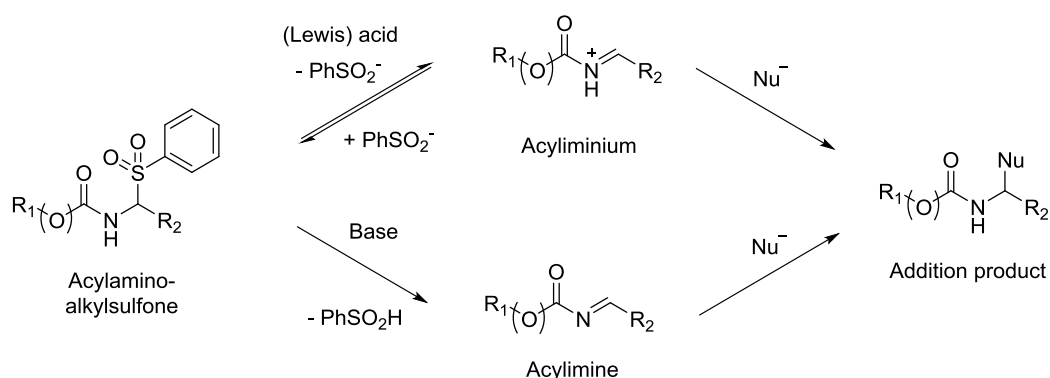


Figure 6.5. *In situ* acylimine/acyliminium formation by activating acylaminoalkylsulfones, followed by the addition reaction with an unspecified nucleophile (Nu).

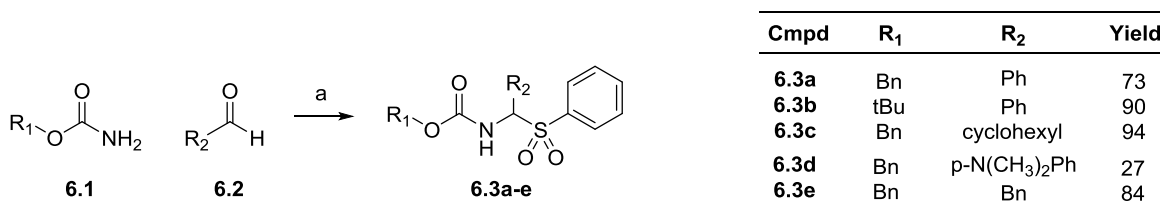
Despite the relative straightforwardness of this two-step approach, we were nonetheless interested in devising a one-pot procedure for the acyliminium-Strecker protocols. Availability of such a procedure could offer significant efficiency benefits in the framework of on-target applications or classical library synthesis. Choice of catalyst, cyanide source, solvent and temperature were considered the reaction parameters that would be focused on primarily. The optimization is divided into two parts; one where sulfones are used as isolated intermediates and one where possible one-pot procedures are explored. Given the exploratory character of these experiments, most reactions were carried out with simple, non-functionalized building blocks: *tert*-butyl carbamate, benzyl carbamate or benzamide as the acylamine reaction partner and benzaldehyde or its homologues as the aldehyde partner. Additional building blocks used include likewise simple aliphatic acylamides and aldehydes and are specified in the Results and Discussion section below.

6.3 Results and discussion

6.3.1 Experiments involving isolation of acylaminoalkylsulfone intermediates

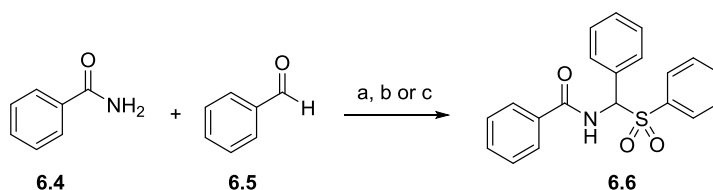
6.3.1.1 Synthesis of acylaminoalkylsulfones

The starting point for studying the first step of the approach (acylaminoalkylsulfone formation and isolation) was a widely used literature procedure in which sodium phenylsulfinate is condensed with the acylamine and aldehyde reaction partners in water:methanol (2:1) in the presence of excess formic acid (**Scheme 6.1**).²⁹ Precipitation of the product from the aqueous medium allowed easy isolation of intermediates **6.3a-e** in pure form by filtration. Acceptable yields (73-94%) were obtained for all carbamates, except for **6.3d** (27%). In case of amide starting material (**6.4**), the yield significantly dropped to 28% (**Table 6.2**, entry a). In addition, anticipating on the possibility to devise a one-pot protocol for the full acyliminium-Strecker reaction, conditions that would not lead to acylaminoalkylsulfone precipitation were subsequently explored. This goal was reached by employing phenylsulfonic acid instead of the corresponding sodium salt, allowing the use of organic solvents as the reaction media.⁴⁰ The choice for dichloromethane as the solvent in this reaction led to an increased yield (62%) in comparison with the original method (**Table 6.2**, entry b). Changing the solvent to tetrahydrofuran (**Table 6.2**, entry c) appeared to provide acylaminoalkylsulfone as well, but hindered easy isolation due to the presence of undesired side products.



Scheme 6.1. Reagents and conditions^[a]: a) Sodium benzenesulfinate, H₂O:MeOH (2:1), formic acid (20 eq.), RT, 4 d, 60-90%.

Table 6.2. Synthesis of acylaminoalkylsulfones with amide starting material

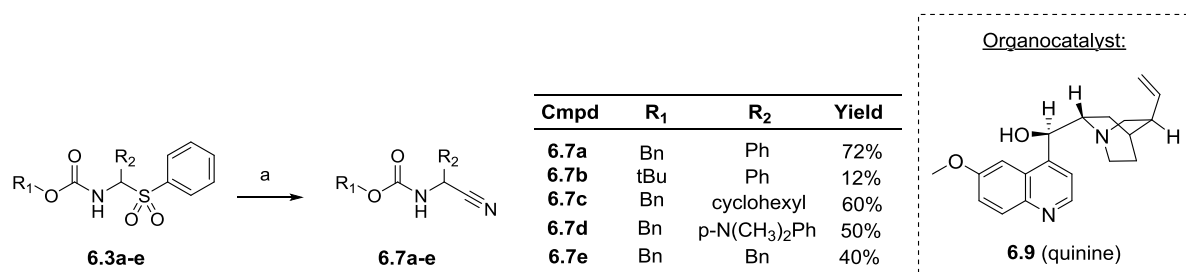


| Entry | Reagents and conditions | Yield |
|-------|--|----------------------------|
| a | Sodium phenylsulfinate, formic acid (20 eq.), H ₂ O:MeOH (2:1), 4 d | 28% |
| b | Phenylsulfonic acid, MgSO ₄ , RT, overnight | DCM 62% |
| c | | THF Purification failed |

6.3.1.2 Transformation of acylaminoalkylsulfones in the corresponding carbonitriles

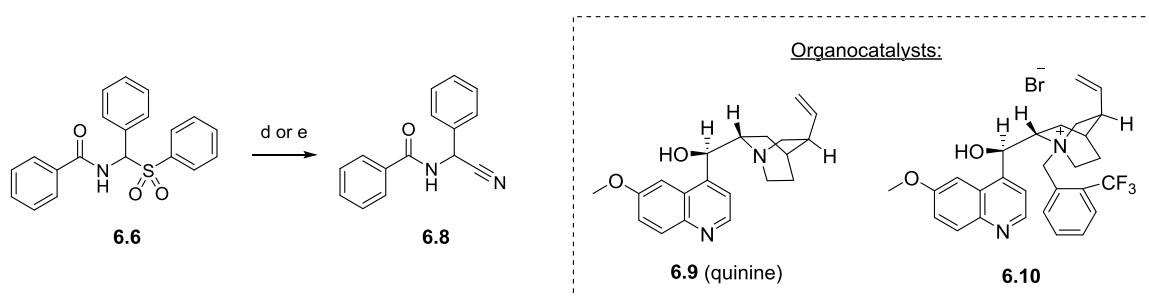
Using organocatalysts

Two literature approaches (Reingruber *et al.* and Herrera *et al.*, respectively) were compared for these experiments. Hallmarks of the procedure by Reingruber are the use of potassium cyanide and quinine (**6.9**), as an asymmetric organocatalyst.²⁹ In case of carbamate-based intermediates (**6.3a-e**), the afforded aminonitriles (**6.7a-e**) were obtained in yields varying from 12% to 72% (**Scheme 6.2**) while a yield of 92% was obtained in case of the amide (**Table 6.3**, entry d). Though the original procedure achieved enantiomeric excesses (*ees*) of the *S*-enantiomer (which would also be the desired configuration in protease inhibitors) ranging from 34 to 80%, we were not able to verify this claim. Exploratory chiral Supercritical Fluid Chromatography (SFC) experiments were performed but baseline separation of the individual enantiomers could not be obtained.



Scheme 6.2. Reagents and conditions: a) KCN, quinine (**9**), THF, -10 °C, 5 h, RT, overnight, 12 - 60%.

Further investigation comprised the exploration of the Herrera protocol (**Table 6.3**, entry e).²⁸ The latter relies on a biphasic solvent system of water and excess toluene, and a quaternary ammonium derivative of quinine (**6.10**) as the catalyst, which was synthesized as reported by the authors of the study. Other characteristics of this procedure are the application of aqueous potassium carbonate as a base and acetone cyanohydrin as an alternative and potentially safer cyanide source. Both the Reingruber and Herrera protocol showed high yields (>92%) and were thus valid candidates for implementation in a one-pot protocol.

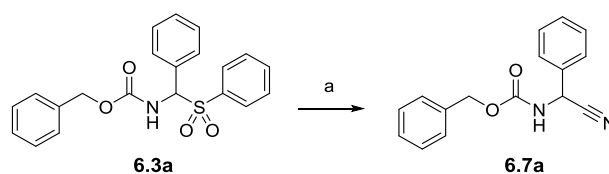
Table 6.3. Transformation of acylaminoalkylsulfones in the corresponding carbonitriles

| Entry | Reagents and conditions | Yield |
|-------|--|-------|
| d | KCN ^[a] (2 eq.), quinine (6.9), THF, -10 °C, 5 h, RT, overnight | 92% |
| e | acetone cyanohydrin (2 eq.), 6.10 , K ₂ CO ₃ ^[b] (5 eq.), toluene, RT, overnight | >99% |

[a] Suspended as a solid in the reaction mixture. [b] Added as a solution of 50% w/w in H₂O.

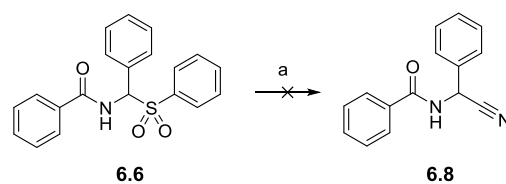
Using Lewis acid catalysts

As mentioned before, in contrast to activating acylaminoalkylsulfones into the corresponding acylimines in basic conditions, activation is also made possible via the use of Lewis acids. Several Lewis acids, such as InCl₃ and BiBr₃, have proven to be successful in classical Strecker reactions.⁴⁶⁻⁴⁸ These examples were also investigated in our setting to provide acylaminonitrile **6.7a** (**Table 6.4**). However, InCl₃ was the only catalyst able to afford the appropriate carbamate-based product. Expanding the use of this Lewis acid towards amide-containing starting material did not give satisfying results (**Scheme 6.3**), most likely due to its low solubility in this solvent. No further elaboration was done on this matter.

Table 6.4. “Consecutive” one-pot protocol for the acyliminium-Strecker reaction

| Entry | Reagents and conditions | Yield ^[a] |
|-------|------------------------------|----------------------|
| a | InCl ₃ (0.1 eq.) | >99% |
| b | BiBr ₃ (0.05 eq.) | 0% ^[b] |

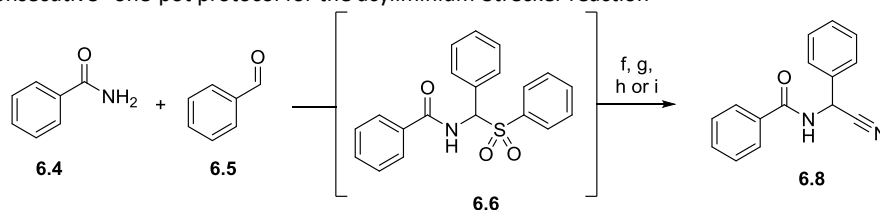
[a] Yields obtained after purification. [b] No product was formed.



6.3.1.3 One-pot protocols for the acyliminium-Strecker reaction

Two different approaches were again followed. The first one consisted of consecutively producing the intermediate acylaminoalkylsulfone and -carbonitrile in the same reaction vessel without intermediary work-up. The starting materials for the sulfone were stirred overnight, after which the cyanide source and catalyst were added for the second reaction. Since the intermediary sulfone had limited solubility in DCM (*vide supra*), the solvents from the Reingruber and Herrera protocols were selected. Moreover, only the reactions in which the reagents and conditions of these protocols were applied, were found to be successful (**Table 6.5**, entry f and i). Interestingly, tetrahydrofuran and toluene did not cause problems for the acylaminoalkylsulfone formation under these reaction configurations. Conversely, experiments involving organocatalyst **6.10** failed to provide product when only tetrahydrofuran was present as the solvent (**Table 6.5**, entry g and h), suggesting that a biphasic system is essential for this catalyst.

Table 6.5. “Consecutive” one-pot protocol for the acyliminium-Strecker reaction



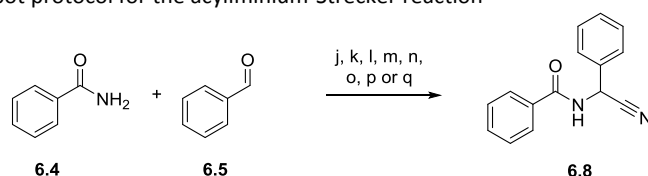
| Entry | Reagents and conditions | | | | Yield ^[a] |
|-------|---------------------------------------|---|------------------------------|----|----------------------|
| f | | KCN (2 eq.), quinine (6.9), 5 d | THF | RT | 54% |
| g | sulfonic acid, overnight, followed by | acetone cyanohydrin (2 eq.), KCN ^[b] (0.1 eq.), 6.10 , 5 d | THF | RT | failed |
| h | | acetone cyanohydrin (2 eq.), K ₂ CO ₃ ^[b] (5 eq.), 6.10 , 5 d | THF | RT | failed |
| i | sulfonic acid, overnight, followed by | acetone cyanohydrin (2 eq.), K ₂ CO ₃ ^[c] (5 eq.), 6.10 , 5 d | toluene/ H ₂ O | RT | 54% |

[a] Yields obtained after purification. [b] Suspended as a solid in the reaction mixture. [c] Added as a solution of 50% w/w in H₂O.

The second one-pot approach comprised simultaneously mixing all reagents in selected solvents or solvent mixtures and prolonged stirring (1-5 day(s)). It was hypothesized that under these conditions *in situ* formed acylaminoalkylsulfones would react further with the available cyanide source to form the desired carbonitriles. These types of reactions were performed in pressure tubes to avoid liberation (and loss) of hydrogen cyanide (**Table 6.6**). Also, in some of the cases only a catalytic amount (0.1 eq.) of phenylsulfonic acid was added, expecting that a continuous turnover of acylaminoalkylsulfones under these conditions would create sufficiently high phenylsulfinate concentrations to efficiently promote the reaction. Unfortunately, in none of the cases product formation was observed. Moreover, intermediate acylaminoalkylsulfone was identified in only one reaction (**Table 6.6**, entry p). A possible rationale for these outcomes might be found in the stoichiometry of acidic (phenylsulfonic acid) and basic (KCN, K₂CO₃) reagents in the reaction mixtures

that were evaluated. While the second reaction step (carbonitrile formation) is known to be catalyzed both by acids and bases, literature examples of acylaminoalkylsulfone formation are, to the best of our knowledge, invariably carried out under acidic conditions. Our preliminary experiments could indicate that acylaminoalkylsulfone formation is not catalyzed efficiently by bicarbonate or hydrogen cyanide. The presence (or even prevalence) of the latter, which are only weak acidic species, could result in the reaction mixture from reaction between phenylsulfonic acid and potassium carbonate or potassium cyanide, respectively. In that perspective, a straightforward modification would be to increase the amount of phenylsulfonic acid up to suprastoichiometric amounts. Additionally, in cases where the neutral cyanide source acetone cyanohydrin was used (entries p-q), change of the solvent into toluene could be considered, reflecting the conditions present in the successful “consecutive” one-pot experiments based on the Herrera protocol. Finally, in entry p, where 0.1 equivalents of potassium cyanide were supposed to help promoting the conversion of acetone cyanohydrin into cyanide ions, it could be worth to create a biphasic system (toluene/water), for example by adding potassium cyanide as an aqueous solution.

Table 6.6. “Direct” one-pot protocol for the acyliminium-Strecker reaction



| Entry | Reagents and conditions | | | Yield ^[a] |
|-------|--|------------------------------|--------|----------------------|
| j | | DCM | RT | failed |
| k | phenylsulfonic acid (0.1 eq.), quinine (6.9), KCN ^[c] (2 eq.), 1 d | DCM | reflux | failed |
| l | | THF | RT | failed |
| m | | THF | reflux | failed |
| n | phenylsulfonic acid (1.1 eq.), 6.10 , KCN ^[b] (1.1 eq.), 1 d | toluene/ H ₂ O | RT | failed |
| o | phenylsulfonic acid (0.1 eq.), 6.10 , KCN ^[b] (1.1 eq.), 1 d | toluene/ H ₂ O | RT | failed |
| p | phenylsulfonic acid (1 eq.), acetone cyanohydrin (2 eq.), KCN ^[c] (0.1 eq.), 6.10 , 5 d | THF | RT | failed |
| q | phenylsulfonic acid (1 eq.), acetone cyanohydrin (2 eq.), K ₂ CO ₃ ^[c] (5 eq.), 6.10 , 1 d | THF | RT | failed |

[a] Yields obtained after purification. [b] Added as a 1 M aqueous solution. [c] Suspended as a solid in the reaction mixture.

It should also be stressed that direct one-pot protocols imply a main competing side reaction: cyanohydrin formation from the aldehyde and (hydrogen) cyanide (**Figure 6.6**). However, since this reaction is readily reversible under the used reaction conditions and the Strecker product is essentially irreversibly formed, it is not believed to cause fundamental problems for the feasibility of the one-pot protocol.

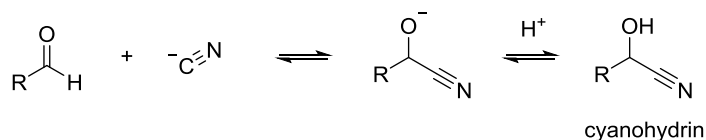


Figure 6.6. The formation of cyanohydrin as a reversible side reaction of the Strecker synthesis.

6.3.2 Preliminary experiments to produce a one-pot protocol without phenylsulfonic acid catalysis

The role of phenylsulfonic acid catalysis in the acyliminium-Strecker reaction can readily be rationalized, given its ability to stabilize the acyliminium intermediate of the reaction. Nonetheless, it seemed desirable to also investigate hypothetical protocols that do not involve this compound, but instead rely on specifically selected (Lewis) acid catalysts for direct condensation of the aldehyde, acylamine and cyanide building block, similar to existing protocols for the classical Strecker reaction.⁴⁹⁻⁵² Thorough exploration of this possibility for the acyliminium-Strecker reaction so far has not been reported in literature, but could be considered highly valuable in the framework of library synthesis. Again, only preliminary experiments were performed with unfunctionalized building blocks (benzylcarbamate, benzaldehyde) used in the foregoing part. Obtained results are summarized in **Table 6.7**. Surprisingly, a one-pot protocol with $\text{Cu}(\text{OTf})_2$ and trimethylsilyl cyanide in tetrahydrofuran delivered the desired product **6.7a** (entry a). However, changing these components led to failure of the reaction. Dichloromethane and methanol as solvent (entry b-c), TiCl_4 as catalyst (entry d) or potassium cyanide and acetone cyanohydrin as cyanide source (entry e-f) were shown to be poor alternatives.

Table 6.7. Preliminary experiments to produce a one-pot protocol without phenylsulfonic acid catalysis

| Entry | Reagents and conditions | | | | | Yield ^[b] |
|-------|---------------------------|-----------------------------|---------|-------------|------|----------------------|
| | Catalyst ^[a] | Cyanide source | Solvent | Temperature | Time | |
| a | $\text{Cu}(\text{OTf})_2$ | TMSCN (2 eq.) | THF | RT | 3 d | 39% |
| b | $\text{Cu}(\text{OTf})_2$ | TMSCN (2 eq.) | MeOH | RT | 3 d | 0% ^[b] |
| c | $\text{Cu}(\text{OTf})_2$ | TMSCN (2 eq.) | DCM | RT | 3 d | 0% ^[b] |
| d | TiCl_4 | TMSCN (2 eq.) | THF | RT | 3 d | 0% ^[b] |
| e | $\text{Cu}(\text{OTf})_2$ | KCN (1 eq.) | THF | RT | 3 d | 0% ^[b] |
| f | $\text{Cu}(\text{OTf})_2$ | acetone cyanohydrin (1 eq.) | THF | RT | 3 d | 0% ^[b] |

[a] 0.1 eq. catalyst was used. [b] Yields obtained after purification. [b] No product was formed.

6.4 Future perspectives

This study indicates that the acyliminium-Strecker reaction could be a strong candidate for efficient library synthesis of carbonitrile-containing inhibitors and, eventually, for target-assisted synthesis.

Nonetheless, it is obvious that further optimization is essential. This is currently pursued by other people in our laboratory. The following aspects are currently investigated:

- 1) The scope of building block types that can be used in the acyliminium-Strecker reaction (including, among others, functionalized aliphatic and aromatic compounds, and amino acid derivatives).
- 2) The generality of (Lewis) acid-catalyzed, direct condensation approaches and the exploration of complementary acyliminium-stabilizing protocols (involving, among others, benzotriazole and aminal-based methods).

Benzotriazole has been extensively described and used as an acyliminium stabilizing group by Katritzky and co-workers.^{41, 53} Comparable to phenylsulfonic acid, the stabilizing effect comes from covalent adduct formation with acyliminium intermediates (**Figure 6.7, A**). The covalent bond formation does not strictly require acid catalysis, although this can be applied according to literature. An alternative, more recently described approach stabilizes acyliminium intermediates derived from an aldehyde and a carbamate by covalent bond formation with an additional equivalent of carbamate.⁵⁴ This leads to an aminal-like structure that, in some cases can be isolated by precipitation. A consecutive acid-catalyzed reaction enables *in situ* generation of the acylimine (**Figure 6.7, B**).

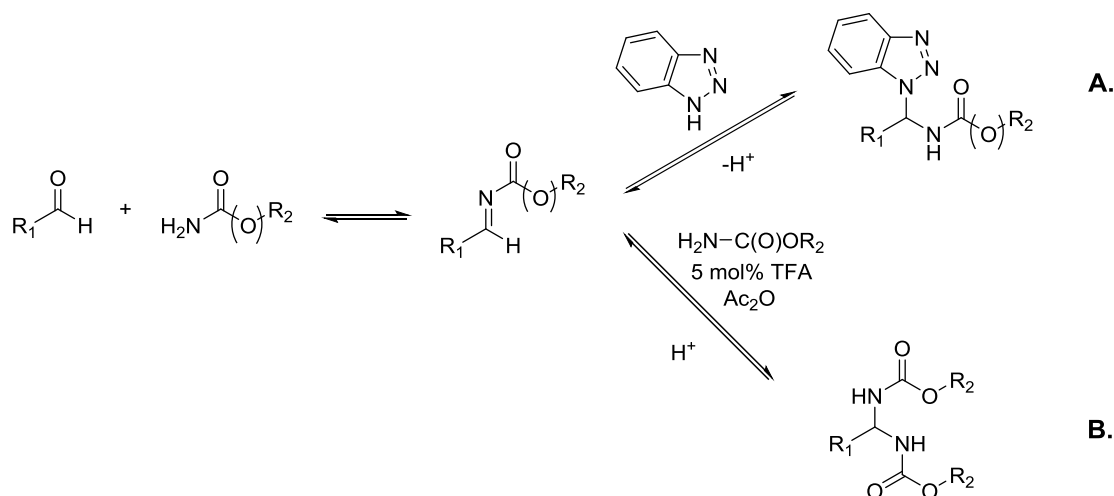
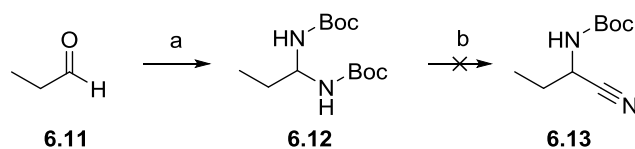


Figure 6.7. Stabilization of acylimines through the formation of acylaminoalkylbenzotriazoles (A) and *N*-acyl aminals (B).

The aminal-based strategy was already superficially evaluated as part of my own research with propanal and *tert*-butyl carbamate as the reaction partners (**Scheme 6.4**). Formation of an aminal intermediate could however not be unequivocally demonstrated and the second step, an exploratory reaction with potassium cyanide under $\text{Cu}(\text{OTf})_2$ catalysis, did not deliver the desired product. The choice of catalyst was determined by its success in reactions with similar aminal-type starting material.⁵⁴



Scheme 6.4. Reagents and conditions: a) Boc-NH₂, TFA (5 mol%), Ac₂O, RT, 15 min; b) Cu(OTf)₂ (0.1 eq.), KCN (5 eq.), DCM, RT, 24 h.

Detailed investigations to check the feasibility of an amination-based methodology are underway.

3) To allow swift quantitative analysis of reaction mixtures without the need for time-consuming product purification and isolation, LC-MS and NMR-based routines are currently under development. These should allow quick and reliable screening of different reaction protocols.

4) Enantioselectivity and/or diastereoselectivity will be taken into account as well.

6.5 Conclusion

In line with creating a protocol that could serve in efficient library and target-aided synthesis of potential caspase inhibitors, the acyliminium-Strecker synthesis was explored. Since this was not yet described before, amides were explored as building blocks for this reaction. Preliminary experiments were carried out with acylaminoalkylsulfone intermediates, in order to stabilize the acyliminium derivatives. A promising one-pot protocol was devised relying on consecutive acylaminoalkylsulfone production, *in situ* generation of acyliminium and quinine-catalyzed Strecker synthesis to afford aminonitriles. Other pathways via amination precursors or without acyliminium-stabilizing precursors were attempted as well, but were less efficient at providing the expected results. Further exploration in the laboratory focuses both on additional methodological innovation and exploration, and in developing analytical routines that facilitate the investigation of the outcome of the reactions.

6.6 Experimental section

6.6.1 Chemistry

Reagents were obtained from Sigma-Aldrich, Acros, Fluorochem or Apollo Scientific and were used without further purification. Synthesized compounds were characterized by ¹H NMR, ¹³C NMR and mass spectrometry. ¹H NMR and ¹³C NMR spectra were recorded with a 400 MHz Bruker Avance DRX 400 spectrometer, and analyzed by use of MestReNova analytical chemistry software. Where necessary, flash purification was performed with a Biotage ISOLERA One flash system equipped with an internal variable dual-wavelength diode array detector (200–400 nm). Purity is >95%, unless otherwise stated. Purities were determined with a Waters Acquity UPLC system coupled to a Waters TUV detector, ESI source and a Waters Acquity Qda Mass Detector. A Waters Acquity UPLC BEH C18 1.7 μm 2.1 x 50 mm column was used. Solvent A: water with 0.1% formic acid, solvent B: acetonitrile

with 0.1% formic acid. The (normal) gradient used started with a flow rate of 0.7 mL/min at 95% A, 5% B for 0.15 min, then in 1.85 min from 95% A, 5% B to 100% B, isocratically at the same percentage for 0.25 min and finally 0.75 min (0.350 mL/min) 95% A, 5% B.

General procedure for the preparation of carbamate-based *N*-acylaminoalkylsulfones in aqueous media (6.3a-e)

A mixture of the carbamate (1 mmol) and benzenesulfinic acid sodium salt (2 mmol) was suspended in a solution of methanol:water (1:2). Afterwards, the aldehyde (1.5 mmol) was added in one portion, followed by formic acid (20 mmol). The resulting mixture was allowed to stir for 2-4 days at room temperature. The resulting white precipitate was filtered and washed with water and diethyl ether to obtain the title compound as a solid. No further purification was required.

Benzyl phenyl(phenylsulfonyl)methylcarbamate (6.3a)

White solid, yield 73%; $R_f = 0.14$ (Hex:EtOAc 4:1, visualization by UV), $^1\text{H NMR}$ (400 MHz, CDCl_3) δ 4.94 (s, 2H, CH, NH), 5.95 (s, 2H, CH_2), 7.24 (d, 1H, benzene H), 7.34–7.47 (m, 11H, benzene H), 7.59–7.63 (m, 1H, benzene H), 7.84 ppm (d, 2H, benzene H).

***tert*-Butyl (phenyl(phenylsulfonyl)methyl)carbamate (6.3b)**

White solid, yield 90%; $^1\text{H NMR}$ (400 MHz, CDCl_3) δ 1.17 (s, 9H, CH_3), 5.81 (bd, 1H CH), 5.88 (bd, 1H, NH), 7.39-7.33 (m, 5H, benzene H), 7.48-7.44 (m, 2H, benzene H), 7.58-7.55 (m, 1H, benzene H), 7.85 ppm (d, 2H, benzene H).

Benzyl (cyclohexyl(phenylsulfonyl)methyl)carbamate (6.3c)

White solid, 94% yield, $^1\text{H NMR}$ (400 MHz, CDCl_3) δ 1.81-1.08 (m, 9H, cyclohexyl), 2.18-2.12 (m, 1H, cyclohexyl), 2.50-2.44 (m, 1H, cyclohexyl), 4.91-4.74 (m, 3H, CH, CH_2), 5.47 (d, 1H, NH), 7.43-7.19 (m, 7H, benzene H), 7.59-7.56 (m, 1H, benzene H), 7.85-7.83 ppm (m, 2H, benzene H).

Benzyl ((4-(dimethylamino)phenyl)(phenylsulfonyl)methyl)carbamate (6.3d)

White solid, 27% yield, $^1\text{H NMR}$ (400 MHz; CDCl_3) δ 3.02 (s, 6H, CH_3) 4.91 (d, 1H, CH_2), 4.95 (1H, d, CH_2), 5.98 (d, 1H, CHNH), 6.22 (d, 1H, NH), 7.23-7.25 (m, 2H, benzene H), 7.45-7.32 (m, 10H, benzene H), 7.60 (t, 1H, benzene H), 7.83 ppm (d, 2H, benzene H).

Benzyl (2-phenyl-1-(phenylsulfonyl)ethyl)carbamate (6.3e)

White solid, 84% yield, $R_f = 0.18$ (Hex:EtOAc 8:2, visualization by UV); $^1\text{H NMR}$ (400 MHz, CDCl_3) δ 3.03 (d, 1H, CH_2), 3.66 (d, 1H, CH), 4.73 (d, 1H, CH_2), 4.77 (d, 1H, CH_2), 5.18 (m, 1H, CH_2), 5.28 (d, 1H, NH),

7.07–7.09 (m, 2H, benzene H), 7.21–7.32 (m, 8H, benzene H), 7.45 (t, 2H, benzene H), 7.61 (t, 1H, benzene H), 7.90–7.92 ppm (m, 2H, benzene H).

Benzenesulfinic acid

Sodium benzenesulfinate (2.46 g, 15 mmol) was dissolved in water (150 mL), and the mixture was stirred until a clear solution was obtained. Diethyl ether (60 mL) was added followed by the slow addition of concentrated aqueous hydrochloric acid (1.6 mL, 15 mmol) over 2 min. The mixture was stirred for an additional 20–30 min and the aqueous layer was removed. The organic layer was concentrated *in vacuo*, and the white solid obtained was dried under vacuum to give benzenesulfinic acid (1 g, 47%). The compound was stored at -20 °C. ¹H NMR (400 MHz, DMSO-*d*₆) δ 7.54 - 7.59 (m, 3H), 7.64 - 7.70 ppm (m, 2H).

***N*-(Phenyl(phenylsulfonyl)methyl)benzamide (6.6, Table 6.2, entry a)**

A mixture of benzamide (1 g, 8.26 mmol) and sodium benzenesulfinate (2.71 g, 16.51 mmol) was suspended in a solution of methanol:water (1:2, 15 mL). Afterwards, benzaldehyde (1.259 mL, 12.38 mmol) was added in one portion, followed by formic acid (6.23 mL, 165 mmol). The resulting mixture was allowed to stir for 4 days at room temperature. The resulting precipitate was filtered and washed with water and diethyl ether. Acylaminoalkylsulfone **6.6** was obtained as a white solid (800 mg, 28%). *R*_f = 0.37 (Hex:EtOAc 1:1, visualization by UV); ¹H NMR (400 MHz, CDCl₃) δ 6.50 (d, *J* = 10.4 Hz, 1H), 7.20 (d, *J* = 10.3 Hz, 1H), 7.38 – 7.57 (m, 9H), 7.58 – 7.72 (m, 3H), 7.89 ppm (d, *J* = 7.5 Hz, 2H); UPLC-MS *m/z*: 374.1 [M+Na]⁺.

***N*-(Phenyl(phenylsulfonyl)methyl)benzamide (6.6, Table 6.2, entry b)**

Benzamide (200 mg, 1.651 mmol) was dissolved in DCM (10 mL) and then benzenesulfinic acid (258 mg, 1.816 mmol), benzaldehyde (0.168 mL, 1.651 mmol) and anhydrous MgSO₄ (40 mg) were sequentially added at room temperature. The mixture was stirred overnight at room temperature, under a nitrogen atmosphere. The formed precipitate was filtered and washed with DCM. The crude was dissolved in THF, filtered over a short pad of Florisil and concentrated *in vacuo*. Acylaminoalkylsulfone **6.6** was obtained as a white solid (360 mg, 62%). Similar analytical properties were obtained as for **6.6**, entry a.

General Procedure for the acyliminium-Strecker reaction to obtain carbamate-based acylaminonitriles (6.7a-e)

A 0.5 M solution of the *N*-carbamoyl- α -(phenylsulfonyl)amine (**6.3a-e**) (1 mmol) and quinine (5 mol%) in CH₂Cl₂ (1.0 mL) was cooled to -10 °C under nitrogen. At this temperature KCN (2 mmol) was added

and the reaction mixture was stirred vigorously for 24 h at room temperature. After completion, the mixture was quenched with saturated aqueous NaHCO₃ (10 mL), extracted with CH₂Cl₂ (2 x 25 mL), dried over Na₂SO₄ and concentrated under vacuum. The resulting residue was further purified by column chromatography to give the pure title compounds.

Benzyl (cyano(phenyl)methyl)carbamate (6.7a)

White solid, 62% yield, R_f = 0.30 (EtOAc:hept 1:2, visualization with UV and PMA); ¹H NMR (400 MHz, CDCl₃), δ 5.12 (s, 2H, CH₂), 5.37 (d, 1H, CH), 5.80 (bd, 1H, NH), 7.55 - 7.24 ppm (m, 10H, benzene H); UPLC-MS *m/z*: 267.1 [M+H]⁺

tert-Butyl (cyano(phenyl)methyl)carbamate (6.7b)

Colorless solid, 12%, mp 81.4–83.1 °C, R_f = 0.61 (EtOAc/cyclohexane 1:1, visualization by KMnO₄); ¹H NMR (400 MHz, CDCl₃) δ 1.47 (s, 9H, CH₃), 5.26 (d, 1H, NH), 5.80 (d, 1H, CHCN), 7.41–7.48 ppm (m, 5H, benzene H).

Benzyl (cyano(cyclohexyl)methyl)carbamate (6.7c)

White solid, 60% yield, ¹H NMR (400 MHz, CDCl₃) δ 1.09–1.29 (m, 5H, cyclohexyl), 1.69–1.87 (m, 6H, cyclohexyl), 4.52 (d, 1H, CHCN), 5.14 (bs, 3H), 7.33–7.40 ppm (m, 5H, benzene H).

Benzyl (cyano(4-(dimethylamino)phenyl)methyl)carbamate (6.7d)

White solid, 50% yield, ¹H NMR (400 MHz, CDCl₃) δ 3.09 (s, 3H, CH₃), 5.12 (s, 2H, CH₂), 5.37 (d, 1H, CH), 5.80 (d, 1H, NH), 7.65–7.34 ppm (m, 9H, benzene H).

Benzyl (1-cyano-2-phenylethyl)carbamate (6.7e)

White solid, 40% yield, ¹H NMR (400 MHz, CDCl₃) δ 2.94 (dd, 1H, CH₂); 3.01 (dd, 1H, CH₂), 4.78 (dd, 1H, CH), 4.94 (d, 1H, NH), 4.98 (s, 2H, CH₂), 7.15–7.13 (m, 2H, benzene H), 7.26–7.20 ppm (m, 8H, benzene H).

N-(Cyano(phenyl)methyl)benzamide (6.8, Table 6.3, entry d)

Acylaminoalkylsulfone **6.6** (0.5 g, 1.423 mmol) and quinine (**6.9**, 0.023 g, 0.071 mmol) were dissolved in THF (50 mL) and cooled to -10 °C under nitrogen atmosphere. At the same temperature potassium cyanide (0.185 g, 2.85 mmol) was added and the reaction mixture was stirred vigorously for 5 h at -10 °C and then overnight at room temperature. The mixture was reduced *in vacuo*, quenched with saturated aqueous NaHCO₃ (30 mL) and extracted with EtOAc (3 x 20 mL). The organic layers were combined, washed with water (30 mL), brine (30 mL), dried over Na₂SO₄ and concentrated *in vacuo*. Flash chromatography was performed to obtain carbonitrile **6.8** as a white solid (310 mg, 92%). R_f =

0,61 (Hept:EtOAc 1:1, visualization by UV); ¹H NMR (400 MHz, CDCl₃) δ 6.36 (d, *J* = 8.3 Hz, 1H), 6.58 (d, *J* = 8.0 Hz, 1H), 7.43 - 7.51 (m, 5H), 7.53 - 7.60 (m, 3H), 7.77 - 7.83 ppm (m, 2H); ¹³C NMR (101 MHz, CDCl₃) δ 44.66, 117.62, 127.20, 127.46, 128.89, 129.52, 129.70, 132.50, 132.63, 133.34, 166.71 ppm; UPLC-MS *m/z*: 237.1 [M+H]⁺.

***N*-(Cyano(phenyl)methyl)benzamide (6.8, Table 6.3, entry e)**

To a solution of *N*-(phenyl(phenylsulfonyl)methyl)benzamide (0.1 g, 0.285 mmol) in toluene (10 mL) was added quaternary quinine (**6.10**) followed by acetone cyanohydrin (0.052 ml, 0.569 mmol) and aqueous potassium carbonate (0.197 g, 1.423 mmol) (50% w/w) in one portion. The reaction mixture was stirred vigorously overnight at room temperature. No precautions were done to exclude moisture or air. The reaction was quenched with saturated NaHCO₃ (20 mL) and the aqueous layer was extracted with DCM (3 x 15 mL). The combined organic layers were washed with water (20 mL), brine (20 mL), dried over Na₂SO₄ and concentrated *in vacuo*. The residue was purified by preparative TLC (1:1 Hex:EtOAc) to afford target compound **6.8** as a yellow solid product (70 mg, >99%). Similar analytical properties were obtained as for **6.8**, entry e.

Benzyl (cyano(phenyl)methyl)carbamate (6.7a), prepared from the corresponding sulfone by using a Lewis acid (Table 6.4, entry a)

Trimethylsilyl cyanide (1.2 mmol) was added dropwise to a solution of an *N*-acylaminoalkylsulfone **6.3a** (1 mmol) and InCl₃ (10 mol%) in CH₂Cl₂ (5 mL) under nitrogen. The mixture was stirred, and the reaction was monitored by TLC. After completion (2 h), the reaction was quenched with distilled H₂O (5 mL) and the mixture was extracted with EtOAc (3 x 10 mL). The combined organic portions were washed with H₂O (2 x 10 mL) and saturated aqueous NH₄Cl solution (2 x 10 mL), dried over anhydrous Na₂SO₄ and concentrated *in vacuo* to obtain pure aminonitrile **6.7a** (>99% yield). Similar analytical properties were obtained as previously described.

***N*-(Cyano(phenyl)methyl)benzamide (6.8, Table 6.5, entry f)**

Benzamide (200 mg, 1.651 mmol) was dissolved in THF (10 mL) and then benzenesulfinic acid (258 mg, 1.816 mmol) and benzaldehyde (0.168 mL, 1.651 mmol) were sequentially added at room temperature. The mixture was stirred overnight at room temperature, under a nitrogen atmosphere. Additional THF (35 mL) was added to facilitate dissolving the formed intermediate. Quinine (27 mg, 0.083 mmol) and potassium cyanide (215 mg, 3.30 mmol) were added and left stirring for 4 days. A similar work-up as for “**6.8**, entry d” was performed to obtain aminonitrile **6.8** as a white solid (210 mg, 54%). Similar analytical properties were obtained as previously described.

***N*-(Cyano(phenyl)methyl)benzamide (6.8, Table 6.5, entry i)**

Benzamide (200 mg, 1.651 mmol) was dissolved in toluene (10 mL) and then benzenesulfonic acid (258 mg, 1.816 mmol) and benzaldehyde (0.168 ml, 1.651 mmol) were sequentially added at room temperature. It takes about 10 minutes before a clear solution is obtained. The mixture was stirred overnight at room temperature, under a nitrogen atmosphere. Additional toluene (55 mL) was added to facilitate dissolving the formed intermediate but no clear solution was obtained. Quaternary quinine (**6.6**), acetone cyanohydrin (0.302 mL, 3.30 mmol) and aqueous potassium carbonate (1141 mg, 8.26 mmol, 50% w/w) were then added and left stirring for 5 d. A similar work-up as for "**6.8**, entry d" was performed to obtain **6.8** as a yellow solid (210 mg, 54%). Similar analytical properties were obtained as previously described.

Benzyl (cyano(phenyl)methyl)carbamate (6.7a), prepared from the corresponding carbamate and aldehyde via a one-pot reaction with a Lewis acid (Table 6.7, entry a)

Benzyl carbamate (0.783 g, 5.18 mmol) and benzaldehyde (0.476 mL, 4.71 mmol) were dissolved in dry THF (6 mL) under inert atmosphere in the presence of MgSO₄. Then catalyst Cu(OTf)₂ (0.170 g, 0.471 mmol) was added and TMSCN (1.179 mL, 9.42 mmol) was added dropwise. The reaction was stirred at room temperature for 3 days. The reaction mixture was diluted with water (50 mL) and extracted with EtOAc (2 x 50 mL). The combined organic phases were washed with brine, dried (Na₂SO₄) and concentrated *in vacuo*. The product was purified by flash chromatography (hept:EtOAc) and recrystallized in a mixture of EtOAc and heptane to obtain **6.7a** as a white crystal (595 mg, 47%). Similar analytical properties were obtained as previously described.

Di-*tert*-butyl propane-1,1-diylidicarbamate (6.12)

Propionaldehyde (444 μL, 6.1 mmol) and *O*-*t*-butyl carbamate (644 mg, 5.5 mmol) were added into acetic anhydride (750 μL, 7.95 mmol). To this suspension was added trifluoroacetic acid (21 μL, 0.274 mmol), which lead to immediate solidifying. Hexane was added to facilitate stirring and the mixture was stirred for 2 h. The *N*-Boc-protected aminal **6.12** was obtained as a white powder by filtration. UPLC-MS showed the presence of target compound, but NMR showed *tert*-butyl carbamate. ¹H NMR (400 MHz, CDCl₃) δ 1.43 (s, 9H), 4.74 ppm (s, 2H); ¹³C NMR (101 MHz, CDCl₃) δ 28.25, 79.68, 156.29 ppm; UPLC-MS *m/z*: 297.1 [M+H]⁺.

References

1. Merino, P.; Marqués-López, E.; Tejero, T.; Herrera, R. P., Organocatalyzed Strecker reactions. *Tetrahedron* **2009**, *65* (7), 1219-1234.
2. Lehn, J. M.; Eliseev, A. V., Chemistry - Dynamic combinatorial chemistry. *Science* **2001**, *291* (5512), 2331-2332.
3. Hu, X. D.; Manetsch, R., Kinetic target-guided synthesis. *Chem. Soc. Rev.* **2010**, *39* (4), 1316-1324.
4. Bosc, D.; Jakhlal, J.; Deprez, B.; Deprez-Poulain, R., Kinetic target-guided synthesis in drug discovery and chemical biology: a comprehensive facts and figures survey. *Future Med. Chem.* **2016**, *8* (4), 381-404.
5. Herrmann, A., Dynamic combinatorial/covalent chemistry: a tool to read, generate and modulate the bioactivity of compounds and compound mixtures. *Chem. Soc. Rev.* **2014**, *43* (6), 1899-1933.
6. Huang, R. J.; Leung, I. K. H., Protein-Directed Dynamic Combinatorial Chemistry: A Guide to Protein Ligand and Inhibitor Discovery. *Molecules* **2016**, *21* (7).
7. Mondal, M.; Hirsch, A. K. H., Dynamic combinatorial chemistry: a tool to facilitate the identification of inhibitors for protein targets. *Chem. Soc. Rev.* **2015**, *44* (8), 2455-2488.
8. Oueis, E.; Sabot, C.; Renard, P. Y., New insights into the kinetic target-guided synthesis of protein ligands. *Chem. Commun.* **2015**, *51* (61), 12158-12169.
9. Nasr, G.; Petit, E.; Supuran, C. T.; Winum, J. Y.; Barboiu, M., Carbonic anhydrase II-induced selection of inhibitors from a dynamic combinatorial library of Schiff's bases. *Bioorg. Med. Chem. Lett.* **2009**, *19* (21), 6014-6017.
10. Nasr, G.; Petit, E.; Vullo, D.; Winum, J. Y.; Supuran, C. T.; Barboiu, M., Carbonic Anhydrase-Encoded Dynamic Constitutional Libraries: Toward the Discovery of Isozyme-Specific Inhibitors. *J. Med. Chem.* **2009**, *52* (15), 4853-4859.
11. Sindelar, M.; Lutz, T. A.; Petrera, M.; Wanner, K. T., Focused Pseudostatic Hydrazone Libraries Screened by Mass Spectrometry Binding Assay: Optimizing Affinities toward gamma-Aminobutyric Acid Transporter 1. *J. Med. Chem.* **2013**, *56* (3), 1323-1340.
12. Sindelar, M.; Wanner, K. T., Library Screening by Means of Mass Spectrometry (MS) Binding Assays-Exemplarily Demonstrated for a Pseudostatic Library Addressing gamma-Aminobutyric Acid (GABA) Transporter 1 (GAT1). *ChemMedChem* **2012**, *7* (9), 1678-1690.
13. Caraballo, R.; Dong, H.; Ribeiro, J. P.; Jimenez-Barbero, J.; Ramstrom, O., Direct STD NMR Identification of beta-Galactosidase Inhibitors from a Virtual Dynamic Hemithioacetal System. *Angew. Chem., Int. Ed.* **2010**, *49* (3), 589-593.
14. Saiz, C.; Castillo, V.; Fontan, P.; Bonilla, M.; Salinas, G.; Rodriguez-Haralambides, A.; Mahler, S., Discovering Echinococcus granulosus thioredoxin glutathione reductase inhibitors through site-specific dynamic combinatorial chemistry. *Mol. Diversity* **2014**, *18* (1), 1-12.
15. Scott, D. E.; Dawes, G. J.; Ando, M.; Abell, C.; Ciulli, A., A Fragment-Based Approach to Probing Adenosine Recognition Sites by Using Dynamic Combinatorial Chemistry. *ChemBioChem* **2009**, *10* (17), 2772-2779.
16. Leung, I. K. H.; Brown, T.; Schofield, C. J.; Claridge, T. D. W., An approach to enzyme inhibition employing reversible boronate ester formation. *MedChemComm* **2011**, *2* (5), 390-395.

17. Arico, F.; Chang, T.; Cantrill, S. J.; Khan, S. I.; Stoddart, J. F., Template-directed synthesis of multiply mechanically interlocked molecules under thermodynamic control. *Chem. - Eur. J.* **2005**, *11* (16), 4655-4666.
18. Manetsch, R.; Krasinski, A.; Radić, Z.; Raushel, J.; Taylor, P.; Sharpless, K. B.; Kolb, H. C., In Situ Click Chemistry: Enzyme Inhibitors Made to Their Own Specifications. *J. Am. Chem. Soc.* **2004**, *126* (40), 12809-12818.
19. Lewis, W. G.; Green, L. G.; Grynszpan, F.; Radić, Z.; Carlier, P. R.; Taylor, P.; Finn, M. G.; Sharpless, K. B., Click Chemistry In Situ: Acetylcholinesterase as a Reaction Vessel for the Selective Assembly of a Femtomolar Inhibitor from an Array of Building Blocks. *Angew. Chem., Int. Ed.* **2002**, *41* (6), 1053-1057.
20. Milanesi, L.; Hunter, C. A.; Sedelnikova, S. E.; Waltho, J. P., Amplification of bifunctional ligands for calmodulin from a dynamic combinatorial library. *Chem. - Eur. J.* **2006**, *12* (4), 1081-1087.
21. Lienard, B. M. R.; Selevsek, N.; Oldham, N. J.; Schofield, C. J., Combined mass spectrometry and dynamic chemistry approach to identify metalloenzyme inhibitors. *ChemMedChem* **2007**, *2* (2), 175-+.
22. Lienard, B. M. R.; Hueting, R.; Lassaux, P.; Galleni, M.; Frere, J. M.; Schofield, C. J., Dynamic combinatorial mass spectrometry leads to metallo-beta-lactamase inhibitors. *J. Med. Chem.* **2008**, *51* (3), 684-688.
23. Leung, I. K. H.; Demetriades, M.; Hardy, A. P.; Lejeune, C.; Smart, T. J.; Szollossi, A.; Kawamura, A.; Schofield, C. J.; Claridge, T. D. W., Reporter Ligand NMR Screening Method for 2-Oxoglutarate Oxygenase Inhibitors. *J. Med. Chem.* **2013**, *56* (2), 547-555.
24. Otto, S.; Furlan, R. L. E.; Sanders, J. K. M., Dynamic combinatorial libraries of macrocyclic disulfides in water. *J. Am. Chem. Soc.* **2000**, *122* (48), 12063-12064.
25. Fleming, F. F.; Yao, L. H.; Ravikumar, P. C.; Funk, L.; Shook, B. C., Nitrile-Containing Pharmaceuticals: Efficacious Roles of the Nitrile Pharmacophore. *J. Med. Chem.* **2010**, *53* (22), 7902-7917.
26. Bone, H. G.; Dempster, D. W.; Eisman, J. A.; Greenspan, S. L.; McClung, M. R.; Nakamura, T.; Papapoulos, S.; Shih, W. J.; Rybak-Feiglin, A.; Santora, A. C.; Verbruggen, N.; Leung, A. T.; Lombardi, A., Odanacatib for the treatment of postmenopausal osteoporosis: development history and design and participant characteristics of LOFT, the Long-Term Odanacatib Fracture Trial. *Osteoporosis Int.* **2015**, *26* (2), 699-712.
27. Scott, L. J., Linagliptin In Type 2 Diabetes Mellitus. *Drugs* **2011**, *71* (5), 611-624.
28. Herrera, R. P.; Sgarzani, V.; Bernardi, L.; Fini, F.; Pettersen, D.; Ricci, A., Phase Transfer Catalyzed Enantioselective Strecker Reactions of α -Amido Sulfones with Cyanohydrins. *J. Org. Chem.* **2006**, *71* (26), 9869-9872.
29. Reingruber, R.; Baumann, T.; Dahmen, S.; Bräse, S., Use of the Chiral Pool - Practical Asymmetric Organocatalytic Strecker Reaction with Quinine. *Adv. Synth. Catal.* **2009**, *351* (7-8), 1019-1024.
30. Yan, H.; Suk Oh, J.; Lee, J. W.; Eui Song, C., Scalable organocatalytic asymmetric Strecker reactions catalysed by a chiral cyanide generator. *Nat. Commun.* **2012**, *3*, 1212.
31. Ooi, T.; Uematsu, Y.; Fujimoto, J.; Fukumoto, K.; Maruoka, K., Advantage of in situ generation of N-arylsulfonyl imines from α -amide sulfones in the phase-transfer-catalyzed asymmetric Strecker reaction. *Tetrahedron Lett.* **2007**, *48* (8), 1337-1340.

32. Hu, X.; Li, R.; Li, Z., Conversion of N-benzyloxycarbonylamino- and N-tosylamino-benzyl phenylsulfones by green Strecker reactions to α -aminobenzyl nitriles using potassium hexacyanoferrate(II). *J. Chem. Res.* **2014**, *38* (7), 432-436.
33. Banphavichit, V.; Chaleawertumpon, S.; Bhanthumnavin, W.; Vilaivan, T., A Convenient Synthesis of N-Boc-Protected α -Aminonitriles from α -Amidosulfones. *Synth. Commun.* **2004**, *34* (17), 3147-3160.
34. Pori, M.; Galletti, P.; Soldati, R.; Giacomini, D., Asymmetric Strecker Reaction with Chiral Amines: a Catalyst-Free Protocol Using Acetone Cyanohydrin in Water. *Eur. J. Org. Chem.* **2013**, *2013* (9), 1683-1695.
35. Ohkuma, T.; Kurono, N., Asymmetric Cyanation with the Chiral Ru-Li Combined Catalysts. *Synlett* **2012**, (13), 1865-1881.
36. Taillades, J.; Commeyras, A., Systemes de strecker et apparentes—II. *Tetrahedron* **1974**, *30* (15), 2493-2501.
37. Ogata, Y.; Kawasaki, A., Mechanistic aspects of the Strecker aminonitrile synthesis. *J. Chem. Soc. B* **1971**, (0), 325-329.
38. Petrini, M.; Torregiani, E., Recent Advances in Stereoselective Syntheses Using N-Acylimines. *Synthesis* **2007**, *2007* (2), 159-186.
39. Meester, W. J. N.; van Maarseveen, J. H.; Kirchsteiger, K.; Hermkens, P. H. H.; Schoemaker, H. E.; Hiemstra, H.; Rutjes, F. P. J. T., Scope and limitations of the solution and solid phase synthesis of homoallylic amines via N-acyliminium ion reactions. *Arkivoc* **2004**, 122-151.
40. Petrini, M.; Seri, M., α -Amido sulfones from natural α -amino acids and their reaction with carbon nucleophiles. *Tetrahedron* **2006**, *62* (5), 960-967.
41. Katritzky, A. R.; Manju, K.; Singh, S. K.; Meher, N. K., Benzotriazole mediated amino-, amido-, alkoxy- and alkylthio-alkylation. *Tetrahedron* **2005**, *61* (10), 2555-2581.
42. Lucchetti, N.; Lancianesi, S.; Petrini, M., α -Acryloylamidoalkyl Sulfones in a Synthetic Approach for the Preparation of 6-Alkyltetrahydropyridin-2-ones. *Eur. J. Org. Chem.* **2014**, *2014* (25), 5433-5441.
43. Sisko, J.; Mellinger, M.; Sheldrake, P. W.; Baine, N. H., An efficient method for the synthesis of substituted TosMIC precursors. *Tetrahedron Lett.* **1996**, *37* (45), 8113-8116.
44. Yin, B. L.; Zhang, Y. X.; Xu, L. W., Recent Applications of α -Amido Sulfones as in situ Equivalents of Activated Imines for Asymmetric Catalytic Nucleophilic Addition Reactions. *Synthesis* **2010**, (21), 3583-3595.
45. Petrini, M., α -Amido sulfones as stable precursors of reactive N-acylimino derivatives. *Chem. Rev.* **2005**, *105* (11), 3949-3977.
46. Kadam, S. T.; Thirupathi, P.; Kim, S. S., Synthetic application of in situ generation of N-acyliminium ions from α -amido p-tolylsulfones for the synthesis of α -amino nitriles. *Tetrahedron* **2010**, *66* (9), 1684-1688.
47. Das, B.; Damodar, K.; Shashikanth, B.; Srinivas, Y.; Kalavathi, I., A Mild and Efficient Catalytic Strecker Reaction of N-Alkoxy carbonylamino Sulfones with Trimethylsilyl Cyanide Using Indium(III) Chloride: A Facile Synthesis of α -Aminonitriles. *Synlett* **2008**, *2008* (20), 3133-3136.
48. Wang, J.; Hu, X. L.; Jiang, J.; Gou, S. H.; Huang, X.; Liu, X. H.; Feng, X. M., Asymmetric activation of tropos 2,2'-biphenol with cinchonine generates an effective catalyst for the asymmetric Strecker reaction of N-Tosyl-protected aldimines and ketoimines. *Angew. Chem., Int. Ed.* **2007**, *46* (44), 8468-8470.

49. Ranu, B. C.; Dey, S. S.; Hajra, A., Indium trichloride catalyzed one-step synthesis of α -amino nitriles by a three-component condensation of carbonyl compounds, amines and potassium cyanide. *Tetrahedron* **2002**, *58* (13), 2529-2532.
50. De, S. K., RuCl₃ Catalyzed One-Pot Synthesis of α -Aminonitriles. *Synth. Commun.* **2005**, *35* (5), 653-656.
51. Kobayashi, S.; Busujima, T., Scandium triflate-catalyzed Strecker-type reactions of aldehydes, amines and tributyltin cyanide in both organic and aqueous solutions. Achievement of complete recovery of the tin compounds toward environmentally-friendly chemical processes. *Chem. Commun.* **1998**, (9), 981-982.
52. De, S. K.; Gibbs, R. A., Praseodymium Trifluoromethylsulfonate as an Efficient and Recyclable Catalyst for the Synthesis of α -Aminonitriles. *Synth. Commun.* **2005**, *35* (7), 961-966.
53. Katritzky, A. R.; Lan, X.; Yang, J. Z.; Denisko, O. V., Properties and Synthetic Utility of N-Substituted Benzotriazoles. *Chem. Rev.* **1998**, *98* (2), 409-548.
54. Kano, T.; Yurino, T.; Asakawa, D.; Maruoka, K., Acid-Catalyzed In Situ Generation of Less Accessible or Unprecedented N-Boc Imines from N-Boc Amins. *Angew. Chem., Int. Ed.* **2013**, *52* (21), 5532-5534.

CONFIDENTIAL

Chapter 7

**Approach to induce caspase-1 degradation via
thalidomide conjugates**

**This chapter has been removed from this thesis due to limited Intellectual Property rights.
Please contact the author for access.**

7 Approach to induce caspase-1 degradation via thalidomide conjugates

This chapter has been removed from this thesis due to limited Intellectual Property rights.

Chapter 8

Conclusions and Outlook

8 Conclusions and Outlook

8.1 Conclusions

One of the main objectives of this PhD thesis was the discovery of improved caspase inhibitors by implementing carboxylate isosteres. First, replacing the acidic function in caspase-1 inhibitor VRT-043198 by acylsulfonamide moieties led to analogues with similar caspase affinities as the carboxylate-based reference inhibitor. Moreover, we discovered that these compounds presented enhanced cell permeability as a consequence of their potential to act as prodrugs. The basis in the understanding of the activation of these aldehyde-containing prodrugs was unraveled by a comprehensive ^1H and ^{13}C NMR study. Next, alteration of the aldehyde warhead into a carbonitrile provided inhibitors without prodrug activation, but the determined IC_{50} values disfavored the suitability for isosteric replacement. The second part of fulfilling this objective consisted of performing the MSAS methodology on caspase-1 and -4, which provided a series of worthy isosteric replacements of the carboxylate functional group that have so far not been described in terms of caspase inhibitor design. Oxadiazolones, the most promising isosteres in this testing, were implemented in caspase inhibitors containing a carbonitrile warhead. Different challenging synthetic routes had to be set up due to the difficulties that we faced during the production of these compounds. Eventually, the final inhibitors were not able to provide significant inhibitory improvements compared to the original carboxylate-based inhibitors. Nevertheless, we strongly believe that further investigation of the oxadiazolone heterocycle with other warhead functionalities could provide improved S1 subsite binding affinities.

Next, an exploratory study was performed with respect to on-target experiments and efficient library synthesis of potential caspase inhibitors. This study consisted of prospectively optimizing the acyliminium-Strecker reaction to afford acylaminoalkylcarbonitriles with a one-pot protocol. A consecutive protocol was created, based on the catalysis of quinine (derivatives). This procedure is a big step towards fast and efficient library production. It should however be highlighted that much effort is still required for the optimization of the reaction conditions in order to generate a biocompatible protocol for on-target experiments.

Finally, the last objective comprised the achievement of CRBN-dependent caspase-1 degradation. Two types of PROTACs of thalidomide and caspase-1 inhibitor VX-765 were designed and synthesized but did not give the desired effect. Since this is most likely due to the low cell permeability of these compounds, we believe that a small variety of cell permeable spacers will have a beneficial effect on achieving this objective.

8.2 Outlook

8.2.1 Further investigation of acylsulfonamide prodrugs

The detailed structural elaboration on acylsulfonamide-based inhibitors, possessing an aldehyde warhead, revealed the mechanism behind the susceptibility of these compounds towards hydrolysis. Moreover, the performed cellular experiments proved the beneficial effect of their improved cell permeability and their advantages as prodrugs. However, further investigation of the pharmacokinetic properties of these molecules is required to achieve a valuable comparison with the currently studied ethyl hemiacetal prodrugs.

8.2.2 Screening of the fragment library against other enzymatic targets

The produced library subset of *N*-acyl aminomethylcoumarins containing carboxylic acids and isosteres thereof, can be readily used for the MSAS application towards other targets. Enzymes with strong affinities for carboxylates in their active site are ideal candidates. In addition, existing drugs for such targets can undergo a similar optimization as in this study. The MSAS approach provides a good way to circumvent any of the drawbacks that are associated to carboxylic acids.

8.2.3 Taking oxadiazolones to the next level with respect to caspase inhibitor discovery

8.2.3.1 Modifications to the warhead

As shown in the inhibitor screening of the MSAS approach, caspases have the ability to accommodate isosteric replacements of carboxylic acid. A perfect fit in the S1 subsite is however essential, including optimal positioning of the warhead towards the caspase's nucleophilic center, in order to achieve high inhibitory potencies. In that perspective, we believe that oxadiazolones combined with other warhead functionalities could provide the optimal fitting that we are aiming for. Aldehydes, for example, have proven to be worthy warheads in terms of caspase inhibitor design. In addition, the investigation of different linkers between isostere and warhead should provide further understanding of the binding sites in the S1 region of caspases. These adjustments lead to the molecules presented in **Figure 8.1**.

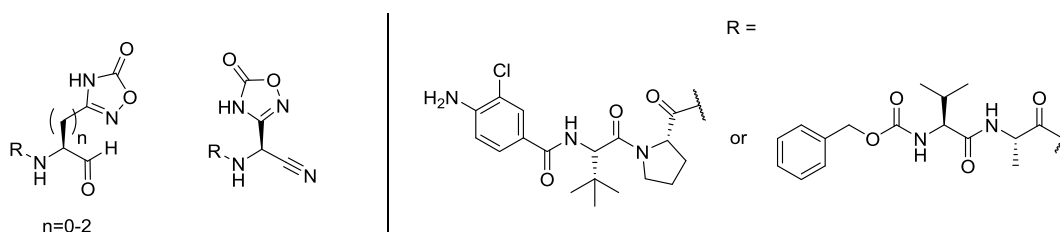


Figure 8.1. Potential oxadiazolone-containing inhibitors that could provide further understanding of the binding sites in the S1 region of caspases.

8.2.3.2 Scaffold-based inhibitors

Besides focusing on peptidic or peptidomimetic inhibitors containing warhead functionalities, it would be highly recommended to also investigate the possibility of combining these promising isosteres with a heterocyclic scaffold. However, this field is much underestimated; so far only few caspase inhibitors exist with such a structure. The absence of a warhead would allow easier adaptation in the enzyme's pocket in order to provide a good fit of the negatively charged isostere towards the caspase arginines. Such a validation has been performed during the MSAS investigation towards potent and druglike uPA inhibitors, and could therefore be considered for caspase inhibitors as well.¹ Due to straightforward synthesis and easy substituent decoration of pyrimidines, these heterocycles are considered excellent scaffolds for the transformation of identified *N*-acyl aminomethylcoumarins into scaffold-based inhibitors (**Figure 8.2**). Moreover, besides the impact of the isosteres, additional scaffold substituents could also contribute to higher levels of caspase selectivity.

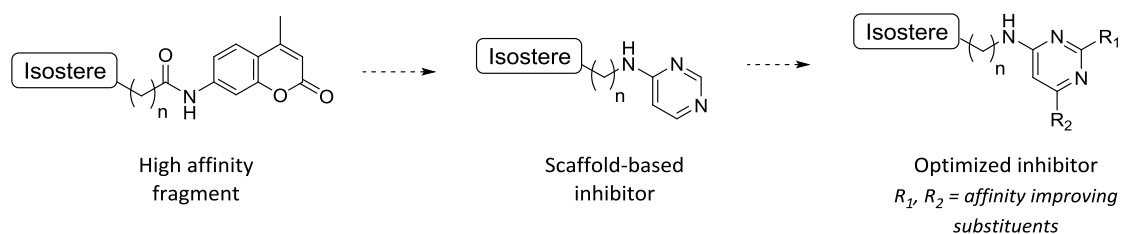


Figure 8.2. Transformation of a high affinity fragment into a scaffold-based inhibitor.

8.2.3.3 Modifications to the oxadiazolone heterocycle

The oxadiazolone moiety can also be subjected to optimization. Small modifications to the heterocycle are easily accomplished and have the potential of inducing a better fit in the caspase active site. In this perspective, we believe that oxathiazolones and oxadiazolethiones could provide valuable information about caspase binding due to the small differences in size and electron distribution (**Figure 8.3**). These heterocycles have already extensively been investigated in the study to replace the carboxylate functionalities in vasorelaxants, nonpeptidic angiotensin II receptor antagonists, BACE1 inhibitors and many others.²⁻⁶ Also optimized caspase-3 inhibitors have been found to incorporate such heterocycles, though these moieties served as S4-subsite binders.⁷

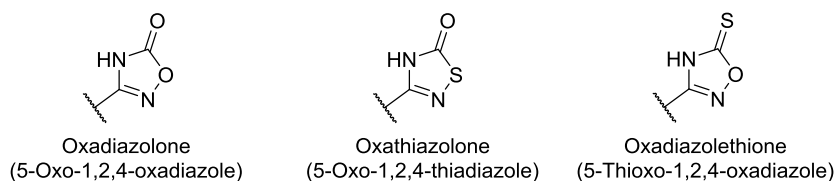


Figure 8.3. Derivatives of the oxadiazolone heterocycle.

8.2.4 Further optimization of the acyliminium-Strecker synthesis

The acyliminium-Strecker reaction is considered a strong candidate for efficient library synthesis of carbonitrile-containing inhibitors and, eventually, for target-assisted synthesis. Nonetheless, it is obvious that further optimization is essential. Besides the future perspectives that have been described in Chapter 6, we hope that the optimized acyliminium-Strecker reaction will allow a large variety of starting materials, such as bigger amide-based fragments (e.g. the peptidomimetic chain of VX-765) and diverse (protected) carboxylate isosteres (**Figure 8.4**). The selection of the latter can be directly derived from the MSAS results in Chapter 4.

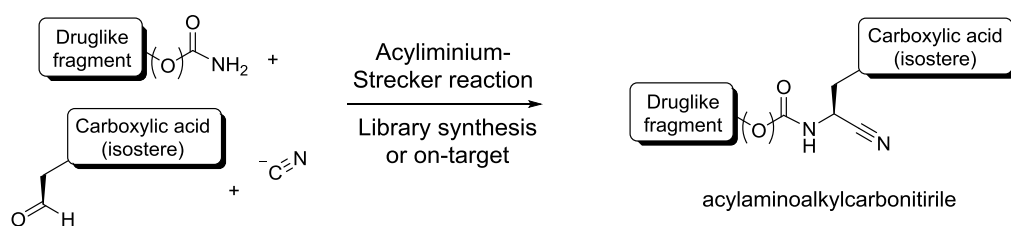


Figure 8.4. Library synthesis and target-assisted drug discovery based on the acyliminium-Strecker reaction to obtain acylaminoalkylcarbonitriles that could serve as caspase-1 inhibitors.

References

1. Gladysz, R.; Adriaenssens, Y.; De Winter, H.; Joossens, J.; Lambeir, A. M.; Augustyns, K.; Van der Veken, P., Discovery and SAR of Novel and Selective Inhibitors of Urokinase Plasminogen Activator (uPA) with an Imidazo[1,2-a]pyridine Scaffold. *J. Med. Chem.* **2015**, *58* (23), 9238-9257.
2. Kimura, T.; Hamada, Y.; Stochaj, M.; Ikari, H.; Nagamine, A.; Abdel-Rahman, H.; Igawa, N.; Hidaka, K.; Nguyen, J. T.; Saito, K.; Hayashi, Y.; Kiso, Y., Design and synthesis of potent beta-secretase (BACE1) inhibitors with P1' carboxylic acid bioisosteres. *Bioorg Med Chem Lett* **2006**, *16* (9), 2380-6.
3. Tagad, H. D.; Hamada, Y.; Nguyen, J. T.; Hamada, T.; Abdel-Rahman, H.; Yamani, A.; Nagamine, A.; Ikari, H.; Igawa, N.; Hidaka, K.; Sohma, Y.; Kimura, T.; Kiso, Y., Design of pentapeptidic BACE1 inhibitors with carboxylic acid bioisosteres at P1' and P4 positions. *Bioorg Med Chem* **2010**, *18* (9), 3175-86.
4. Alvarez, G.; Aguirre-Lopez, B.; Cabrera, N.; Marins, E. B.; Tinoco, L.; Batthyany, C. I.; de Gomez-Puyou, M. T.; Puyou, A. G.; Perez-Montfort, R.; Cerecetto, H.; Gonzalez, M., 1,2,4-thiadiazol-5(4H)-ones: a new class of selective inhibitors of Trypanosoma cruzi triosephosphate isomerase. Study of the mechanism of inhibition. *J Enzyme Inhib Med Chem* **2013**, *28* (5), 981-9.
5. Falck, J. R.; Koduru, S. R.; Mohapatra, S.; Manne, R.; Atcha, K. R.; Atcha, R.; Manthathi, V. L.; Capdevila, J. H.; Christian, S.; Imig, J. D.; Campbell, W. B., 14,15-Epoxyeicosa-5,8,11-trienoic Acid (14,15-EET) surrogates: carboxylate modifications. *J Med Chem* **2014**, *57* (16), 6965-72.
6. Kohara, Y.; Kubo, K.; Imamiya, E.; Wada, T.; Inada, Y.; Naka, T., Synthesis and angiotensin II receptor antagonistic activities of benzimidazole derivatives bearing acidic heterocycles as novel tetrazole bioisosteres. *J. Med. Chem.* **1996**, *39* (26), 5228-5235.
7. Allen, D. A.; Pham, P.; Choong, I. C.; Fahr, B.; Burdett, M. T.; Lew, W.; DeLano, W. L.; Gordon, E. M.; Lam, J. W.; O'Brien, T.; Lee, D., Identification of potent and novel small-Molecule inhibitors of caspase-3. *Bioorganic & Medicinal Chemistry Letters* **2003**, *13* (21), 3651-3655.

Chapter 9

Summary

9 Summary

9.1 The therapeutic relevance of caspases

Human caspases, a family of aspartic acid-directed cysteinyl proteases, are typically divided into two main groups, depending on their structural similarities, which are generally associated with their cellular functions. The first group, the inflammatory caspases, includes caspase-1, -4, -5 and -12, and participate in the activation of inflammasomes to initiate inflammation and pyroptosis, an inflammatory and lytic form of programmed cell death.¹ The second group, the apoptotic caspases, are typically subdivided into initiators (caspase-2, -8, -9 and -10) and executioners (caspase-3, -6 and -7) of an immunologically silent form of programmed cell death known as apoptosis.²⁻³ Upon dysregulation of caspases, these processes become impaired and consequently play central roles in many common medical conditions. Dysregulated caspase-1 for example, one of the most studied members, is involved in the pathogenesis of inflammatory conditions such as atherosclerosis, type 2 diabetes, gout and rare autoinflammatory disorders.⁴ These enzymes are therefore considered excellent targets for influencing these pathological processes via inhibitor-mediated blocking of protease activity. Since selective inhibition of one member of the caspase family remains a major obstacle in drug discovery, only five inhibitors have found their way into clinical trials. The lack of selectivity for individual caspases is mainly due to the overlapping substrate specificity among caspases.⁵⁻⁶ In general, caspases have a strong preference for aspartic acid in the S1 binding site, leading to the presence of carboxylic acids in most of the known peptidic and non-peptidic caspase inhibitors.⁷ Consequently, enhancing selectivity could be achieved by replacing the carboxylate functional group by an isostere thereof. The application of bioisosteres has been adopted as a fundamental tactical approach to overcome a number of handicaps associated with design and development of drug candidates.⁸ Yet, limited cases of carboxylic acid isosteres have been reported for caspase inhibitor discovery. The initial goal of this PhD was to identify isosteric replacements for carboxylates with respect to inhibitor discovery for inflammatory caspases-1 and -4.

9.2 Carboxylate isosteres for caspase inhibitors: the acylsulfonamide case revisited

As part of our interest in discovering caspase-1 inhibitors with an optimized selectivity and biopharmaceutical profile, *N*-acylsulfonamides were explored as carboxylate isosteres. Previously, Okamoto *et al.* reported that the use acylsulfonamides resulted in similar potency for caspase-1 in a biochemical evaluation, a fourfold increase of inhibitory activity in cellular assays and a drastically improved cell permeability compared to the carboxylate reference.⁹ Notwithstanding these promising results, the full potential of this functional group for caspase research was never further investigated. Likewise, no data on caspase selectivity, physicochemical properties and *in vitro* pharmacokinetic

profile are available for the published compound. We therefore thoroughly investigated acylsulfonamide-containing analogues of existing caspase-1 inhibitors VRT-043198 (**9.1**) and NCGC00183434 (**9.2**), and *pan*-caspase inhibitor Z-VAD-CHO (**9.3**) (**Figure 9.1**). Analogous to Okamoto *et al.*, acylsulfonamide-based inhibitors, possessing an aldehyde warhead (**9.5**, **9.7-9.8**), were found to have similar inhibitory potencies compared to the carboxylate references. Moreover, specific caspase-1 and -11 dependent cellular experiments indicated improved cell permeability. This phenomenon was discovered to be a consequence of prodrug activation of the acylsulfonamide moieties into the corresponding carboxylates. The basis in the understanding of the activation of these prodrugs was unraveled by a comprehensive ^1H and ^{13}C NMR study. Small fragments were used as a model, which indicated the preference of the cyclic hemiaminal tautomer in case of acylsulfonamide-containing aldehyde inhibitors. Alteration of the aldehyde warhead into a carbonitrile provided inhibitor NCGC00183434 (**9.2**) and its acylsulfonamide analogue (**9.6**). The first inhibitor was confirmed to show strongly improved selectivity for human and murine caspase-1. The acylsulfonamide analogue **9.6** compound showed improved stabilities in comparison with its aldehyde counterpart, but the determined IC_{50} values disfavored the suitability for isosteric replacement.

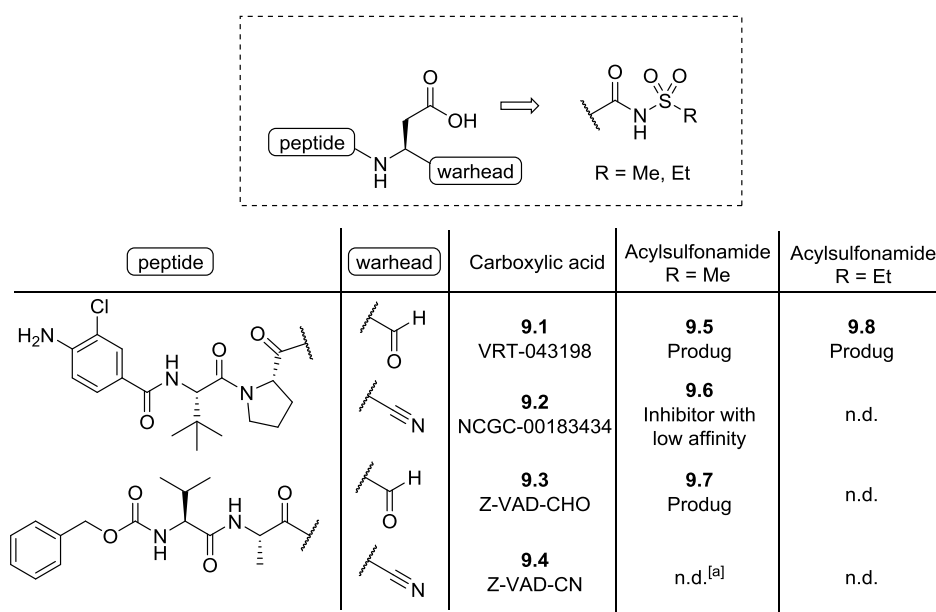


Figure 9.1. Isosteric replacement of the carboxylic acid functional group by an acylsulfonamide, in existing caspase inhibitors. [a] not determined.

9.3 The identification of isosteric replacements for carboxylic acids in (inflammatory) caspase inhibitors, determined by the Modified Substrate Activity Screening (MSAS)

Besides acylsulfonamides, the reported examples of carboxylate isosteres in caspase inhibitors are rather limited. In order to explore a variety of isosteric replacements suitable for caspase inhibitor design, we applied the Modified Substrate Activity Screening (MSAS, **Figure 9.2**). This methodology

was recently devised by our group and has so far been validated in inhibitor discovery for urokinase plasminogen activator (uPA), a trypsin-like serine protease that is overexpressed in metastasizing solid tumors,¹⁰⁻¹¹ and Atg4B, a cysteine hydrolase that plays a key role in autophagy.¹²

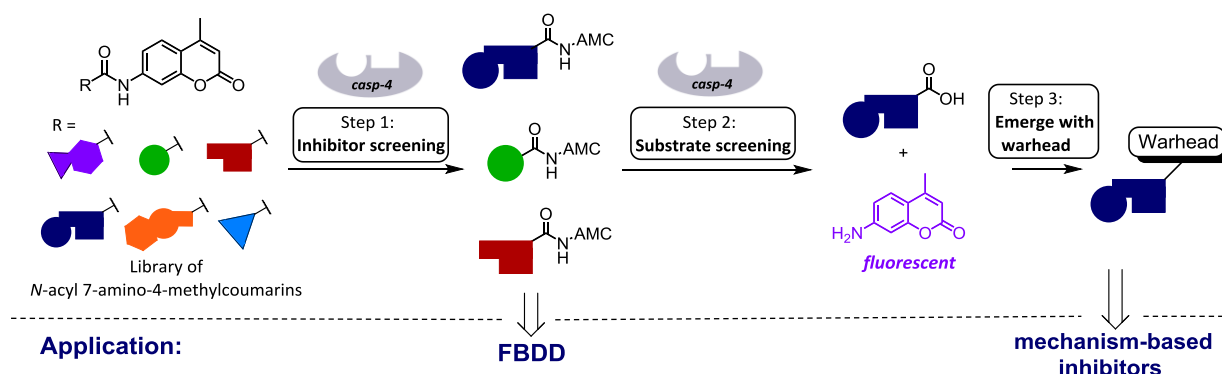


Figure 9.2. Outline of the MSAS approach. Figure was taken from ref [11].

In this project, we expanded MSAS's applicability towards caspase-1 and -4. The first phase in this bottom-up drug design comprised the enzymatic identification of building blocks that bind to the S1 region of the target protease. An existing library consisting of 171 *N*-acyl aminomethylcoumarins (AMC) with non-peptidic, low molecular-weight *N*-acyl groups (MW < 150), was supplemented with 51 new AMC-based compounds, structurally inspired by moieties that are known or reasonably expected to bind the S1 pocket/region of caspases. Particularly, a number of acidic residues (carboxylate, sulfonate, phosphonate or bioisosteres thereof) was selected that could mimic the P1 Asp-residue in the peptide substrates of caspases. The isosteric subset was tested for their inhibitory capacity against caspase-1, -3, and -4. The most promising results consisted of acylsulfonamide **9.9** and oxadiazolones **9.10** and **9.11** (**Figure 9.3**). The identification of the acylsulfonamide moiety confirmed the previously demonstrated impact on caspase inhibition, as well as the accuracy of the MSAS methodology.

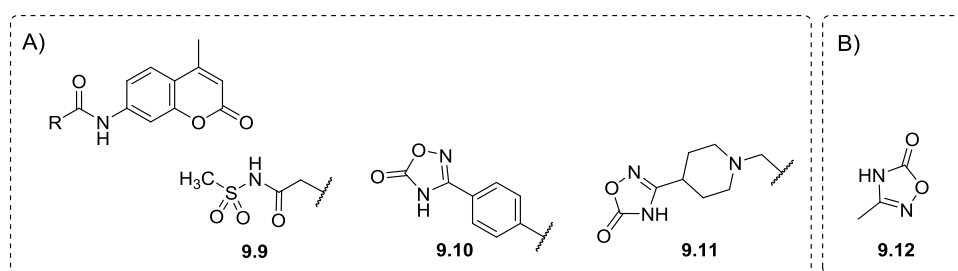


Figure 9.3. Most promising results from the inhibitor screening for the library of *N*-acyl AMCs (A) and small fragments (B).

To expand the scope of the MSAS methodology, an additional set of small acetic acid-based fragments was created and their inhibitory potency was determined. Though the required high fragment concentrations complicated the analysis of the results, the oxadiazolone fragment (**9.12**) was exclusively identified with a noticeable increase of potency. The considerable impact of oxadiazolones

on caspases is quite promising since, so far, these heterocycles have never been reported as S1 subsite binding partners in the development of caspase inhibitors.

During the second step of the MSAS methodology no substrates were identified. The direct substrate conversion into warhead-based inhibitors was thus not possible (step 3) so the results from the inhibitor screening were considered the main starting point for the validation. However, oxadiazolones connected to aldehyde warheads via an alkyl/aryl linker did not provide the expected inhibitory effects. In response, we have set our focus on incorporating these isosteres in existing caspase inhibitors, similar to the implementation of the acylsulfonamide moiety in the previous chapter.¹³⁻¹⁴ This however appeared to be a real challenge; one chapter is devoted to development of different approaches for the synthesis of an oxadiazolone-containing aspartic acid derivative. An acyliminium-Strecker-type synthesis and a Schiff base synthetic pathway did not seem successful. Nevertheless, our group achieved at producing oxadiazolone-containing analogues of NCGC-00183434 (**9.2**) and Z-VAD-CN (**9.4**) by an intensive and complicated pathway starting from aspartic acid ($n=1$) and glutamic acid ($n=2$) (**Figure 9.4**). As expected, the glutamic derivative **9.15** did not provide good inhibition. Regarding the aspartic analogues (**9.13-9.14**), the inhibitory potencies were generally lower than the reference inhibitors. Nonetheless, their stability and expected beneficial biopharmaceutical properties support oxadiazolones to remain subject of further investigation towards improved caspase inhibitors.

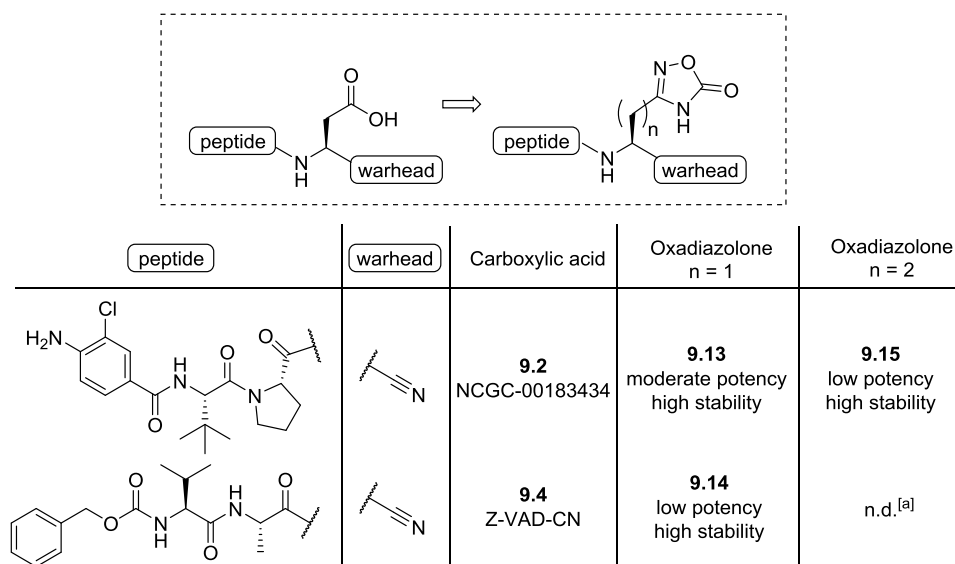


Figure 9.4. Isosteric replacement of the carboxylate functional group by an oxadiazolone, in existing caspase inhibitors. [a] not determined.

9.4 Optimization of the acyliminium-Strecker synthesis

This chapter describes the exploratory study towards easy library synthesis using the acyliminium-Strecker reaction. The purpose is to produce large sets of aminonitriles in a time-efficient way. Aminonitriles are considered highly suitable for caspase drug design because of their direct

implementation of a warhead functionality. Focus was set on using terminal amides and aldehydes as building blocks. This combination has not yet been described in the exploration of the Strecker synthesis, but is considered highly advantageous for the production of biocompatible molecules.¹⁵⁻¹⁶ Preliminary experiments were carried out with amidosulfone intermediates, in order to stabilize the acyliminium derivatives.¹⁷ A promising one-pot protocol was devised with consecutive amidosulfone production (**9.18**) and a quinine-catalyzed Strecker synthesis to afford aminonitriles (**9.19**) (**Figure 9.5**).

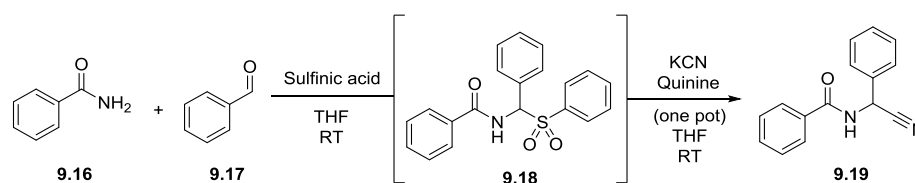


Figure 9.5. Optimized one-pot acyliminium-Strecker synthesis of carbonitriles.

The scope of this protocol could be enlarged by employing amide analogues of amino acids as suitable starting materials, which directly provides potential caspase inhibitors. Other pathways via aminal precursors or without acyliminium-stabilizing precursors were attempted as well, but were unable at providing the expected results.

References

1. Lamkanfi, M.; Dixit, V. M., Mechanisms and Functions of Inflammasomes. *Cell* **2014**, *157* (5), 1013-1022.
2. Man, S. M.; Kanneganti, T. D., Converging roles of caspases in inflammasome activation, cell death and innate immunity. *Nat. Rev. Immunol.* **2016**, *16* (1), 7-21.
3. Fuchs, Y.; Steller, H., Live to die another way: modes of programmed cell death and the signals emanating from dying cells. *Nat. Rev. Mol. Cell Biol.* **2015**, *16* (6), 329-344.
4. Winkler, S.; Rosen-Wolff, A., Caspase-1: an integral regulator of innate immunity. *Semin. Immunopathol.* **2015**, *37* (4), 419-427.
5. Poreba, M.; Strozyk, A.; Salvesen, G. S.; Drag, M., Caspase substrates and inhibitors. *Cold Spring Harbor Perspect. Biol.* **2013**, *5* (8), a008680.
6. Poreba, M.; Szalek, A.; Kasperkiewicz, P.; Rut, W.; Salvesen, G. S.; Drag, M., Small Molecule Active Site Directed Tools for Studying Human Caspases. *Chem. Rev.* **2015**, *115* (22), 12546-12629.
7. Wilson, K. P.; Black, J. A. F.; Thomson, J. A.; Kim, E. E.; Griffith, J. P.; Navia, M. A.; Murcko, M. A.; Chambers, S. P.; Aldape, R. A.; Raybuck, S. A.; Livingston, D. J., Structure and Mechanism of Interleukin-1-Beta Converting-Enzyme. *Nature* **1994**, *370* (6487), 270-275.
8. Meanwell, N. A., Synopsis of some recent tactical application of bioisosteres in drug design. *J. Med. Chem.* **2011**, *54* (8), 2529-91.
9. Okamoto, Y.; Anan, H.; Nakai, E.; Morihira, K.; Yonetoku, Y.; Kurihara, H.; Sakashita, H.; Terai, Y.; Takeuchi, M.; Shibamura, T.; Isomura, Y., Peptide based interleukin-1 beta converting enzyme (ICE) inhibitors: Synthesis, structure activity relationships and crystallographic study of the ICE-inhibitor complex. *Chem. Pharm. Bull.* **1999**, *47* (1), 11-21.
10. Gladysz, R.; Adriaenssens, Y.; De Winter, H.; Joossens, J.; Lambeir, A. M.; Augustyns, K.; Van der Veken, P., Discovery and SAR of Novel and Selective Inhibitors of Urokinase Plasminogen Activator (uPA) with an Imidazo[1,2-a]pyridine Scaffold. *J. Med. Chem.* **2015**, *58* (23), 9238-9257.
11. Gladysz, R.; Cleenewerck, M.; Joossens, J.; Lambeir, A. M.; Augustyns, K.; Van der Veken, P., Repositioning the Substrate Activity Screening (SAS) Approach as a Fragment-Based Method for Identification of Weak Binders. *ChemBioChem* **2014**, *15* (15), 2238-47.
12. Cleenewerck, M.; Grootaert, M. O. J.; Gladysz, R.; Adriaenssens, Y.; Roelandt, R.; Joossens, J.; Lambeir, A.-M.; De Meyer, G. R. Y.; Declercq, W.; Augustyns, K.; Martinet, W.; Van der Veken, P., Inhibitor screening and enzymatic activity determination for autophagy target Atg4B using a gel electrophoresis-based assay. *Eur. J. Med. Chem.* **2016**, *123*, 631-638.
13. Boxer, M. B.; Quinn, A. M.; Shen, M.; Jadhav, A.; Leister, W.; Simeonov, A.; Auld, D. S.; Thomas, C. J., A highly potent and selective caspase 1 inhibitor that utilizes a key 3-cyanopropanoic acid moiety. *ChemMedChem* **2010**, *5* (5), 730-8.
14. Adriaenssens, Y.; Fernández, D. J.; Vande Walle, L.; Elvas, F.; Joossens, J.; Lambeir, A. M.; Augustyns, K.; Lamkanfi, M.; Van der Veken, P., Carboxylate Isosteres for Caspase Inhibitors: the Acylsulfonamide Case Revisited. *Unpublished work*.
15. Ohkuma, T.; Kurono, N., Asymmetric Cyanation with the Chiral Ru-Li Combined Catalysts. *Synlett* **2012**, (13), 1865-1881.
16. Cai, X. H.; Xie, B., Recent advances in asymmetric Strecker reactions. *Arkivoc* **2014**, 205-248.

17. Petrini, M., alpha-Amido sulfones as stable precursors of reactive N-acylimino derivatives. *Chem. Rev.* **2005**, *105* (11), 3949-3977.

Chapter 10

Samenvatting

10 Samenvatting

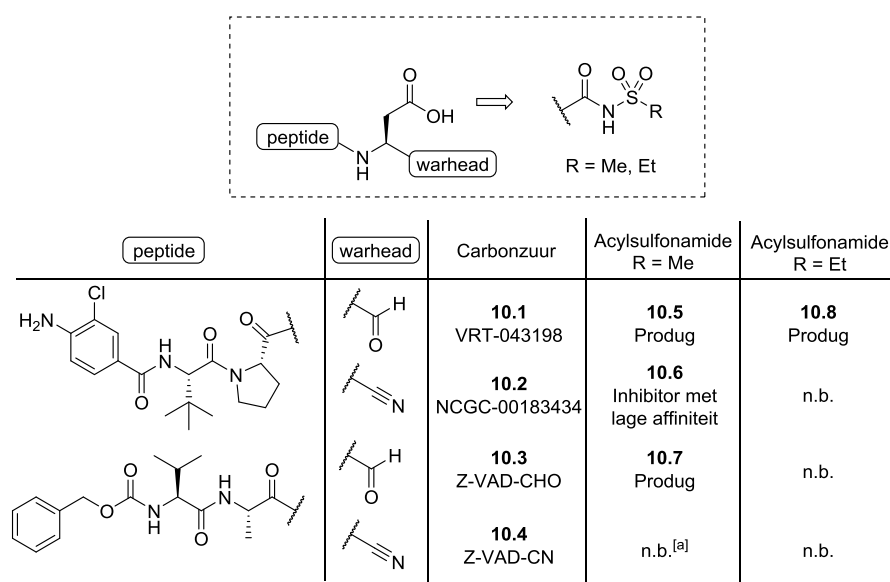
10.1 Therapeutisch belang van caspases

Humane caspases zijn aspartaatgerichte cysteineproteasen die gewoonlijk worden ingedeeld in twee groepen, afhankelijk van hun structurele overeenkomsten die in het algemeen gepaard gaan met hun cellulaire functies. De eerste groep, de inflammatoire caspases, omvat caspase-1, -4, -5 en -12, en speelt mee in de activering van het inflammasoom, die op zijn beurt ontsteking en pyroptose, een lytische vorm van geprogrammeerde celdood, teweegbrengt.¹ De tweede groep, de apoptotische caspases, wordt typisch onderverdeeld in initiators (caspase-2, -8, -9 en -10) en executors (caspase-3, -6 en -7) van een niet-immunologische vorm van geprogrammeerde celdood, apoptose genaamd.²⁻³ Indien caspases verstoord geraken, zullen deze processen ontregelen. Daarom spelen caspases een centrale rol in veel voorkomende medische aandoeningen. Verstoord caspase-1 bijvoorbeeld, één van de meest bestudeerde leden van de caspasefamilie, is betrokken bij de pathogenese van inflammatoire aandoeningen zoals atherosclerose, type 2 diabetes, jicht en zeldzame auto-inflammatoire ziekten.⁴ Deze enzymen worden bijgevolg beschouwd als uitstekende doelwitten voor het beïnvloeden van deze pathologische processen via inhibitor-gemedieerde blokkering van proteaseactiviteit. Aangezien selectieve inhibitie van één lid van de caspasefamilie een beduidend groot obstakel in geneesmiddelontwikkeling is, zijn slechts vijf caspase-inhibitoren toegelaten tot de klinische studies. Het gebrek aan selectiviteit voor individuele caspases is voornamelijk te wijten aan de overlappende substraatspecificiteit onder de caspases.⁵⁻⁶ In het algemeen hebben caspases een sterke voorkeur voor aspartaat in hun S1 bindingsplaats, met als gevolg dat het merendeel van de gepubliceerde caspase-inhibitoren carbonzuren bevatten.⁷ In dit opzicht lijkt het ons uiterst aangewezen dat sterke selectiviteitsverhoging bereikt kan worden door de aspartaatzijgroep isosterisch te modificeren. De toepassing van bioisosteren wordt beschouwd als een fundamenteel tactische benadering voor het omzeilen van handicaps die gepaard gaan met het ontwerp en de ontwikkeling van geneesmiddelen.⁸ Desalniettemin zijn slechts een beperkt aantal gevallen van carbonzuurisosteren beschreven in het onderzoek naar caspase-inhibitoren. Het oorspronkelijke doel van dit doctoraat was de identificatie van carbonzuurisosteren met het oog op de ontwikkeling van caspase-1 en -4 remmers.

10.2 Carbonzuurisosteren voor remmers van caspases: acylsulfonamides herbekeken

Als deel van ons onderzoek om caspase-1 inhibitoren te ontdekken met een geoptimaliseerde selectiviteit en biofarmaceutisch profiel, werden *N*-acylsulfonamides beschouwd als potentiële carbonzuurisosteren. Okamoto *et al.* hebben reeds gerapporteerd dat het gebruik van acylsulfonamides resulteerde in gelijkaardige remmende vermogens voor caspase-1 in een biochemische evaluatie, een viervoudige inhibitietoename in cellulaire experimenten en een sterk

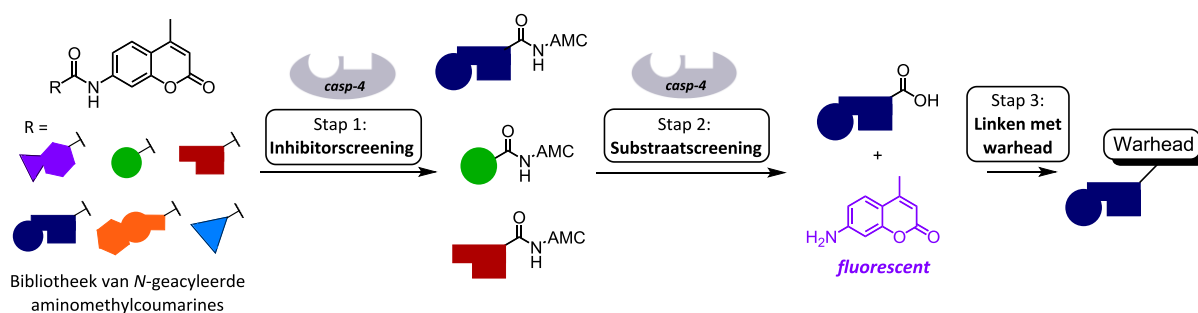
verhoogde celpermeabiliteit vergeleken met de carbonzuurreferenties.⁹ Ondanks deze veelbelovende resultaten werd het volledige potentieel van deze functionele groep voor caspase-onderzoek nooit verder onderzocht. Bovendien werden er ook geen gegevens over caspaseselectiviteit, fysicochemische eigenschappen en *in vitro* farmacokinetisch profiel gerapporteerd voor de gepubliceerde verbinding. Daarom hebben wij een grondig onderzoek uitgevoerd naar acylsulfonamide-analogen van bestaande caspase-1 remmers VRT-043198 (**10.1**) en NCGC00183434 (**10.2**) en *pan*-caspase remmer Z-VAD-CHO (**10.3**) (**Figuur 10.1**). Gelijkaardig aan het werk van Okamoto *et al.* hadden acylsulfonamide-gebaseerde inhibitoren, die aldehyde *warheads* bezitten (**10.5**, **10.7-10.8**), dezelfde remmende sterktes in vergelijking met de carbonzuurreferenties. Bovendien resulteerden cellulaire experimenten met muis caspase-1 en -11 in verbeterde celpermeabiliteit. Dit effect werd verklaard als een gevolg van produgactivatie van het acylsulfonamide in het overeenkomstig carbonzuur. De basis van deze activatie werd ontdekt door een uitgebreide ¹H en ¹³C NMR studie. Kleine fragmenten werden gebruikt als model, die de voorkeur benadrukten van het cyclische hemiaminaltautomeer in het geval van deze acylsulfonamide-bevattende aldehyde inhibitoren. Vervolgens werd de aldehyde *warhead* gewijzigd in een carbonitril, wat inhibitor NCGC00183434 (**10.2**) en zijn analoog acylsulfonamide (**10.6**) opleverde. De sterk verbeterde selectiviteit van **10.2** werd bevestigd voor menselijk en muis caspase-1. Hoewel de stabiliteit van het acylsulfonamide analoog **10.6** beduidend hoger was in vergelijking met de aldehyde tegenhangers, bleek deze molecuul geen geschikte kandidaat voor isosterische vervanging vanwege zijn verminderd remmend vermogen.



Figuur 10.1. Het gebruik van acylsulfonamides als carbonzuurisosteren bij bestaande caspase inhibitoren. [a] niet bepaald.

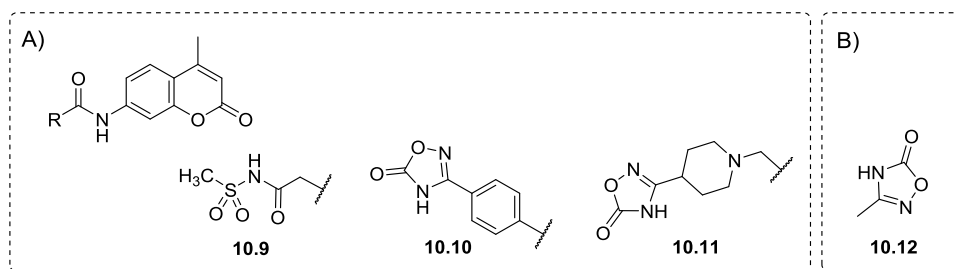
10.3 Identificatie van carbonzuurisosteren voor remmers van inflammatoire caspases, bepaald door de Gemodificeerde Substraat Activiteit Screening (MSAS)

Naast acylsulfonamides zijn de gerapporteerde voorbeelden van carbonzuurisosteren in remmers van caspases zeer beperkt. Met oog op het verkennen van een verscheidenheid aan isosterische vervangingen die geschikt zijn voor het ontwerp van caspase-inhibitoren, hebben we de Gemodificeerde Substraat Activiteit Screening (MSAS) toegepast (**Figuur 10.2**). Deze methodologie werd onlangs door onze groep ontwikkeld, en is reeds gevalideerd op urokinase plasminogeenactivator (uPA), een trypsine-achtige serine protease dat in overexpressie wordt gebracht in metastaserende tumoren,¹⁰⁻¹¹ en Atg4B, een cysteine hydrolase dat een belangrijke rol speelt in autofagie.¹²



Figuur 10.2. Overzicht van de MSAS-benadering. Figuur werd overgenomen van ref [11].

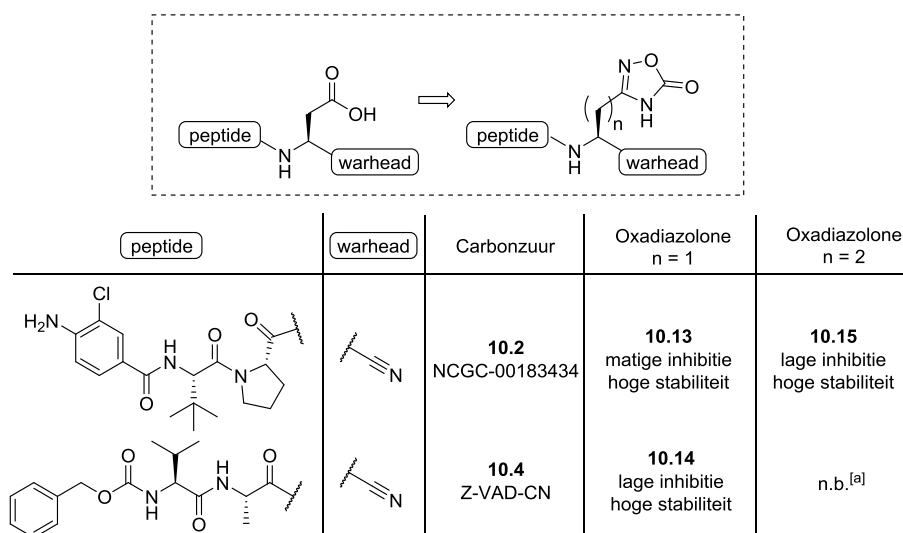
De intentie in dit deel van het project is het onderzoeken van de toepasbaarheid van MSAS op caspase-1 en -4. De eerste fase in deze “bottom-up” benadering bestaat uit de enzymatische identificatie van bouwstenen die zich binden aan de S1 regio van het doelwit. Een reeds geproduceerde bibliotheek, bestaande uit 171 *N*-geacyleerde aminomethylcoumarines (AMC) met niet-peptidische, laagmoleculaire *N*-acylgroepen (MM <150) werd aangevuld met 51 nieuwe AMC-gebaseerde verbindingen, structureel geïnspireerd door residuen waarvan bekend is of waarvan redelijkerwijs verwacht wordt dat ze binden in de S1 regio van caspases. Een set van zure functionele groepen (carboxylaat, sulfonaat, fosfonaat of bioisosteren daarvan) werd geselecteerd die het P1 Asp-residu kan nabootsen in de peptidesubstraten van caspases. De isosterische subgroep werd getest op zijn remmende vermogen tegen caspase-1, -3 en -4. De meest belovende resultaten uit deze set bevatten acylsulfonamide **10.9** en oxadiazolonen **10.10** en **10.11** (**Figuur 10.3**). De identificatie van de acylsulfonamide-eenheid bevestigt de reeds aangetoonde impact van acylsulfonamides op caspase-inhibitie, alsook de accuraatheid van de MSAS-methodologie.



Figuur 10.3. Meest belovende resultaten van de inhibitorscreening na het testen van de volledige bibliotheek van *N*-geacyleerde AMCs (A) en kleine fragmenten (B).

Om de omvang van de MSAS-methodiek uit te breiden, werd een bijkomende set van kleine azijnzuur-gebaseerde fragmenten samengesteld en getest naar hun remmend vermogen. Hoewel de vereiste hoge fragmentconcentraties de analyse van de resultaten heeft bemoeilijkt, werd uitsluitend het oxadiazolon-bevattend fragment (**10.12**) geïdentificeerd met een merkbare verhoging van remmend vermogen. De impact van oxadiazolonen op caspases wordt erg veelbelovend ingeschat aangezien tot op heden deze heteroringen nog nooit werden gerapporteerd als S1-bindingspartners in de ontwikkeling van caspaseremmers.

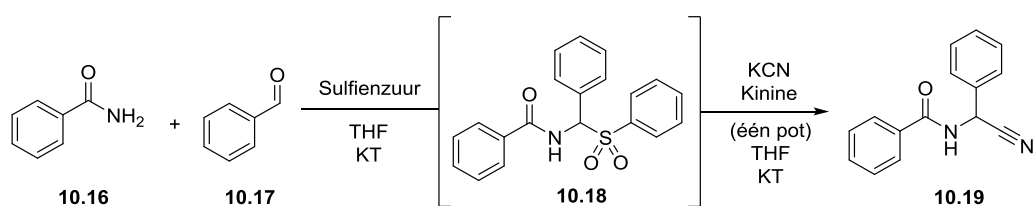
Tijdens de tweede stap van de MSAS-benadering werden geen substraten geïdentificeerd. Om die reden was de directe omzetting tot substraat-gebaseerde inhibitoren door het linken met een *warhead* niet mogelijk (stap 3). Daarom werden de resultaten van de inhibitorscreening beschouwd als het belangrijkste uitgangspunt voor de validatie. Echter, oxadiazolonen gelinkt aan aldehyde *warheads* via een alkyl/aryl linker brachten niet de verwachte remmende effecten teweeg. Hierdoor werd de focus gelegd op het implementeren van deze isosteren in bestaande caspase-inhibitoren, op een gelijkaardige manier als bij de acylsulfonamides in het vorige hoofdstuk.¹³⁻¹⁴ Dit bleek echter een grote uitdaging; één hoofdstuk werd toegewijd aan de ontwikkeling van verschillende benaderingen voor de synthese van een oxadiazolon-bevattend aspartaatderivaat. Een acyliminium-Strecker-type synthese en een *Schiff*-base syntheseroute werden beiden onsuccesvol bevonden. Desalniettemin is onze groep geslaagd in de productie van oxadiazolon-analogen van NCGC-00183434 (**10.2**) en Z-VAD-CN (**10.4**) door een intensief en ingewikkeld synthesepad te hanteren, uitgaande vanaf de originele aspartaat- ($n = 1$) en glutamaatstructuur ($n = 2$) (**Figuur 10.4**). Zoals verwacht bracht het glutamaatderivaat **10.15** geen noemenswaardige inhibitie teweeg. De aspartaatanalogen (**10.13-10.14**) werden in het algemeen gekarakteriseerd door licht lagere remmende vermogens. Desondanks wordt verwacht dat de hoge stabiliteit en de vermoedelijke gunstige biofarmaceutische eigenschappen van de oxadiazolonen een belangrijke rol zullen spelen om deze heteroringen onderwerp te maken van nader onderzoek naar geoptimaliseerde caspase-remmers.



Figuur 10.4. Het gebruik van oxadiazolonen als carbonzuurisosteren bij bestaande caspase inhibitoren. [a] niet bepaald.

10.4 Optimalisatie van de acyliminium-Streckersynthese

Dit hoofdstuk omvatte de verkennende studie naar gemakkelijke en efficiënte bibliotheeksynthese met behulp van de acyliminium-Streckerreactie. Dit zou de snelle productie van grote reeksen aminonitrillen mogelijk maken, die geschikt zijn voor de ontwikkeling van caspase-inhibitoren. De focus werd gelegd op het gebruik van eindstandige amiden en aldehyden als bouwstenen; een gebied dat nog niet verkend is in het verleden maar erg belangrijk wordt geschat voor het creëren van biocompatibele moleculen.¹⁵⁻¹⁶ De eerste experimenten werden uitgevoerd met amidosulfon-tussenproducten, met het oog op het stabiliseren van de acyliminiumderivaten.¹⁷ Een veelbelovend éénpotsprotocol werd ontwikkeld met achtereenvolgende amidosulfonproductie en kinine-gekatalyseerde Streckersynthese met als gevolg dat het aminonitril werd gegenereerd (**Figuur 10.5**).



Figuur 10.5. Geoptimaliseerde éénpotsacyliminium-Streckersynthese van aminonitrillen.

Het toepassingsgebied van dit protocol kan naderhand worden uitgebreid door amide-analogen van aminozuren te gebruiken als geschikte uitgangsmaterialen, wat rechtstreeks potentiële caspaseremmers zou opleveren. Andere synthesesetrajecten via aminal-tussenproducten of zonder acyliminium-stabiliserende tussenproducten werden tevens onderzocht, maar waren niet in staat om de verwachte resultaten teweeg te brengen.

Referenties

1. Lamkanfi, M.; Dixit, V. M., Mechanisms and Functions of Inflammasomes. *Cell* **2014**, *157* (5), 1013-1022.
2. Man, S. M.; Kanneganti, T. D., Converging roles of caspases in inflammasome activation, cell death and innate immunity. *Nat. Rev. Immunol.* **2016**, *16* (1), 7-21.
3. Fuchs, Y.; Steller, H., Live to die another way: modes of programmed cell death and the signals emanating from dying cells. *Nat. Rev. Mol. Cell Biol.* **2015**, *16* (6), 329-344.
4. Winkler, S.; Rosen-Wolff, A., Caspase-1: an integral regulator of innate immunity. *Semin. Immunopathol.* **2015**, *37* (4), 419-427.
5. Poreba, M.; Strozyk, A.; Salvesen, G. S.; Drag, M., Caspase substrates and inhibitors. *Cold Spring Harbor Perspect. Biol.* **2013**, *5* (8), a008680.
6. Poreba, M.; Szalek, A.; Kasperkiewicz, P.; Rut, W.; Salvesen, G. S.; Drag, M., Small Molecule Active Site Directed Tools for Studying Human Caspases. *Chem. Rev.* **2015**, *115* (22), 12546-12629.
7. Wilson, K. P.; Black, J. A. F.; Thomson, J. A.; Kim, E. E.; Griffith, J. P.; Navia, M. A.; Murcko, M. A.; Chambers, S. P.; Aldape, R. A.; Raybuck, S. A.; Livingston, D. J., Structure and Mechanism of Interleukin-1-Beta Converting-Enzyme. *Nature* **1994**, *370* (6487), 270-275.
8. Meanwell, N. A., Synopsis of some recent tactical application of bioisosteres in drug design. *J. Med. Chem.* **2011**, *54* (8), 2529-91.
9. Okamoto, Y.; Anan, H.; Nakai, E.; Morihira, K.; Yonetoku, Y.; Kurihara, H.; Sakashita, H.; Terai, Y.; Takeuchi, M.; Shibamura, T.; Isomura, Y., Peptide based interleukin-1 beta converting enzyme (ICE) inhibitors: Synthesis, structure activity relationships and crystallographic study of the ICE-inhibitor complex. *Chem. Pharm. Bull.* **1999**, *47* (1), 11-21.
10. Gladysz, R.; Adriaenssens, Y.; De Winter, H.; Joossens, J.; Lambeir, A. M.; Augustyns, K.; Van der Veken, P., Discovery and SAR of Novel and Selective Inhibitors of Urokinase Plasminogen Activator (uPA) with an Imidazo[1,2-a]pyridine Scaffold. *J. Med. Chem.* **2015**, *58* (23), 9238-9257.
11. Gladysz, R.; Cleenewerck, M.; Joossens, J.; Lambeir, A. M.; Augustyns, K.; Van der Veken, P., Repositioning the Substrate Activity Screening (SAS) Approach as a Fragment-Based Method for Identification of Weak Binders. *ChemBioChem* **2014**, *15* (15), 2238-47.
12. Cleenewerck, M.; Grootaert, M. O. J.; Gladysz, R.; Adriaenssens, Y.; Roelandt, R.; Joossens, J.; Lambeir, A.-M.; De Meyer, G. R. Y.; Declercq, W.; Augustyns, K.; Martinet, W.; Van der Veken, P., Inhibitor screening and enzymatic activity determination for autophagy target Atg4B using a gel electrophoresis-based assay. *Eur. J. Med. Chem.* **2016**, *123*, 631-638.
13. Boxer, M. B.; Quinn, A. M.; Shen, M.; Jadhav, A.; Leister, W.; Simeonov, A.; Auld, D. S.; Thomas, C. J., A highly potent and selective caspase 1 inhibitor that utilizes a key 3-cyanopropanoic acid moiety. *ChemMedChem* **2010**, *5* (5), 730-8.
14. Adriaenssens, Y.; Fernández, D. J.; Vande Walle, L.; Elvas, F.; Joossens, J.; Lambeir, A. M.; Augustyns, K.; Lamkanfi, M.; Van der Veken, P., Carboxylate Isosteres for Caspase Inhibitors: the Acylsulfonamide Case Revisited. *Unpublished work*.
15. Ohkuma, T.; Kurono, N., Asymmetric Cyanation with the Chiral Ru-Li Combined Catalysts. *Synlett* **2012**, (13), 1865-1881.
16. Cai, X. H.; Xie, B., Recent advances in asymmetric Strecker reactions. *Arkivoc* **2014**, 205-248.

17. Petrini, M., alpha-Amido sulfones as stable precursors of reactive N-acylimino derivatives. *Chem. Rev.* **2005**, *105* (11), 3949-3977.

Chapter 11

Curriculum Vitae

11 Curriculum Vitae

Personal information

| | |
|-------------------------|---|
| First name: | Yves |
| Surname: | Adriaenssens |
| Date and place of birth | October 6 th 1989, Jette (Belgium) |
| E-mail | yves.adriaenssens@outlook.com |
| Nationality | Belgian |

Education

| | |
|-----------|---|
| 2012-2016 | PhD in Pharmaceutical Sciences, Laboratory of Medicinal Chemistry (UAMC, University of Antwerp) |
| 2010-2012 | Master in Chemistry, University of Antwerp (<i>achieved with distinction</i>) |
| 2010-2011 | Erasmus Program: Biomolecular Chemistry, University of Montpellier (France) |
| 2007-2010 | Bachelor in Chemistry, University of Antwerp (<i>achieved with great distinction</i>) |
| 2001-2007 | Secondary education: Sciences-Mathematics, OLVE Edegem |

Scientific research

Publications

Gladysz, R.; **Adriaenssens, Y.**; De Winter, H., Joossens, J.; Lambeir, A.-M.; Augustyns, K.; Van der Veken, P. Discovery and SAR of novel and selective inhibitors of urokinase plasminogen activator (uPA) with an imidazo[1,2-a]pyridine scaffold, *Journal of Medicinal Chemistry* **2015**, *58*, 9238-9257.

Cleenewerck, M.; Grootaert, M. O. J.; Gladysz, R.; **Adriaenssens, Y.**; Roelandt, R.; Joossens, J.; Lambeir, A.-M.; De Meyer, G. R. Y.; Declercq, W.; Augustyns, K.; Martinet, W.; Van der Veken, P., Inhibitor screening and enzymatic activity determination for autophagy target Atg4B using a gel electrophoresis-based assay. *European Journal of Medicinal Chemistry* **2016**, *123*, 631-638.

Adriaenssens, Y.; Fernández, D. J.; Vande Walle, L.; Elvas, F.; Joossens, J.; Lambeir, A. M.; Augustyns, K.; Lamkanfi, M.; Van der Veken, P.; Carboxylate Isosteres for Caspase Inhibitors: the Acylsulfonamide Case Revisited; *submitted to Organic and Biomolecular Chemistry*.

Elvas, F.; Vanden Berghe, T.; **Adriaenssens, Y.**; Vandenabeele, P.; Augustyns, K.; Staelens, S.; Stroobants, S.; Van der Veken, P.; wyffels, L.; Peptide-Based Positron Emission Tomography Probes Targeting Caspase-3/-7 for Molecular Imaging of Apoptosis; *submitted to Journal of Medicinal Chemistry*.

Adriaenssens, Y.; Gladysz, R.; Zonnekeijn, L.; Peeraer, A.; Cleenewerck, M.; Elvas, F.; Joossens, J.; Lambeir, A. M.; Augustyns, K.; Van der Veken, P.; The identification of isosteric replacements for carboxylic acids in inflammatory caspase inhibitors, determined by the Modified Substrate Activity Screening (MSAS); *In preparation*.

Oral presentations

Carboxylate Isosteres for Caspase Inhibitors: the Acylsulfonamide Case Revisited (Edition 2), presented at the Departmental Research Day of Pharmaceutical Sciences, Antwerp, **2016**.

Carboxylate Isosteres for Caspase Inhibitors: the Acylsulfonamide Case Revisited (Edition 1), presented at the 13th Chemistry Conference for Young Scientists (ChemCYS 2016), Blankenberge, **2016**.

Validation of the Modified Substrate Activity Screening (MSAS) approach in the discovery of selective inhibitors of caspase-4, presented during the 5th RSC-BMCS Fragment-based Drug Discovery symposium (Fragments 2015), Cambridge, UK, **2015**.

Poster presentations

Carboxylate Isosteres for Caspase Inhibitors: the N-Acylsulfonamide Case Revisited, presented at the 17th Tetrahedron Symposium, Sitges, Spain, **2016**.

Validation of the Modified Substrate Activity Screening (MSAS) approach in the discovery of selective inhibitors of caspase-4 (Edition 3), presented at:

- Frontiers in Medicinal Chemistry (FMC 2015), Antwerp, **2015**.
- the EFMC Young Medicinal Chemist Symposium (EFMC-YMCS 2015), Antwerp, **2015**.

Validation of the Modified Substrate Activity Screening (MSAS) approach in the discovery of selective inhibitors of caspase-4 (Ed.2), presented at the 5th RSC-BMCS Fragment-based Drug Discovery symposium (Fragments 2015), Cambridge, UK, **2015**.

Validation of the Modified Substrate Activity Screening (MSAS) approach in the discovery of selective inhibitors of caspase-4 (Edition 1), presented at the 18th Sigma-Aldrich Symposium, Blankenberge, **2014**.

Investigation of the Modified Substrate Activity Screening (MSAS) Approach in the Discovery of Selective Inhibitor of Caspase-4, presented at the Annual One-Day Meeting on Medicinal Chemistry of SRC & KVCV, Liège, **2013**.

Supervision of Master students

02/2016 - 07/2016 Thibault Monheim, Master student, Farmaceutical sciences, University of Antwerp

Chapter 12

Dankwoord

12 Dankwoord

Nu de laatste hand aan mijn thesis gelegd is, neem ik even tijd om stil te staan bij de mensen die de afgelopen vijf jaren bewust of onbewust hebben bijgedragen tot de realisatie van dit meesterwerk.

Eerst en vooral ben ik **Prof. dr. Pieter Van Der Veken** en **Prof. dr. Koen Augustyns** zeer dankbaar voor de kans die ze deze chemist hebben gegeven om een doctoraat te beginnen in hun laboratorium vol farmaceuten. Hun deur stond steeds wagenwijd open om mij te helpen bij allerhande farmaceutische, chemische en zelfs irrelevante vragen! **Pieter**, u zou ik in het bijzonder willen bedanken voor de vele raadgevingen, aanmoedigen na de onvermijdelijke teleurstellingen en het uitvoerig corrigeren van mijn thesis. Ik genoot ook telkens van onze chemisch getinte gesprekken waarbij we de meest efficiënte manier zochten om tot onze doelmoleculen te geraken. Hieruit heb ik voornamelijk geleerd om het onderste uit de kan te halen wat betreft kennis en denkvermogen.

Ik zou deze thesis willen toewijden aan **Prof. dr. Sandra Apers**, die op een veel te jonge leeftijd in februari 2017 is heengegaan. Tijdens de jaarlijkse tussenverdediging heb ik kunnen genieten van uw opbouwende commentaar, maar ik heb u helaas nooit het eindresultaat kunnen tonen.

Prof. dr. Adrian Covaci, bedankt om in te springen in mijn doctoraatscommissie in deze ongelukkige situatie en het voorzitterschap op u te nemen. Tevens heb ik uw gevatte en constructieve feedback na het lezen van de proefthesis erg geapprecieerd.

Prof. dr. Ingrid De Meester, bedankt om deel te maken van mijn interne jury, alsook voor de constructieve opmerkingen die u tijdens mijn doctoraat en na het lezen van de thesis hebt gedeeld. Uw kijk op het onderzoek heeft belangrijke vorderingen teweeggebracht die het geheel vervolledigde.

Vervolgens zou ik **Prof. dr. Mo Lamkanfi** willen bedanken. Niet enkel voor de taak van extern lid van mijn doctoraatscommissie te accepteren, maar ook voor de vlotte samenwerking tijdens dit vierjarig onderzoek. Uw ideeën hebben mij enorm veel bijgebracht. Bovendien zeg ik er graag bij dat er twee mooie hoofdstukken uit die samenwerking zijn gevloeid.

Ook **Prof. dr. Steven Ballet** zou ik willen bedanken voor het accepteren van de taak als extern lid van mijn doctoraatscommissie en voor het lezen van de proefthesis. Bovendien, wie weet kruisen we elkaar nogmaals binnenkort in de volleybalclub van Mortsels...

Ik wil tevens mijn dankbaarheid uitten aan **Prof. dr. Anne-Marie Lambeir**. Uw uitvoerige kennis heeft mij enorm geholpen tijdens het opstellen van de biochemische experimenten en de interpretatie van de resultaten. Ik heb overigens de gedetailleerde feedback op artikels of posters enorm geapprecieerd.

In het bijzonder zou ik **dr. Jurgen Joossens** willen bedanken voor zijn inspirerende ideeën en verruimende blik. Door u ben ik meer out-of-the-box beginnen denken. Overigens apprecieer ik ook enorm hoe je mij hebt geholpen in mijn verdere carrièrekeuzes.

I wish to thank the colleagues from the University of Gent for the nice collaboration we had. **Prof. dr. Mo Lamkanfi**, I enjoyed the discussions we had in order to tackle the problems we faced together. **Daniel**, thanks for all your help with the IC₅₀ determinations. You made pipetting go a lot faster as usual! **Nina** en **Lieselotte**, bedankt om alle biologische assays zo duidelijk mogelijk uit te leggen. Ik vond het trouwens erg leuk om eens een dagje met jullie mee te volgen. Ik wens jullie alvast nog veel succes met de thalidomide-structuren. Ik hoop ten zeerste dat er nog iets veelbelovend uit de bus komt!

Voor alle vragen omtrent problemen in het labo was er altijd één adres waar ik terecht kon; bij **Sophie**. Bedankt voor de diverse hulp en professionele houding! **Ingmar**, jij kwam als een engel uit de hemel om mijn biochemische evaluatie over te nemen. Wat was ik blij dat we samen op caspasen konden vloeken!

I really had a lot of fun with my lab mates. **Rafaëla, David, Jens** (unfortunately only for a short period before they took you away!), **Dries** (let's call it virtual lab sharing ;-)), **Lara** and **Anke**, I really enjoyed spending all those days in the lab with you. I learnt a lot about the Polish language (which I already forgot, sorry!), French habits (some of which I did not want to know...), Belgian kittens (Dries, what was that with all the pictures?), Portuguese boyfriends (which I got to meet eventually!) and Dutch lab safety rules (Anke, glad your safe and sound!).

Special thanks go to you, **Rafi**, for teaching me the tricks to become a good medicinal chemist. I wish you the best of luck with the on-target experiments! Ook voor jullie, **Lara** en **Anke**, dat het caspase-onderzoek nog veel positieve ontdekkingen mag teweegbrengen. The same for you, **Filipe**, never give up on the caspases! ;-)

In het bijzonder zou ik **Jens, Sam, Dries** en **Lars** willen bedanken. Als het even minder ging kon ik steeds terecht bij jullie voor een spontane lach. Jullie zijn topkerels! Dat we nog veel spartaanse veldlopen mogen meemaken...

Many thanks go to you, **Antonella**, for all the help you gave me with the set-up of a good Strecker protocol. Though we were facing some communication challenges, I enjoyed working with you and I really appreciated the energy you have put in this project.

In general, the atmosphere at the lab was always very amusing. I really appreciated working with all my (ex-)colleagues. Not only in the lab, but we also had a great time during the conferences, football events and teambuilding activities. **Irene, Eduardo, Carlos, An, Jeroen, Hans, Maciej, Olga, Pedro, Fabio, Eleni, Naiara, Matthias Cleenewerck, Koen, Matthias Breugelmans, Leen, Jonas, Kurt, Artem, Oxana, Venkat, Marion, Giuliana, Agnese, Thomas, Somhairle, Aneta and Dieter**, many thanks for all the nice moments! I wish you all the best for your further career.

Hoewel ze niets essentieels hebben bijgedragen tot deze thesis is ook de inbreng van mijn **vrienden** niet te onderschatten. Ook al begrepen jullie er zo weinig van, jullie waren altijd erg geïnteresseerd als ik mijn thesisonderwerp nogmaals wou uitleggen... of deden jullie tenminste erg goed alsof! De vele leuke momenten samen gaven me telkens weer voldoende energie om volledig te 'knallen' tijdens het afwerken van mijn thesis. Ik hoop dat we dergelijke fantastische momenten nog veel mogen herhalen.

Uiteraard had ik nooit zo ver geraakt zonder mijn ouders. **Mutti, Padre**, dikke merci om al 27 jaar met raad en daad achter mij te staan. Jullie hebben mij altijd gesteund, welke beslissing ik ook genomen heb. Ook mijn drie geweldige **broers** zou ik niet willen vergeten. Jullie zijn niet enkel broers, maar echte vrienden! Wat ben ik blij dat ik jullie schaapje mag zijn!

Ten slotte rest er nog één bijzonder lief meisje om te bedanken; de rots in mijn branding, mijn complement, mijn moordgriet, mijn sardientje, mijn zonnetje in huis, mijn verloofde ... **Sandrine**. Ik kan mij geen beter lief inbeelden dan jou. Je hebt jezelf altijd op de tweede plaats gezet om er voor mij te kunnen zijn. Ik zal je daarom nooit genoeg kunnen bedanken voor de enorme steun die je mij hebt gegeven tijdens deze thesis. Na dit doctoraat kan ik me helemaal terug op jou storten en kunnen we samen dat huwelijksbootje verder versieren! ;-)

All of you...

THANK YOU!!